



Universidade do Minho
Escola de Medicina

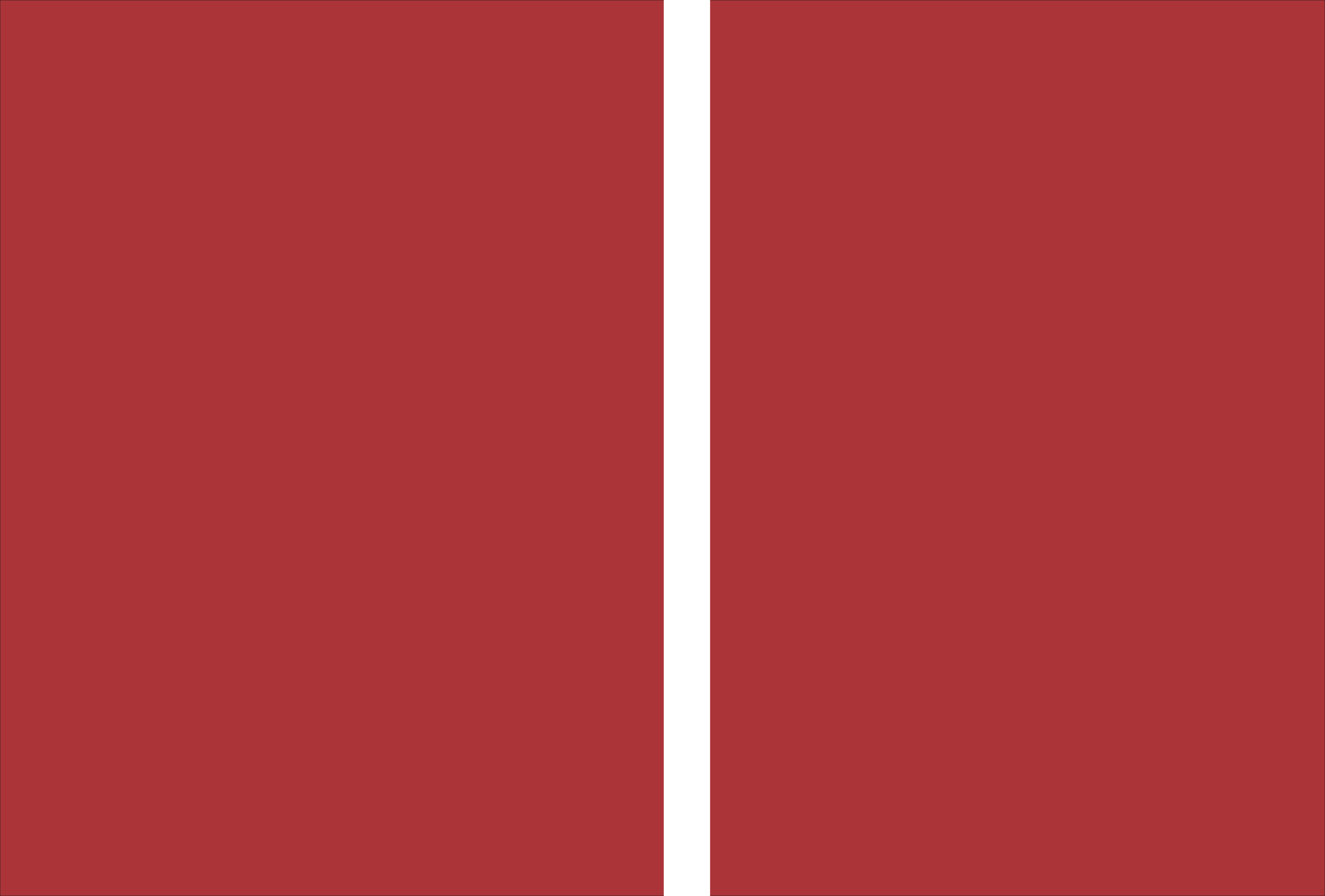
André Miguel Lopes Miranda

Endolysosomal dysfunction and exosome secretion: implications for neurodegenerative disorders

André Miguel Lopes Miranda
Endolysosomal dysfunction and exosome secretion: implications for neurodegenerative disorders

FCT
Fundação para a Ciência e a Tecnologia
MINISTÉRIO DA EDUCAÇÃO E CIÊNCIA







Universidade do Minho
Escola de Medicina

André Miguel Lopes Miranda

**Endolysosomal dysfunction and exosome
secretion: implications for neurodegenerative
disorders**

Tese de Doutoramento em Medicina

Trabalho efetuado sob a orientação do
Doutor Gilbert Di Paolo
e do
Doutor Tiago Gil Rodrigues Oliveira

abril de 2018

DECLARAÇÃO

Nome: André Miguel Lopes Miranda

Endereço eletrónico: id5609@alunos.uminho.pt

Título da Tese de Doutoramento:

Endolysosomal dysfunction and exosome secretion: implications for neurodegenerative disorders

Orientadores:

Doutor Gilbert Di Paolo

Doutor Tiago Gil Rodrigues Oliveira

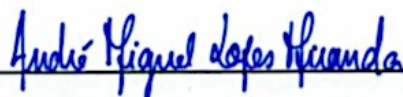
Ano de conclusão: 2018

Doutoramento em Medicina

É AUTORIZADA A REPRODUÇÃO INTEGRAL DESTA TESE, APENAS PARA EFEITOS DE INVESTIGAÇÃO, MEDIANTE A DECLARAÇÃO ESCRITA DO INTERESSADO, QUE A TAL SE COMPROMETE.

Universidade do Minho, 25 de abril de 2018

Assinatura: _____



(André Miguel Lopes Miranda)

STATEMENT OF INTEGRITY

I hereby declare having conducted my thesis with integrity. I confirm that I have not used plagiarism or any form of falsification of results in the process of the thesis elaboration.

I further declare that I have fully acknowledged the Code of Ethical Conduct of the University of Minho.

University of Minho, 25 of April of 2018

Full Name: André Miguel Lopes Miranda

Signature: André Miguel Lopes Miranda

“The heavier the burden, the closer our lives
come to the earth, the more real and truthful
they become.”

Milan Kundera

ACKNOWLEDGEMENTS

To Professor Gilbert Di Paolo, for his fantastic support and great mentorship over the past four years. Thank you for helping me develop a great passion and enthusiasm for science and become an independent and critical thinker.

To Tiago Gil Oliveira, for his trust and belief since the moment we met and for always pushing me to the best of my potential. It has been a pleasure to follow your early steps as a group leader and I hope to continue to contribute to your success.

To Professor Mikael Shelanski, for all the support during my stay at Columbia University.

To all faculty at Escola de Medicina, for the continuous effort in pushing medical education forward in Portugal, without whom the MD/PhD program would have not been possible.

To all the members of the Di Paolo lab, to whom I owe the great working environment, enthusiasm for science, friendship and companion.

To all my friends, for all the support and great adventures.

To my family, who has supported me all the way through these years, always inspired me to achieve the highest degree of excellence, and hardly endured the cost of my absence.

Financial support was provided by Fundação para a Ciência e Tecnologia (PD/BD/105915/2014) in the context of the University of Minho MD/PhD Program.

ABSTRACT

Endolysosomal dysfunction and exosome secretion: implications for neurodegenerative disorders

Defects in endolysosomal and autophagic functions are increasingly viewed as key pathological features of neurodegenerative disorders. A master regulator of these functions is phosphatidylinositol-3-phosphate (PI3P), a phospholipid synthesized primarily by class III PI 3-kinase Vps34. Here we report that disruption of neuronal Vps34 function *in vitro* and *in vivo* impairs autophagy, lysosomal degradation as well as lipid metabolism, causing endolysosomal membrane damage. PI3P deficiency also promotes secretion of unique exosomes enriched for undigested lysosomal substrates, including amyloid precursor protein C-terminal fragments (APP-CTFs), specific sphingolipids and the phospholipid bis(monoacylglycero)phosphate (BMP), which normally resides in the internal vesicles of endolysosomes. Secretion of these exosomes requires neutral sphingomyelinase 2 and sphingolipid synthesis. Our results reveal a homeostatic response counteracting lysosomal dysfunction via secretion of atypical exosomes eliminating lysosomal waste and define exosomal APP-CTFs and BMP as candidate biomarkers for endolysosomal dysfunction associated with neurodegenerative disorders. Moreover, we characterized the lipid profile of several brain regions and along the longitudinal axis of the hippocampus, specifically. We observed regional molecular identity and identified a continuous molecular gradient along the dorsal and ventral extremities of the hippocampus, subject to differential modulation of lipid pathways upon treatment with corticosterone, a known mediator of the pathological effects of chronic stress. Thus, our results suggest a multipartite view of the brain based on its lipid signature and highlight lipid metabolism as an important mediator of stress, with potential implications for mood and neurodegenerative disorders. Altogether, our findings highlight the importance of the study of basic cellular mechanisms such as endolysosomal traffic, lipid metabolism and exosome secretion for a better understanding of the pathophysiology of neuronal loss and identification of new biomarkers and therapeutic targets in neurodegenerative disorders associated with endolysosomal dysfunction.

RESUMO

Disfunção endolisossomal e secreção de exossomas: implicações para doenças neurodegenerativas

Defeitos na função endolisossomal e autofagia têm sido cada vez mais associados aos achados patológicos de doenças neurodegenerativas. Um dos principais reguladores destes sistemas é o fosfatidilinositol-3-fosfato (PI3P), um fosfolípido sintetizado primariamente pela PI-3 cinase classe III Vps34. Neste estudo relatamos que a inibição da função da Vps34 em neurónios *in vitro* e *in vivo* bloqueia a autofagia, degradação lisossomal e o metabolismo lipídico, causando o dano de membranas endolisossomais. O déficit de PI3P promove a secreção de exossomas únicos, enriquecidos em substratos lisossomais não degradados, incluindo o fragmento C-terminal da proteína precursora da amiloide (APP-CTFs), esfingolípidos específicos e o fosfolípido bis(monoacilglicerol)fosfato (BMP), exclusivamente localizado nas vesículas internas de endolisossomas. A secreção dos referidos exossomas requer a enzima esfingomielinase neutra 2 e a síntese de esfingolípidos. Assim, os nossos resultados revelam uma resposta homeostática combatendo a disfunção lisossomal por meio de secreção de exossomas atípicos que facilitam a eliminação de material não degradado, e definem os APP-CTFs e BMP como potenciais biomarcadores de disfunção endolisossomal associada a doenças neurodegenerativas. Adicionalmente, caracterizamos o perfil lipídico de várias regiões cerebrais e especificamente ao longo do eixo longitudinal do hipocampo. Além de observar uma identidade molecular regional, identificamos um gradiente molecular ao longo da região dorsal-ventral do hipocampo, sujeito a modulação diferencial de vias lipídicas após tratamento com corticosterona, um conhecido mediador dos efeitos patológicos de stress crónico. Como tal, os nossos resultados apontam para uma visão multipartida do cérebro, com base na sua composição lipídica, e destacam o metabolismo lipídico como importante mediador dos efeitos do stress, potencialmente com implicação para distúrbios do humor e doenças neurodegenerativas. Sumariamente, os nossos resultados destacam a importância do estudo de mecanismos celulares básicos, como o tráfego endolisossomal, metabolismo lipídico e secreção de exossomas, para uma melhor compreensão da fisiopatologia da morte neuronal e identificação de novos biomarcadores e alvos terapêuticos em doenças neurodegenerativas associadas a disfunção endolisossomal.

TABLE OF CONTENTS

ACKNOWLEDGEMENTS	vii
ABSTRACT	ix
RESUMO	xi
TABLE OF CONTENTS	xiii
ABBREVIATIONS	xv
1. INTRODUCTION	1
1.1 The Endolysosomal system	3
1.2 Autophagy	5
1.3 Exosomes	7
1.4 Lipids and membrane trafficking	10
1.4.1 Phosphoinositides	13
1.4.2 PI3P: Master Regulator of the endolysosomal and autophagy pathways	15
1.5 Lysosomal storage disorders and neurodegeneration	18
1.5.1 PI3P and neurodegeneration	20
Aims	22
References	23
2. EXPERIMENTAL WORK	31
2.1 Neuronal lysosomal dysfunction releases exosomes harboring APP C-terminal fragments and unique lipid signatures	33
2.1.1 Supplementary Information	75
2.2 Differential lipid composition and regulation along the hippocampal longitudinal axis	95
3. DISCUSSION, CONCLUSION AND FUTURE PERSPECTIVES	127
4. ANNEXES	149
4.1 Lipids under stress - a lipidomic approach for the study of mood disorders	151
4.2 Endolysosomal dysfunction and exosome secretion: implications for neurodegenerative disorders	163
4.3 Peer Review Electronic File	175

ABBREVIATIONS

24-OHC, 24(S)-hydroxycholesterol	GM3 – monosialodihexosylganglioside
27-OHC, 27(S)-hydroxycholesterol	GR – glucocorticoid receptor
A β – amyloid- β	HexCer - hexosylceramide
AD – Alzheimer’s disease	HOPS - homotypic fusion and protein sorting
ALS – amyotrophic lateral sclerosis	ILV – intraluminal vesicle
APP – amyloid precursor protein	LacCer – lactosylceramide
APP-CTFs – amyloid precursor protein c-terminal fragments	LAMP-1 – lysosomal membrane associated protein 1
APS - acyl-phosphatidylserine.	LBPA – lysobisphosphatidic acid
Atg – autophagy-related gene	LOAD – late onset Alzheimer’s disease
BACE1 – β -secretase enzyme	LPC – lysophosphatidylcholine
BafA1 – bafilomycin 1	LPCE - ether lysophosphatidylcholine
BMP – bis(monoacylglycerol)phosphate	LPE – lysophosphatidylethanolamine
CatD – cathepsin D	LPEp - plasmalogen lysophosphatidylethanolamine
CE – cholesteryl ester	LPI – lysophosphatidylinositol
Cer - ceramide	LSD – lysosomal storage disorder
CLEAR – coordinated lysosomal expression and regulation	MhCer - monohexylceramide
COP1 – coating protein I	MG - monoacylglycerol
CORT – corticosterone	MR – mineralocorticoid receptor
CTRL – control	MTMR – myotubularin
CUS – chronic unpredictable stress	mTOR – mammalian target of rapamycin
DG - diacylglycerol	MVE – multivesicular endosome
dhCer - dihydroceramide	PA - phosphatidic acid
dhSM – dihydrosphingomyelin	PC – phosphatidylcholine
EM – electronic microscopy	PCe - ether phosphatidylcholine
ESCRT - endosomal sorting complexes required for transport	PD – Parkinson’s disease
EV – extracellular vesicle	PE – phosphatidylethanolamine
FC – free cholesterol	Pep - plasmalogen phosphatidylethanolamine
FTD – frontotemporal dementia	PG – phosphatidylglycerol
	PI – phosphatidylinositol

PS - phosphatidylserine

PIP – phosphatidylinositolphosphate

SM - sphingomyelin

SNX – sorting nexins

Sulf – sulfatides

Sulf(2OH) - 2-hydroxy N-acyl sulfatide

TG - triglyceride

VEH- vehicle

Vps34 – vacuolar sorting protein 34

CHAPTER 1

INTRODUCTION

INTRODUCTION

1.1 The endolysosomal system

The endosomal-lysosomal system is a fundamental feature of eukaryotic cells (Wideman et al. 2014). This system is broadly configured by three major populations of vesicular compartments, early and late endosomes as well as lysosomes (Figure 1) (Maxfield and Mukherjee 2004).

Endocytosis starts with membrane invagination and internalization of molecules in membrane pits which then pinch off to generate vesicles that ultimately fuse with early endosomes. Endosomes act as important sorting platforms receiving vesicles from the *trans*-Golgi network, recycling cell surface receptors and sorting cargo for degradation in lysosomes. While endocytosis is an effective mechanism to downregulate activated membrane surface receptors, early endosomes also act as important signaling platforms providing scaffold for second messengers as well as kinases or transcription factors and facilitating crosstalk of multiple signaling pathways (Di Fiore and von Zastrow 2014). Importantly, early endosomes are a group of heterogeneous organelles with different spatial distributions and cargo sorting activities, although dynamically interacting and communicating with each other (Villaseñor, Kalaidzidis, and Zerial 2016). Morphologically, early endosomes are characterized by tubules extending from a typically electron lucent central vacuole (Klumperman and Raposo 2014). These structures are important membrane carriers that mediate outgoing traffic from early endosomes, promoting recycling of proteins and lipids back to the plasma membrane. Recycling may occur directly from the tubules emerging from early endosomes or mediated through a relay station called the endocytic recycling compartment. Importantly, in addition to their molecular make up (e.g. Rab GTPases), recycling endosomes are characterized by the absence of endocytic cargo destined for degradation in late endocytic compartments (Maxfield and Mukherjee 2004; Wandinger-Ness and Zerial 2014).

The following compartment in the endocytic pathway is the late endosome. This transition is characterized by a dramatic remodeling of endocytic compartments. The tubular morphology is converted to a globular shape with numerous intraluminal vesicles (ILVs) while the lumen is acidified (Luzio et al. 2014). The intraluminal trapping of membranes sequesters receptors from the cytosol and thus terminates signaling, while also facilitating internal membrane exposure to hydrolases upon fusion with lysosomes (Bissig and Gruenberg 2013). Multiple mechanisms for ILV formation have been described, including sorting by the endosomal sorting complexes required for transport (ESCRT) pathway, tetraspanins or via local synthesis of specific lipids, namely ceramides or

bis(monoacylglycero)phosphate (BMP), also known as lysobisphosphatidic acid (LBPA), both of which spontaneously induce ILV budding *in vitro* at acidic pH (Raiborg and Stenmark 2009; Pols and Klumperman 2009; Trajkovic et al. 2008; Matsuo et al. 2004). In fact, BMP is exclusively found in ILVs and used as a *bona fide* marker of late endosomes (Kobayashi et al. 1999). The local enrichment of lipids such as sphingolipids, BMP and cholesterol suggests that most of the cargo found in ILVs is stringently selected and is, in most cases, destined to the lysosomes for degradation (Huotari and Helenius 2011; Kobayashi et al. 1999; Möbius et al. 2003). Alternatively, multivesicular endosomes (MVEs) can fuse with the plasma membrane and release ILVs as exosomes (see below) (Raposo and Stoorvogel 2013). Importantly, late endosomes depend on the permanent influx of new components from the *trans*-Golgi network, other endosomes and lysosomes to properly provide lysosomes with hydrolases and membrane proteins crucial for degradative function (Huotari and Helenius 2011).

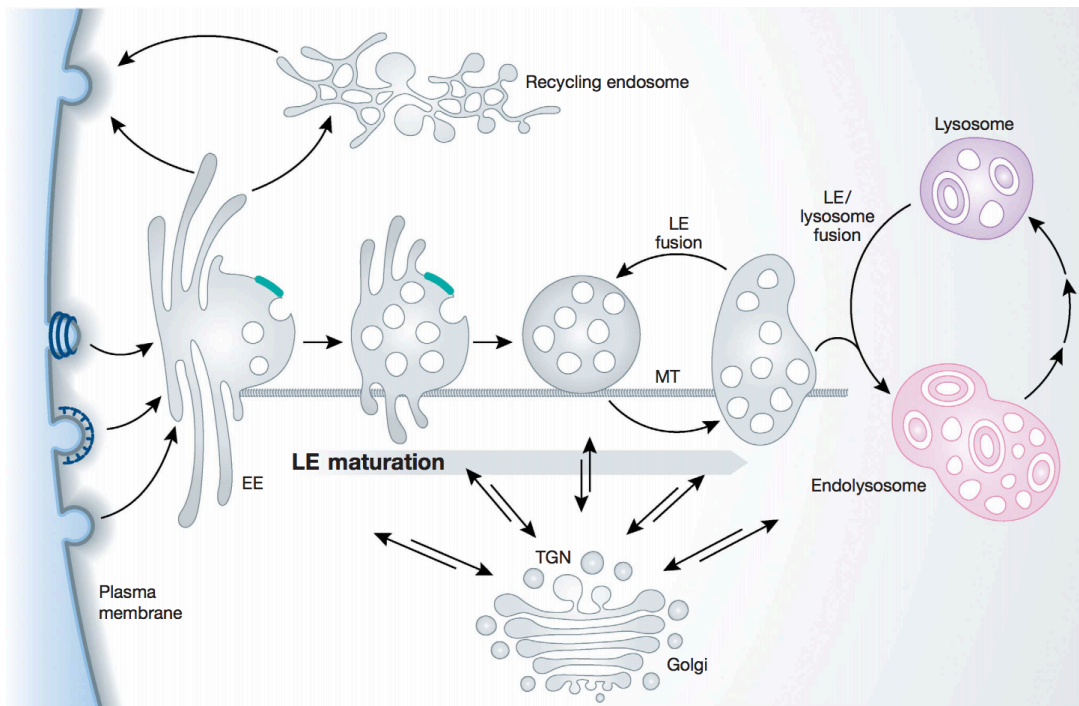


Figure 1. The endolysosomal system. Upon internalization, the immediate endocytic structures fuse with early endosomes, large endocytic compartments characterized by extensive tubulation. Cargo is sorted for recycling or transferred to late endosomes, which gradually reduce the number of tubules and increase budding of intraluminal vesicles (ILVs) as they mature. Late endosomes communicate with lysosomes through vesicular transport (not shown) or heterotypic fusion, forming endolysosomes (adapted from Huotari and Helenius, 2011).

Lysosomes are the end stage of the endocytic pathway and are the primary degradative compartments of cells. They are responsible for the breakdown of proteins, lipids, sugars and nucleic acids, which, in conditions of compromised function, accumulate as indigestible materials (Settembre

et al. 2013). Lysosomes are characterized by the presence of lysosome-associated membrane proteins (*e.g.*, LAMP-1), acidic pH, enrichment of hydrolytic enzymes and lack of mannose-6-phosphate receptors (Saftig and Klumperman 2009). Of all endocytic compartments, lysosomes show the broadest composition and morphology, particularly between different cell types, in which lysosome-related organelles display specialized functions (*e.g.*, melanosomes and lytic organelles) (Marks, Heijnen, and Raposo 2013). Lysosomal heterogeneity may also result from the diversity of feeding pathways that provide the different lysosomal membrane constituents as well as types of cargo, including electron-dense hydrolases or electron-lucid lysosomal membrane proteins. Since some lysosomes fuse with late endosomes and the resulting hybrid compartment shares common morphological features with the previous, these are also commonly called endolysosomes (Huotari and Helenius 2011).

Altogether, the endolysosomal pathway is composed by a continuum of intermediate structures that are responsible for the internalization of external and surface molecules, which, in turn, can be recycled back to the plasma membrane or degraded in endolysosomes. Of note, different models have been proposed for endosomal maturation and include maturation of a single compartment through the varying stages, vesicular transport between heterotypic compartments, *kiss-and-run* events by transfer of material through transient physical interactions of heterotypic vesicles (Luzio, Pryor, and Bright 2007). Given the dynamic nature and ongoing trafficking of material between compartments, it is extremely challenging to unambiguously identify these structures. As such, classification of endocytic structures is based on combinatorial characterization of ultrastructural morphology and molecular composition. Examples of commonly used organelle markers are Rab GTPases and phosphoinositides (PIPs) (Wandinger-Ness and Zerial 2014). Both are responsible for the timely and spatially restricted recruitment of protein effectors that mediate important aspects of endosomal maturation as transport, fusion, tubulation and fission. Importantly, disruption of PIP metabolism or *on-off* conversion of Rab GTPases causes the accumulation of abnormal hybrid organelles and significantly impairs cellular degradation and signaling, implying a restrict regulation of endocytic trafficking for proper function (Wandinger-Ness and Zerial 2014).

1.2 Autophagy

The endolysosomal compartment communicates with several other cellular organelles, among which autophagosomes play a critical role as part of a set of lysosomal degradation pathways collectively

referred to as autophagy. Autophagy is a largely conserved process responsible for bulk and selective turnover of cytosolic cargo inaccessible to the endosomal lumen (Figure 2) (Bento et al. 2016). Autophagy cargo is commonly endogenous, including both soluble and particulate molecules (*e.g.*, protein aggregates) or even whole organelles, typically compromised or damaged and targeted for degradation. Autophagy may also contribute to the turnover of exogenous material, most commonly endocytic cargo that escapes permeabilized vesicles (*e.g.*, bacteria) (Galluzzi et al. 2017).

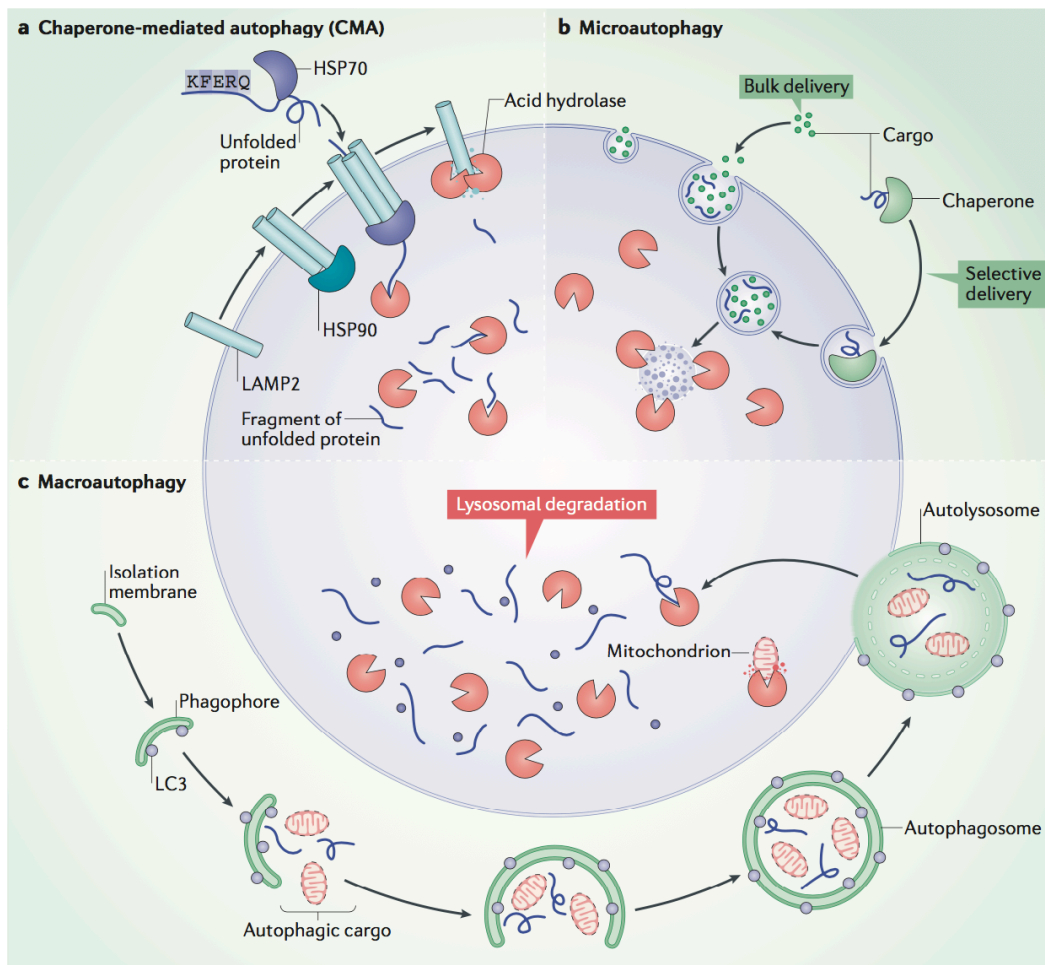


Figure 2. Overview of autophagy. **a.** Chaperone-mediated autophagy involves protein unfolding by molecular chaperones and internalization through pore-like structures assembled by clustering of LAMP-2 transmembrane proteins. **b.** Microautophagy occurs through direct invagination of endolysosomal membranes. **c.** In macroautophagy, cargo is captured in bulk or selectively by a growing phagophore. Following closure, autophagosomes fuse with endosomes (not shown) or lysosomes (adapted from Galluzzi et al. 2016).

Importantly, autophagy is intrinsically associated with the endolysosomal pathway. First, microautophagy relies in the luminal sorting of cytosolic cargo by direct invagination of the endolysosomal membrane. This process has been more widely described in yeast but also recently

reported in mammals (Sahu et al. 2011). Secondly, chaperone-mediated autophagy mediates the lysosomal incorporation of soluble proteins by unfolding and shuttling through a pore-like membrane translocation complex in lysosomes (Cuervo and Wong 2013). Thirdly, macroautophagy (hereafter referred to as autophagy) mediates bulk or selective degradation of cytoplasmic material by capturing cargo with a double-membrane phagophore that elongates and fuses to form an enclosed vesicle, the autophagosome (Bento et al. 2016; Galluzzi et al. 2016). Autophagosomes fuse with late endosomes and lysosomes for degradation of the engulfed material. Of note, autophagosome fusion shares the same molecular machinery required for homo- and heterotypic endosomal fusion (Tooze, Abada, and Elazar 2014). Given the convergence between autophagy and the endolysosomal system, autophagy disturbances also play an important role in the physiology of endolysosomal defects that lead to lysosomal storage disorders (LSDs) (Lamb, Yoshimori, and Tooze 2013).

1.3 Exosomes

Extracellular vesicles (EVs) are a heterogeneous group of vesicles that are referred to as exosomes or ectosomes, whether they originate from the endolysosomal system or shed from the plasma membrane, respectively (Figure 3) (Cocucci and Meldolesi 2015). Their candidate role as vehicles for intercellular communication and relative accessibility in biological fluids has recently drawn a lot of attention, particularly in the fields of neurodegenerative disorders and biomarker discovery (van Niel, D'Angelo, and Raposo 2018).

Exosomes are small 30-100nm diameter vesicles released from the fusion of endolysosomal membranes with the plasma membrane. Thus, exosomes are in essence ILVs secreted in the extracellular milieu. In contrast, ectosomes (also commonly called microvesicles) show a broader range in size (50-1000nm) and derive directly from outward budding of the plasma membrane. Nevertheless, despite distinct morphologies, origins and likely mechanisms, exosomes and subpopulations of microvesicles share common properties, including lipid and protein cargoes, since endolysosomal membranes also partially derive from the plasma membrane. In the absence of more specific purification and characterization tools to distinguish small EVs, the enrichment of endosome-associated proteins and lipids allows for the distinction of exosomes from vesicles of other origin, such as ectosomes and apoptotic bodies (Kowal et al. 2016; Skotland, Sandvig, and Llorente 2017). Another challenging, yet fascinating, observation is that exosome secretion greatly depends on cell-

type, not only quantitatively but also qualitatively, and composition will vary depending on the cellular state (Kowal et al. 2016).

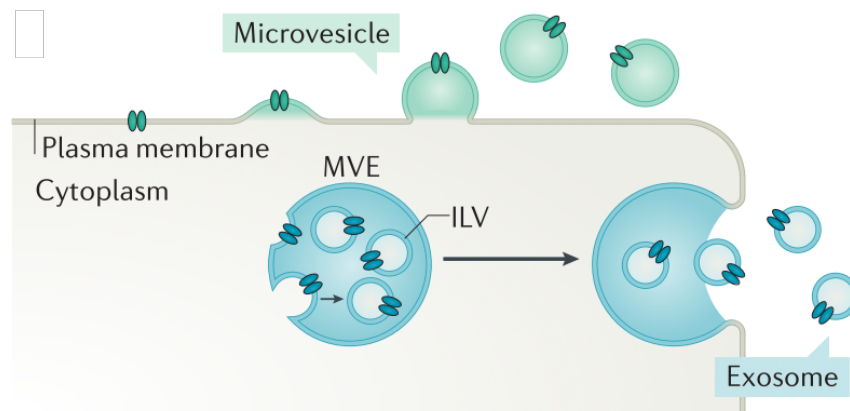


Figure 3. Biogenesis of extracellular vesicles. Microvesicles bud directly from the plasma membrane; exosomes derive from ILVs released upon fusion of MVE with the plasma membrane (adapted from van Niel, D'Angelo and Raposo 2018).

By definition, exosomes require the budding of ILVs in MVEs. A fundamental question is which mechanisms sort ILVs for degradation in lysosomes *vs.* secretion as exosomes. A partial answer may imply different ILV budding mechanisms, which invariably starts with cargo clustering on microdomains of MVE's limiting membrane. The ESCRT pathway was initially implicated in exosome biogenesis given its role in intraluminal sorting of membrane proteins and detection of ESCRT components in exosome preparations (Colombo et al. 2013). Importantly, ESCRT-depleted cells are still able to form ILVs and secrete exosomes, although likely of different composition (Stuffers et al. 2009; Colombo et al. 2013; Edgar, Eden, and Futter 2014). Alternatively, tetraspanins CD63, CD81, CD82 and CD9 have also been involved in ILV sorting by clustering, binding to cholesterol and inducing inward budding of microdomains of the limiting membrane (van Niel, D'Angelo, and Raposo 2018). In addition, another proposed mechanism of ESCRT-independent mechanisms of exosome biogenesis has been ceramide synthesis by neutral type II sphingomyelinase and BMP-dependent ILV sorting (Trajkovic et al. 2008; Matsuo et al. 2004). Notably, the aforementioned mechanisms are linked to luminal sorting of membrane associated proteins, whether through recognition of ubiquitin residues by ESCRT or sorting to membrane subdomains enriched in tetraspanins or ceramides and BMP. It is noteworthy that cytosolic cargo has also been detected in exosomes, including proteins, RNA and DNA, but their sorting mechanisms are more elusive (van Niel, D'Angelo, and Raposo 2018). Therefore, cells possess multiple mechanisms for ILV sorting and exosome secretion that likely results

in vesicle subpopulations of distinct composition. Remarkably, it is still unclear what cargo is preferentially sorted by each of the aforementioned pathways, whether these different sorting pathways compete with each other for substrate loading into ILVs or if exosome subpopulations originate from common or exclusive endolysosomal compartments (Colombo et al. 2013; Baietti et al. 2012; van Niel, D'Angelo, and Raposo 2018; Willms et al. 2016). In addition to ILV biogenesis, exosome secretion will also depend on the machinery controlling the fusion of MVEs with the plasma membrane or other endocytic compartments (e.g., Rabs and ARFs) (Baietti et al. 2012; Ghossoub et al. 2014; Ostrowski et al. 2010). Consequently, PIPs may also play an important role in exosome dynamics as they recruit GTPases and modulate endosomal microdomain assembly and vesicle budding (Hessvik et al. 2016; Jean and Kiger 2012). As a result of such a complex regulatory network, what molecular checkpoints or structural components commit MVEs to secretion or degradation remains a central question in the field.

Once exosomes are released, they may exert downstream effects by directly fusing with acceptor cells' membrane or by being internalized through endocytosis and having their contents released into the cytosol upon back fusion with the limiting endocytic membrane (Cocucci and Meldolesi 2015). Specificity of cell transfer is likely determined by the molecular landscape of both exosomes and acceptor membranes. For instance, subpopulations of exosomes released by neurons can be exclusively targeted to other neurons or both neurons and glial cells (Laulagnier et al. 2017; Chivet et al. 2014). Exosomes will transfer many different cargoes and thus are likely endowed with distinct cellular responses in acceptor cells. In neurodegenerative diseases, exosomes may transfer pathological proteins (e.g. amyloid- β ($A\beta$), tau, TDP43 and α -synuclein) and thus facilitate the transcellular propagation of protein aggregates (Coleman and Hill 2015).

Altogether, there is a growing interest and a critical need to better understand the biology of exosomes as well as their physiological and pathophysiological roles. While the accessibility of bodily fluids endows exosomes great diagnostic and prognostic potential, the complexity of exosome biogenesis, diversity of subpopulations and lack of standard isolation protocols have limited their practical application. Therefore, the molecular characterization of exosomes and mechanistic understanding of how their biogenesis and secretion operate will significantly help to understand their potential as reporters of cellular activities or overall status.

1.4 Lipids and membrane trafficking

Cellular membranes are predominantly composed of lipids, which are critical molecules not only for their structural organization and compartmentalization, a unique feature of eukaryotic cells, but also for cellular signaling (Klose, Surma, and Simons 2013; Wideman et al. 2014). The vast physicochemical diversity of lipids allows for multiple functions at the cellular level in addition to membrane trafficking, including direct ion channel modulation, amplification of signaling cascades and cell-cell communication (Piomelli, Astarita, and Rapaka 2007).

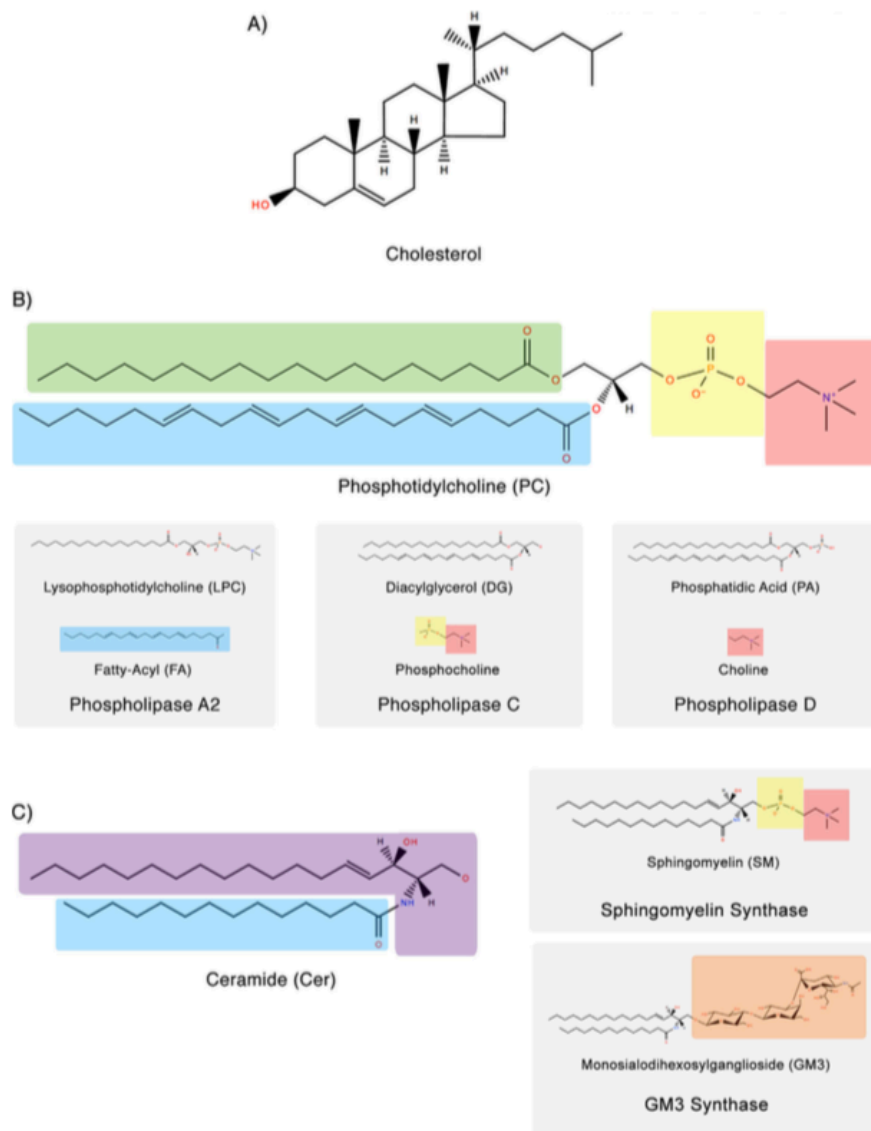


Figure 4. Major lipid categories in mammalian cells. a. Cholesterol is the most abundant sterol in mammals. It contains an inflexible four-ring core that confers high hydrophobicity and interferes with acyl chain packing in membranes, promoting the assembly of lipid microdomains. Cholesterol plays an important role on the physical properties of membranes, namely fluidity, thickness, and permeability. **b.** Glycerophospholipids are divided in classes according to the nature of the head group linked to the glycerol backbone. These vary in shape and charge, determining their

location within membranes in cells. The insight boxes show the site of cleavage by phospholipases A2, C, and D. The respective products contribute to changes in membrane properties, such as induction of curvature (lysoPC and PA), or act as intracellular signaling molecules (acyl chains and DG). **c.** Sphingolipids contain a sphingoid backbone, which is acylated to form a ceramide. Addition of polar head groups, phosphate or sugars, yields more complex classes, such as phosphosphingolipids and gangliosides (adapted from Miranda and Oliveira, 2015).

Classification of lipids is based on their chemical structure and physical properties. In mammalian cells, the main lipid categories are sterols (cholesterol), glycerophospholipids and sphingolipids (Figure 4). Lipid categories are divided in lipid classes depending on their head group, while species refer to the acyl chain composition. Importantly, the hydrocarbon chain moiety can vary in length, saturation and hydroxylation, while polar head groups can differ in shape and charge (Fahy et al. 2005). This variety at the atomic level provides lipids distinct physical properties such as propensity to assemble rigid, impermeable membrane domains, typical of sterols and sphingolipids, or flexible, curved membranes rich in glycerophospholipids (Simons and Sampaio 2011).

Cholesterol is the most abundant lipid in mammalian cells (Harayama and Riezman 2018). The presence of a highly hydrophobic core promotes tight membrane lipid packing, facilitating the assembly of membrane subcompartments known as lipid rafts (Simons and Sampaio 2011). These nanoscale subdomains are not only enriched in cholesterol but also in sphingolipids and glycerolipids of long and saturated hydrocarbon chains. These structures allow for the lateral segregation of specific proteins (*e.g.*, neurotransmitter receptors or ion channels) and promote the interaction between substrate and enzyme complexes [amyloid precursor protein (APP) and β -secretase 1 (BACE-1)]. Protein recruitment is determined by hydrophobic matching, a physical interaction between the transmembrane domains and the surrounding lipids (Mouritsen 2011). Also, cytosolic proteins may be recruited to these compartments by post-translational modifications, such as palmitoylation and prenylation (Simons and Sampaio 2011). Excess free cholesterol can be converted to cholesteryl esters and stored in lipid droplets (Chang et al. 2006).

Sphingolipids share a sphingosine backbone that can be acylated and differ in polar head groups. The first step in sphingolipid synthesis is mediated by serine palmitoyltransferase, which reduces sphingosine to dihydrosphingosine. Dihydrosphingosine undergoes additional acylation and desaturation to generate ceramide, which in turn is then converted to sphingomyelin or glucosylceramide, a substrate for more complex glycosphingolipids (Hannun and Obeid 2008; Hannun and Obeid 2017). Sphingolipids are characterized by long and saturated acyl chains that determine their tall cylindrical shape, a trait that promotes lateral sorting in tightly packed lipid rafts. Their

hydrophobicity facilitates clustering and limited lateral movement, unless they are specifically transported (Hannun and Obeid 2017).

In addition to acting as scaffolds for assembly of membrane subdomains, some sphingolipids act as important bioactive molecules, namely ceramides and sphingosine-1-phosphate. Ceramides are potent modulators of apoptosis and autophagy in response to stressors while sphingosine 1-phosphate modulates G protein-coupled receptors and intracellular signaling (Hannun and Obeid 2008; Morad and Cabot 2013). Notably, degradation of membrane sphingolipids occurs through internalization of membranes via the endolysosomal pathway. Sphingolipids and glucosylceramides are degraded in lysosomes where sphingomyelinases and glucosylceramidases are localized. Mistrafficking of enzymes and sphingolipids or defective lysosomal clearance frequently lead to sphingolipid storage, a common feature of LSDs (Platt 2014).

Glycerophospholipids are the second most abundant lipid category in eukaryotic cells, after cholesterol. Their structure is based on a glycerol backbone linked to one or two acyl substituents present at *sn1* and *sn2* positions and a polar head group at the position *sn3*. The phosphate group links glycerol to another alcohol that determines the glycerophospholipid class, such as phosphatidylcholine (PC), phosphatidylserine (PS) and phosphatidylinositol (PI) (Fahy et al. 2005). Atypical phospholipids are cardiolipin and BMP which not only have very unique physical properties but are also spatially restricted to mitochondria and ILVs, respectively (Paradies et al. 2014; Bissig and Gruenberg 2013). The different classes of glycerophospholipids differ significantly in abundance and cellular distribution. PC is a cylindrical phospholipid that is typically unsaturated and, as the main glycerophospholipid in eukaryotic membranes, confers planarity and fluidity to membranes. Interestingly, PC can be rapidly catabolized into conical derivatives lysophosphatidylcholine (LPC) phosphatidic acid (PA) by phospholipases A and D, respectively, to induce membrane curvature and allow vesiculation or tubulation in planar membranes. Also, anionic phospholipids confer negative charge to membrane leaflets, particularly cytosolic, and mediate functional interactions with positively charged adaptors (Holthuis and Menon 2014).

In addition to the molecular complexity of lipids, the lipid network is also regulated by spatial distribution. Most *de novo* lipid synthesis takes place in the endoplasmic reticulum (van Meer, Voelker, and Feigenson 2008) and lipids are shuttled to the Golgi apparatus and plasma membrane through secretory vesicles or non-vesicular lipid transfer proteins (Lev 2010; Schauder et al. 2014). The unidirectional transport of sterol and sphingolipids along the secretory pathway is established by the exclusion of both from coat protein I (COPI) vesicles that retrogradely transport proteins and lipids

back to the endoplasmic reticulum, generating a gradient of increasing concentration of sterols and sphingolipids (Shevchenko and Simons 2010). Moreover, the spatial restriction of lipid metabolizing enzymes facilitates the enrichment of certain lipids in specific subcellular compartments which will confer these compartments particular traits, either membrane surface charge (e.g. PIP kinases and phosphatases) or fluidity and curvature, based on acyl chain and saturation specificity (e.g. ceramide synthases and phospholipases A) (Hannun and Obeid 2008). The crosstalk between metabolic pathways of distinct lipid categories, particularly sphingolipids and glycerophospholipids, allows the integration of lipids in a more generalized homeostatic system (Miranda and Oliveira 2015). As such, impairment of specific lipid pathways may disturb the overall lipid equilibrium, with important impact in organelle function.

1.4.1 Phosphoinositides

PIPs are a class of glycerophospholipids that is essential for membrane trafficking (Schink, Tan, and Stenmark 2016). PI can be reversibly phosphorylated at the 3', 4' and 5'-hydroxyl groups of the inositol residue to generate seven PIPs (Figure 5). Strategic localization and coordinated actions of PIP kinases and phosphatases cause PIPs to be differentially localized subcellularly, providing organelles a membrane identity code (Di Paolo and De Camilli 2006). The heterogeneous distribution and the reversible recruitment of distinct effector proteins, each with PIP-specific binding motifs, mediates membrane dynamics and allows for directionality in membrane transport (Schink, Tan, and Stenmark 2016).

PI is the precursor of all PIPs and constitutes about 10-20% of total cellular glycerophospholipids. It is synthesized in the endoplasmic reticulum and transported to the plasma membrane by both vesicular and non-vesicular transport. Although its localization is not particularly specific, it acts as the main pool for the synthesis of PI3P and PI4P, two of the most abundant PIPs (Hammond and Balla 2015). PI4P is the most abundant, corresponding to approximately 5% of PI, and is predominantly found in the Golgi and several endosomal compartments, although a pool is also available at the plasma membrane for PI(4,5)P₂ synthesis. PI3P is the second most abundant PIP, accounting for 5-10% of PI4P (Zolov et al. 2012). PI3P is predominantly localized to endosomal structures, although a subpopulation has been detected in ILVs of MVBs. Also, PI3P is detected in nascent autophagosomes (Raiborg, Schink, and Stenmark 2013). PI5P is the least abundant of the singly phosphorylated PIPs (Zolov et al. 2012). The absence of reliable molecular probes to detect this scant lipid has prevented a clear view of its intracellular localization. Of the polyphosphorylated

PIPs, PI(4,5)P₂ is the most abundant and is predominantly found at the plasma membrane. It mostly derives from phosphorylation of PI4P by PI4P 5-kinases and is rapidly turned over by 5'-phosphatases during endocytosis. PI(3,5)P₂ mainly derives from phosphorylation of PI3P, hence its endosomal localization, and despite its minor abundance, is a critical regulator of late stages of the endolysosomal pathway (Ho, Alghamdi, and Botelho 2012). PI(3,4)P₂ and PI(3,4,5)P₃ are both synthesized by Class I PI3K and have been implicated in the maturation of clathrin-coated vesicles and phagocytic cups, respectively (Schink, Tan, and Stenmark 2016). Despite the simultaneous presence of certain PIPs in distinct organelles, precise recruitment of membrane effectors is ensured by co-incidental detection, a combinatorial system requiring not only PIP-binding specificity but also a second interaction either driven by membrane curvature or coincidental presence of small GTPases, such as Rabs or ARFs (Hammond and Balla 2015).

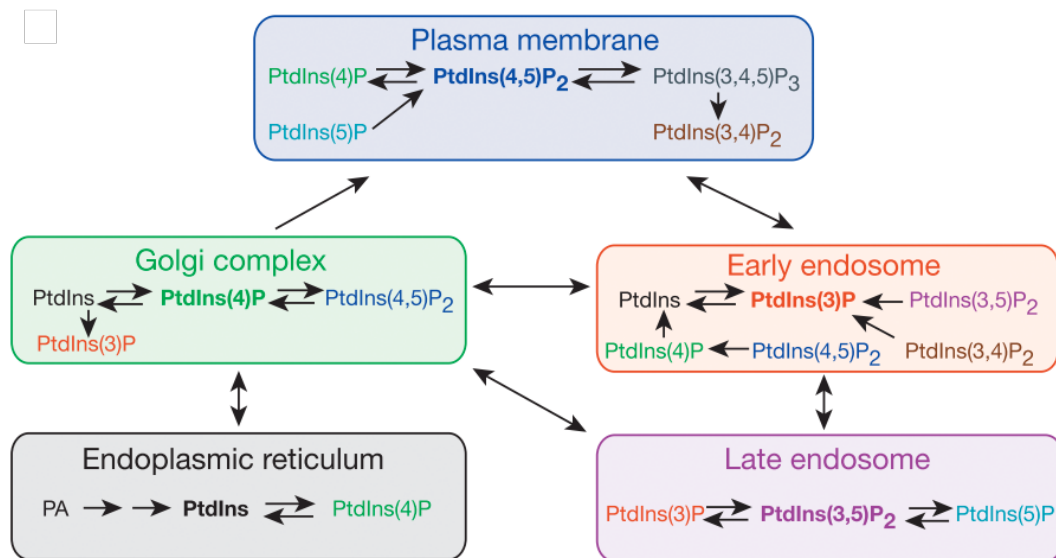


Figure 5. Conversion and subcellular localization of PIPs. Predominant cellular compartmentalization indicated by colored boxes; arrows indicate possible phosphorylation/dephosphorylation conversion between PIPs (adapted from Di Paolo and De Camilli 2006).

Despite some degree of redundancy of the different PIP kinase and phosphatase isoforms, the differential subcellular targeting of these enzymes allows for spatially and timely restricted PIP synthesis and turnover, causing membranes to become particularly sensitive to imbalances in PIP metabolism. Not surprisingly, experimental knock-out models of PIP kinases and phosphatases are commonly embryonically lethal and several human disorders have been genetically linked to mutations in PIP metabolizing enzymes, most of which result in loss of function (Staiano et al. 2015).

Altogether, these observations support the importance of carefully characterizing basic cellular mechanisms mediated by PIPs for the understanding of fundamental mechanisms of disease, particularly those associated with endosomal anomalies, for which therapeutic targets are still a current need.

1.4.2 PI3P: Master Regulator of the endolysosomal and autophagy pathways

PI3P is the third most abundant PIP in eukaryotic cells. It is primarily synthesized by phosphorylation of PI in the 3'-hydroxyl group by Class III PI3K, also known as Vacuolar Protein Sorting 34 (Vps34), which occurs as a multiprotein complex. While the kinase domain of Vps34 represents the catalytic subunit of the Vps34 complex, Vps15 acts as a scaffold and Beclin 1 as the regulatory unit of the complex. Two complexes can be formed with an additional fourth interacting partner, ATG14L or UVRAG (Itakura et al. 2008). Vps34 Complex I includes ATG14L which directs the complex to the omegasome, an endoplasmic reticulum subdomain enriched for PI3P that serves as the autophagy initiation site, while Complex II includes UVRAG and is mostly localized to endosomes. Importantly, there is co-dependence between the Vps34 components such that deregulation of a member destabilizes its interacting partners (Devereaux et al. 2013). Also, as autophagy shares the endosomal machinery for fusion with lysosomes and degradation of cargo, Complex I and II may act sequentially, in autophagosome formation and late stage fusion respectively (Backer 2016). Alternatively, minor pools of PI3P can be synthesized by class II PI3K by similar phosphorylation of PI or consecutive dephosphorylations of PI(3,4,5)P₃ by type II inositol 5'-phosphatase and type Iα 4'-phosphatase (Schink, Raiborg, and Stenmark 2013). Likewise, PI3P turnover can also be mediated by sequential phosphorylation or dephosphorylation. PIKFyve is a PI3P 5-kinase that phosphorylates PI3P to PI(3,5)P₂. While this is the main reaction for PI(3,5)P₂ synthesis, PI3P levels are an order of magnitude more abundant than PI(3,5)P₂ (Zolov et al. 2012). Thus, local PI(3,5)P₂ synthesis may not serve as a major turnover pathway but as an important regulator of spatially and temporally restricted PI3P fluctuations. Alternatively, PI3P can be dephosphorylated by myotubularins (MTMR) (Ketel et al. 2016). Similarly to PIKFyve, MTMR3 and MTMR4 contain a FYVE domain that targets them preferentially to PI3P-enriched domains comparatively to other active members of the MTMR family (Schink, Raiborg, and Stenmark 2013). Therefore, the redundancy of PI3P metabolizing pathways suggests that each likely corresponds to a distinct subcellular pool of PI3P.

The early stages of endocytosis are predominantly characterized by the presence of PI(4,5)P₂. The coincidence of PIPs and membrane cargo sequentially recruits the adaptor protein complex AP2

and clathrin, which invaginates the plasma membrane and forms a coated vesicle (Cocucci et al. 2012). While a brief spike of PI3P production was recently reported short after clathrin coat disassembly, presumably by PI3KC2 α , PI3P signaling has been repeatedly excluded from early stages of endosomal formation (Petiot et al. 2003; Futter et al. 2001; He et al. 2017). In fact, a fraction of vesicles positive for the early endosomal marker APPL1 are negative for PI3P and act as peripheral transient stations *en route* to PI3P-positive endosomes. The transition for PI3P positivity occurs upon recruitment of Vps34 to Rab5-positive endosomes and causes the association of PI3P-binding proteins, such as WDFY2 and EEA1, which mediate important aspects of endosome dynamics and cargo sorting (Zoncu et al. 2009). EEA1 is a tethering protein that binds to PI3P via its C-terminus and active Rab5 via its N-terminus; an allosteric conformational change caused by GTP bound Rab5 induces the collapse of EEA1 coiled-coil and facilitates homotypic fusion (Murray et al. 2016; Christoforidis et al. 1999; Simonsen et al. 1998). Notably, the binding properties of EEA1 to PI3P have been repeatedly used as a reporter of PI3P levels upon manipulation of Vps34 (Petiot et al. 2003; Zoncu et al. 2009; Futter et al. 2001).

In addition to fusion, PI3P also mediates other aspects of early endosomal function. PI3P recruits kinesin-3 KIF16B and regulates transport of early endosomes to the plus end of microtubules (Hoepfner et al. 2005). Sorting nexins (SNX) are a family of proteins characterized by PX and BAR domains. These domains facilitate the binding of SNX to PIPs, including PI3P (*e.g.* SNX1 and SNX3), and induce and stabilize membrane curvature, allowing early endosome tubulation and recycling of proteins back to the plasma membrane or to the *trans*-Golgi network (Zhong et al. 2005; Carlton et al. 2004). Selection of cargo to be retrieved from endosomes is performed by retromer, a trimeric core of Vps26-Vps29-Vps35, that binds the tubulation machinery and thus indirectly depends on PI3P (Cullen and Korswagen 2011; Small and Petsko 2015). Moreover, PI3P is central to the recruitment of the homotypic fusion and protein sorting (HOPS) complex that triggers the molecular switch between Rab GTPases Rab5 and Rab7, driving early to late endosome conversion (Rink et al. 2005; Poteryaev et al. 2010). In late endosomes, cargo is sorted to ILVs, a morphological trait of this compartment. Not only has PI3P been detected in these vesicles but it is also required for the recruitment of early effectors of the ESCRT pathway (Gillooly et al. 2000). This pathway is implicated in the degradation of ubiquitinated cargo proteins and membrane lipids by inducing budding of the limiting endosomal membrane into the lumen of the MVE. Indeed, heterodimer ESCRT-0, containing the FYVE-domain protein Hrs [also commonly used as a PI3P reporter (Di Paolo and De Camilli 2006)], binds and concentrates membrane proteins by simultaneously binding PI3P and ubiquitin residues.

The recruitment of the following ESCRT-I, -II and -III complexes mediates invagination and scission of mature ILVs (Schmidt and Teis 2012). Supporting an important role for PI3P in this pathway, pharmacological inhibition of Vps34 or knockdown of Hrs has a profound effect in the number of ILVs per endosome; however, late endosomes still display ILVs (Petiot et al. 2003; Futter et al. 2001; Bache et al. 2003). In fact, ILV formation can be found even in the absence of all ESCRT complexes and is thus not exclusive of the PI3P/ESCRT pathway (Stuffers et al. 2009). Overexpression of SNX3, a PI3P interacting protein partner, may bypass ESCRT-deficiency, but PI3P-independent mechanisms have also been proposed, involving tetraspanins, BMP and ceramides (Pons et al. 2008; Matsuo et al. 2004; Trajkovic et al. 2008).

PI3P has also been intrinsically implicated in distinct steps of autophagy, including phagophore nucleation, expansion and fusion with lysosomes (Dall'Armi, Devereaux, and Di Paolo 2013). Autophagy initiation requires the activation of the ULK1 complex by phosphorylation and translocation to the autophagy initiation site (Hurley and Young 2017). An important substrate of ULK1 kinase is the Vps34 Complex I that locally synthesizes PI3P in the pre-autophagosomal site. However, Vps34 function may require additional modulation by post-translational modifications, such as phosphorylation or ubiquitination, that mediate stability of the complex and interaction with autophagy regulators (*e.g.*, AMBRA1, VMP1 and NBRF2) (Furuya et al. 2010; Liu et al. 2011; Nascimbeni, Codogno, and Morel 2017). Next, most models suggest that PI3P acts as a membrane platform for protein effectors containing PI3P-binding domains, including DFCP1 and members of the WIPI family (Nascimbeni, Codogno, and Morel 2017). Specifically, WIPI2 recruits the autophagy-related gene (Atg) triad ATG12-Atg5-Atg16L1 that mediates LC3 lipidation and hence autophagosome expansion (Dooley et al. 2014). Alfy is another FYVE-domain containing protein that acts as a scaffold and bridges ubiquitinated protein aggregates and growing autophagosomes (Filimonenko et al. 2010). In addition to autophagosome biogenesis, PI3P may also play a role in later stages of autophagy, including autophagosome fusion to endosomes (amphisome) and lysosomes (autolysosomes) through mediation of tethering and fusion events (Klionsky, Eskelinen, and Deretic 2014). While KIF16b regulates early endosome transportation via microtubules, FYCO1 interacts with LC3, Rab7 and PI3P and mediates trafficking of amphisomes (Pankiv et al. 2010). Finally, efficient turnover of PI3P is also required. PI3P is the main substrate for PI(3,5)P₂ synthesis by Pikfyve and inhibition of this phosphorylation step causes accumulation of autophagosomes and autophagy substrates, suggesting impairment of late stages of autophagy, in addition to more global changes in the morphology of endolysosomes (Ferguson, Lenk, and Meisler 2009; de Lartigue et al. 2009; Martin et al. 2013).

Importantly, autophagy is also mediated by dephosphorylation of PI3P by myotubularins MTMR3 and MTMR14 (Jumpy), regulating size and autophagosome initiation (Vergne et al. 2009; Taguchi-Atarashi et al. 2010).

The timely production of PI3P is required for critical steps in endosomal traffic and lysosomal degradation. The identification and characterization of these events is particularly challenging considering the transient nature of endosomal PI3P pools and the recruitment of a myriad of PI3P-binding proteins. Yet, a better understanding of these cellular events is of high therapeutic relevance as dysfunctional endolysosomal and autophagy pathways are a common pathogenic hallmark of many neurodegenerative disorders. Consequently, correction of these defects may be beneficial to maintain cellular homeostasis and prevent accumulation of toxic material associated with neurodegenerative disorders (Sharma et al. 2018).

1.5 Lysosomal storage disorders and neurodegeneration

LSDs are rare inherited metabolic disorders caused by mutations in genes related to endolysosomal function, where a common histological hallmark is accumulation of lysosomal substrates, hence the concept of storage disorder. In most cases, the biochemical nature of the storage material is tightly linked to the genetic cause of the disease, prompting experts in the field to initially classify primary LSDs based on the the type of storage material. Decreased expression levels, instability or reduced functionality of the affected lysosomal enzymes determine the severity of metabolic impairment (Boustany 2013).

The degradative function of lysosomes depends on adequate and timely interaction between hydrolases and substrate, which is in turn regulated by post-translational modifications and maturations of enzymes as well as vesicular trafficking (Braulke and Bonifacino 2009; Pols et al. 2013). Maintenance of lysosomal integrity, homo- and heterotypic endolysosomal fusion and lumen acidification are therefore all essential aspects required for proper enzymatic activity (Saftig and Klumperman 2009). Recent progress in molecular genetics have implicated genes other than those encoding lysosomal enzymes in abnormal storage of lysosomal material (Platt, Boland, and van der Spoel 2012). Disorders classified as secondary LSDs are associated with mutation in genes encoding various proteins, including lysosomal transporters, hydrolase activators or lysosomal ion channels that collectively disrupt vesicular traffic, ion homeostasis, proton gradients, triggering pathological cascades leading to intralysosomal substrate accumulation (Settembre et al. 2013). In addition to the metabolic defects, downstream events drive widespread cellular dysfunction and potentially cell death,

causing inflammation and degeneration in peripheral tissues and in some cases, the brain. This common pathological cascade in both primary and secondary LSDs has prompted the need to develop holistic therapeutic approaches of potentially broad application (Platt 2018; Parenti, Andria, and Ballabio 2015).

The early onset of neurological symptoms and aggressive progression of neuronal dysfunction in LSDs suggest that neurons are particularly susceptible to endolysosomal defects. In fact, several neurodegenerative diseases share similar histological findings and pathogenic mechanisms with LSDs, implicating defects in the endolysosomal system in their etiology. The loss of ability to divide through mitosis decreases the ability of neurons to alleviate the storage burden while their axonal and dendritic polarization requires transport of significant volumes of membranes and cytosolic content to fulfill their high physiologic demands. Thus, interference with the dynamic and efficient maturation and transport of endolysosomal organelles invariably leads to dystrophic swelling and accumulation of lysosomal substrates, either within the endolysosomal compartment itself (*e.g.*, glycosphingolipids), in the cytoplasm (*e.g.*, tau, α -synuclein, ubiquitin inclusions) or in the extracellular environment (*e.g.*, amyloid plaques) (Nixon 2013; Platt 2014; Settembre et al. 2013). Altogether, the analogy between neurodegenerative disorders and LSDs highlights the importance of understanding key aspects of endolysosomal homeostasis and value these rare metabolic disorders as study models of great potential for the understanding of pathogenic cascades and identification of new candidate therapeutic targets (Platt 2018).

In addition to the histological hallmarks, the causal relationship between endolysosomal dysfunction and neurodegeneration is supported by genetics, in which homozygous carriers of certain gene mutations develop LSDs (*e.g.*, *GBA* and *GRM*), while heterozygous carriers for the same mutations have instead a much greater risk of developing late-onset neurodegenerative diseases, such as Parkinson's disease (PD) and frontotemporal dementia (FTD), respectively (Abeliovich and Gitler 2016; Kao et al. 2017). Additional mutations in a variety of genes involved in the control of endolysosomal function have also been shown to cause autosomal dominant familial PD (*e.g.*, *LRKK2*) or some forms of parkinsonism (*e.g.*, *VPS35*, *SYNJ1*, *ATP13A2*) (Abeliovich and Gitler 2016; Clague and Rochin 2016).

In Alzheimer's disease (AD), familial dominant mutations in the genes encoding APP and presenilin-1 (PSEN1) and -2 (PSEN2), which either affect the substrate or the proteases generating A β , respectively, collectively lead to increased extracellular A β deposition and plaque formation (Selkoe and Hardy 2016). These observations led to the dominant "amyloid cascade hypothesis", in

which increased production of aggregate-prone A β species induces severe synaptotoxicity and is ultimately responsible for tau pathology, neuronal loss and cognitive impairment (Karran, Mercken, and Strooper 2011; Selkoe and Hardy 2016). Despite the tight link between A β metabolism and familial early-onset forms of the disease, the vast majority of cases are sporadic and late-onset (LOAD), in which amyloid plaques poorly correlate with cognitive decline [unlike other indicators, including neurofibrillary tangles (Braak et al. 2006)]. This has led to a major effort in identifying new genetic risk *loci* for LOAD. After the historical identification of *APOE4* as the main genetic risk factor for LOAD by Roses and colleagues in the early 90's, recent genome-wide association studies confirmed *APOE4* as the main hit, but also identified different new candidate genes associated with high risk for AD, many of which involved in the regulation of endolysosomal function, lipid metabolism and innate immunity (Lambert et al. 2013; Van Cauwenberghe, Van Broeckhoven, and Sleegers 2016). The implication of *ApoE4*, the major risk *loci* detected, and *ABCA7* supports a role of lipids in AD risk, which is strengthened by the effects of cholesterol metabolism on A β pathology (Djelti et al. 2015; Di Paolo and Kim 2011). Another set of genes mapped are intrinsically related to endosomal traffic (e.g., *SORL1*, *BIN1*, *PICALM*, and *CD2AP*). Interestingly, primary alterations in these genes induce early endosomal enlargement and may mediate events upstream of APP processing and A β pathology (Small et al. 2017). Indeed, several lines of evidence suggest a parallelism between the disruption of the endolysosomal system seen in the context of AD and LSDs. Endocytic anomalies have been proposed as the earliest cellular phenotype in AD, long before onset A β plaque assembly and symptomatology, which may thus contribute to amyloidogenic processing of APP, which in turn feeds a positive feedback loop to perpetuate imbalances in the endocytic pathway (Rajendran and Annaert 2012; Nixon 2017; Nixon 2013). Altogether, these observations suggest that, in addition to A β -lowering therapies, enhancement of endosomal traffic and prevention of *jammed* enlarged endosomes are an emerging goal in the context of AD, similarly to enhancing lysosomal and autophagic clearance in LSDs (Small et al. 2017; Sharma et al. 2018). In this line, phosphoinositides are promising targets as fundamental drivers of endosomal sorting and maturation.

1.5.1 PI3P and neurodegeneration

The growing implication of endosomal anomalies in neurodegeneration has prompted a great interest in the molecular machinery regulating endosomal traffic. As previously mentioned, PI3P is a master regulator of both endosomal and autophagy pathways, mediating a variety of critical processes, such as endosomal fusion, ILV budding, endosomal motility as well as biogenesis and

maturation of autophagosomes (Dall'Armi, Devereaux, and Di Paolo 2013; Schink, Tan, and Stenmark 2016). In line with the consensus that neuronal cells are particularly susceptible to endolysosomal defects, the PI3P/PI(3,5)P₂ has been extensively implicated in neurodegeneration. First, postnatal neuronal conditional knock-out of *Pik3c3* (gene encoding Vps34) in mice causes progressive synaptic loss followed by extensive gliosis and neurodegeneration (Wang, Budolfson, and Wang 2011; Zhou et al. 2010). In humans, a truncation in *Pik3c3* and a mutation in *PIK3R4* (encoding Vps15) cause severe cortical atrophy and deep learning disabilities (Inaguma et al. 2016; Gstrein et al. 2018). Additionally, genetic ablation of *PIKfyve* and interacting partners *Fig4* or *Vac14* causes spongiform neurodegeneration in mice (Zolov et al. 2012; Zhang et al. 2007; Chow et al. 2007). In humans, mutations in *FIG4* and *VAC14* have also been genetically linked to Amyotrophic Lateral Sclerosis, Charcot-Marie-Tooth Type 4J and PD (Mccartney, Zhang, and Weisman 2014; Taghavi et al. 2017). Moreover, a recent study from our group reported that PI3P is selectively deficient in the brain of patients with AD and mouse models thereof (Morel et al. 2013). Remarkably, silencing Vps34 in primary neurons was shown to cause early endosomal anomalies and altered sorting and amyloidogenic processing of APP, both of which are important pathological features of AD (Morel et al. 2013; R.A. Nixon 2013). Overall, these studies implicate dysregulation of the PI3P pathway and associated endolysosomal perturbation in neurodegeneration.

Aims

The growing association of endolysosomal defects in the pathogenesis of neurodegenerative diseases highlights the importance of the study of basic cellular mechanisms such as endosomal traffic and autophagy for a better understanding of the events driving disease onset and progression. PIPs, particularly PI3P, regulate fundamental aspects of membrane trafficking previously linked to neurodegeneration and are thus promising experimental models for the identification of cellular and molecular pathways of diagnostic or therapeutic value.

The main goal of the present thesis is to understand the role of endolysosomal dysfunction, particularly mediated by lipid dysregulation, in the pathogenesis of neurodegenerative disorders. The specific aims of this project are:

- **To characterize the impact of phosphatidylinositol-3-phosphate deficiency in endolysosomal function *in vitro* and *in vivo*;**
- **To investigate the impact of endolysosomal dysfunction in exosome secretion;**
- **To study the lipid composition of the brain and relationship with regional susceptibility to neurodegenerative disorders.**

REFERENCES

- Abeliovich, Asa, and Aaron D Gitler. 2016. "Defects in Trafficking Bridge Parkinson's Disease Pathology and Genetics." *Nature* 539 (7628): 207–16. doi:10.1038/nature20414.
- Bache, Kristi G., Andreas Brech, Anja Mehlum, and Harald Stenmark. 2003. "Hrs Regulates Multivesicular Body Formation via ESCRT Recruitment to Endosomes." *Journal of Cell Biology* 162 (3): 435–42. doi:10.1083/jcb.200302131.
- Backer, J. M. 2016. "The Intricate Regulation and Complex Functions of the Class III Phosphoinositide 3-Kinase Vps34." *Biochemical Journal* 473 (15): 2251–71. doi:10.1042/BCJ20160170.
- Baietti, Maria Francesca, Zhe Zhang, Eva Mortier, Aurélie Melchior, Gisèle Degeest, Annelies Geeraerts, Ylva Ivarsson, et al. 2012. "Syndecan–syntenin–ALIX Regulates the Biogenesis of Exosomes." *Nature Cell Biology* 14 (7): 677–85. doi:10.1038/ncb2502.
- Bento, Carla F., Maurizio Renna, Ghita Ghislat, Claudia Puri, Avraham Ashkenazi, Mariella Vicinanza, Fiona M. Menzies, and David C. Rubinsztein. 2016. "Mammalian Autophagy: How Does It Work?" *Annual Review of Biochemistry* 85 (1): 685–713. doi:10.1146/annurev-biochem-060815-014556.
- Bissig, Christin, and Jean Gruenberg. 2013. "Lipid Sorting and Multivesicular Endosome Biogenesis." *Cold Spring Harbor Perspectives in Biology*. Cold Spring Harbor Laboratory Press. doi:10.1101/cshperspect.a016816.
- Boustany, Rose-Mary Naaman. 2013. "Lysosomal Storage Diseases—the Horizon Expands." *Nature Publishing Group* 9 (10). doi:10.1038/nrneurol.2013.163.
- Braak, Heiko, Irina Alafuzoff, Thomas Arzberger, Hans Kretschmar, and Kelly Del Tredici. 2006. "Staging of Alzheimer Disease-Associated Neurofibrillary Pathology Using Paraffin Sections and Immunocytochemistry." *Acta Neuropathologica* 112 (4): 389–404. doi:10.1007/s00401-006-0127-z.
- Braulke, Thomas, and Juan S. Bonifacino. 2009. "Sorting of Lysosomal Proteins." *Biochimica et Biophysica Acta (BBA) - Molecular Cell Research* 1793 (4). Elsevier: 605–14. <https://www.sciencedirect.com/science/article/pii/S0167488908003716>.
- Carlton, Jez, Miriam Bujny, Brian J. Peter, Viola M.J. Oorschot, Anna Rutherford, Harry Mellor, Judith Klumperman, Harvey T. McMahon, and Peter J. Cullen. 2004. "Sorting Nexin-1 Mediates Tubular Endosome-to-TGN Transport through Coincidence Sensing of High-Curvature Membranes and 3-Phosphoinositides." *Current Biology* 14 (20): 1791–1800. doi:10.1016/j.cub.2004.09.077.
- Chang, Ta-Yuan, Catherine C Y Chang, Nobutaka Ohgami, and Yoshio Yamauchi. 2006. "Cholesterol Sensing, Trafficking, and Esterification." *Annual Review of Cell and Developmental Biology* 22: 129–57. doi:10.1146/annurev.cellbio.22.010305.104656.
- Chivet, Mathilde, Charlotte Javalet, Karine Laulagnier, Béatrice Blot, Fiona J Hemming, and Rémy Sadoul. 2014. "Exosomes Secreted by Cortical Neurons upon Glutamatergic Synapse Activation Specifically Interact with Neurons." *Journal of Extracellular Vesicles* 3: 24722. <http://www.ncbi.nlm.nih.gov/pubmed/25398455>.
- Chow, Clement Y., Yanling Zhang, James J. Dowling, Natsuko Jin, Maja Adamska, Kensuke Shiga, Kinga Szigeti, et al. 2007. "Mutation of FIG4 Causes Neurodegeneration in the Pale Tremor Mouse and Patients with CMT4J." *Nature* 448 (7149): 68–72. doi:10.1038/nature05876.
- Christoforidis, Savvas, Heidi M. McBride, Robert D. Burgoyne, and Marino Zerial. 1999. "The Rab5 Effector EEA1 Is a Core Component of Endosome Docking." *Nature* 397 (6720): 621–25. doi:10.1038/17618.
- Clague, Michael J., and Leila Rochin. 2016. "Parkinson's Disease: A Traffic Jam?" *Current Biology* 26 (8). Elsevier Ltd: R332–34. doi:10.1016/j.cub.2016.03.001.
- Cocucci, Emanuele, François Aguet, Steeve Boulant, and Tom Kirchhausen. 2012. "The First Five Seconds in the Life of a Clathrin-Coated Pit." *Cell* 150 (3): 495–507. doi:10.1016/j.cell.2012.05.047.
- Cocucci, Emanuele, and Jacopo Meldolesi. 2015. "Ectosomes and Exosomes: Shedding the Confusion between Extracellular Vesicles." *Trends in Cell Biology* 25: 364–72. doi:10.1016/j.tcb.2015.01.004.
- Coleman, Bradley M., and Andrew F. Hill. 2015. "Extracellular Vesicles – Their Role in the Packaging and Spread of Misfolded Proteins Associated with Neurodegenerative Diseases." *Seminars in Cell & Developmental Biology* 40 (April). Academic Press: 89–96. doi:10.1016/J.SEMCDB.2015.02.007.
- Colombo, Marina, Catarina Moita, Guillaume van Niel, Joanna Kowal, James Vigneron, Philippe Benaroch, Nicolas Manel, Luis F Moita, Clotilde Théry, and Graça Raposo. 2013. "Analysis of ESCRT Functions in Exosome Biogenesis, Composition and Secretion Highlights the Heterogeneity of Extracellular Vesicles." *Journal of Cell Science* 126 (24): 5553–65. doi:10.1242/jcs.128868.
- Cuervo, Ana Maria, and Esther Wong. 2013. "Chaperone-Mediated Autophagy: Roles in Disease and Aging." *Nature Publishing Group* 24 (24): 92–104. doi:10.1038/cr.2013.153.
- Cullen, Peter J, and Hendrik C Korswagen. 2011. "Sorting Nexins Provide Diversity for Retromer-Dependent Trafficking Events." *Nature Cell Biology* 14 (1). Europe PMC Funders: 29–37. doi:10.1038/ncb2374.
- Dall'Armi, Claudia, Kelly a Devereaux, and Gilbert Di Paolo. 2013. "The Role of Lipids in the Control of Autophagy." *Current Biology* : CB 23 (1). Elsevier Ltd: R33-45. doi:10.1016/j.cub.2012.10.041.

- de Lartigue, Jane, Hannah Polson, Morri Feldman, Kevan Shokat, Sharon a. Tooze, Sylvie Urbé, and Michael J. Clague. 2009. "PIKfyve Regulation of Endosome-Linked Pathways." *Traffic* 10 (7): 883–93. doi:10.1111/j.1600-0854.2009.00915.x.
- Devereaux, Kelly, Claudia Dall'Armi, Abel Alcazar-Roman, Yuta Ogasawara, Xiang Zhou, Fan Wang, Akitsugu Yamamoto, Pietro de Camilli, and Gilbert Di Paolo. 2013. "Regulation of Mammalian Autophagy by Class II and III PI 3-Kinases through PI3P Synthesis." *PLoS ONE* 8 (10): 10–12. doi:10.1371/journal.pone.0076405.
- Di Fiore, P. P., and M. von Zastrow. 2014. "Endocytosis, Signaling, and Beyond." *Cold Spring Harbor Perspectives in Biology* 6 (8): a016865–a016865. doi:10.1101/cshperspect.a016865.
- Di Paolo, Gilbert, and Pietro De Camilli. 2006. "Phosphoinositides in Cell Regulation and Membrane Dynamics." *Nature* 443 (7112): 651–57. doi:10.1038/nature05185.
- Di Paolo, Gilbert, and Tae-Wan Kim. 2011. "Linking Lipids to Alzheimer's Disease: Cholesterol and Beyond." *Nature Reviews. Neuroscience* 12 (5). Nature Publishing Group: 284–96. doi:10.1038/nrn3012.
- Djelti, Fathia, Jerome Braudeau, Eloise Hudry, Marc Dhenain, Jennifer Varin, Ivan Bièche, Catherine Marquer, et al. 2015. "CYP46A1 Inhibition, Brain Cholesterol Accumulation and Neurodegeneration Pave the Way for Alzheimer's Disease." *Brain*, awv166. doi:10.1093/brain/awv166.
- Dooley, Hannah C., Minoo Razi, Hannah E.J. Polson, Stephen E. Girardin, Michael I. Wilson, and Sharon A. Tooze. 2014. "WIP1 Links LC3 Conjugation with PI3P, Autophagosome Formation, and Pathogen Clearance by Recruiting Atg12–5–16L1." *Molecular Cell* 55 (2). Cell Press: 238–52. doi:10.1016/J.MOLCEL.2014.05.021.
- Edgar, James R., Emily R. Eden, and Clare E. Futter. 2014. "Hrs- and CD63-Dependent Competing Mechanisms Make Different Sized Endosomal Intraluminal Vesicles." *Traffic* 15 (2). John Wiley & Sons A/S: 197–211. doi:10.1111/tra.12139.
- Fahy, Eoin, Shankar Subramaniam, H Alex Brown, Christopher K Glass, Alfred H Merrill, Robert C Murphy, Christian R H Raetz, et al. 2005. "A Comprehensive Classification System for Lipids." *Journal of Lipid Research* 46 (5): 839–61. doi:10.1194/jlr.E400004-JLR200.
- Ferguson, Cole J., Guy M. Lenk, and Miriam H. Meisler. 2009. "Defective Autophagy in Neurons and Astrocytes from Mice Deficient in PI(3,5)P2." *Human Molecular Genetics* 18 (24). Oxford University Press: 4868–78. doi:10.1093/hmg/ddp460.
- Filimonenko, Maria, Pauline Isakson, Kim D. Finley, Monique Anderson, Hyun Jeong, Thomas J. Melia, Bryan J. Bartlett, et al. 2010. "The Selective Macroautophagic Degradation of Aggregated Proteins Requires the PI3P-Binding Protein Alfy." *Molecular Cell* 38 (2). Cell Press: 265–79. doi:10.1016/J.MOLCEL.2010.04.007.
- Furuya, Tsuyoshi, Minsu Kim, Marta Lipinski, Juying Li, Dohoon Kim, Tao Lu, Yong Shen, et al. 2010. "Negative Regulation of Vps34 by Cdk Mediated Phosphorylation." *Molecular Cell* 38 (4): 500–511. doi:10.1016/j.molcel.2010.05.009.
- Futter, C. E., L. M. Collinson, J. M. Backer, and C. R. Hopkins. 2001. "Human VPS34 Is Required for Internal Vesicle Formation within Multivesicular Endosomes." *Journal of Cell Biology* 155 (7). Rockefeller University Press: 1251–63. doi:10.1083/jcb.200108152.
- Galluzzi, Lorenzo, Eric H Baehrecke, Andrea Ballabio, Patricia Boya, José Manuel Bravo-San Pedro, Francesco Cecconi, Augustine M Choi, et al. 2017. "Molecular Definitions of Autophagy and Related Processes." *The EMBO Journal*, e201796697. doi:10.15252/embj.201796697.
- Galluzzi, Lorenzo, José Manuel Bravo-San Pedro, Klas Blomgren, and Guido Kroemer. 2016. "Autophagy in Acute Brain Injury." *Nature Reviews Neuroscience* 17 (8). Nature Publishing Group: 467–84. doi:10.1038/nrn.2016.51.
- Ghossoub, Rania, Frédérique Lembo, Aude Rubio, Carole Baron Gaillard, Jérôme Bouchet, Nicolas Vitale, Josef Slavik, Miroslav Machala, and Pascale Zimmermann. 2014. "Syntenin-ALIX Exosome Biogenesis and Budding into Multivesicular Bodies Are Controlled by ARF6 and PLD2." *Nature Communications* 5 (January): 3477. doi:10.1038/ncomms4477.
- Gillooly, D. J., I C Morrow, M Lindsay, R Gould, N J Bryant, J M Gaullier, R G Parton, and H Stenmark. 2000. "Localization of Phosphatidylinositol 3-Phosphate in Yeast and Mammalian Cells." *The EMBO Journal* 19 (17): 4577–88. doi:10.1093/emboj/19.17.4577.
- Gstrein, Thomas, Andrew Edwards, Anna Přistoupilová, Ines Leca, Martin Breuss, Sandra Pilat-Carotta, Andi H. Hansen, et al. 2018. "Mutations in Vps15 Perturb Neuronal Migration in Mice and Are Associated with Neurodevelopmental Disease in Humans." *Nature Neuroscience* 21 (February). Springer US. doi:10.1038/s41593-017-0053-5.
- Hammond, Gerald R.V., and Tamas Balla. 2015. "Polyphosphoinositide Binding Domains: Key to Inositol Lipid Biology." *Biochimica et Biophysica Acta (BBA) - Molecular and Cell Biology of Lipids* 1851 (6). Elsevier B.V.: 746–58. doi:10.1016/j.bbalip.2015.02.013.
- Hannun, Yusuf A., and Lina M. Obeid. 2017. "Sphingolipids and Their Metabolism in Physiology and Disease." *Nature Reviews Molecular Cell Biology*. Nature Publishing Group. doi:10.1038/nrm.2017.107.
- Hannun, Yusuf a, and Lina M Obeid. 2008. "Principles of Bioactive Lipid Signalling: Lessons from Sphingolipids." *Nature Reviews. Molecular Cell Biology* 9 (2): 139–50. doi:10.1038/nrm2329.
- Harayama, Takeshi, and Howard Riezman. 2018. "Understanding the Diversity of Membrane Lipid Composition." *Nature*

- Reviews Molecular Cell Biology, February. Nature Publishing Group. doi:10.1038/nrm.2017.138.
- He, Kangmin, Robert Marsland Iii, Srigokul Upadhyayula, Eli Song, Song Dang, Benjamin R Capraro, Weiming Wang, et al. 2017. "Dynamics of Phosphoinositide Conversion in Clathrin-Mediated Endocytic Traffic." Nature Publishing Group 552. doi:10.1038/nature25146.
- Hessvik, Nina Pettersen, Anders Øverbye, Andreas Brech, Maria Lyngaas Torgersen, Ida Seim Jakobsen, Kirsten Sandvig, and Alicia Llorente. 2016. "PIKfyve Inhibition Increases Exosome Release and Induces Secretory Autophagy." Cellular and Molecular Life Sciences. Springer International Publishing. doi:10.1007/s00018-016-2309-8.
- Ho, Cheuk Y., Tamadher A. Alghamdi, and Roberto J. Botelho. 2012. "Phosphatidylinositol-3,5-Bisphosphate: No Longer the Poor PIP 2." Traffic. Blackwell Publishing Ltd. doi:10.1111/j.1600-0854.2011.01246.x.
- Hoepfner, Sebastian, Fedor Severin, Alicia Cabezas, Bianca Habermann, Anja Runge, David Gillyooly, Harald Stenmark, and Marino Zerial. 2005. "Modulation of Receptor Recycling and Degradation by the Endosomal Kinesin KIF16B." Cell 121 (3): 437–50. doi:10.1016/j.cell.2005.02.017.
- Holthuis, Joost C M, and Anant K Menon. 2014. "Lipid Landscapes and Pipelines in Membrane Homeostasis." Nature 510 (7503): 48–57. doi:10.1038/nature13474.
- Huotari, Jatta, and Ari Helenius. 2011. "Endosome Maturation." The EMBO Journal 30 (17). European Molecular Biology Organization: 3481–3500. doi:10.1038/emboj.2011.286.
- Hurley, James H, and Lindsey N Young. 2017. "Mechanisms of Autophagy Initiation." Annu. Rev. Biochem 86: 225–44. doi:10.1146/annurev-biochem.
- Inaguma, Yutaka, Ayumi Matsumoto, Mariko Noda, Hidenori Tabata, Akihiko Maeda, Masahide Goto, Daisuke Usui, et al. 2016. "Role of Class III Phosphoinositide 3-Kinase in the Brain Development: Possible Involvement in Specific Learning Disorders." Journal of Neurochemistry 139 (2): 245–55. doi:10.1111/jnc.13832.
- Itakura, Eisuke, Chieko Kishi, Kinji Inoue, and Noboru Mizushima. 2008. "Beclin 1 Forms Two Distinct Phosphatidylinositol 3-Kinase Complexes with Mammalian Atg14 and UVRAG." Molecular Biology of the Cell 19 (12). American Society for Cell Biology: 5360–72. doi:10.1091/mbc.E08-01-0080.
- Jean, Steve, and Amy A. Kiger. 2012. "Coordination between RAB GTPase and Phosphoinositide Regulation and Functions." Nature Reviews Molecular Cell Biology. doi:10.1038/nrm3379.
- Kao, Aimee W, Andrew Mckay, Param Priya Singh, Anne Brunet, and Eric J Huang. 2017. "Progranulin, Lysosomal Regulation and Neurodegenerative Disease." Nature Reviews Neuroscience 18: 325–333.
- Karran, Eric, Marc Mercken, and Bart De Strooper. 2011. "The Amyloid Cascade Hypothesis for Alzheimer's Disease: An Appraisal for the Development of Therapeutics." Nature Reviews. Drug Discovery 10 (September). Nature Publishing Group: 698–712. doi:10.1038/nrd3505.
- Ketel, Katharina, Michael Krauss, Anne-Sophie Nicot, Dmytro Puchkov, Marnix Wieffer, Rainer Müller, Devaraj Subramanian, Carsten Schultz, Jocelyn Laporte, and Volker Haucke. 2016. "A Phosphoinositide Conversion Mechanism for Exit from Endosomes." Nature 529 (7586). Nature Publishing Group: 408–12. doi:10.1038/nature16516.
- Klionsky, Daniel J, Eeva Liisa Eskelinen, and Vojo Deretic. 2014. "Autophagosomes, Phagosomes, Autolysosomes, Phagolysosomes, Autophagolysosomes... Wait, I'm Confused." Autophagy. Taylor & Francis. doi:10.4161/auto.28448.
- Klose, Christian, Michal a. Surma, and Kai Simons. 2013. "Organellar Lipidomics-Background and Perspectives." Current Opinion in Cell Biology 25 (4). Elsevier Ltd: 406–13. doi:10.1016/j.ceb.2013.03.005.
- Klumperman, Judith, and Graça Raposo. 2014. "The Complex Ultrastructure of the Endolysosomal System." Cold Spring Harbor Perspectives in Biology 6 (10). Cold Spring Harbor Laboratory Press: a016857. doi:10.1101/cshperspect.a016857.
- Kobayashi, T, M H Beuchat, M Lindsay, S Frias, R D Palmiter, H Sakuraba, R G Parton, and J Gruenberg. 1999. "Late Endosomal Membranes Rich in Lysobisphosphatidic Acid Regulate Cholesterol Transport." Nature Cell Biology 1 (2): 113–18. doi:10.1038/10084.
- Kowal, Joanna, Guillaume Arras, Marina Colombo, Mabel Jouve, Jakob Paul Morath, Bjarke Primdal-Bengtson, Florent Dingli, Damaris Loew, Mercedes Tkach, and Clotilde Théry. 2016. "Proteomic Comparison Defines Novel Markers to Characterize Heterogeneous Populations of Extracellular Vesicle Subtypes." Proceedings of the National Academy of Sciences 113 (8): E968–77. doi:10.1073/pnas.1521230113.
- Lamb, Christopher A., Tamotsu Yoshimori, and Sharon A. Tooze. 2013. "The Autophagosome: Origins Unknown, Biogenesis Complex." Nature Reviews Molecular Cell Biology 14 (12). Nature Publishing Group: 759–74. doi:10.1038/nrm3696.
- Lambert, Jean-Charles, Carla A Ibrahim-Verbaas, Denise Harold, Adam C Naj, Rebecca Sims, Celine Bellenguez, Gyungah Jun, et al. 2013. "Meta-Analysis of 74,046 Individuals Identifies 11 New Susceptibility Loci for Alzheimer's Disease." Nature Genetics 45 (12): 1452–58. doi:10.1038/ng.2802.
- Laulagnier, Karine, Charlotte Javalet, Fiona J. Hemming, Mathilde Chivet, Gaëlle Lachenal, Béatrice Blot, Christine Chatellard, and Rémy Sadoul. 2017. "Amyloid Precursor Protein Products Concentrate in a Subset of Exosomes

- Specifically Endocytosed by Neurons." *Cellular and Molecular Life Sciences*, February 27. doi:10.1007/s00018-017-2664-0.
- Lev, Sima. 2010. "Non-Vesicular Lipid Transport by Lipid-Transfer Proteins and beyond." *Nature Publishing Group* 11 (10). *Nature Publishing Group*: 739–50. doi:10.1038/nrm2971.
- Liu, Junli, Hongguang Xia, Minsu Kim, Lihua Xu, Ying Li, Lihong Zhang, Yu Cai, et al. 2011. "Beclin1 Controls the Levels of p53 by Regulating the Deubiquitination Activity of USP10 and USP13." *Cell* 147 (1): 223–34. doi:10.1016/j.cell.2011.08.037.
- Luzio, J. Paul, Paul R. Pryor, and Nicholas A. Bright. 2007. "Lysosomes: Fusion and Function." *Nature Reviews. Molecular Cell Biology* 8 (8): 622–32. doi:10.1038/nrm2217.
- Luzio, J Paul, Yvonne Hackmann, Nele M G Dieckmann, and Gillian M Griffiths. 2014. "The Biogenesis of Lysosomes and Lysosome-Related Organelles." *Cold Spring Harbor Perspectives in Biology* 6 (9): a016840–a016840. doi:10.1101/cshperspect.a016840.
- Marks, Michael S, Harry FG Heijnen, and Graça Raposo. 2013. "Lysosome-Related Organelles: Unusual Compartments Become Mainstream." *Current Opinion in Cell Biology* 25 (4): 495–505. doi:10.1016/j.ccb.2013.04.008.
- Martin, Sally, Callista B. Harper, Linda M. May, Elizabeth J. Coulson, Frederic a. Meunier, and Shona L. Osborne. 2013. "Inhibition of PIKfyve by YM-201636 Dysregulates Autophagy and Leads to Apoptosis-Independent Neuronal Cell Death." *PLoS ONE* 8 (3). doi:10.1371/journal.pone.0060152.
- Matsuo, Hirokami, Julien Chevallier, Nathalie Mayran, Isabelle Le Blanc, Charles Ferguson, Julien Fauré, Nathalie Sartori Blanc, et al. 2004. "Role of LBPA and Alix in Multivesicular Liposome Formation and Endosome Organization." *Science* 303 (5657): 531–34. doi:10.1126/science.1092425.
- Maxfield, Frederick R., and Sushmita Mukherjee. 2004. "The Endosomal–lysosomal System." In *Lysosomal Disorders of the Brain*, 3–31. Oxford University Press. doi:10.1093/acprof:oso/9780198508786.003.0001.
- Mccartney, Amber J., Yanling Zhang, and Lois S. Weisman. 2014. "Phosphatidylinositol 3,5-Bisphosphate: Low Abundance, High Significance." *BioEssays* 36 (1): 52–64. doi:10.1002/bies.201300012.
- Miranda, André Miguel, and Tiago Gil Oliveira. 2015. "Lipids under Stress - a Lipidomic Approach for the Study of Mood Disorders." *BioEssays* 37 (11): 1226–35. doi:10.1002/bies.201500070.
- Möbius, W, E. van Donselaar, Y. Ohno-Iwashita, Y. Shimada, H. F. G. Heijnen, J. W. Slot, and H. J. Geuze. 2003. "Recycling Compartments and the Internal Vesicles of Multivesicular Bodies Harbor Most of the Cholesterol Found in the Endocytic Pathway." *Traffic (Copenhagen, Denmark)* 4 (1). Munksgaard International Publishers: 222–31. doi:072 [pii].
- Morad, Samy A.F., and Myles C. Cabot. 2013. "Ceramide-Orchestrated Signalling in Cancer Cells." *Nature Reviews Cancer* 13 (1): 51–65. doi:10.1038/nrc3398.
- Morel, Etienne, Zeina Chamoun, Zofia M Lasiacka, Robin B Chan, Rebecca L Williamson, Christopher Vetanovetz, Claudia Dall'Armi, et al. 2013. "Phosphatidylinositol-3-Phosphate Regulates Sorting and Processing of Amyloid Precursor Protein through the Endosomal System." *Nature Communications* 4 (January): 2250. doi:10.1038/ncomms3250.
- Mouritsen, Ole G. 2011. "Model Answers to Lipid Membrane Questions." *Cold Spring Harbor Perspectives in Biology* 3 (9): 1–15. doi:10.1101/cshperspect.a004622.
- Murray, David H., Marcus Jahnel, Janelle Lauer, Mario J. Avellaneda, Nicolas Brouilly, Alice Cezanne, Hernán Morales-Navarrete, et al. 2016. "An Endosomal Tether Undergoes an Entropic Collapse to Bring Vesicles Together." *Nature* 537 (7618). *Nature Publishing Group*: 107–11. doi:10.1038/nature19326.
- Nascimbeni, Anna Chiara, Patrice Codogno, and Etienne Morel. 2017. "Phosphatidylinositol-3-Phosphate in the Regulation of Autophagy Membrane Dynamics." *The FEBS Journal* 284 (9): 1267–78. doi:10.1111/febs.13987.
- Nixon, R.A. 2013. "The Role of Autophagy in Neurodegenerative Disease." *Nat Med*. doi:10.1038/nm.3232.
- Nixon, Ralph a. 2013. "The Role of Autophagy in Neurodegenerative Disease." *Nature Medicine* 19 (8). *Nature Publishing Group*: 983–97. doi:10.1038/nm.3232.
- Nixon, Ralph A. 2017. "Amyloid Precursor Protein and Endosomal – Lysosomal Dysfunction in Alzheimer ' S Disease : Inseparable Partners in a Multifactorial Disease." *FASEB Journal : Official Publication of the Federation of American Societies for Experimental Biology* 31 (7): 2729–43. doi:10.1096/fj.201700359.
- Ostrowski, Matias, Nuno B. Carmo, Sophie Krumeich, Isabelle Fanget, Graça Raposo, Ariel Savina, Catarina F. Moita, et al. 2010. "Rab27a and Rab27b Control Different Steps of the Exosome Secretion Pathway." *Nature Cell Biology* 12 (1): 19–30. doi:10.1038/ncb2000.
- Pankiv, Serhiy, Endalkachew A Alemu, Andreas Brech, Jack-Ansgar Bruun, Trond Lamark, Aud Overvatn, Geir Bjørkøy, and Terje Johansen. 2010. "FYCO1 Is a Rab7 Effector That Binds to LC3 and PI3P to Mediate Microtubule plus End-Directed Vesicle Transport." *The Journal of Cell Biology* 188 (2). *Rockefeller University Press*: 253–69. doi:10.1083/jcb.200907015.
- Paradies, Giuseppe, Valeria Paradies, Valentina De Benedictis, Francesca M. Ruggiero, and Giuseppe Petrosillo. 2014. "Functional Role of Cardiolipin in Mitochondrial Bioenergetics." *Biochimica et Biophysica Acta (BBA) - Bioenergetics* 1837 (4). Elsevier: 408–17. doi:10.1016/J.BBABI.2013.10.006.

- Parenti, Giancarlo, Generoso Andria, and Andrea Ballabio. 2015. "Lysosomal Storage Diseases: From Pathophysiology to Therapy." *Annual Review of Medicine* 66 (1): 471–86. doi:10.1146/annurev-med-122313-085916.
- Petiot, A., J. Fauré, H. Stenmark, and J. Gruenberg. 2003. "PI3P Signaling Regulates Receptor Sorting but Not Transport in the Endosomal Pathway." *The Journal of Cell Biology* 162 (6): 971–79. doi:10.1083/jcb.200303018.
- Piomelli, Daniele, Giuseppe Astarita, and Rao Rapaka. 2007. "A Neuroscientist's Guide to Lipidomics." *Nature Reviews. Neuroscience* 8 (10): 743–54. doi:10.1038/nrn2233.
- Platt, Frances M. 2014. "Sphingolipid Lysosomal Storage Disorders." *Nature* 510 (7503): 68–75. doi:10.1038/nature13476.
- Platt, Frances M. 2018. "Emptying the Stores: Lysosomal Diseases and Therapeutic Strategies." *Nature Reviews Drug Discovery* 17 (2): 133–50. doi:10.1038/nrd.2017.214.
- Platt, Frances M, Barry Boland, and Aarnoud C van der Spoel. 2012. "The Cell Biology of Disease: Lysosomal Storage Disorders: The Cellular Impact of Lysosomal Dysfunction." *The Journal of Cell Biology* 199 (5): 723–34. doi:10.1083/jcb.201208152.
- Pols, Maaïke S., and Judith Klumperman. 2009. "Trafficking and Function of the Tetraspanin CD63." *Experimental Cell Research*. doi:10.1016/j.yexcr.2008.09.020.
- Pols, Maaïke S, Eline Van Meel, Viola Oorschot, Corlinda Ten Brink, Minoru Fukuda, M G Swetha, Satyajit Mayor, and Judith Klumperman. 2013. "ARTICLE hVps41 and VAMP7 Function in Direct TGN to Late Endosome Transport of Lysosomal Membrane Proteins." *Nature Communications* 4. doi:10.1038/ncomms2360.
- Pons, Véronique, Pierre-Philippe Luyet, Etienne Morel, Laurence Abrami, F. Gisou van der Goot, Robert G Parton, and Jean Gruenberg. 2008. "Hrs and SNX3 Functions in Sorting and Membrane Invagination within Multivesicular Bodies." Edited by Suzanne Pfeffer. *PLoS Biology* 6 (9): e214. doi:10.1371/journal.pbio.0060214.
- Poteryaev, Dmitry, Sunando Datta, Karin Ackema, Marino Zerial, and Anne Spang. 2010. "Identification of the Switch in Early-to-Late Endosome Transition." *Cell* 141 (3). Elsevier Ltd: 497–508. doi:10.1016/j.cell.2010.03.011.
- Raiborg, Camilla, Kay O Schink, and Harald Stenmark. 2013. "Class III Phosphatidylinositol 3-Kinase and Its Catalytic Product PtdIns3P in Regulation of Endocytic Membrane Traffic." *The FEBS Journal* 280 (12): 2730–42. doi:10.1111/febs.12116.
- Raiborg, Camilla, and Harald Stenmark. 2009. "The ESCRT Machinery in Endosomal Sorting of Ubiquitylated Membrane Proteins." *Nature* 458 (7237): 445–52. doi:10.1038/nature07961.
- Rajendran, Lawrence, and Wim Annaert. 2012. "Membrane Trafficking Pathways in Alzheimer's Disease." *Traffic* 13: 759–70. doi:10.1111/j.1600-0854.2012.01332.x.
- Raposo, Graça, and Willem Stoorvogel. 2013. "Extracellular Vesicles: Exosomes, Microvesicles, and Friends." *Journal of Cell Biology* 200 (4): 373–83. doi:10.1083/jcb.201211138.
- Rink, Jochen, Eric Ghigo, Yannis Kalaidzidis, and Marino Zerial. 2005. "Rab Conversion as a Mechanism of Progression from Early to Late Endosomes." *Cell* 122 (5). Cell Press: 735–49. doi:10.1016/J.CELL.2005.06.043.
- Saftig, Paul, and Judith Klumperman. 2009. "Lysosome Biogenesis and Lysosomal Membrane Proteins: Trafficking Meets Function." *Nature Reviews. Molecular Cell Biology* 10 (9). Nature Publishing Group: 623–35. doi:10.1038/nrm2745.
- Sahu, Ranjit, Susmita Kaushik, Cristina C. Clement, Elvira S. Cannizzo, Brian Scharf, Antonia Follenzi, Ilaria Potolicchio, Edward Nieves, Ana Maria Cuervo, and Laura Santambrogio. 2011. "Microautophagy of Cytosolic Proteins by Late Endosomes." *Developmental Cell* 20 (1). Elsevier: 131–39. doi:10.1016/j.devcel.2010.12.003.
- Schauder, Curtis M, Xudong Wu, Yasunori Saheki, Pradeep Narayanaswamy, Federico Torta, Markus R Wenk, Pietro De Camilli, and Karin M Reinisch. 2014. "Structure of a Lipid-Bound Extended Synaptotagmin Indicates a Role in Lipid Transfer." *Nature* 10(7506). Nature Publishing Group: 552–55. doi:10.1038/nature13269.
- Schink, Kay O., Camilla Raiborg, and Harald Stenmark. 2013. "Phosphatidylinositol 3-Phosphate, a Lipid That Regulates Membrane Dynamics, Protein Sorting and Cell Signalling." *BioEssays* 35 (10): 900–912. doi:10.1002/bies.201300064.
- Schink, Kay O., Kia-Wee Tan, and Harald Stenmark. 2016. "Phosphoinositides in Control of Membrane Dynamics." *Annual Review of Cell and Developmental Biology* 32 (1): 143–71. doi:10.1146/annurev-cellbio-111315-125349.
- Schmidt, Oliver, and David Teis. 2012. "The ESCRT Machinery." *Current Biology* 22 (4). Cell Press: R116–20. doi:10.1016/J.CUB.2012.01.028.
- Selkoe, Dennis J, and John Hardy. 2016. "The Amyloid Hypothesis of Alzheimer's Disease at 25 Years." *EMBO Molecular Medicine* 8 (6): 595–608. doi:10.15252/emmm.201606210.
- Settembre, Carmine, Alessandro Fraldi, Diego L Medina, and Andrea Ballabio. 2013. "Signals from the Lysosome: A Control Centre for Cellular Clearance and Energy Metabolism." *Nature Reviews. Molecular Cell Biology* 14 (5). Nature Publishing Group: 283–96. doi:10.1038/nrm3565.
- Sharma, Jaiprakash, Alberto di Ronza, Parisa Lotfi, and Marco Sardiello. 2018. "Lysosomes and Brain Health." *Annual Review of Neuroscience*, no. April: 255–76. doi:10.1146/annurev-neuro-080317-061804.
- Shevchenko, Andrej, and Kai Simons. 2010. "Lipidomics: Coming to Grips with Lipid Diversity." *Nature Reviews. Molecular*

- Cell Biology 11 (8). Nature Publishing Group: 593–98. doi:10.1038/nrm2934.
- Simons, Kai, and Ji Sampaio. 2011. “Membrane Organization and Lipid Rafts.” *Cold Spring Harbor ...*, 1–18. <http://cshperspectives.cshlp.org/content/3/10/a004697.short>.
- Simonsen, a, R Lippé, S Christoforidis, J M Gaullier, a Brech, J Callaghan, B H Toh, C Murphy, M Zerial, and H Stenmark. 1998. “EEA1 Links PI(3)K Function to Rab5 Regulation of Endosome Fusion.” *Nature* 394 (JULY): 494–98. doi:10.1038/28879.
- Skotland, Tore, Kirsten Sandvig, and Alicia Llorente. 2017. “Lipids in Exosomes: Current Knowledge and the Way Forward.” *Progress in Lipid Research*. doi:10.1016/j.plipres.2017.03.001.
- Small, Scott A., and Gregory A. Petsko. 2015. “Retromer in Alzheimer Disease, Parkinson Disease and Other Neurological Disorders.” *Nature Reviews Neuroscience* 16 (3): 126–32. doi:10.1038/nrn3896.
- Small, Scott A., Sabrina Simoes-Spassov, Richard Mayeux, and Gregory A. Petsko. 2017. “Endosomal Traffic Jams Represent a Pathogenic Hub and Therapeutic Target in Alzheimer’s Disease.” *Trends in Neurosciences* 40 (10): 592–602. doi:10.1016/j.tins.2017.08.003.
- Staiano, Leopoldo, Maria Giovanna De Leo, Maria Persico, and Maria Antonietta De Matteis. 2015. “Mendelian Disorders of PI Metabolizing Enzymes.” *Biochimica et Biophysica Acta (BBA) - Molecular and Cell Biology of Lipids* 1851 (6). Elsevier B.V.: 867–81. doi:10.1016/j.bbalip.2014.12.001.
- Stuffers, Susanne, Catherine Sem Wegner, Harald Stenmark, and Andreas Brech. 2009. “Multivesicular Endosome Biogenesis in the Absence of ESCRTs.” *Traffic* 10 (7): 925–37. doi:10.1111/j.1600-0854.2009.00920.x.
- Taghavi, Shaghayegh, Rita Chaoui, Abbas Tafakhori, Luis J. Azcona, Saghar Ghasemi Firouzabadi, Mir Davood Omrani, Javad Jamshidi, et al. 2017. “A Clinical and Molecular Genetic Study of 50 Families with Autosomal Recessive Parkinsonism Revealed Known and Novel Gene Mutations.” *Molecular Neurobiology*. *Molecular Neurobiology*. doi:10.1007/s12035-017-0535-1.
- Taguchi-Atarashi, Naoko, Maho Hamasaki, Kohichi Matsunaga, Hiroko Omori, Nicholas T. Ktistakis, Tamotsu Yoshimori, and Takeshi Noda. 2010. “Modulation of Local PtdIns3P Levels by the PI Phosphatase MTMR3 Regulates Constitutive Autophagy.” *Traffic* 11 (4): 468–78. doi:10.1111/j.1600-0854.2010.01034.x.
- Tooze, Sharon A, Adi Abada, and Zvulun Elazar. 2014. “Endocytosis and Autophagy: Exploitation or Cooperation?” *Cold Spring Harbor Perspectives in Biology* 6 (5). Cold Spring Harbor Laboratory Press: a018358. doi:10.1101/cshperspect.a018358.
- Trajkovic, Katarina, Chieh Hsu, Salvatore Chiantia, Lawrence Rajendran, Dirk Wenzel, Felix Wieland, Petra Schwille, et al. 2008. “Ceramide Triggers Budding of Exosome Vesicles into Multivesicular Endosomes.” *Science (New York, N.Y.)* 319 (April): 1244–47. doi:10.1126/science.1153124.
- Van Cauwenberghe, Caroline, Christine Van Broeckhoven, and Kristel Slegers. 2016. “The Genetic Landscape of Alzheimer Disease: Clinical Implications and Perspectives.” *Genetics in Medicine* 18 (5): 421–30. doi:10.1038/gim.2015.117.
- van Meer, Gerrit, Dennis R Voelker, and Gerald W Feigenson. 2008. “Membrane Lipids: Where They Are and How They Behave.” *Nature Reviews. Molecular Cell Biology* 9 (2): 112–24. doi:10.1038/nrm2330.
- van Niel, Guillaume, Gisela D’Angelo, and Graça Raposo. 2018. “Shedding Light on the Cell Biology of Extracellular Vesicles.” *Nature Reviews Molecular Cell Biology*. Nature Publishing Group. doi:10.1038/nrm.2017.125.
- Vergne, Isabelle, Esteban Roberts, Rasha A Elmaoued, Valérie Tosch, Mónica A Delgado, Tassula Proikas-Cezanne, Jocelyn Laporte, and Vojo Deretic. 2009. “Control of Autophagy Initiation by Phosphoinositide 3-Phosphatase Jumpy.” *The EMBO Journal* 28 (15): 2244–58. doi:10.1038/emboj.2009.159.
- Villaseñor, Roberto, Yannis Kalaidzidis, and Marino Zerial. 2016. “Signal Processing by the Endosomal System.” *Current Opinion in Cell Biology*. Elsevier Current Trends. doi:10.1016/j.ceb.2016.02.002.
- Wandinger-Ness, A., and M. Zerial. 2014. “Rab Proteins and the Compartmentalization of the Endosomal System.” *Cold Spring Harbor Perspectives in Biology*. doi:10.1101/cshperspect.a022616.
- Wang, L., K. Budolfson, and F. Wang. 2011. “Pik3c3 Deletion in Pyramidal Neurons Results in Loss of Synapses, Extensive Gliosis and Progressive Neurodegeneration.” *Neuroscience* 172. Elsevier Inc.: 427–42. doi:10.1016/j.neuroscience.2010.10.035.
- Wideman, Jeremy G., Ka Fai Leung, Mark C. Field, and Joel B. Dacks. 2014. “The Cell Biology of the Endocytic System from an Evolutionary Perspective.” *Cold Spring Harbor Perspectives in Biology* 6 (4). doi:10.1101/cshperspect.a016998.
- Willms, Eduard, Henrik J Johansson, Imre Mäger, Yi Lee, K. Emelie M. Blomberg, Mariam Sadik, Amr Alaarg, et al. 2016. “Cells Release Subpopulations of Exosomes with Distinct Molecular and Biological Properties.” *Scientific Reports* 6. doi:10.1038/srep22519.
- Zhang, Yanling, Sergey N Zolov, Clement Y Chow, Shalom G Slutsky, Simon C Richardson, Robert C Piper, Baoli Yang, et al. 2007. “Loss of Vac14, a Regulator of the Signaling Lipid Phosphatidylinositol 3,5-Bisphosphate, Results in Neurodegeneration in Mice.” *Proceedings of the National Academy of Sciences of the United States of America* 104 (44). National Academy of Sciences: 17518–23. doi:10.1073/pnas.0702275104.

- Zhong, Qi, Martin J Watson, Cheri S Lazar, Andrea M Hounslow, Jonathan P Waltho, and Gordon N Gill. 2005. "Determinants of the Endosomal Localization of Sorting Nexin 1." *Molecular Biology of the Cell* 16 (4). American Society for Cell Biology: 2049–57. doi:10.1091/mbc.E04-06-0504.
- Zhou, Xiang, Liangli Wang, Hiroshi Hasegawa, Priyanka Amin, Bao-Xia Han, Shinjiro Kaneko, Youwen He, and Fan Wang. 2010. "Deletion of PIK3C3/Vps34 in Sensory Neurons Causes Rapid Neurodegeneration by Disrupting the Endosomal but Not the Autophagic Pathway." *Proceedings of the National Academy of Sciences of the United States of America* 107: 9424–29. doi:10.1073/pnas.0914725107.
- Zolov, Sergey N, Dave Bridges, Yanling Zhang, Wei-Wei Lee, Ellen Riehle, Rakesh Verma, Guy M Lenk, et al. 2012. "In Vivo, Ptkfyve Generates PI(3,5)P₂, Which Serves as Both a Signaling Lipid and the Major Precursor for PI5P." *Proceedings of the National Academy of Sciences of the United States of America* 109 (43). National Academy of Sciences: 17472–77. doi:10.1073/pnas.1203106109/-/DCSupplemental. www.pnas.org/cgi/doi/10.1073/pnas.1203106109.
- Zoncu, Roberto, Rushika M Perera, Daniel M Balkin, Michelle Pirruccello, Derek Toomre, and Pietro De Camilli. 2009. "A Phosphoinositide Switch Controls the Maturation and Signaling Properties of APPL Endosomes." *Cell* 136 (6). Elsevier Ltd: 1110–21. doi:10.1016/j.cell.2009.01.032.

CHAPTER 2

EXPERIMENTAL WORK

Chapter 2.1

André M. Miranda, Zofia M. Lasiecka, Yimeng Xu, Jessi Neufeld, Sanjid Shahriar, Sabrina Simoes,
Robin B. Chan, Tiago Gil Oliveira, Scott A. Small, Gilbert Di Paolo

Neuronal lysosomal dysfunction releases exosomes harboring APP C-terminal fragments and unique lipid signatures

Nature Communications **9**(1):291 (2018)

DOI: [10.1038/s41467-017-02533-w](https://doi.org/10.1038/s41467-017-02533-w)

Neuronal lysosomal dysfunction releases exosomes harboring APP C-terminal fragments and unique lipid signatures

André M. Miranda^{1,2,3,4}, Zofia M. Lasiicka¹, Yimeng Xu¹, Jessi Neufeld^{2,5}, Sanjid Shahriar¹, Sabrina Simoes^{2,5}, Robin B. Chan^{1,2}, Tiago Gil Oliveira^{3,4}, Scott A. Small^{2,5}, Gilbert Di Paolo^{1,2,6,*}

¹ Department of Pathology and Cell Biology, Columbia University Medical Center, New York City, NY 10032, USA.

² Taub Institute for Research on Alzheimer's disease and the Aging Brain, Columbia University Medical Center, New York City, NY 10032, USA.

³ Life and Health Sciences Research Institute (ICVS), School of Medicine, University of Minho, Braga 4710-057, Portugal

⁴ ICVS/3B's, PT Government Associate Laboratory, Braga/Guimarães 4710-057, Portugal

⁵ Departments of Neurology, Columbia University Medical Center, New York City, NY 10032, USA

⁶Present address: Denali Therapeutics, South San Francisco, CA 94080, USA

*Correspondence should be addressed to G.D.P. (e-mail: gd2175@cumc.columbia.edu or dipaolo@dnli.com)

Abstract

Defects in endolysosomal and autophagic functions are increasingly viewed as key pathological features of neurodegenerative disorders. A master regulator of these functions is phosphatidylinositol-3-phosphate (PI3P), a phospholipid synthesized primarily by class III PI 3-kinase Vps34. Here we report that disruption of neuronal Vps34 function *in vitro* and *in vivo* impairs autophagy, lysosomal degradation as well as lipid metabolism, causing endolysosomal membrane damage. PI3P deficiency also promotes secretion of unique exosomes enriched for undigested lysosomal substrates, including amyloid precursor protein C-terminal fragments (APP-CTFs), specific sphingolipids and the phospholipid bis(monoacylglycero)phosphate (BMP), which normally resides in the internal vesicles of endolysosomes. Secretion of these exosomes requires neutral sphingomyelinase 2 and sphingolipid synthesis. Our results reveal a homeostatic response counteracting lysosomal dysfunction via secretion of atypical exosomes eliminating lysosomal waste and define exosomal APP-CTFs and BMP as candidate biomarkers for endolysosomal dysfunction associated with neurodegenerative disorders.

Introduction

A variety of neurodegenerative disorders are associated with major defects in the endolysosomal pathway. These include Alzheimer's disease (Nixon 2013; Small et al. 2017) (AD), Parkinson's disease (Abeliovich and Gitler 2016) (PD), frontotemporal dementia (FTD) (Kao et al. 2017) and several lysosome storage disorders (LSD) (Settembre et al. 2013; Nixon 2013). The causal relationship between endolysosomal dysfunction and neurodegeneration is demonstrated by the occurrence of rare, LSD-causing familial mutations that affect genes encoding key endolysosomal proteins, typically resulting in aggressive, childhood-onset LSDs associated with neurodegeneration (e.g., Niemann-Pick disease type C or NPC) (Settembre et al. 2013; Platt 2014). More recently, mutations in a variety of genes involved in endocytic or endolysosomal function have been shown to cause PD (e.g., *LRRK2*) or some forms of parkinsonism (e.g., *VPS35*, *SYNJ1*, *ATP13A2*) (Abeliovich and Gitler 2016). Importantly, homozygous mutations in certain genes cause LSDs (e.g., *GBA* and *GRN*), while heterozygous mutations of the same genes are major genetic risk factors for late-onset neurodegenerative diseases, such as PD and FTD, respectively (Abeliovich and Gitler 2016; Kao et al. 2017). Finally, several genes involved in the regulation of endolysosomal function have also been linked to late-onset AD (LOAD) suggesting this process to be a key driver of disease onset and progression (Karch and Goate 2015).

Lysosomes are central organelles for the degradation of a large number of macromolecules targeted to this compartment via the endocytic and autophagic pathways (Nixon 2013; Settembre et al. 2013; Platt 2014). Failure to properly degrade these substrates leads to their accumulation, within the endolysosomal compartment itself (e.g., glycosphingolipids), in the cytoplasm (e.g., tau, α -synuclein, ubiquitin inclusions) or in the extracellular environment (e.g., amyloid plaques) (Nixon 2013; Settembre et al. 2013; Platt 2014). A key molecular pathway controlling endolysosomal function and autophagy is the class III phosphatidylinositol 3-kinase (PI3K-III)/Vps34 signaling pathway, which leads to the phosphorylation of PI on the 3' position of the inositol ring, generating PI3P. Vps34 interacts with p150/Vps15 and Beclin 1, forming either complex I with ATG14L or complex II with UVRAG. While complex I synthesizes PI3P on pre-autophagosomal membranes, complex II produces PI3P on early endosomes (Backer 2016; Dall'Armi, Devereaux, and Di Paolo 2013). PI3P, in turn, controls the membrane recruitment of a variety of cytosolic effectors harboring PI3P-binding domains, including FYVE and PX modules (Dall'Armi, Devereaux, and Di Paolo 2013; Schink, Tan, and Stenmark 2016). PI3P also serves as a substrate for the synthesis of PI(3,5)P₂ by the PI3P 5-kinase PIKfyve on late endosomes, controlling additional aspects of endolysosomal function (Schink, Tan, and Stenmark

2016; McCartney, Zhang, and Weisman 2014). Altogether, this pathway mediates a variety of critical processes, such as endosomal fusion, intraluminal vesicle budding, endosomal motility as well as the biogenesis and maturation of autophagosomes during macroautophagy (simply referred as autophagy)(Dall'Armi, Devereaux, and Di Paolo 2013; Schink, Tan, and Stenmark 2016).

In neurons, conditional knock-out of Vps34 causes progressive synaptic loss followed by extensive gliosis and neurodegeneration(Wang, Budolfson, and Wang 2011; Zhou et al. 2010). While no human mutations in *PIK3C3*, the gene encoding Vps34, have been associated with neurodegenerative disorders, the relevance of the PI3P/PI(3,5)P₂ pathway in neurological disorders is supported by the existence of Amyotrophic Lateral Sclerosis (ALS) and Charcot-Marie-Tooth 4J (CMT4J) causing mutations in *FIG4* as well as PD causing mutations in *VAC14*, both of which are key components of the PIKfyve complex controlling PI(3,5)P₂ metabolism(McCartney, Zhang, and Weisman 2014; Taghavi et al. 2017). In addition, we have recently reported that PI3P is selectively deficient in the brain of patients with AD and mouse models thereof(Morel et al. 2013). Furthermore, silencing Vps34 in primary neurons was shown to cause endosomal anomalies and altered amyloidogenic processing of amyloid precursor protein (APP), which are important pathological features of AD(Nixon 2013; Small et al. 2017). Overall, these studies implicate dysregulation of the PI3P pathway and associated endolysosomal perturbation in neurodegeneration.

In this study, we employ pharmacological inhibition and genetic ablation of Vps34 in mice to assess the impact of PI3P deficiency on neuronal autophagy and endolysosomal function, with emphasis on APP and lipid metabolism. We confirm that disruption of Vps34 function impairs endolysosomal function and report a profound alteration of cellular lipid metabolism consistent with a LSD. PI3P depletion promoted the physical disruption of endolysosomal membranes and secretion of exosomes harboring APP C-terminal fragments (APP-CTFs) and unique lipid signatures, including an enrichment of the endolysosomal phospholipid bis(monoacylglycero)phosphate (BMP) (also known as lysobisphosphatidic acid or LBPA)(Bissig and Gruenberg 2013). We show that release of these atypical exosomes is blocked by inhibition of neutral sphingomyelinase 2 (nSMase2) and *de novo* sphingolipid synthesis. Together, our results demonstrate that endolysosomal dysfunction triggers a homeostatic response leading to the secretion of atypical exosomes, allowing for elimination of lysosomal contents that cannot be efficiently degraded. They further highlight the potential of exosomes as biomarkers for neurodegenerative disorders involving endolysosomal dysfunction.

Results

PI3P depletion causes endosomal dysfunction

To test the role of PI3P in endosomal function, we used the newly developed highly specific Vps34 kinase inhibitor VPS34IN1 (Bago et al. 2014) (see also (Dowdle et al. 2014; Ronan et al. 2014)), which selectively decreased PI3P by ~50% after 24 hrs in the murine neuroblastoma line N2a (Supplementary Fig. 1a). Drug treatment increased Beclin 1 levels, but did not downregulate its other interacting partners from complex I, namely ATG14L and Vps15, in contrast to knockout of Vps34 (Devereaux et al. 2013), ruling out indirect effects of destabilization of these proteins (Supplementary Fig. 1b). Importantly, a 24 hr treatment with VPS34IN1 did not affect neuronal cell viability *in vitro* (Supplementary Fig. 1c).

Next, we investigated the impact of Vps34 inhibition on early endosomal trafficking in primary mouse cortical neurons. Pharmacological inhibition of Vps34 for 3 hr caused a ~50% increase in the diameter of EEA1-positive endosomal puncta (Fig. 1a), in agreement with previous Vps34 silencing experiments in neurons (Morel et al. 2013). EEA1 fluorescence intensity was decreased by ~30% after Vps34 inhibition (Fig. 1a), likely reflecting reduced membrane association of this PI3P-interacting protein (Schink, Tan, and Stenmark 2016; Dall'Armi, Devereaux, and Di Paolo 2013). This was confirmed in N2a cells fractionated in particulate and soluble fractions, showing higher levels of soluble EEA1, but not Rab5, in VPS34IN1-treated cells (Supplementary Fig. 1d). Rab5 puncta intensity and size were also significantly increased (Fig. 1a and Supplementary Fig. 1e). Upon Vps34 inhibition, Rab5 showed increased colocalization with APPL1 (Fig. 1b), a protein that associates with PI3P-negative early endosomes (Zoncu et al. 2009). These observations confirm the key role of Vps34 kinase activity in early endosomal traffic in neurons.

Vps34 inhibition slows lysosomal degradation of APP-CTFs

Vps34 controls endolysosomal function in non-neuronal cells, in part by mediating sorting *via* the ESCRT pathway and delivery of hydrolases to lysosomes (Schink, Tan, and Stenmark 2016). Here we found that neurons treated with VPS34IN1 for 4 hr show delayed degradation of the EGF receptor (EGFR) following EGF stimulation (Supplementary Fig. 2a). The remaining degradation was blocked by V-ATPase inhibitor bafilomycin A1 (BafA1), suggesting that Vps34 inhibition only partially impairs lysosomal function (Supplementary Fig. 2b). Next, we assessed the maturation of Cathepsin D (CatD), a lysosomal hydrolase produced in the biosynthetic pathway as precursor proCatD (~50kDa) and sorted to the endolysosomal compartment, where it is processed into a mature form (~30kD) at acidic

pH(Braulke and Bonifacino 2009). Vps34 inhibition for 24 hr caused a defect in CatD maturation, based on the decreased CatD/proCatD ratio, but not in total levels (Fig. 1c). However, confocal analysis of CatD showed that its sorting into the endolysosomal lumen was not grossly affected (Fig. 1c).

We next investigated the impact of acute PI3P depletion on the processing of endogenous APP. The C-terminal fragments of APP α (APP-CTF α) and β (APP-CTF β), which are produced by α - and β -secretase, respectively, and further processed by γ -secretase, are known to accumulate as a result of lysosomal dysfunction(Boland et al. 2010). Vps34 inhibition caused a \sim 40% increase in APP-CTF α/β (hereafter referred to as APP-CTFs) levels without altering levels of full-length APP (FL-APP, Fig. 1d). Of note, the BACE1 cleavage product, APP-CTF β , was also increased by \sim 40%. Contrary to effects observed upon Vps34 silencing(Morel et al. 2013), levels of secreted γ -secretase products A β 40 and A β 42 were decreased by \sim 20-25% after Vps34 inhibition (Fig. 1d). Blocking Vps34 in N2a cells caused a more robust increase in total APP-CTF levels and APP-CTF β specifically, while A β 40 and A β 42 secretion was decreased by 40-65% (Fig. 1e).

To test if APP-CTF accumulation results from decreased lysosomal degradation rather than decreased γ -secretase processing, we pulse-treated N2a cells with protein synthesis inhibitor cycloheximide and monitored FL-APP and APP-CTF levels for 6 hr (Supplementary Fig. 2c). While VPS34IN1 did not affect FL-APP turnover, it caused a delay in APP-CTF degradation, particularly at 2 hr (Supplementary Fig. 2c). To exclude processing defects by γ -secretase, cells were also co-incubated with the γ -secretase inhibitor, compound XXI (XXI γ -inhibitor) (Supplementary Fig. 2d). XXI γ -inhibitor extended APP-CTF half-life relative to cycloheximide alone (*i.e.*, from 2 to 4 hr), confirming that γ -secretase cleavage is a main pathway for the clearance of APP-CTFs. However, Vps34 inhibition still significantly delayed APP-CTF clearance despite γ -secretase inhibition (Supplementary Fig. 2d), confirming that a significant amount of APP-CTFs are degraded in lysosomes in a Vps34-dependent fashion.

Vps34 inhibition blocks autophagy initiation

Next, we assessed the autophagic flux by treating neurons for 3 hr with BafA1 to block the clearance of autophagosomes in the presence or absence of VPS34IN1. While BafA1 alone caused a \sim 2-fold increase in the fluorescence of LC3-positive structures (Fig. 2a) and a \sim 5-fold increase in lipidated LC3 (LC3-II) by immunoblotting (Supplementary Fig. 3a), these effects were blocked by Vps34 inhibition, indicating inhibition of autophagosome formation. Next, we investigated the autophagy

adaptor p62, which delivers polyubiquitinated cargoes to growing autophagosomes via its ubiquitin-associated domain and LC3-interacting region. As an autophagy substrate, p62 accumulates and aggregates in ubiquitin-positive structures when autophagy is impaired (Katsuragi, Ichimura, and Komatsu 2015). Vps34 inhibition caused a ~2-fold increase in the fluorescence of p62-positive structures (Fig. 2a), similar to BafA1 alone or after combined treatments (Supplementary Fig. 3a). Remarkably, super-resolution Airyscan confocal images showed that p62-positive puncta do not accumulate in the lumen of LAMP-1-positive late endosomes/lysosomes upon Vps34 inhibition, while they were observed in those of BafA1-treated cells (Fig. 2b). This suggests that sorting of p62 structures into late endosomes/lysosomes requires PI3P-dependent autophagosome formation, a process that is not altered by BafA1. Electron microscopic (EM) analysis of VPS34IN1-treated cortical neurons revealed enlarged vacuoles with decreased intraluminal material and previously observed electron dense structures (Kishi-Itakura et al. 2014) in the vicinity of endocytic compartments (Supplementary Fig. 3b), which morphologically resemble LAMP-1 and p62-positive structures detected by immunofluorescence (Fig. 2b). Additionally, ubiquitin-positive inclusions co-localizing with p62 were revealed by confocal microscopy after a 24 hr treatment with VPS34IN1 (Fig. 2c), consistent with the accumulation of poly-ubiquitinated proteins and p62 observed by immunoblotting (Supplementary Fig. 3c). These results were confirmed in primary cortical neurons lacking Vps34 as a result of lentiviral expression of *Cre* recombinase in a *Pik3c3^{lox/lox}* background (Supplementary Fig. 3d,e) and therefore highlight the essential role of Vps34 and its kinase activity in neuronal autophagy.

Lipid metabolism is severely affected by Vps34 inhibition

Given the deleterious impact of Vps34 inhibition on endolysosomal/autophagic function, we hypothesized that a broader, secondary lipid dysregulation may result from PI3P deficiency. We used liquid chromatography-mass spectrometry (LC-MS) to analyze the lipid composition of cultured cortical neurons following Vps34 inhibition. Of all lipid classes, sphingolipids were the most significantly impaired, particularly ceramide (Cer), dihydroceramide (dhCer) and dihydrosphingomyelin (dhSM) (Fig. 3a), for which many molecular species were increased (Supplementary Fig. 4a). Additionally, levels of BMP were quantified. BMP is predominantly enriched in the ILVs of late endosomes (Bissig and Gruenberg 2013) and is known to be elevated in LSDs, such as NPC (Kobayashi et al. 1999) as well as in the brain of AD patients (Chan et al. 2012). Although no changes in total BMP levels were found after VPS34IN1 treatment, several molecular species of this phospholipid were increased (Fig. 3a, Supplementary Fig. 4b). While only diffuse immunostaining of

BMP was detected in primary neurons, immunostaining of N2a cells confirmed the luminal localization of this phospholipid in LAMP-1 compartments in both control and treated conditions, suggesting that no gross alteration of BMP localization occurs in these organelles upon Vps34 inhibition, which also caused a clear accumulation of p62 in their vicinity (Supplementary Fig. 4c). Overall, these data indicate that reducing PI3P synthesis causes a secondary perturbation of lipid metabolism.

Vps34 inhibition causes endolysosomal membrane damage

Next, we tested if endolysosomal compartments are physically disrupted by Vps34 inhibition. We thus stained VPS34IN1-treated primary cortical neurons for galectin-3, a recently established marker for endolysosomal membrane damage (Maejima et al. 2013), and observed an increase in the number of galectin-3-positive structures (Fig. 3b,c). Galectin-3 puncta greatly colocalized with p62, as well as ubiquitin, and were generally juxtaposed to and distinct from LAMP-1 compartments. In fact, super resolution confocal and linescan analyses evidenced the segregation of p62/galectin-3 intensity peaks from LAMP-1 membranes and luminal exclusion of these structures (Fig. 3b,c). We also found colocalization between galectin-3, p62 and flotillin-2, a membrane-associated protein commonly used to identify cholesterol- and sphingolipid-enriched microdomains (Banning, Tomasovic, and Tikkanen 2011) (Fig. 3d). Although APP-CTFs accumulate in VPS34IN1-treated neurons, immunostainings of APP and APP-CTFs did not colocalize with p62 (Supplementary Fig. 4d), suggesting that APP does not accumulate on damaged endolysosomal structures. Together with the finding that genetic ablation of Vps34 in cultured neurons also increases the number of galectin-3 puncta and their colocalization with p62 (Supplementary Fig. 5), our data suggest that Vps34 inhibition results in physical damage of endolysosomal membranes. Proximity to but lack of luminal sorting into LAMP-1 compartments indicates these damaged organelles are marked for degradation via ubiquitination and recruitment of autophagy adapter p62, but they are not efficiently eliminated by selective autophagy (Maejima et al. 2013), likely from the reduced ability to lipidate LC3 upon Vps34 inhibition. Whether these damaged organelles are early endosome or late endosomes/lysosomes that have lost their membrane markers through proteolysis as a result of membrane damage remains unclear.

APP-CTFs are secreted in BMP-enriched exosomes

Lysosomal stress has been hypothesized to cause the release of extracellular vesicles (EVs), such as exosomes, as an alternative pathway mediating the elimination of cellular waste, including toxic protein aggregates and lipids (Eitan et al. 2016; Strauss et al. 2010; Chivet et al. 2013). Exosomes

are small 40–100nm vesicles that are released when multivesicular endosomes fuse with the plasma membrane(Raposo and Stoorvogel 2013).

The association of flotillin-2 with damaged endolysosomal membranes and the fact that flotillins have been reported on EVs(Raposo and Stoorvogel 2013) prompted us to determine if VPS34IN1-induced endolysosomal dysfunction promotes EV release. EVs were purified by filtration and ultracentrifugation of cell media(Théry et al. 2006; Kowal et al. 2016) (Supplementary Fig. 6a,b). In primary cortical neurons, Vps34 inhibition increased secretion of three EV markers (ALIX, Flotillin-1 and Flotillin-2) by ~3-fold, while levels of the same markers were unaffected in cell lysates (Fig. 4a,b). Given the effect of Vps34 blockade on APP metabolism, we examined levels of FL-APP and APP-CTFs in EVs (Fig. 4b). Remarkably, APP-CTFs were increased to a greater extent than FL-APP (6-fold vs. 3-fold, resp.), suggesting that APP-CTFs are sorted more efficiently to EVs. However, since APP-CTFs levels were also higher in lysates from VPS34IN1-treated cells (Fig. 1d), the fold-increase in EV secretion was comparable for FL-APP and APP-CTFs when normalized to lysate levels of the same proteins (Fig. 4b). Since poly-ubiquitinated proteins as well as p62 have been previously reported on EVs(Huebner et al. 2016; Hessvik et al. 2016), we blotted the EV fractions with anti-ubiquitin and -p62 antibodies and found increased levels upon VPS34IN1 treatment, supporting the hypothesis that EVs can be used as a vehicle for the disposal of undigested material (Fig. 4b).

We next analyzed EV lipid composition by LC-MS. EVs from VPS34IN1-treated cortical neurons were enriched for cholesterol and specific sphingolipid subclasses, namely dhSM, monohexosylceramide (MhCer) and lactosylceramide (LacCer) (Fig. 4c) relative to controls. The most robust change, however, was a ~2.5-fold increase in total BMP (Fig. 4c), reflecting increase in multiple molecular species of this phospholipid (Supplementary Fig. 6c). These results were validated in N2a cells, as EV-associated APP-CTFs, FL-APP, flotillin-1 and -2 levels were all increased (Fig. 4d,e). Of note, proteins typically associated with the number of exosomes, ALIX and CD63, or ESCRT-dependent ILV sorting, Tsg101 and Hrs, were minimally affected, suggesting that Vps34 inhibition likely affects composition rather than quantity of EVs in an ESCRT-independent fashion (Fig. 4d and data not shown). Lipidomic profiling showed an increase in an overlapping set of sphingolipid subclasses, such as MhCer and LacCer, and a striking ~20-fold increase in BMP levels, including all individual molecular species detected (Fig. 4e, Supplementary Fig. 6d). Additionally, while a ~70% increase in dhSM levels was also detected ($p=0.05$), Cer levels were increased by ~50% in contrast to the ~10% decrease found in primary neuron-derived EVs (Fig. 4c). These results were also confirmed using a chemically-distinct Vps34 kinase inhibitor, SAR405(Ronan et al. 2014), indicating on-target effects

(data not shown). Altogether, our observations suggest that EVs secreted upon PI3P depletion result from endolysosomal/autophagic dysfunction and are exosomes, based on the fact that BMP is associated with ILVs(Bissig and Gruenberg 2013) and is thus a *bona fide* marker for these organelles(Bissig and Gruenberg 2013).

APP-CTF secretion requires endolysosomal dysfunction

To investigate if APP-CTF exosomal secretion merely reflects intracellular accumulation, we compared the effect of Vps34 inhibition to γ -secretase inhibition, which dramatically increases cellular APP-CTF levels, but does not cause major alterations of the endolysosomal system(Lee et al. 2010). N2a cells were treated for 24 hr with the XXI γ -inhibitor and VPS34IN1, either singly or in combination. Cellular APP-CTF levels were increased by XXI γ -inhibitor to a higher extent than VPS34IN1 alone, while they were additively increased by combined treatment (Supplementary Fig. 7a). Consistent with a lack of impact on autophagic/lysosomal function, the XXI γ -inhibitor alone did not affect total p62 levels (Supplementary Fig. 7a). Remarkably, despite the robust accumulation of APP-CTFs observed after XXI γ -inhibitor(Sharples et al. 2008), a smaller proportion was released on EVs relative to vehicle or VPS34IN1 treatment (Supplementary Fig. 7b, low and high exposure panels). Combined treatments caused an additive increase in EV-associated APP-CTFs relative to VPS34 inhibition alone, but to a lesser extent than that observed in lysates (Supplementary Fig. 7b). These data suggest that active sorting of APP-CTFs into EVs occurs as a result of Vps34 inhibition and that the amount of EV-associated APP-CTF does not simply reflect cellular APP-CTF levels.

Next, we sought to precisely delineate the role of autophagy blockade *vs.* endolysosomal dysfunction by VPS34IN1 on exosomal secretion of APP-CTFs. To specifically assess the contribution of autophagy, we used CRISPR-Cas9 gene-edited N2a cells lacking *Atg5* (*Atg5* KO), a core component of the autophagy machinery(Bento et al. 2016). *Atg5* ablation was confirmed by the absence of Atg12-Atg5 conjugates (Supplementary Fig. 7c). *Atg5* KO N2a cell lysates showed increased basal cellular levels of p62 and APP-CTFs relatively to isogenic controls. Interestingly, Vps34 inhibition caused a similar fold increase in cellular p62 and APP-CTF levels in both cell lines, in addition to baseline effects induced by *Atg5* KO (Supplementary Fig. 7c). While *Atg5* KO alone showed a trend for increased secretion of the EV markers analyzed, VPS34IN1 treatment caused a much more dramatic effect in EV-associated APP-CTFs and a comparable fold-increase in both naïve and *Atg5* KO cells (Supplementary Fig. 7d). Therefore, we conclude that the increase of APP-CTF secretion *via* EVs

induced by Vps34 inhibition occurs independently of major autophagy defects and suggests it originates from other aspects of endolysosomal dysfunction.

We also investigated whether exosomal APP-CTF levels are affected by endolysosomal alkalization induced by treating N2a cells with BafA1 for 24 hr. Western blot analysis of cell lysates showed that BafA1 treatment causes a dramatic increase in p62 levels as well as in APP-CTFs (Fig. 5a). In contrast, cellular flotillin-2 levels were decreased by ~50% upon BafA1 treatment. BafA1-treated cells showed a striking increase in flotillin-2, p62 and APP-CTFs in EVs, although the later was proportional to cellular levels (Fig. 5b). In addition, LC-MS analysis of EVs from BafA1-treated cells showed a ~20% enrichment for cholesterol and a ~2-fold increase in the sphingolipid subclasses Cer, dhCer, MhCer and LacCer (Fig. 5c). BMP levels were increased by ~2-fold as seen in N2a cells and primary neurons treated with VPS34IN1 (Fig. 5c). Altogether, these results suggest that release of EVs enriched for APP-CTFs and lipids of late endocytic/lysosomal compartments is intrinsically related to endolysosomal dysfunction.

Exosome secretion is modulated by ceramide synthesis

Ceramide production by nSMase2 has been directly implicated in exosome biogenesis and secretion (Trajkovic et al. 2008; Asai et al. 2015). Considering the impact of Vps34 inhibition on ceramide metabolism, we tested if GW4869, a nSMase2 inhibitor, affects exosomal secretion of APP-CTFs induced by VPS34IN1. Cotreatment of primary cortical neurons with VPS34IN1 and GW4869 increased the cellular accumulation of APP-CTFs relative to VPS34IN1 alone (Fig. 6a). In contrast, no changes were observed for cellular flotillin-2 levels (Fig. 6a). GW4869 caused an overall decrease in EV secretion, based on the reduction of ALIX, flotillin-2, APP-CTFs and poly-ubiquitinated protein levels observed in EV fractions (Fig. 6b). The effect of nSMase2 inhibition on exosomes was largely phenocopied by treatment with myriocin, which inhibits serine palmitoyl transferase, *i.e.* the enzyme catalyzing the first step in *de novo* sphingolipid synthesis (Fig. 6c,d). These results suggest that exosome secretion quantitatively alleviates intracellular burden and implicate sphingolipid metabolism in the sorting and secretion of APP-CTFs in exosomes.

Vps34 ablation in neurons alters brain exosome composition

To validate the role of neuronal Vps34 in endolysosomal function and exosome secretion *in vivo*, we conditionally deleted the gene encoding Vps34 in forebrain excitatory pyramidal neurons by crossing *CaMKII-Cre* transgenic mice with *Pik3c3^{fllox/fllox}* mice (*Pik3c3* cKO). Mutant mice show extensive gliosis

and progressive neuronal loss in the hippocampus and cortex, as described previously (Wang, Budolfson, and Wang 2011). Here, mouse hippocampi were analyzed at 2 months of age, approximately a month after *Cre* expression in the forebrain and prior to neurodegeneration, as shown with comparable MAP2 stainings in neurons from both genotypes, in contrast with 3 month old mice which show a profound decrease in MAP2 stainings in *Pik3c3* cKO brain (Fig. 7a and Supplementary Fig. 8a) (Wang, Budolfson, and Wang 2011). Total Vps34 and Beclin 1 protein levels were decreased by ~30% in *Pik3c3* cKO mice, with the remaining expression likely resulting from glial cells as well as inhibitory neurons (Fig. 7b). As expected, *Pik3c3* cKO mice showed accumulation of poly-ubiquitinated proteins and p62, indicating endolysosomal/autophagic defects (Fig. 7b). As seen *in vitro*, Vps34 deficiency increased levels of APP-CTFs (including APP-CTF β) but not FL-APP (Fig. 7c). However, hippocampal A β 40 and A β 42 levels were unchanged (Fig. 7c).

Next, we characterized the hippocampal lipidome. As observed *in vitro*, sphingolipid metabolism was affected with increased Cer and dhCer in *Pik3c3* cKO relative to control mice (CTRL) (Fig. 7d). BMP levels were also increased, consistent with endolysosomal impairment. We also found an increase in monoacylglycerol (MG) and, more striking, in cholesterol esters (CE), perhaps reflecting reactive gliosis and phagocytic activity (Nielsen et al. 2016).

To investigate the secretion of APP-CTFs *via* EVs, brain exosomes were purified by step gradient fractionation (Perez-Gonzalez et al. 2012; Asai et al. 2015) (Supplementary Fig. 8b,c,d). Analysis of exosomal markers revealed a ~2.5-fold increase in ALIX but no changes in flotillin-1 or flotillin-2 in exosomes from *Pik3c3* cKO brain, relative to controls (Fig. 7e). Importantly, we observed a ~2-fold increase in exosomal poly-ubiquitinated proteins and APP-CTFs in *Pik3c3* cKO brain (Fig. 7e). FL-APP and p62 were not detected in purified exosomes, in contrast to those purified *in vitro*. Furthermore, lipidomic analysis of brain EVs revealed an increase in total SM, LacCer and BMP, with an increase in most BMP species detected (Fig. 7f and Supplementary Fig. 8e). While changes were generally more subtle than those observed *in vitro*, a more global alteration of phospholipids was found in hippocampal exosomes as well as increases in CE and MG, as seen in hippocampal tissue (Fig. 7d). Altogether, these results confirm that ablation of Vps34 in neurons *in vivo* induces endolysosomal dysfunction and lipid dysregulation, which are associated with the release of exosomes enriched for APP-CTFs and various lipids, including BMP.

Discussion

Based on our previous work showing a deficiency of PI3P in AD brain (Morel et al. 2013), we have investigated the impact of neuronal Vps34 kinase inhibition and genetic ablation on endolysosomal function, autophagy and APP metabolism. We found that blocking Vps34 leads to a profound dysregulation of lipid metabolism and endolysosomal membrane disruption, accumulation and secretion of APP-CTFs on a subpopulation of exosomes also enriched for ubiquitinated proteins and atypical lipids such as BMP, demonstrating that neurons have the capacity to eliminate undigested, potentially toxic endolysosomal cargoes *via* exosomes.

Dysregulation of the endocytic pathway in neurons is increasingly viewed as one of the earliest pathological events in the pre-clinical stage of LOAD, even preceding autophagy disturbances also reported in this disease (Peric and Annaert 2015). In this study, we show that Vps34 inhibition recapitulates some of the endolysosomal defects seen in early stages of AD, namely enlargement of EEA1-positive early endosomes (Jiang et al. 2010), stabilization of APPL1/Rab5-positive endosomes and elevated APP-CTF β (Kim et al. 2016). Interestingly, Vps34 kinase inhibition led to a decrease in A β secretion in contrast to the previously reported increase in secreted A β resulting from partial knockdown of Vps34 in neurons (Morel et al. 2013). This discrepancy may reflect kinase-dependent effects *vs.* effects related to the destabilization of the Vps34 complex, including Beclin 1 (Devereaux et al. 2013), resulting from loss of Vps34 protein scaffold. In fact, our results are supported by previous findings reporting that low specificity PI3K inhibitors decrease A β secretion (Petanceska and Gandy 1999). In addition, silencing ESCRT component Hrs, which mediates PI3P-dependent sorting of ubiquitinated cargoes into ILVs, drastically impairs A β secretion in N2a cells (Edgar et al. 2015). However, the most striking APP-related phenotype observed in cultured neurons as well as *in vivo* is the accumulation of APP-CTFs, which is reminiscent of NPC (Maulik et al. 2015).

A key finding reported in this study is that reduction of PI3P causes lipid dysregulation and physically-damaged endolysosomal membranes, as demonstrated by the enrichment of galectin-3 and flotillin-2 on p62- and ubiquitin-positive structures. Because these structures were also detected in Vps34 KO primary neurons (which present lower Beclin 1 levels (Devereaux et al. 2013)), we exclude that secondary effects of pharmacological inhibition of Vps34, namely upregulation of Beclin 1, underlie these phenotypes. While the exact mechanism affecting endolysosomal integrity is unknown, it likely results from lysosomal substrate accumulation. The aberrant accumulation of sphingolipids, such as dihydrosphingolipids and ceramide (Gabandé-Rodríguez et al. 2014; Blom et al. 2015), and sterols (Rodríguez-Navarro et al. 2012) can potentially decrease lysosomal enzymatic activity and

destabilize endolysosomal membranes. Alternatively, deficient trafficking or glycosylation of lysosomal membrane proteins may decrease protection from hydrolases and compromise membrane integrity(Li et al. 2016). This phenotype may be striking after Vps34 inhibition since both autophagy and sorting of p62 into lysosomes are reduced, thus preventing clearance of these damaged organelles by lysophagy-like mechanisms(Maejima et al. 2013). Relevant for neurodegenerative disorders, extracellular aggregates of proteins and peptides such as α -synuclein(Freeman et al. 2013) and tau(Papadopoulos et al. 2017; Calafate et al. 2016) have been shown to cause endolysosomal membrane rupture, perhaps facilitating their cell-to-cell transmission. One of the potential implications of our study is that endolysosomal membrane destabilization caused by PI3P deficiency may sensitize neurons to aggregate-induced toxicity and pathology spreading.

Another important finding is the striking secretion of APP-CTFs in exosomes derived from neurons undergoing endolysosomal stress. Exosomes are increasingly associated with the transmission of aggregation-prone proteins(Levy 2017), but little is known about the molecular mechanisms regulating their biogenesis, cargo selection and secretion(Raposo and Stoorvogel 2013). Recent studies have shown that lysosomal alkalization by chloroquine promotes secretion of exosomes harboring α -synuclein(Alvarez-Erviti et al. 2011) as well as the intracellular domain of APP, but not APP-CTFs(Vingtdeux et al. 2007). While the latter result appears to be at odds with our BafA1 findings, it can be potentially explained by the fact that BafA1 causes an irreversible increase in lysosomal pH, unlike chloroquine. In fact, we found that neither chloroquine nor ammonium chloride increase exosomal levels of APP-CTFs, despite causing increases in their cellular levels (data not shown). Importantly, the fact that BafA1 partially phenocopies VPS34IN1 treatment suggests that blocking Vps34 may affect the V-type ATPase, which will be tested in future work. We also found that exosomal APP-CTF secretion upon Vps34 inhibition largely occurs independently of the core autophagy machinery, as Atg5-deficient N2a cells accumulate APP-CTFs intracellularly but do not secrete them to the same extent as Vps34-inhibited cells. Similarly, γ -secretase inhibition also fails to secrete large amounts of APP-CTFs on exosomes, despite their cellular accumulation, providing additional evidence that endolysosomal dysfunction, rather than intracellular APP-CTF accumulation *per se*, is the mechanism driving exosomal secretion of APP-CTFs. This process may minimize intracellular processing of these APP metabolites by γ -secretase, thus reducing A β generation and toxicity.

Our previous work showed that APP and APP-CTFs are sorted into the ILVs of multivesicular endosomes through ESCRT machinery in a pathway requiring PI3P and APP ubiquitination(Morel et al. 2013; Schink, Tan, and Stenmark 2016). Of note, a subset of ILVs are known to be PI3P-positive

within these endosomes(Bissig and Gruenberg 2013). Because APP-CTFs are coenriched with BMP on exosomes induced by Vps34 inhibition, PI3P deficiency may shunt APP-CTFs into a distinct subpopulation of ILVs which are BMP-positive and committed to the exosomal pathway. This is consistent with the longstanding view that PI3P- and BMP-positive ILVs are distinct within multivesicular endosomes(Bissig and Gruenberg 2013). Importantly, it agrees with the view that PI3P/ESCRT-independent pathways contribute to ILV biogenesis, including the nSMase2 pathway(Trajkovic et al. 2008) as well as BMP itself(Bissig and Gruenberg 2013). Supporting this view, APP-CTFs lacking ubiquitination sites in the cytodomain(Williamson et al. 2017), thus preventing sorting via the ESCRT pathway(Morel et al. 2013), are released through exosomes as efficiently as wild-type APP-CTF upon Vps34 inhibition (data not shown). Interestingly, a recent study showed that inhibition of autophagosome-lysosomal fusion by tetraspanin-6 (TSPAN6) overexpression slowed the degradation of APP-CTFs and increased secretion of EVs in a process requiring syntenin(Guix et al. 2017). This protein has been shown to interact with ALIX, a modulator of BMP biological functions, which include regulation of lysosomal lipases and storage of endolysosomal cholesterol(Bissig and Gruenberg 2013). Whether TSPAN6-dependent exosomes share the same biological properties as those induced by Vps34 inhibition is unclear. We also note that other studies have not reported a BMP enrichment in exosomes(Laulagnier et al. 2004; Wubbolts et al. 2003), likely reflecting the fact that BMP-enriched exosomes are not secreted constitutively, but rather released under endolysosomal stress.

Our study has also critical implications for biomarker discovery. Indeed, increased BMP levels are a common feature of several LSDs, including NPC(Kobayashi et al. 1999) and have been reported in the brain of patients with AD(Chan et al. 2012) and Lewy Body disease (LBD)(Clark et al. 2015), both of which associated with endolysosomal dysfunction(Nixon 2013). Our study suggests that detection of BMP in bodily fluids, such as blood, cerebrospinal fluid (CSF) and urine, may be more indicative of exosomal secretion in response to LSD than a simple measure of phospholipidosis(Meikle et al. 2008). APP-CTFs have also been reported in human CSF(García-Ayllón et al. 2017), suggesting that they can be helpful biomarkers in clinical settings. In sum, APP-CTFs and BMP should be explored as exosome-related biomarkers for a range of neurodegenerative disorders, including AD, PD, LBD, FTD, ALS and many LSDs.

Finally, an important question is whether exosomes released upon endolysosomal dysfunction are endowed with specific cell non-autonomous functions. Changes in EVs collected from *Pik3c3* cKO brain were subtler than those found *in vitro*, likely reflecting the dynamic turnover and metabolism of

exosomes *in vivo*. For instance, they could convey "eat-me" signals directed to microglia, ensuring the proper elimination of unhealthy neurons through efferocytosis(Heneka, Golenbock, and Latz 2015) as well as of the neuronal waste they carry. They could also present danger-associated molecular patterns ("DAMPs") affecting immune receptors(Heneka, Golenbock, and Latz 2015). Alternatively, they could be vectors for the aggregation and/or spreading of pathological proteins, including aberrant tau and A β (Asai et al. 2015; Dinkins et al. 2016), or constitute intracellular antigens triggering autoimmune responses(Dinkins et al. 2016).

In summary, our study reveals a specific homeostatic response counteracting endolysosomal dysfunction via secretion of atypical exosomes to eliminate lysosomal waste and define exosomal APP-CTFs and BMP as candidate biomarkers diagnostic of endolysosomal dysfunction associated with neurodegenerative disorders.

Methods

Reagents and Antibodies

The following compounds were used: BafA1 (25 or 50nM, 023-11641, Wako), Cycloheximide (50 µg/ml, C4859, Sigma-Aldrich), EGF (200 ng/ml, 01-101, EMD Millipore), GW4869 (10µM, 13127, Cayman Chemicals), SAR405 (1µM, HY-12481, MedChem Express), VPS34IN1 (1 or 3µM, Dundee University), γ -secretase Inhibitor XXI, Compound E (2µM, 565790, EMD Millipore). All compounds were dissolved in dimethyl sulfoxide (DMSO) and control cells treated with 0.01% DMSO (Sigma-Aldrich). The following antibodies were purchased from commercial sources: ALIX (pab0204, Rabbit (Rb), 1:2000 in Western Blot (WB) of cell lysates and EVs, Covalab), ALIX (ABC40, Rb, 1:1000 in WB of forebrain EVs, EMD Millipore), Amyloid Precursor Protein C1/6.1 C-Terminal Fragment (802801, Mouse (Ms), Biologend, 1:500 in WB), APPL1 (ab59592, Rb, Abcam, 1:200 in IF), Atg12-Atg5 (2011, Rb, Cell Signaling, 1:1000 in WB), Beclin 1 (3738, Rb, Cell Signaling, 1:1000 in WB), β -Amyloid M3.2 (805701, Ms, Biologend, 1:500 in WB), BIII-Tubulin (801201, Ms, Biologend, 1:1000 in immunofluorescence (IF)), Calnexin (ab31290, Ms, Abcam, 1:200 in WB), EEA1 (sc-6415, Goat, Santa Cruz, 1:300 in IF), EEA1 (C45B10, Rb, Cell Signalling, 1:1000 in WB), EGFR (06-847, Rabbit (Rb), EMD Millipore, 1:1000 in WB), Flotillin-1 (610820, Ms, BD Biosciences, 1:1000 in WB), Flotillin-2 (610383, Ms, BD Biosciences, 1:50 for IF and 1:1000 in WB), GAPDH (MCA-1D4, Ms, Encor Biotech, 1:4000 in WB), Galectin-3 (sc-23938, Rat, Santa Cruz, 1:50 in IF), GM130 (610823, Ms, BD Biosciences, 1:500 in WB), LAMP1 (1D4B, Rat, Developmental Studies Hybridoma Bank, 1:400 in IF), LAMP1 (ab24170, Rb, Abcam, 1:400 in IF), LC3 (M152-3, Ms, MBL, 1:300 in IF), LC3 (NB100-2220, Rb, Novus Biomedical, 1:1000 in WB), MAP2 (ab5392, Chicken, Abcam, 1:2000 in IF), p62 (03-GP62-C, Guinea Pig, American Research Productions, 1:1000 for IF and WB), Rab5 (108011, Ms, Synaptic Systems, 1:100 in IF and 1:500 in WB), Rab7 (9367, Rb, Cell Signaling, 1:1000 in WB), Ubiquitin (sc-8017, Ms, Santa Cruz, 1:1000 in WB, 1:100 in IF), Tubulin (T6074, Ms, Sigma-Aldrich, 1:5000 in WB), Vps15 (H00030849-M02, Ms, Abnova, 1:1000 in WB), Vps34 (4263, Rb, Cell Signaling, 1:1000 in WB). Antibodies raised against ATG14L (Rb, 1:500 in WB) were a generous gift from Dr. Zhenyu Yue (Icahn School of Medicine at Mount Sinai), anti-Cathepsin D (Rb, 1:10.000 in WB, 1:200 in IF) were a generous gift from Dr. Ralph Nixon (Nathan Kline Institute) and anti-BMP/LBPA (Ms, 1:50 in IF) were a generous gift from Dr. Jean Gruenberg (University of Geneva).

Cell culture

Murine neuroblastoma N2a cells were maintained at 37°C in a humidified 5% CO₂ atmosphere in DMEM with GlutaMAX supplemented with 10% fetal bovine serum and penicillin (100 U/ml), streptomycin (100 ug/ml) (Thermofisher). Cells were negative for mycoplasma contamination. CRISPR-Cas9 gene-edited ATG5 KO and isogenic N2a cells were a kind gift from Dr. Hermann Schaeztl (University of Calgary). Twenty-four hr before drug treatment, cells were plated at 50% confluence. Primary cortical neurons were generated from newborn wild-type C57BL/6 or *Pik3c3*^{lox/lox} mice. Briefly, cortices were dissected and chemically digested in 0.25% trypsin for 20min at 37°C. Cells were dissociated with a Pasteur pipette, plated on poly-ornithine-coated dishes or glass coverslips at a density of 50,000-100,000 cells/cm² and allowed to mature in Neurobasal-A supplemented with 2mM Glutamax and 2% B27 (Thermofisher). Vps34 KO neurons were cultured from *Pik3c3*^{lox/lox} mice and infected with lentivirus carrying catalytically active *Cre* recombinase or catalytically-dead *Cre* (Δ Cre)(Devereaux et al. 2013) after 7 days *in vitro* and grown up to 15 days. Lentiviruses were generated by transfecting HEK-293T with lentiviral vectors and pPACK-H1 packaging mix (System Biosciences), using lipofectamine LTX (Thermofisher). HEK-293T media was collected 72h post transfection, passed through a 45nm syringe filter, and applied to neuronal media. Drug treatments were performed after 15-18 days *in vitro* in fresh medium containing Neurobasal-A supplemented with 2% B27. Neuronal cell viability was determined following manufacturer's protocol using CCK8 kit (Dojindo) in cortical neurons grown in 96-well plates, seeded at a density of 30,000 cells/well and grown for 15 days *in vitro*.

Animals

Animals were used in full compliance with National Institute of Health/Columbia University Institutional Animal Care and Use Committee guidelines. The animal protocol was approved by the Committee on the Ethics of Animal Experiments of Columbia University. *Pik3c3*^{lox/lox} mice were a kind gift of Dr. Fan Wang (Duke University School of Medicine) and have been previously described(Zhou et al. 2010; Wang, Budolfson, and Wang 2011). Mice were crossed with transgenic mice expressing *Cre*-recombinase under the promoter of *CaMKII* to conditionally knock-out *Pik3c3* in excitatory forebrain neurons. At 2 and 3 months of age, mice were killed by cervical dislocation, brains immediately macro-dissected, frozen in liquid nitrogen and stored at -80°C. In all experiments, littermate *Pik3c3*^{lox/lox}; *CaMKII-Cre* (cKO) of both sexes were compared to *Pik3c3*^{lox/lox} (CTRL).

Immunofluorescence and confocal microscopy

Cultured cortical neurons were fixed in 2% paraformaldehyde (PFA, Alfa Aesar), 2% sucrose (Sigma-Aldrich) in culture media for 15 min and permeabilized with 0.05% saponin in phosphate-buffered saline (PBS, Boston Bioproducts) supplemented with 1% bovine serum albumin (BSA, Sigma-Aldrich). Primary and Alexa Fluor conjugated secondary antibodies (Thermofisher, Jackson ImmunoResearch) were sequentially incubated for 1 hr in the same buffer. Coverslips were mounted in ProLong Gold antifade mountant (Thermofisher). For immunohistochemistry, mice were transcardially perfused with PBS. Brains were dissected and fixed overnight in 4% PFA in PBS at 4°C, followed by incubation in 30% sucrose (Sigma-Aldrich) for 48 hr in PBS. Brains were sectioned in coronal planes with a cryostat (Leica Biosystems). Immunostaining was performed by blocking free-floating brain sections in 5% Donkey Serum (Thermofisher), 1% BSA and 0.2% Triton X-100 (Fisher Scientific) in PBS for 1 hr. Primary antibodies were incubated overnight at 4°C and secondary antibodies for 2 hr at room temperature, both in blocking solution. Slices were mounted in ProLong Gold antifade mountant (Thermofisher). Confocal stacks and super-resolution images were acquired using a Zeiss LSM 800 confocal microscope equipped with Airyscan module (Zeiss). Fluorescence was collected with x40 and x63 plan apochromat immersion oil objectives. Extraction of single z-frame and maximum intensity projections were performed with ImageJ software. Colocalization was calculated with JACoP plugin of ImageJ and is expressed as Manders' coefficient. Object number, size and intensity were detected and quantified with the ICY software. Each experiment was independently repeated at least three times, unless indicated otherwise.

Conventional electron microscopy

Cultured cortical neurons were fixed with 2.5% glutaraldehyde in 0.1 M cacodylate buffer (Electron Microscopy Sciences) for 24 hr and processed as described previously (Morel et al. 2013). Ultrathin sections were prepared with an EM UC6 ultracryomicrotome (Leica). Exosomes purified from mice brain (see below) were suspended in PBS and fixed with a mixture of 2% PFA/0.065% glutaraldehyde in 0.2M PBS at 4°C. The suspension was loaded onto formvar-carbon-coated EM grids (Electron Microscopy Sciences) and fixed a second time. Samples were contrasted and embedded in a mixture of uranyl acetate and methylcellulose (Electron Microscopy Sciences). Images were acquired using a Philips CM-12 electron microscope (FEI) and digital acquisitions made with a Gatan (4k x2.7k) digital camera (Gatan).

Protein biochemistry and immunoblotting

Cells were washed in PBS and scraped in Radioimmunoprecipitation assay buffer (RIPA) (Pierce) supplemented with protease and phosphatase inhibitor cocktail (Roche). Homogenates were centrifuged for 10 min at 16,000 g at 4°C. Subcellular fractionation of particulate and soluble fractions was performed as previously described (de Araújo and Huber 2007). Supernatants were processed for protein dosage (BCA, Pierce) and samples diluted to equal concentration. SDS-PAGE was carried out per manufacturer's protocol (ThermoFisher). Samples (20-40 µg protein) were prepared with NuPage LDS sample buffer and NuPage reducing reagent and loaded in NuPAGE 4-12% Bis-Tris gels; separation was carried out using MES running buffer (ThermoFisher). Wet transfer was performed on 0.22µm nitrocellulose membranes (Amersham) at 80 V for 1h45 min at 4°C using 0.05% SDS tris-glycine buffer (Boston BioProducts). Membranes were blocked with 5% BSA for 45 min at room temperature. Primary antibodies were diluted in blocking buffer and incubated overnight at 4°C; HRP-conjugated secondary antibodies were incubated for 90 min at room temperature. Membrane development was performed with Immobilon Western Chemiluminescent HRP Substrate (EMD Millipore) and the chemiluminescent signal was imaged with ImageQuant LAS4000 mini (GE Healthcare). Quantification was performed with ImageJ. Analysis of APP-CTFs was done using NuPage 10-20% Tricine gels (ThermoFisher). For analysis of mouse brain tissue, samples were homogenized in 10 volumes of RIPA supplemented with protease and phosphatase inhibitor cocktail (Roche). Homogenates were centrifuged at 16,000g for 15min and supernatants processed as described above. Uncropped blots are shown in Supplementary Fig. 9.

Aβ measurements

Cortical neurons were grown 15 to 18 days in vitro. Neurons were placed in fresh culture medium containing Neurobasal A and 2% B27 and treated for 24 hr. Conditioned media was collected, treated with AEBSF protease inhibitor (1mM, ThermoFisher), centrifuged at 2,000g for 5min and stored at -80°C. Levels of Aβ40 and Aβ42 were measured using V-PLEX Aβ Peptide Panel 1 (4G8) kit (MesoScaleDiscovery, MSD) following the manufacturer's protocol. Mouse hippocampi were homogenized in 10 volumes of tissue homogenization buffer (250 mM sucrose, 20 mM Tris base, 1 mM EDTA, 1 mM EGTA) and diluted 1:2 in 0.4% diethanolamine, 100mM NaCl to extract soluble β-amyloid. Samples were ultracentrifuged for 60min, at 4°C and 100,000g using a TLA55 rotor (Beckman Coulter) and equilibrated with Tris-HCl (0.05M). Murine Aβ40 and Aβ42 were measured using Aβ40 and Aβ42 Mouse ELISA Kits (ThermoFisher) following the manufacturer's protocol. In both

cases, samples were measured in duplicates and values were normalized to protein concentration of cell or brain lysates, respectively.

Exosome Isolation

Primary cortical neurons were grown in 100mm dishes or 6-well plates at a density of 100,000 cells/cm². Conditioned media was collected 24 to 36 hr after treatment and exosomes isolated by differential centrifugation as previously described (Théry et al. 2006; Sharples et al. 2008), with minor modifications. Briefly, samples were cleared of cellular debris at 2000g for 20min, filtered through a 0.2µm PES filter (Worldwide Life Sciences) and ultracentrifuged for 90min at 4°C and 100,000 g using a Sw41 or TLA55 rotor (Beckman Coulter). Exosome pellets were washed in PBS and ultracentrifuged for 90min at 4°C and 100,000 g. Pellets were resuspended in RIPA buffer for Western blotting or in PBS for lipid analysis (see below). Equal volumes of exosome resuspension were loaded on SDS-Page. For analysis of N2a cell derived exosomes, FBS was exosome-depleted by ultracentrifugation for 18h, at 4°C and 100,000 g. Cells were grown in 10% FBS and media was processed as described above. Purification of exosomes was confirmed by comparison of exosomal and non-exosomal markers levels in lysates and EVs. Brain exosomes were isolated as previously described (Perez-Gonzalez et al. 2012; Asai et al. 2015) with slight modifications. Briefly, cortices were minced and digested in hibernate A and papain for 20 min at 37°C (ThermoFisher). Digestion was halted with the addition of excess hibernate A containing protease and phosphatase inhibitors (Roche). The tissue was homogenized gently with a serological pipette and cells were removed by centrifugation for 10 min at 4°C and 300 g. The supernatant was passed through a 40µm strainer (BD Bioscience) followed by a 0.2µm PES filter and subjected to serial centrifugations for 10 min at 2,000 g and 30 min at 10,000 g; at 4°C, to remove cellular debris. The resulting supernatant was centrifuged for 70 min at 4°C and 100,000 g, washed with PBS and centrifuged again. Pellets were suspended in 3mL of 40% Optiprep (Sigma Aldrich), overlaid with 3mL of 20%, 10%, and 5% Optiprep solutions and centrifuged for 18 hr at 4°C and 200,000 g. One-mL fractions were collected, diluted in PBS, and centrifuged again for 70min at 4°C and 100,000 g. Pellets were resuspended in RIPA for immunoblotting or PBS for EM and lipid analysis. Fraction density was calculated by diluting a sample in 3 volumes of 0.25M sucrose and measuring optical density at 340nm (Axis-Shield Density Gradient Media). Validation of exosome purification was performed in wild-type C57BL/6 mice by buoyancy, EM and enrichment of exosome markers ALIX and Flotillin-1. Fractions containing exosomes were pooled together for downstream analyses.

Lipid analysis

Lipid extracts were prepared using a modified Bligh/Dyer extraction as previously described (Morel et al. 2013). Briefly, cells or mice hippocampi were resuspended and homogenized in a solution of methanol:chloroform (2:1) and lipids extracted using chloroform:KCl (3:2, 1M). Extracted lipids were dried under vacuum and stored at -80°C . Extracts were spiked with appropriate internal standards and analyzed by liquid chromatography-mass spectrometry (LC-MS). For analysis of anionic phospholipids and phosphoinositide, extracted lipids were deacylated and analyzed by anion-exchange high-performance liquid chromatography with suppressed conductivity (Morel et al. 2013). Lipid levels are expressed as average Mol% of the total sum of moles of lipids detected. The nomenclature abbreviations are: FC, free cholesterol; CE, cholesterol ester; MG, monoacylglycerol; DG, diacylglycerol; TG, triacylglycerol; Cer, ceramide; dhCer, dihydroceramide; SM, sphingomyelin; dhSM, dihydrosphingomyelin; MhCer, monohexosylceramide; Sulf, sulfatide; LacCer, lactosylceramide; GM3, monosialodihexosylganglioside; PA, phosphatidic acid; PC, Phosphatidylcholine; PCe, ether phosphatidylcholine, PE, phosphatidylethanolamine, PEp, plasmalogen phosphatidylethanolamine, PS, phosphatidylserine; PI, phosphatidylinositol; PG, phosphatidylglycerol; BMP, bis(monoacyl)glycerol; LPC, lysophosphatidylcholine, LPCe, ether lysophosphatidylcholine; LPE, lysophosphatidylethanolamine; LPEp, plasmalogen lysophosphatidylethanolamine; LPI, lysophosphatidylinositol.

Statistics

Statistical analysis was performed using Prism software (Graphpad). All the data are given as mean \pm s.e.m for a given N of biological replicates. Results were pooled from independent experiments as indicated. No statistical method was used to determine sample size. Mice were randomized per litter with age-matched controls and results pooled from at least two distinct litters. No blinding was done for biochemical analyses. For comparison of two experimental conditions, two-tailed Student's t -test was performed. One-way ANOVA followed by Holm-Sidak's multiple comparisons test was performed for analysis of additional experimental groups. Analysis of time-course experiments was performed with two-way ANOVA repeated measures followed by Holm-Sidak's multiple comparisons test. Exact P values are reported in Supplementary Table 1.

References

- Abeliovich, Asa, and Aaron D Gitler. 2016. "Defects in Trafficking Bridge Parkinson's Disease Pathology and Genetics." *Nature* 539 (7628): 207–16. doi:10.1038/nature20414.
- Alvarez-Erviti, Lydia, Yiqi Seow, Anthony H. Schapira, Chris Gardiner, Ian L. Sargent, Matthew J A Wood, and J. Mark Cooper. 2011. "Lysosomal Dysfunction Increases Exosome-Mediated Alpha-Synuclein Release and Transmission." *Neurobiology of Disease* 42 (3). Elsevier Inc.: 360–67. doi:10.1016/j.nbd.2011.01.029.
- Asai, Hirohide, Seiko Ikezu, Satoshi Tsunoda, Maria Medalla, Jennifer Luebke, Tarik Haydar, Benjamin Wolozin, Oleg Butovsky, Sebastian Kügler, and Tsuneya Ikezu. 2015. "Depletion of Microglia and Inhibition of Exosome Synthesis Halt Tau Propagation." *Nature Neuroscience* 18 (11): 1584–93. doi:10.1038/nn.4132.
- Backer, J. M. 2016. "The Intricate Regulation and Complex Functions of the Class III Phosphoinositide 3-Kinase Vps34." *Biochemical Journal* 473 (15): 2251–71. doi:10.1042/BCJ20160170.
- Bago, Ruzica, Nazma Malik, Michael J. Munson, Alan R. Prescott, Paul Davies, Eeva Sommer, Natalia Shpiro, et al. 2014. "Characterization of VPS34-IN1, a Selective Inhibitor of Vps34, Reveals That the Phosphatidylinositol 3-Phosphate-Binding SGK3 Protein Kinase Is a Downstream Target of Class III Phosphoinositide 3-Kinase." *Biochemical Journal* 463 (3): 413–27. doi:10.1042/BJ20140889.
- Banning, Antje, Ana Tomasovic, and Ritva Tikkanen. 2011. "Functional Aspects of Membrane Association of Reggie/Flotillin Proteins." *Current Protein & Peptide Science* 12 (8): 725–35. doi:10.2174/138920311798841708.
- Bento, Carla F., Maurizio Renna, Ghita Ghislat, Claudia Puri, Avraham Ashkenazi, Mariella Vicinanza, Fiona M. Menzies, and David C. Rubinsztein. 2016. "Mammalian Autophagy: How Does It Work?" *Annual Review of Biochemistry* 85 (1): 685–713. doi:10.1146/annurev-biochem-060815-014556.
- Bissig, Christin, and Jean Gruenberg. 2013. "Lipid Sorting and Multivesicular Endosome Biogenesis." *Cold Spring Harbor Perspectives in Biology*. Cold Spring Harbor Laboratory Press. doi:10.1101/cshperspect.a016816.
- Blom, Tomas, Shiqian Li, Andrea Dichlberger, Nils Bäck, Young Ah Kim, Ursula Loizides-Mangold, Howard Riezman, Robert Bittman, and Elina Ikonen. 2015. "LAPTM4B Facilitates Late Endosomal Ceramide Export to Control Cell Death Pathways." *Nature Chemical Biology* 11 (10): 799–806. doi:10.1038/nchembio.1889.
- Boland, Barry, David A. Smith, Declan Mooney, Sonia S. Jung, Dominic M. Walsh, and Frances M. Platt. 2010. "Macroautophagy Is Not Directly Involved in the Metabolism of Amyloid Precursor Protein." *Journal of Biological Chemistry* 285 (48): 37415–26. doi:10.1074/jbc.M110.186411.
- Braulke, Thomas, and Juan S. Bonifacino. 2009. "Sorting of Lysosomal Proteins." *Biochimica et Biophysica Acta (BBA) - Molecular Cell Research* 1793 (4). Elsevier: 605–14. <https://www.sciencedirect.com/science/article/pii/S0167488908003716>.
- Calafate, Sara, William Flavin, Patrik Verstreken, and Diederik Moechars. 2016. "Loss of Bin1 Promotes the Propagation of Tau Pathology." *Cell Reports* 17: 931–40. doi:10.1016/j.celrep.2016.09.063.
- Chan, Robin B., Tiago G. Oliveira, Ety P. Cortes, Lawrence S. Honig, Karen E. Duff, Scott a. Small, Markus R. Wenk, Guanghou Shui, and Gilbert Di Paolo. 2012. "Comparative Lipidomic Analysis of Mouse and Human Brain with Alzheimer Disease." *Journal of Biological Chemistry* 287: 2678–88. doi:10.1074/jbc.M111.274142.
- Chivet, Mathilde, Charlotte Javalet, Fiona Hemming, Karin Pernet-Gallay, Karine Laulagnier, Sandrine Fraboulet, and Rémy Sadoul. 2013. "Exosomes as a Novel Way of Interneuronal Communication." *Biochemical Society Transactions* 41 (1): 241–44. doi:10.1042/BST20120266.
- Clark, Lorraine N., Robin Chan, Rong Cheng, Xinmin Liu, Naeun Park, Nancy Parmalee, Sergey Kisselev, et al. 2015. "Gene-Wise Association of Variants in Four Lysosomal Storage Disorder Genes in Neuropathologically Confirmed Lewy Body Disease." Edited by Coro Paisan-Ruiz. *PLOS ONE* 10 (5): e0125204. doi:10.1371/journal.pone.0125204.
- Dall'Armi, Claudia, Kelly a Devereaux, and Gilbert Di Paolo. 2013. "The Role of Lipids in the Control of Autophagy." *Current Biology : CB* 23 (1). Elsevier Ltd: R33-45. doi:10.1016/j.cub.2012.10.041.
- de Araújo, Mariana Eça Guimarães, and Lukas Alfons Huber. 2007. "Subcellular Fractionation." *Methods in Molecular Biology* 357: 73–85. doi:10.1385/1-59745-214-9:73.
- Devereaux, Kelly, Claudia Dall'Armi, Abel Alcazar-Roman, Yuta Ogasawara, Xiang Zhou, Fan Wang, Akitsugu Yamamoto, Pietro de Camilli, and Gilbert Di Paolo. 2013. "Regulation of Mammalian Autophagy by Class II and III PI 3-Kinases through PI3P Synthesis." *PLoS ONE* 8 (10): 10–12. doi:10.1371/journal.pone.0076405.
- Dinkins, Michael B, John Enasko, Caterina Hernandez, Guanghu Wang, Jina Kong, Inas Helwa, Yutao Liu, Alvin V. Terry, and Erhard Bieberich. 2016. "Neutral Sphingomyelinase-2 Deficiency Ameliorates Alzheimer's Disease Pathology and Improves Cognition in the 5XFAD Mouse." *The Journal of Neuroscience* 36 (33): 8653–67. doi:10.1523/JNEUROSCI.1429-16.2016.
- Dowdle, William E, Beat Nyfeler, Jane Nagel, Robert A Elling, Shanming Liu, Ellen Triantafellow, Suchithra Menon, et al. 2014. "Selective VPS34 Inhibitor Blocks Autophagy and Uncovers a Role for NCOA4 in Ferritin Degradation and

- Iron Homeostasis in Vivo” 16 (11). doi:10.1038/ncb3053.
- Edgar, James R., Katarina Willén, Gunnar K. Gouras, and Clare E. Futter. 2015. “ESCRTs Regulate Amyloid Precursor Protein Sorting in Multivesicular Bodies and Intracellular Amyloid- β Accumulation.” *Journal of Cell Science* 128 (14). <http://jcs.biologists.org/content/128/14/2520.long>.
- Eitan, Erez, Caitlin Suire, Shi Zhang, and Mark P. Mattson. 2016. “Impact of Lysosome Status on Extracellular Vesicle Content and Release.” *Ageing Research Reviews* 32. Elsevier B.V.: 65–74. <http://dx.doi.org/10.1016/j.arr.2016.05.001>.
- Freeman, David, Rudy Cedillos, Samantha Choyke, Zana Lukic, Kathleen McGuire, Shauna Marvin, Andrew M. Burrage, et al. 2013. “Alpha-Synuclein Induces Lysosomal Rupture and Cathepsin Dependent Reactive Oxygen Species Following Endocytosis.” Edited by Philipp J. Kahle. *PLoS ONE* 8 (4). Public Library of Science: e62143. doi:10.1371/journal.pone.0062143.
- Gabandé-Rodríguez, E, P Boya, V Labrador, C G Dotti, and M D Ledesma. 2014. “High Sphingomyelin Levels Induce Lysosomal Damage and Autophagy Dysfunction in Niemann Pick Disease Type A.” *Cell Death and Differentiation* 21 (6). Nature Publishing Group: 864–75. doi:10.1038/cdd.2014.4.
- García-Ayllón, María-Salud, Inmaculada Lopez-Font, Claudia P Boix, Juan Fortea, Raquel Sánchez-Valle, Alberto Lleó, José-Luis Molinuevo, Henrik Zetterberg, Kaj Blennow, and Javier Sáez-Valero. 2017. “C-Terminal Fragments of the Amyloid Precursor Protein in Cerebrospinal Fluid as Potential Biomarkers for Alzheimer Disease.” *Scientific Reports* 7 (1). Nature Publishing Group: 2477. doi:10.1038/s41598-017-02841-7.
- Guix, Francesc X., Ragna Sannerud, Fedor Berditchevski, Amaia M. Arranz, Katrien Horr , An Snellinx, Amantha Thathiah, et al. 2017. “Tetraspanin 6: A Pivotal Protein of the Multiple Vesicular Body Determining Exosome Release and Lysosomal Degradation of Amyloid Precursor Protein Fragments.” *Molecular Neurodegeneration* 12 (1). *Molecular Neurodegeneration*: 25. doi:10.1186/s13024-017-0165-0.
- Heneka, Michael T, Douglas T Golenbock, and Eicke Latz. 2015. “Innate Immunity in Alzheimer’s Disease.” *Nature Immunology* 16 (3): 229–36. doi:10.1038/ni.3102.
- Hessvik, Nina Pettersen, Anders Øverbye, Andreas Brech, Maria Lyngaas Torgersen, Ida Seim Jakobsen, Kirsten Sandvig, and Alicia Llorente. 2016. “PIKfyve Inhibition Increases Exosome Release and Induces Secretory Autophagy.” *Cellular and Molecular Life Sciences*. Springer International Publishing. doi:10.1007/s00018-016-2309-8.
- Huebner, Alyssa R, Lei Cheng, Poorichaya Somporn, Mark A Knepper, Robert A Fenton, and Trairak Pisitkun. 2016. “Deubiquitylation of Protein Cargo Is Not an Essential Step in Exosome Formation.” *Molecular & Cellular Proteomics: MCP* 15 (5). American Society for Biochemistry and Molecular Biology: 1556–71. doi:10.1074/mcp.M115.054965.
- Jiang, Ying, Kerry A Mullaney, Corrinne M Peterhoff, Shaoli Che, Stephen D Schmidt, Anne Boyer-Boiteau, Stephen D Ginsberg, Anne M Cataldo, Paul M Mathews, and Ralph A Nixon. 2010. “Alzheimer’s-Related Endosome Dysfunction in Down Syndrome Is A -Independent but Requires APP and Is Reversed by BACE-1 Inhibition.” *Proceedings of the National Academy of Sciences* 107 (4). National Academy of Sciences: 1630–35. doi:10.1073/pnas.0908953107.
- Kao, Aimee W, Andrew Mckay, Param Priya Singh, Anne Brunet, and Eric J Huang. 2017. “Progranulin, Lysosomal Regulation and Neurodegenerative Disease.” *Nature Reviews Neuroscience* 18: 325–333.
- Karch, Celeste M., and Alison M. Goate. 2015. “Alzheimer’s Disease Risk Genes and Mechanisms of Disease Pathogenesis.” *Biological Psychiatry*. doi:10.1016/j.biopsych.2014.05.006.
- Katsuragi, Yoshinori, Yoshinobu Ichimura, and Masaaki Komatsu. 2015. “p62/SQSTM1 Functions as a Signaling Hub and an Autophagy Adaptor.” *FEBS Journal* 282: n/a-n/a. doi:10.1111/febs.13540.
- Kim, S, Y Sato, P S Mohan, C Peterhoff, A Pensalfini, A Rigoglioso, Y Jiang, and R A Nixon. 2016. “Evidence That the rab5 Effector APPL1 Mediates APP- β CTF-Induced Dysfunction of Endosomes in Down Syndrome and Alzheimer’s Disease.” *Molecular Psychiatry* 21 (5): 707–16. doi:10.1038/mp.2015.97.
- Kishi-Itakura, Chieko, Ikuko Koyama-Honda, Eisuke Itakura, and Noboru Mizushima. 2014. “Ultrastructural Analysis of Autophagosome Organization Using Mammalian Autophagy-Deficient Cells.” *Journal of Cell Science* 127 (22): 4984–4984. doi:10.1242/jcs.164293.
- Kobayashi, T, M H Beuchat, M Lindsay, S Frias, R D Palmiter, H Sakuraba, R G Parton, and J Gruenberg. 1999. “Late Endosomal Membranes Rich in Lysobisphosphatidic Acid Regulate Cholesterol Transport.” *Nature Cell Biology* 1 (2): 113–18. doi:10.1038/10084.
- Kowal, Joanna, Guillaume Arras, Marina Colombo, Mabel Jouve, Jakob Paul Morath, Bjarke Primdal-Bengtson, Florent Dingli, Damaris Loew, Mercedes Tkach, and Clotilde Th ry. 2016. “Proteomic Comparison Defines Novel Markers to Characterize Heterogeneous Populations of Extracellular Vesicle Subtypes.” *Proceedings of the National Academy of Sciences* 113 (8): E968–77. doi:10.1073/pnas.1521230113.
- Laulagnier, Karine, Claude MOTTA, Safouane HAMDJ, S bastien ROY, Florence FAUVELLE, Jean-Fran ois PAGEAUX, Toshihide KOBAYASHI, et al. 2004. “Mast Cell- and Dendritic Cell-Derived Exosomes Display a Specific Lipid

- Composition and an Unusual Membrane Organization." *Biochemical Journal* 380 (1): 161–71. doi:10.1042/bj20031594.
- Lee, Ju-Hyun Hyun, W. Haung Yu, Asok Kumar, Sooyeon Lee, Panaiyur S. Mohan, Corrinne M. Peterhoff, Devin M. Wolfe, et al. 2010. "Lysosomal Proteolysis and Autophagy Require Presenilin 1 and Are Disrupted by Alzheimer-Related PS1 Mutations." *Cell* 141 (7). Elsevier Ltd: 1146–58. doi:10.1016/j.cell.2010.05.008.
- Levy, Efrat. 2017. "Exosomes in the Diseased Brain: First Insights from In Vivo Studies." *Frontiers in Neuroscience* 11. Frontiers Media SA: 142. doi:10.3389/fnins.2017.00142.
- Li, Yuan, Baohui Chen, Wei Zou, Xin Wang, Yanwei Wu, Dongfeng Zhao, Yanan Sun, et al. 2016. "The Lysosomal Membrane Protein SCAV-3 Maintains Lysosome Integrity and Adult Longevity." *Journal of Cell Biology* 215 (2): 167–85. doi:10.1083/jcb.201602090.
- Maejima, Ikuko, Atsushi Takahashi, Hiroko Omori, Tomonori Kimura, Yoshitsugu Takabatake, Tatsuya Saitoh, Akitsugu Yamamoto, et al. 2013. "Autophagy Sequesters Damaged Lysosomes to Control Lysosomal Biogenesis and Kidney Injury." *The EMBO Journal* 32: 2336–47. doi:10.1038/emboj.2013.171.
- Maulik, Mahua, Kyle Peake, Ji Yun Chung, Yanlin Wang, Jean E. Vance, and Satyabrata Kar. 2015. "APP Overexpression in the Absence of NPC1 Exacerbates Metabolism of Amyloidogenic Proteins of Alzheimer's Disease." *Human Molecular Genetics* 24 (24): 7132–50. doi:10.1093/hmg/ddv413.
- Mccartney, Amber J., Yanling Zhang, and Lois S. Weisman. 2014. "Phosphatidylinositol 3,5-Bisphosphate: Low Abundance, High Significance." *BioEssays* 36 (1): 52–64. doi:10.1002/bies.201300012.
- Meikle, Peter J., Stephen Duplock, David Blacklock, Phillip D. Whitfield, Gemma Macintosh, John J. Hopwood, and Maria Fuller. 2008. "Effect of Lysosomal Storage on Bis(monoacylglycerol)phosphate." *Biochemical Journal* 411 (1). <http://www.biochemj.org/content/411/1/71>.
- Morel, Etienne, Zeina Chamoun, Zofia M Lasiacka, Robin B Chan, Rebecca L Williamson, Christopher Vetanovetz, Claudia Dall'Armi, et al. 2013. "Phosphatidylinositol-3-Phosphate Regulates Sorting and Processing of Amyloid Precursor Protein through the Endosomal System." *Nature Communications* 4 (January): 2250. doi:10.1038/ncomms3250.
- Nielsen, Mette M. B., Kate L. Lambertsen, Bettina H. Clausen, Morten Meyer, Dhaka R. Bhandari, Søren T. Larsen, Steen S. Poulsen, Bernhard Spengler, Christian Janfelt, and Harald S. Hansen. 2016. "Mass Spectrometry Imaging of Biomarker Lipids for Phagocytosis and Signalling during Focal Cerebral Ischaemia." *Scientific Reports* 6 (1). Nature Publishing Group: 39571. doi:10.1038/srep39571.
- Nixon, Ralph a. 2013. "The Role of Autophagy in Neurodegenerative Disease." *Nature Medicine* 19 (8). Nature Publishing Group: 983–97. doi:10.1038/nm.3232.
- Papadopoulos, Chrisovalantis, Philipp Kirchner, Monika Bug, Daniel Grum, Lisa Koerver, Nina Schulze, Robert Poehler, et al. 2017. "VCP/p97 Cooperates with YOD1, UBXD1 and PLAA to Drive Clearance of Ruptured Lysosomes by Autophagy." *The EMBO Journal* 36 (2): 135–150. doi:10.15252/embj.
- Perez-Gonzalez, Rocio, Sebastien A. Gauthier, Asok Kumar, and Efrat Levy. 2012. "The Exosome Secretory Pathway Transports Amyloid Precursor Protein Carboxyl-Terminal Fragments from the Cell into the Brain Extracellular Space." *Journal of Biological Chemistry* 287 (51): 43108–15. doi:10.1074/jbc.M112.404467.
- Peric, Aleksandar, and Wim Annaert. 2015. "Early Etiology of Alzheimer's Disease: Tipping the Balance toward Autophagy or Endosomal Dysfunction?" *Acta Neuropathologica* 129 (3): 363–81. doi:10.1007/s00401-014-1379-7.
- Petanceska, Suzana S., and Sam Gandy. 1999. "The Phosphatidylinositol 3-Kinase Inhibitor Wortmannin Alters the Metabolism of the Alzheimer's Amyloid Precursor Protein." *Journal of Neurochemistry* 73 (6). Blackwell Science Ltd.: 2316–20. doi:10.1046/j.1471-4159.1999.0732316.x.
- Platt, Frances M. 2014. "Sphingolipid Lysosomal Storage Disorders." *Nature* 510 (7503): 68–75. doi:10.1038/nature13476.
- Raposo, Graça, and Willem Stoorvogel. 2013. "Extracellular Vesicles: Exosomes, Microvesicles, and Friends." *Journal of Cell Biology* 200 (4): 373–83. doi:10.1083/jcb.201211138.
- Rodriguez-Navarro, Jose Antonio, Susmita Kaushik, Hiroshi Koga, Claudia Dall'Armi, Guanghou Shui, Markus R. Wenk, Gilbert Di Paolo, and Ana Maria Cuervo. 2012. "Inhibitory Effect of Dietary Lipids on Chaperone-Mediated Autophagy." *Proceedings of the National Academy of Sciences of the United States of America* 109 (12): E705-14. doi:10.1073/pnas.1113036109.
- Ronan, Baptiste, Odile Flamand, Lionel Vescovi, Christine Dureuil, Laurence Durand, Florence Fassy, Marie-France Bachelot, et al. 2014. "A Highly Potent and Selective Vps34 Inhibitor Alters Vesicle Trafficking and Autophagy." *Nature Chemical Biology* 10 (12): 1013–19. doi:10.1038/nchembio.1681.
- Schink, Kay O., Kia-Wee Tan, and Harald Stenmark. 2016. "Phosphoinositides in Control of Membrane Dynamics." *Annual Review of Cell and Developmental Biology* 32 (1): 143–71. doi:10.1146/annurev-cellbio-111315-125349.
- Settembre, Carmine, Alessandro Fraldi, Diego L Medina, and Andrea Ballabio. 2013. "Signals from the Lysosome: A Control Centre for Cellular Clearance and Energy Metabolism." *Nature Reviews. Molecular Cell Biology* 14 (5). Nature Publishing Group: 283–96. doi:10.1038/nrm3565.
- Sharples, Robyn A, Laura J Vella, Rebecca M Nisbet, Ryan Naylor, Keyla Perez, Kevin J Barnham, Colin L Masters, and

- Andrew F Hill. 2008. "Inhibition of Gamma-Secretase Causes Increased Secretion of Amyloid Precursor Protein C-Terminal Fragments in Association with Exosomes." *FASEB Journal : Official Publication of the Federation of American Societies for Experimental Biology* 22 (5). Federation of American Societies for Experimental Biology: 1469–78. doi:10.1096/fj.07-9357com.
- Small, Scott A., Sabrina Simoes-Spassov, Richard Mayeux, and Gregory A. Petsko. 2017. "Endosomal Traffic Jams Represent a Pathogenic Hub and Therapeutic Target in Alzheimer's Disease." *Trends in Neurosciences* 40 (10): 592–602. doi:10.1016/j.tins.2017.08.003.
- Strauss, Katrin, Cornelia Goebel, Heiko Runz, Wiebke Möbius, Sievert Weiss, Ivo Feussner, Mikael Simons, and Anja Schneider. 2010. "Exosome Secretion Ameliorates Lysosomal Storage of Cholesterol in Niemann-Pick Type C Disease." *Journal of Biological Chemistry* 285 (34): 26279–88. doi:10.1074/jbc.M110.134775.
- Taghavi, Shaghayegh, Rita Chaoui, Abbas Tafakhori, Luis J. Azcona, Saghar Ghasemi Firouzabadi, Mir Davood Omrani, Javad Jamshidi, et al. 2017. "A Clinical and Molecular Genetic Study of 50 Families with Autosomal Recessive Parkinsonism Revealed Known and Novel Gene Mutations." *Molecular Neurobiology*. *Molecular Neurobiology*. doi:10.1007/s12035-017-0535-1.
- Théry, Clotilde, Aled Clayton, Sebastian Amigorena, Graça Raposo, and Aled Clayton. 2006. "Isolation and Characterization of Exosomes from Cell Culture Supernatants." *Current Protocols in Cell Biology / Editorial Board, Juan S. Bonifacino ... [et Al.] Chapter 3 (April)*. Hoboken, NJ, USA: John Wiley & Sons, Inc.: 1–29. doi:10.1002/0471143030.cb0322s30.
- Trajkovic, Katarina, Chieh Hsu, Salvatore Chiantia, Lawrence Rajendran, Dirk Wenzel, Felix Wieland, Petra Schwille, et al. 2008. "Ceramide Triggers Budding of Exosome Vesicles into Multivesicular Endosomes." *Science (New York, N.Y.)* 319 (April): 1244–47. doi:10.1126/science.1153124.
- Vingtdoux, Valérie, Malika Hamdane, Anne Loyens, Patrick Gelé, Hervé Drobeck, Séverine Bégard, Marie Christine Galas, et al. 2007. "Alkalinizing Drugs Induce Accumulation of Amyloid Precursor Protein by-Products in Luminal Vesicles of Multivesicular Bodies." *Journal of Biological Chemistry* 282 (25): 18197–205. doi:10.1074/jbc.M609475200.
- Wang, L., K. Budolfson, and F. Wang. 2011. "Pik3c3 Deletion in Pyramidal Neurons Results in Loss of Synapses, Extensive Gliosis and Progressive Neurodegeneration." *Neuroscience* 172. Elsevier Inc.: 427–42. doi:10.1016/j.neuroscience.2010.10.035.
- Williamson, Rebecca L., Karine Laulagnier, André Miguel Miranda, Marty A. Fernandez, Michael S. Wolfe, Rémy Sadoul, and Gilbert Di Paolo. 2017. "Disruption of Amyloid Precursor Protein Ubiquitination Selectively Increases Amyloid Beta (A β 40 Levels via Presenilin 2-Mediated Cleavage." *Journal of Biological Chemistry*, October. American Society for Biochemistry and Molecular Biology, jbc.M117.818138. doi:10.1074/jbc.M117.818138.
- Wubbolts, Richard, Rachel S. Leckie, Peter T M Veenhuizen, Guenter Schwarzmann, Wiebke Möbius, Joerg Hoernschmeyer, Jan Willem Slot, et al. 2003. "Proteomic and Biochemical Analyses of Human B Cell-Derived Exosomes: Potential Implications for Their Function and Multivesicular Body Formation." *Journal of Biological Chemistry* 278 (13): 10963–72. doi:10.1074/jbc.M207550200.
- Zhou, Xiang, Liangli Wang, Hiroshi Hasegawa, Priyanka Amin, Bao-Xia Han, Shinjiro Kaneko, Youwen He, and Fan Wang. 2010. "Deletion of PIK3C3/Vps34 in Sensory Neurons Causes Rapid Neurodegeneration by Disrupting the Endosomal but Not the Autophagic Pathway." *Proceedings of the National Academy of Sciences of the United States of America* 107: 9424–29. doi:10.1073/pnas.0914725107.
- Zoncu, Roberto, Rushika M Perera, Daniel M Balkin, Michelle Pirruccello, Derek Toomre, and Pietro De Camilli. 2009. "A Phosphoinositide Switch Controls the Maturation and Signaling Properties of APPL Endosomes." *Cell* 136 (6). Elsevier Ltd: 1110–21. doi:10.1016/j.cell.2009.01.032.

Author Contributions

A.M.M., T.G.O., S.A.S. and G.D.P. designed the research. A.M.M. coordinated and carried out the bulk of the experiments. Z.M.L. performed the characterization of cKO neurons and mice. A.M.M., Z.M.L., Y.X., S.S. and R.B.C. designed and carried out the lipid biochemistry. J.N. purified and characterized exosomes from mice brain. S.S. performed the EM analyses. A.M.M. and G.D.P. wrote the manuscript. All co-authors edited the manuscript. G.D.P. conceived the project and supervised the study.

Acknowledgements

We thank Fan Wang for the kind gift of the *Pi3kc3^{lox/lox}* mice. We thank Basant Abdulrahman and Hermann Schaezel for providing the gene-edited *Atg5* KO N2a cells. We are also grateful to Zhenyu Yue, Ralph Nixon and Jean Gruenberg for the kind gift of anti-Atg14L, Cathepsin D and BMP antibodies, respectively. We thank Thomas Südhof for sharing *Cre* recombinase lentiviruses. We thank the OCS Microscopy Core of New York University Langone Medical Center for the support of the EM work and Rocio Perez-Gonzalez and Efrat Levy of New York University for their support during optimization of the brain exosome isolation technique. We thank Elizabeta Micevska for the maintenance and genotyping of the animal colony and Bowen Zhou for the preliminary lipidomic analysis of conditional *Pi3kc3* cKO mice. We also thank Rebecca Williams and Catherine Marquer for critically reading the manuscript. This work was supported by grants from the Fundação para a Ciência e Tecnologia (PD/BD/105915/2014 to A.M.M.); the National Institute of Health (R01 NS056049 to G.D.P, transferred to Ron Liem, Columbia University; T32-MH015174 to Rene Hen (Z.M.L.)). Z.M.L. and R.B.C. received pilot grants from ADRC grant P50 AG008702 to S.A.S.

Competing Financial Interest

The authors declare no competing financial interests. G.D.P. is a full-time employee of Denali Therapeutics Inc.

Figure legends

Figure 1. Vps34 inhibition induces early endosomal abnormalities and causes accumulation of APP-CTFs.

A-B) Representative confocal images of cultured cortical neurons treated with vehicle or VPS34IN1 at 3 μ M for 3 hr. A) Super-resolution Airyscan insets and arrows highlight EEA1 endosomes. Bar graphs indicate average EEA1-puncta size, per cell (mean \pm SEM, N=37 and 44 cells resp., from three independent experiments) and average EEA1/Rab5 puncta intensity, per cell (mean \pm SEM, N=55 and 63 for vehicle and VPS34IN1 resp.). B) Airyscan insets highlight colocalization between APPL1 and Rab5. Bar graph indicates fraction of APPL1 signal co-localizing with Rab5 (mean \pm SEM, N=35 cells, from three independent experiments). Scale bar, 10 μ m. ***p<0.001 in two-tailed Student's t-test. C) Western blot analysis of Cathepsin D levels in primary cortical neurons treated with vehicle or VPS34IN1 at 3 μ M for 24 hr. Bar graph represents average protein levels of total CatD (sum of CatD and proCatD) or ratio of CatD/proCatD, normalized to vehicle (mean \pm SEM, N=7, from two independent experiments). Right panel, representative confocal images of primary cortical neurons. Airyscan insets highlight luminal sorting of Cathepsin D in LAMP-1-positive compartments. Scale bar, 10 μ m. ***p<0.001 in two-tailed Student's t-test. D-E) Western blot analysis of APP metabolites from primary cortical neurons treated as in C) or N2a cells treated with VPS34IN1 at 1 μ M for 24 hr. Bar graph denotes average protein levels normalized to vehicle (mean \pm SEM, N=6 and 7 resp. for primary neurons; N=8 and 7 resp. for N2a cells, from two independent experiments) and murine A β 40 and A β 42 levels measured by MSD from culture media (mean \pm SEM, N=12 and 13 resp. for primary neurons; N=8 and 7 resp. for N2a cells, from two independent experiments). A β levels were normalized to lysate total protein. *p<0.05, **p<0.01, ***p<0.001 in two-tailed Student's t-test.

Figure 2. Vps34 inhibition blocks autophagy initiation and causes accumulation of ubiquitin- and p62-positive structures.

A) Representative confocal images of cortical neurons treated with vehicle, Bafilomycin A1 (BafA1) at 50nM, VPS34IN1 at 3 μ M or co-treated for 3 hr. Arrows highlight LC3 and p62 structures. Right panel, bar graphs denote average object intensity, per cell (mean \pm SEM, N=49-60 cells, from three independent experiments). Scale bar, 10 μ m. ***p<0.001 in one-way ANOVA, Holm-Sidak's multiple comparisons test. B) Representative confocal images of cortical neurons treated as in A) and immunostained for LAMP-1, LC3 and p62. Airyscan insets highlight position of LC3 and p62 structures relative to LAMP-1-positive membranes. Scale bar, 10 μ m. C) Representative confocal images of

cultured cortical neurons treated with vehicle or VPS34IN1 at 3 μ M for 24 hr. Arrows highlight p62 and ubiquitin colocalization. Scale bar, 10 μ m.

Figure 3. Vps34 inhibition causes cellular accumulation of sphingolipids and induces endolysosomal membrane damage.

A) LC-MS analysis of lipids extracted from primary cortical neurons treated with vehicle or VPS34IN1 at 3 μ M for 24 hr. For lipid nomenclature, see methods section. Values are expressed as average Mol% of total lipid measured, normalized to vehicle (mean \pm SEM, N=8, from two independent experiments). *p<0.05, **p<0.01 in two-tailed Student's t-test. B-D) Representative confocal images of cultured cortical neurons treated as in A). B) Airyscan insets highlight triple colocalization between galectin-3, ubiquitin and p62. Bar graphs indicate average number of galectin-3 puncta per cell (mean \pm SEM, N=40 cells, from three independent experiments), fraction of galectin-3 co-localizing with p62 and ubiquitin co-localizing with galectin-3 (mean \pm SEM, N=30 cells, from three independent experiments). C) Airyscan insets highlight p62 and galectin-3 colocalization in close proximity to LAMP-1-positive membranes. Right panel, linescan intensity profile for adjacent p62/galectin-3 and LAMP-1 structures. D) Airyscan insets and linescan intensity profile highlight triple colocalization between galectin-3, p62 and flotillin-2. Scale bar, 10 μ m.

Figure 4. VPS34IN1 treatment causes secretion of extracellular vesicles (EVs) enriched for APP-CTFs, sphingolipids and BMP.

A-B) Western blot analysis of cell lysates and EVs from primary cortical neurons treated with vehicle or VPS34IN1 at 3 μ M for 24 hr. EV protein levels were normalized to lysate total protein (EV total) or lysate levels of the corresponding protein (EV/Lysate ratio). Bar graph denotes average protein levels normalized to vehicle (mean \pm SEM, N=4 for cell lysates, N=6 for EVs, from two independent experiments). **p<0.01, ***p<0.001 in two-tailed Student's t-test. C) LC-MS analysis of lipids extracted from EVs collected from primary cortical neuron culture media after treatment as in A). Values are expressed as average Mol% of total lipid measured, normalized to vehicle (mean \pm SEM, N=3, each from a pool of two biological replicates). * p<0.05, ** p<0.01, ***P<0.01 in two-tailed Student's t-test. D-E) Western blot and LC-MS analysis of lipids extracted from EVs collected from N2a cell culture media after treatment with vehicle or VPS34IN1 at 1 μ M for 24 hr. EV protein levels were normalized to lysate total protein (EV total) or lysate levels of the corresponding protein (EV/Lysate ratio). For complete lipid panel, see Supplementary Fig. 6d (mean \pm SEM, N=6, from two independent

experiments). Lipid values are expressed as average Mol% of total lipids measured, normalized to vehicle (mean \pm SEM N=7, each from a pool of two biological replicates) * $p < 0.05$, ** $p < 0.01$, *** $p < 0.001$ in two-tailed Student's t-test.

Figure 5. Inhibition of V-ATPase promotes secretion of EVs enriched for APP-CTF and BMP.

A-B) Western blot analysis of cell lysates and EVs from N2a cells treated with vehicle or BafA1 at 25nM for 24 hr. EV protein levels were normalized to lysate total protein (EV total) or lysate levels of the corresponding protein (EV/Lysate ratio). Bar graph denotes average protein levels normalized to vehicle (mean \pm SEM, N=4 for lysates, N=6 for EVs, from two independent experiments). ** $p < 0.01$, *** $p < 0.001$ in two-tailed Student's t-test. C) LC-MS analysis of lipids extracted from EVs collected from N2a cells treated as in A). Values are expressed as average Mol% of total lipids measured, normalized to vehicle (mean \pm SEM, N=5, each from a pool of two biological replicates) * $p < 0.05$, ** $p < 0.01$, *** $p < 0.001$ in two-tailed Student's t-test.

Figure 6. Pharmacological blockade of neutral Sphingomyelinase 2 or inhibition of *de novo* sphingolipid synthesis inhibit VPS34IN1-induced release of exosomal APP-CTFs.

A-D) Western blot analysis of cell lysates and EVs from cortical neurons treated with vehicle, VPS34IN1 at 3 μ M or co-treated with GW4869 at 10 μ M or Myriocin at 1 μ M for 36 hr. EV protein levels were normalized to lysate total protein (EV total) or lysate levels of the corresponding protein (EV/Lysate ratio). Bar graph denotes average protein levels normalized to vehicle (mean \pm SEM, N=5 for vehicle, N=6 for treated groups, from two independent experiments). * $p < 0.05$, ** $p < 0.01$, *** $p < 0.001$ in one-way ANOVA, Holm-Sidak's multiple comparisons test.

Figure 7. Neuronal Vps34 deficiency *in vivo* leads to endolysosomal dysfunction and increased exosomal APP-CTF sorting.

A) Brain sections from 2 month-old *Pik3c3*^{lox/lox} (CTRL) and *Pik3c3*^{lox/lox}; *CaMKII-Cre* (*Pik3c3* cKO) mice immunostained for MAP2 and p62. Scale bar, 500 μ m. B-C) Western blot analysis of hippocampus lysates from 2 month-old CTRL and cKO mice (mean \pm SEM, N=7 and 8, resp. in B; N=8 in C), from two independent experiments). C) Right panel, soluble A β 42 and A β 40 levels in hippocampus lysates of 2 month-old CTRL and cKO mice (mean \pm SEM, N=9 mice, from two independent experiments). * $p < 0.05$, ** $p < 0.01$, *** $p < 0.001$ in two-tailed Student's t-test. D) LC-MS analysis of lipids extracted

from hippocampus lysates of 2 month-old CTRL and cKO mice. Values are expressed as average Mol% of total lipids measured, normalized to CTRL. (mean \pm SEM, N=8 and 9 resp., from two independent experiments). * $p < 0.05$, *** $p < 0.001$ in two-tailed Student's t-test. E) Western blot analysis of EVs isolated from the forebrain of 2 month-old CTRL and cKO mice. Bar graph denotes average protein levels normalized to CTRL (mean \pm SEM, N=4 mice, from two independent experiments). * $p < 0.05$ in two-tailed Student's t-test. F) LC-MS analysis of EVs from 2 month-old CTRL and *Pik3c3* cKO mice. Values are expressed as average Mol% of total lipids measured, normalized to CTRL. For complete lipid panel and BMP species analysis, see Supplementary Fig. 8e. (mean \pm SEM, N=6 mice, from two independent experiments). * $p < 0.05$, ** $p < 0.01$ in two-tailed Student's t-test.

Figures

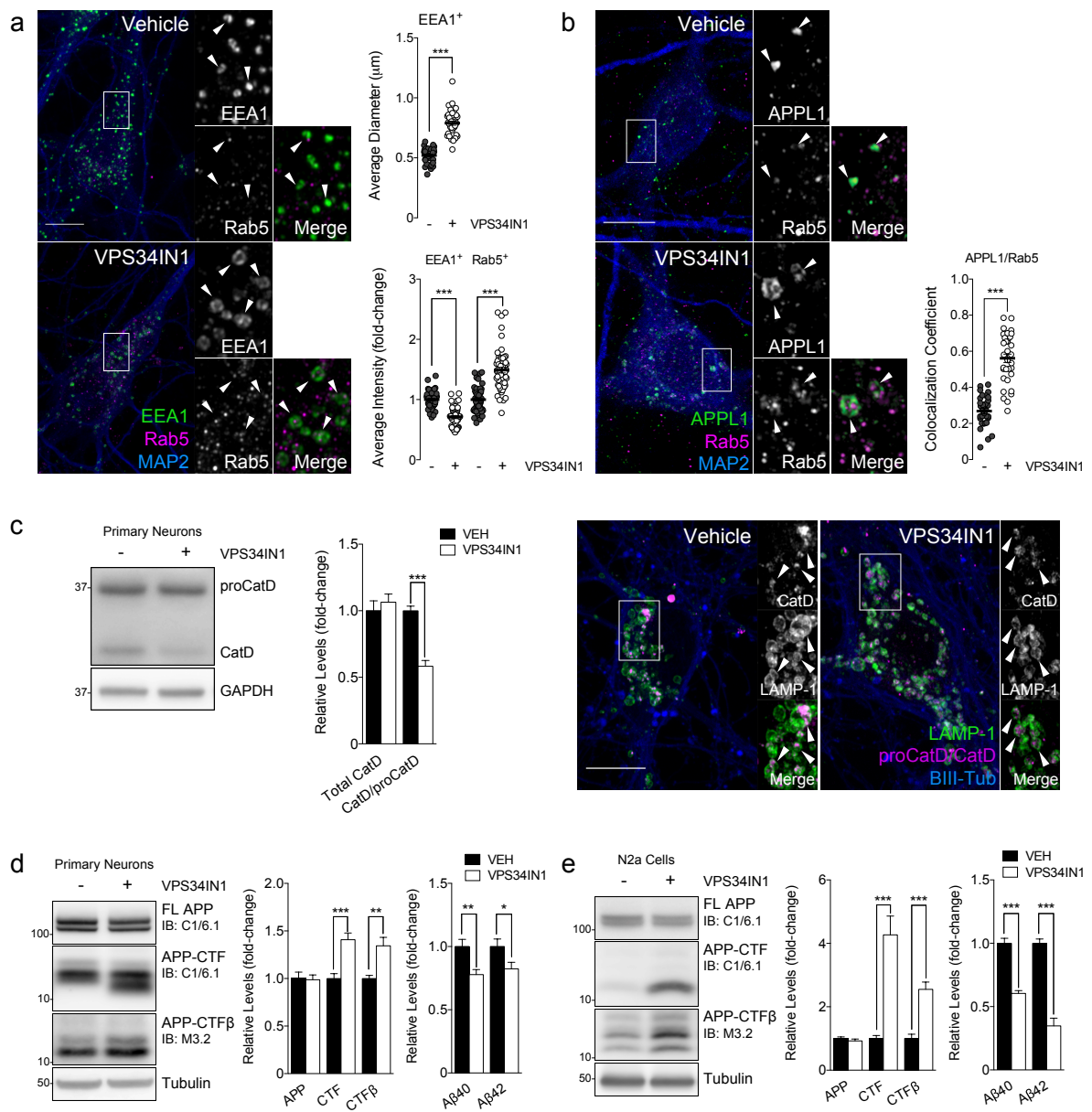


Figure 1 - Miranda et al

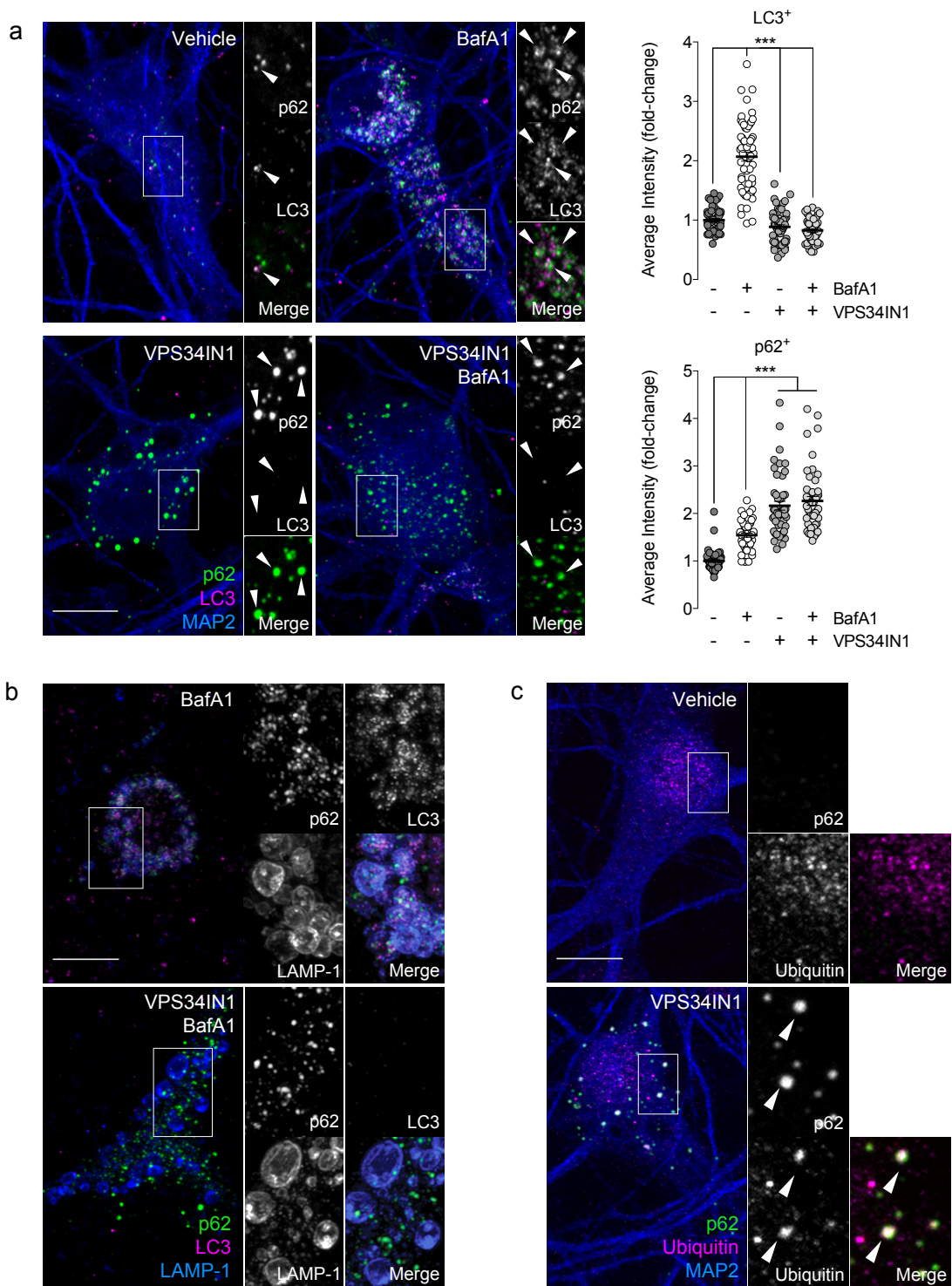


Figure 2- Miranda et al

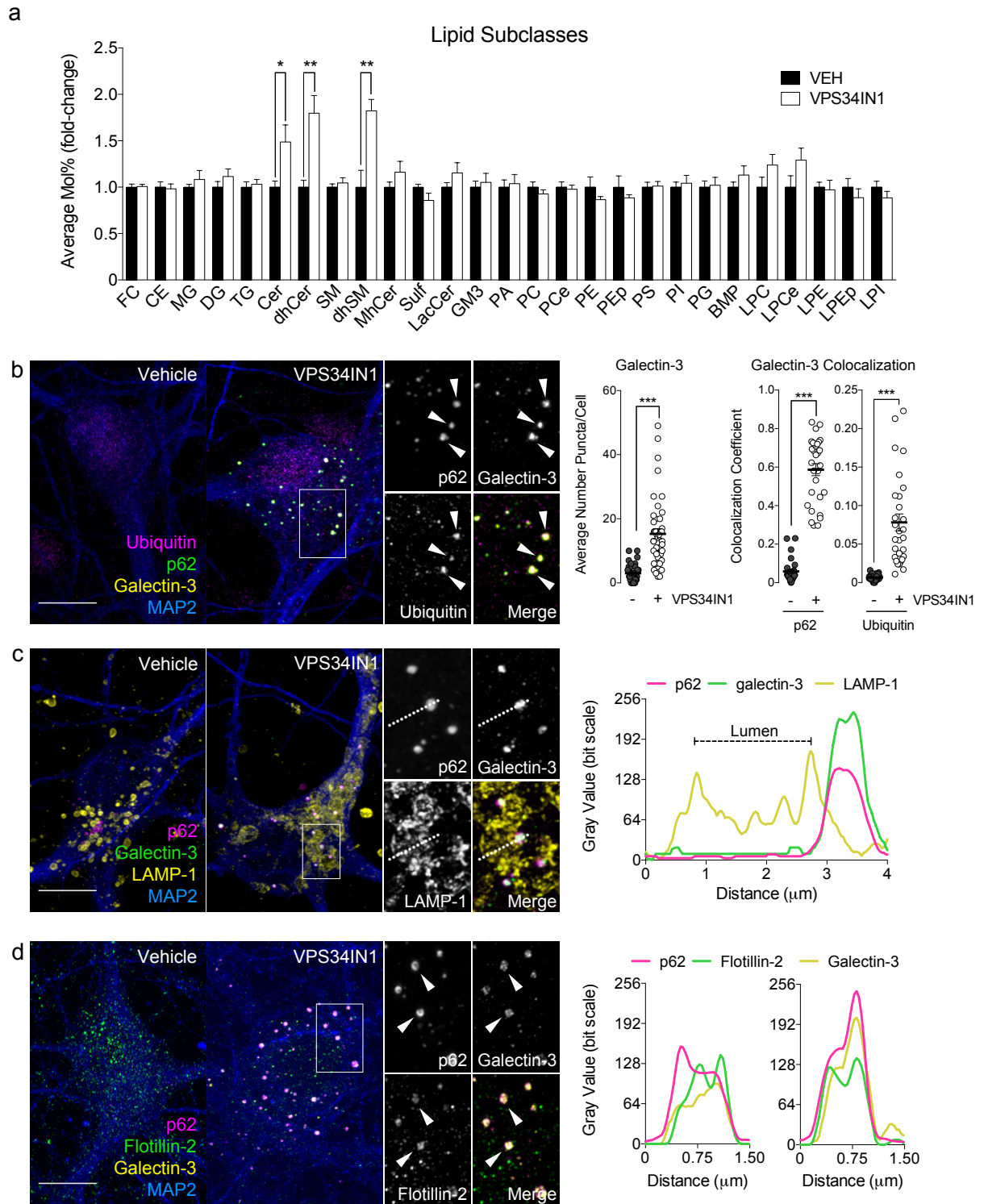


Figure 3 - Miranda et al

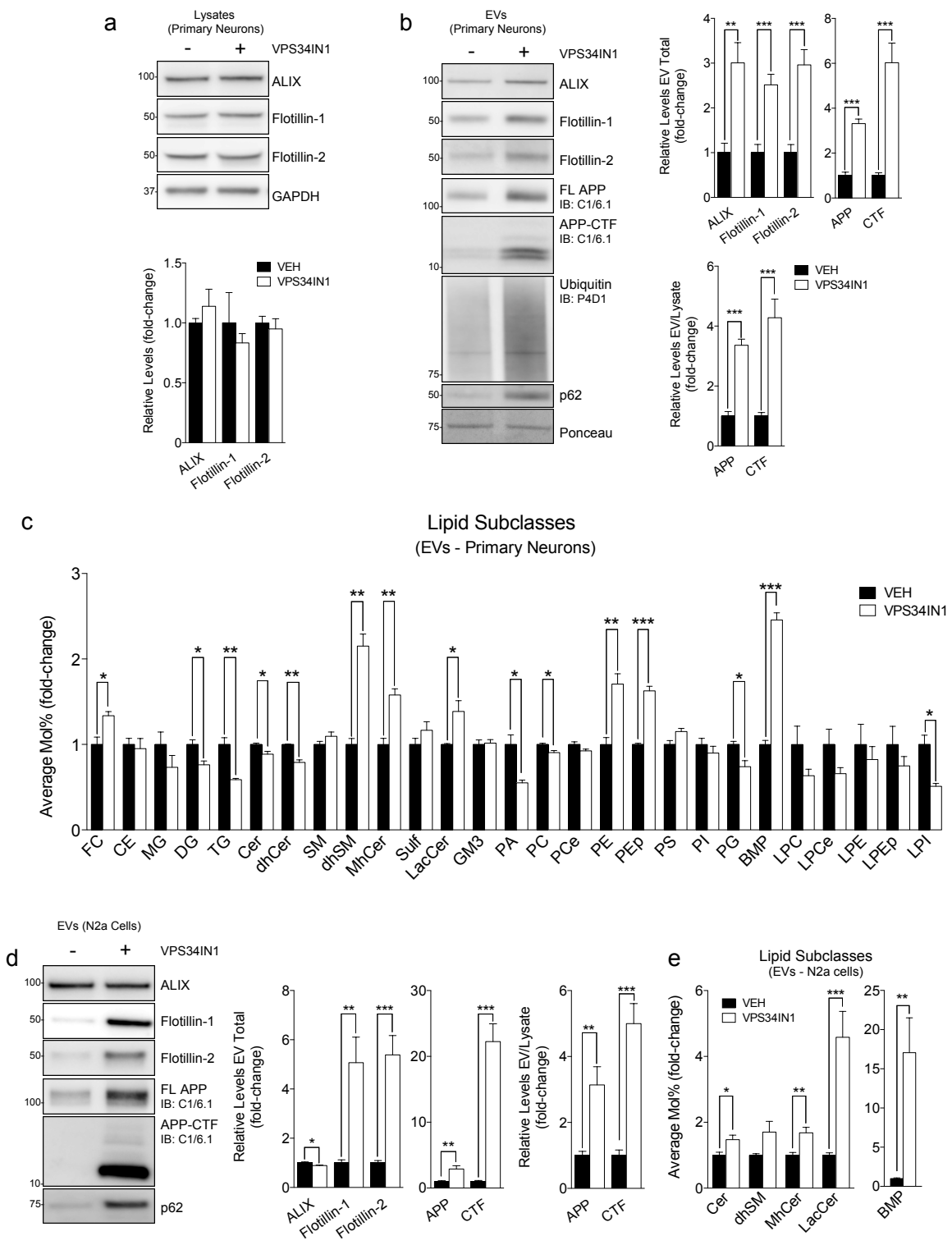


Figure 4 - Miranda et al

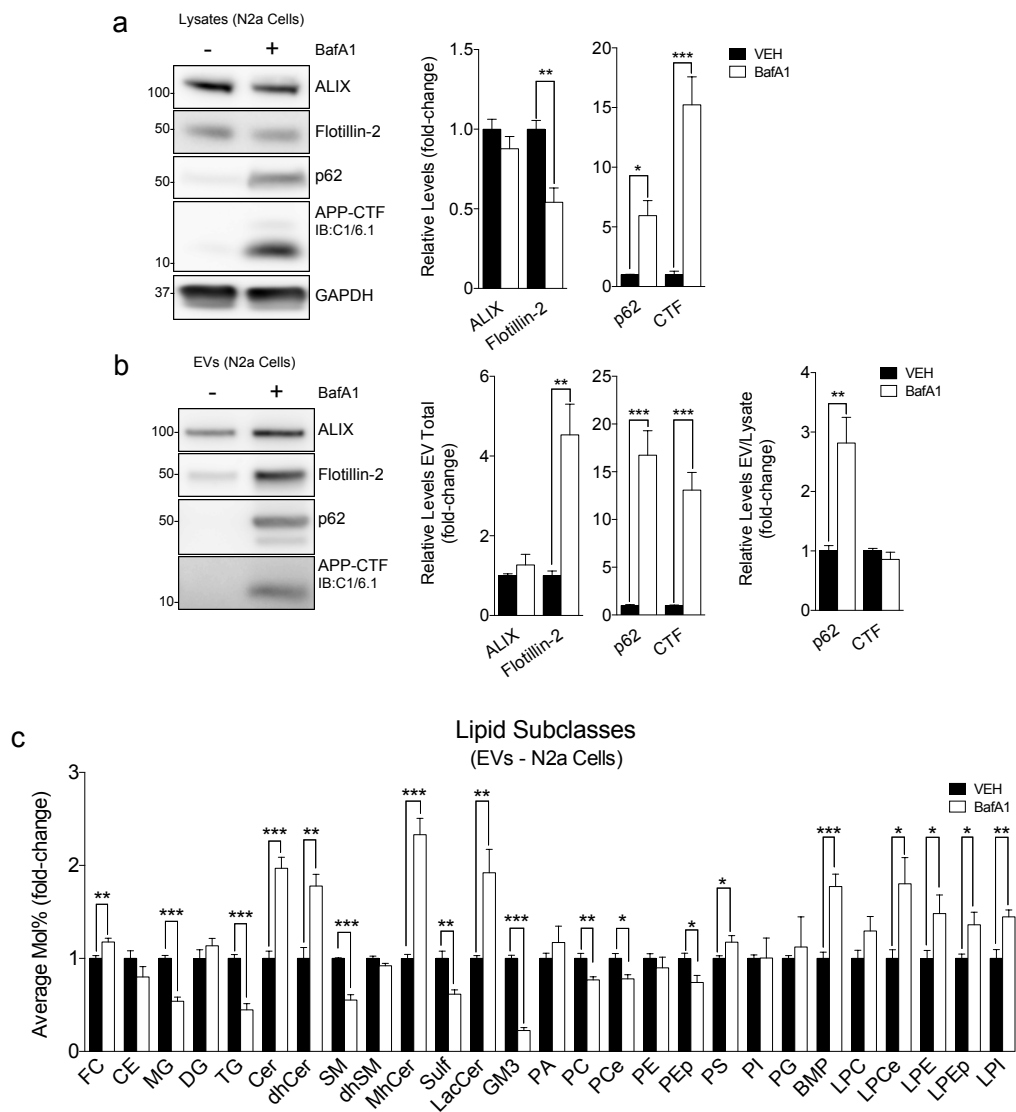


Figure 5 - Miranda et al

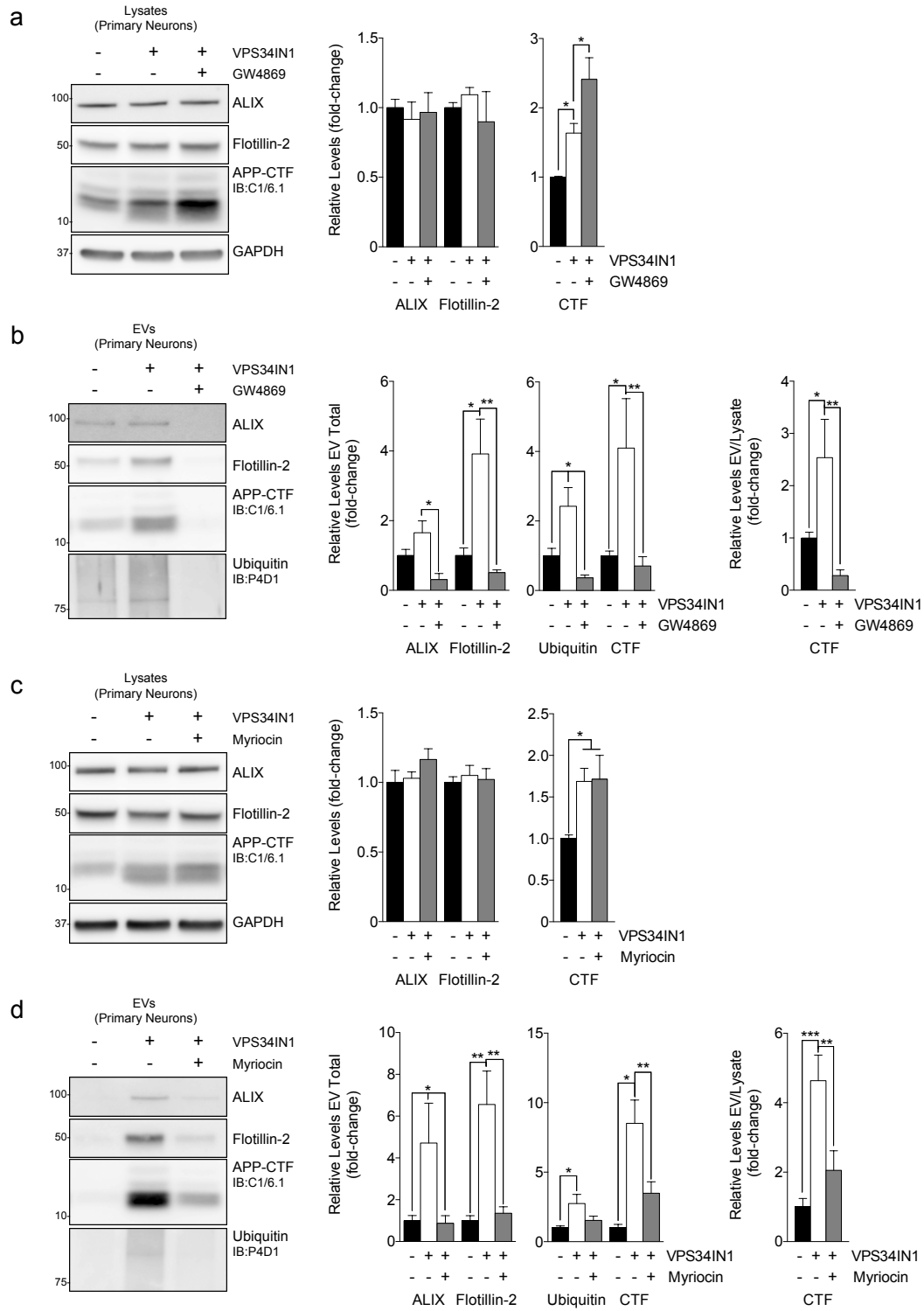


Figure 6 - Miranda et al

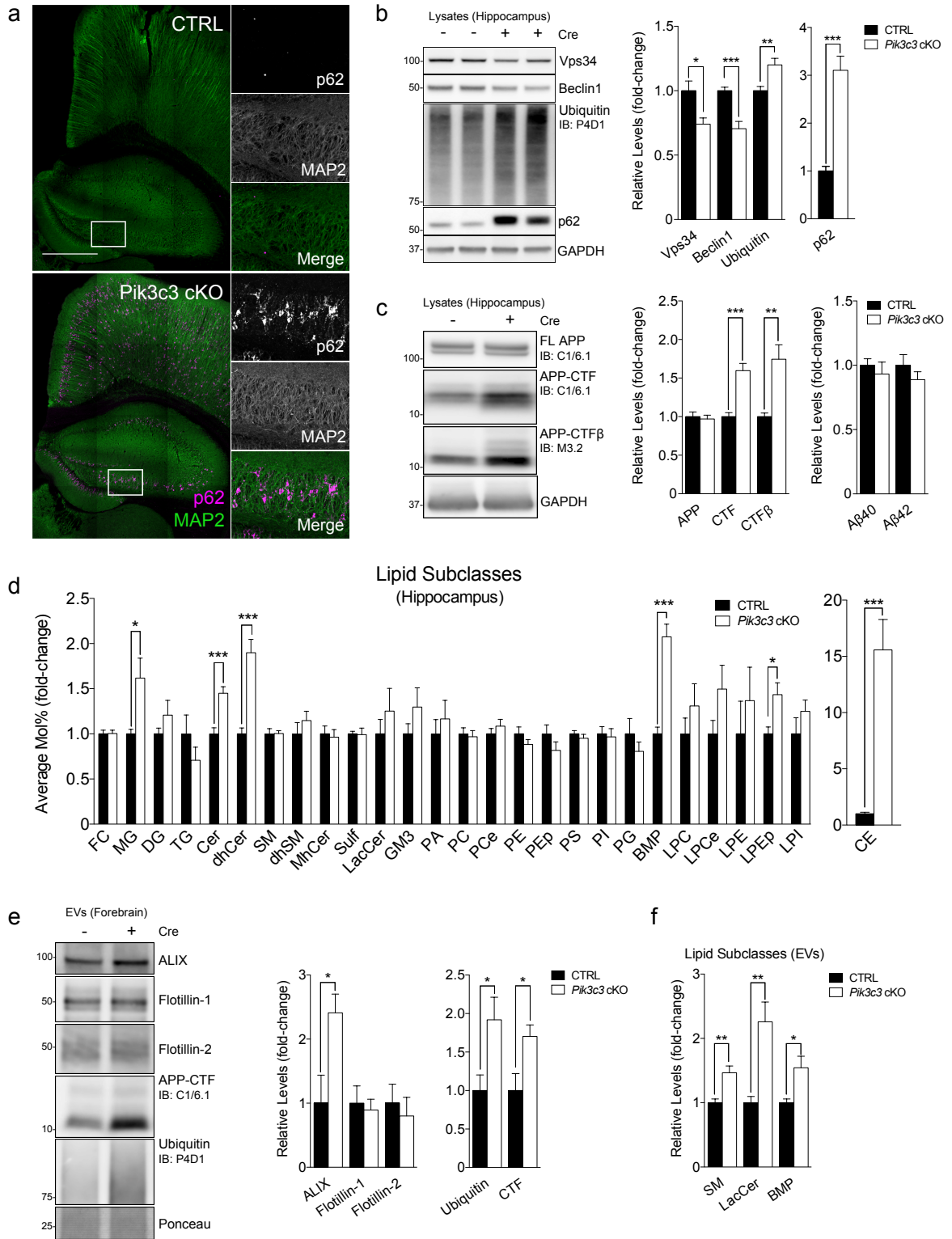


Figure 7 - Miranda et al

Chapter 2.1.1

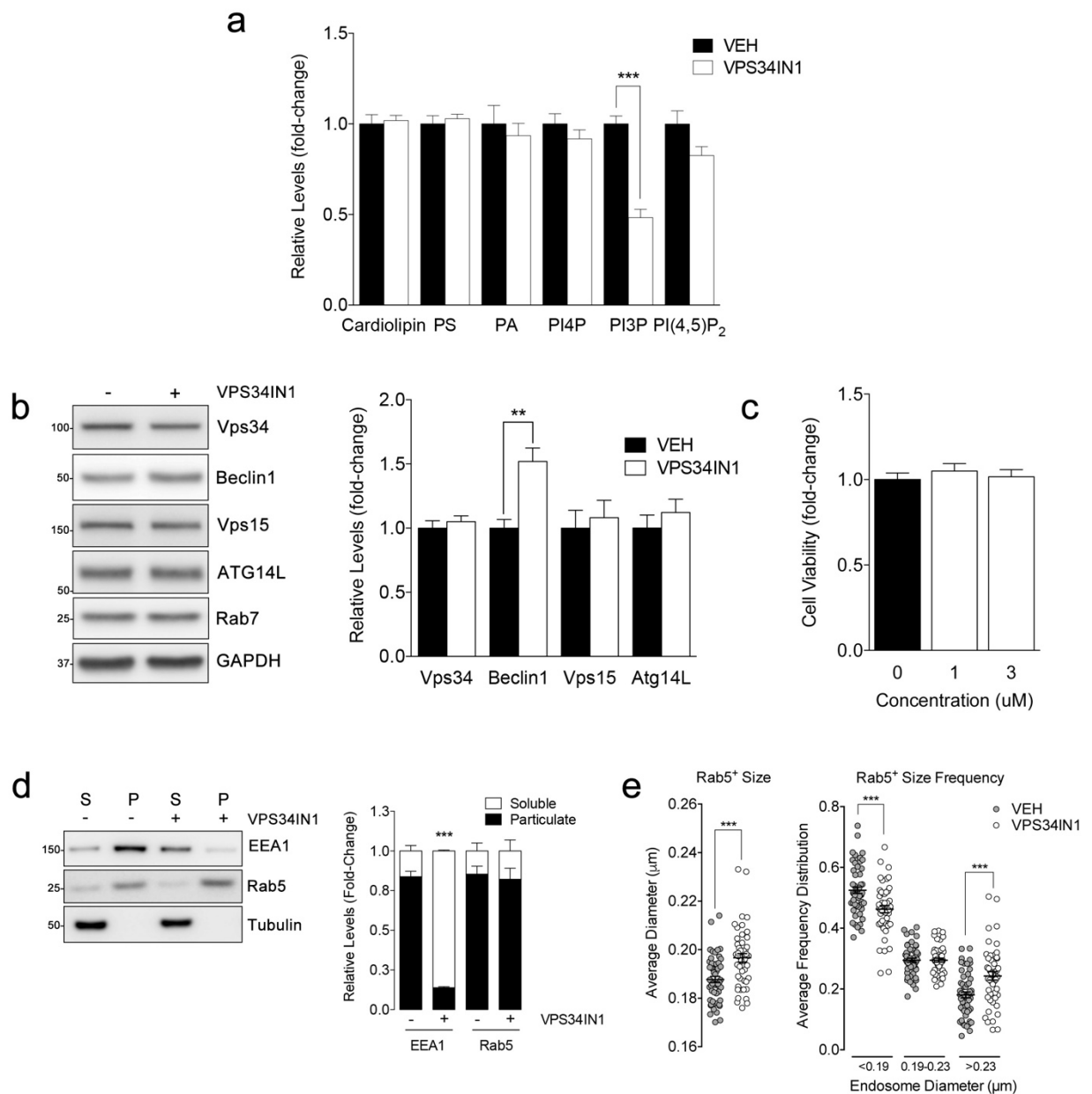
André M. Miranda, Zofia M. Laseicka, Yimeng Xu, Jessi Neufeld, Sanjid Shahriar, Sabrina Simoes,
Robin B. Chan, Tiago Gil Oliveira, Scott A. Small, Gilbert Di Paolo

**Neuronal lysosomal dysfunction releases exosomes harboring APP C-terminal
fragments and unique lipid signatures**

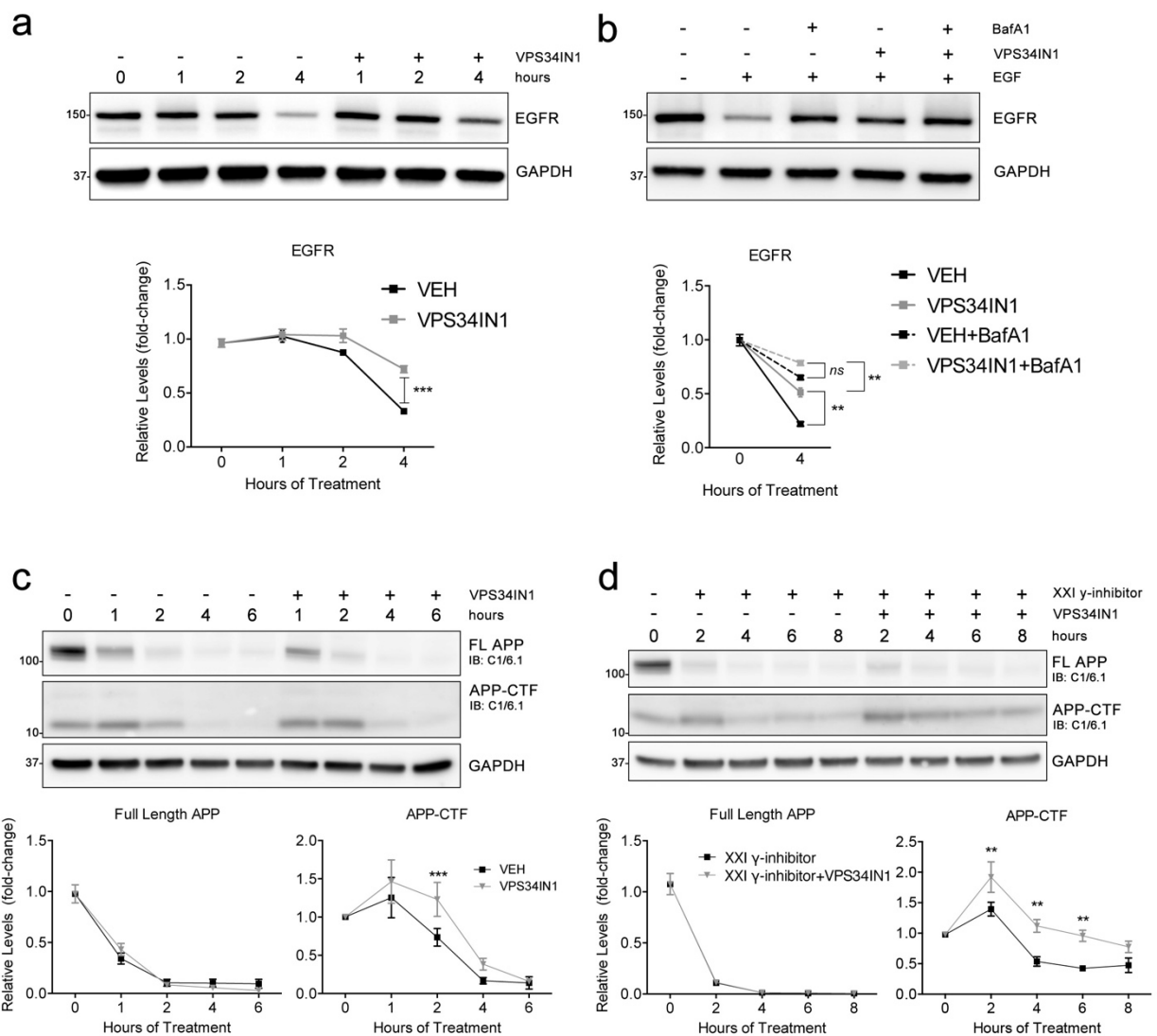
Supplementary Information

Nature Communications **9**(1):291 (2018)

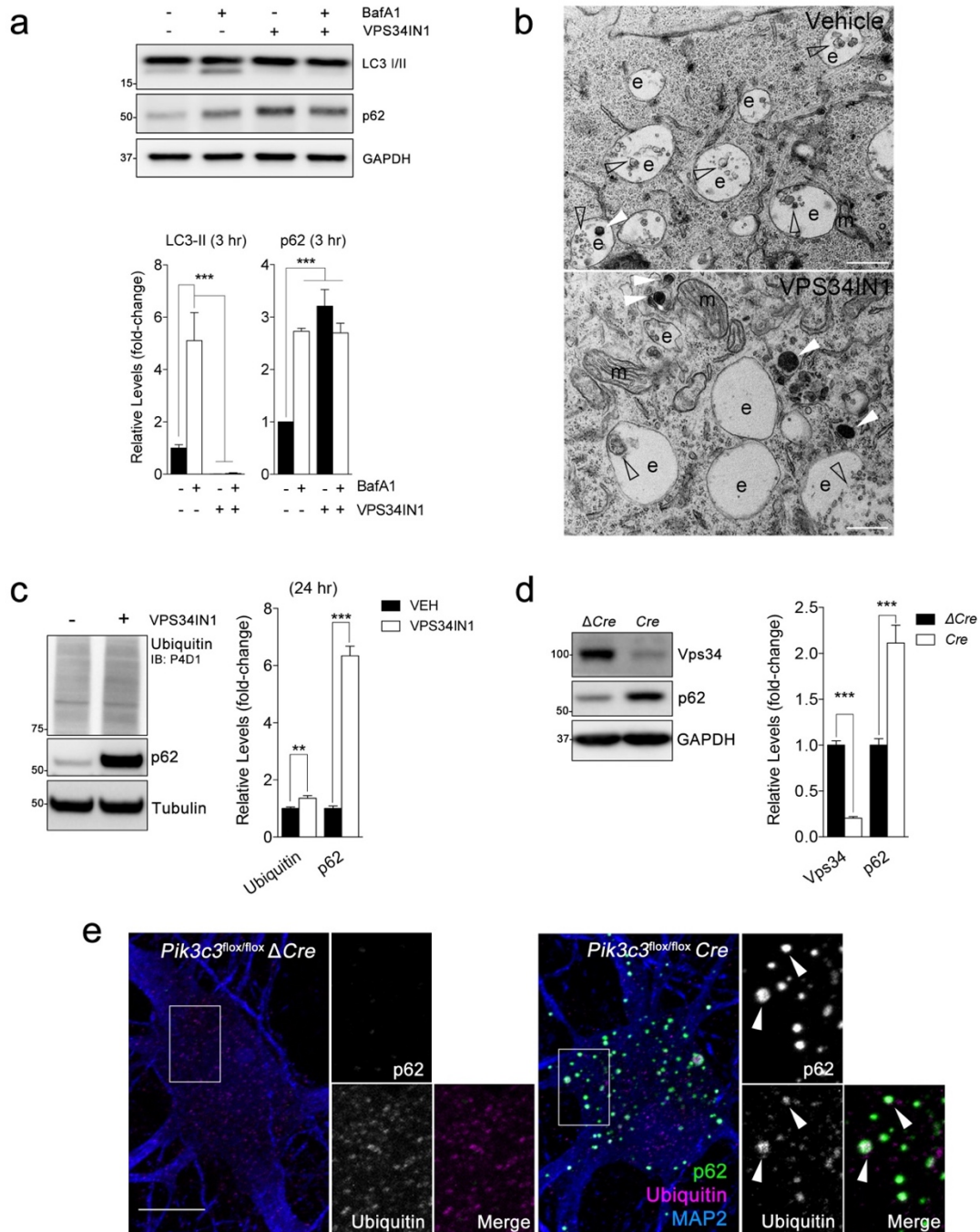
DOI: [10.1038/s41467-017-02533-w](https://doi.org/10.1038/s41467-017-02533-w)



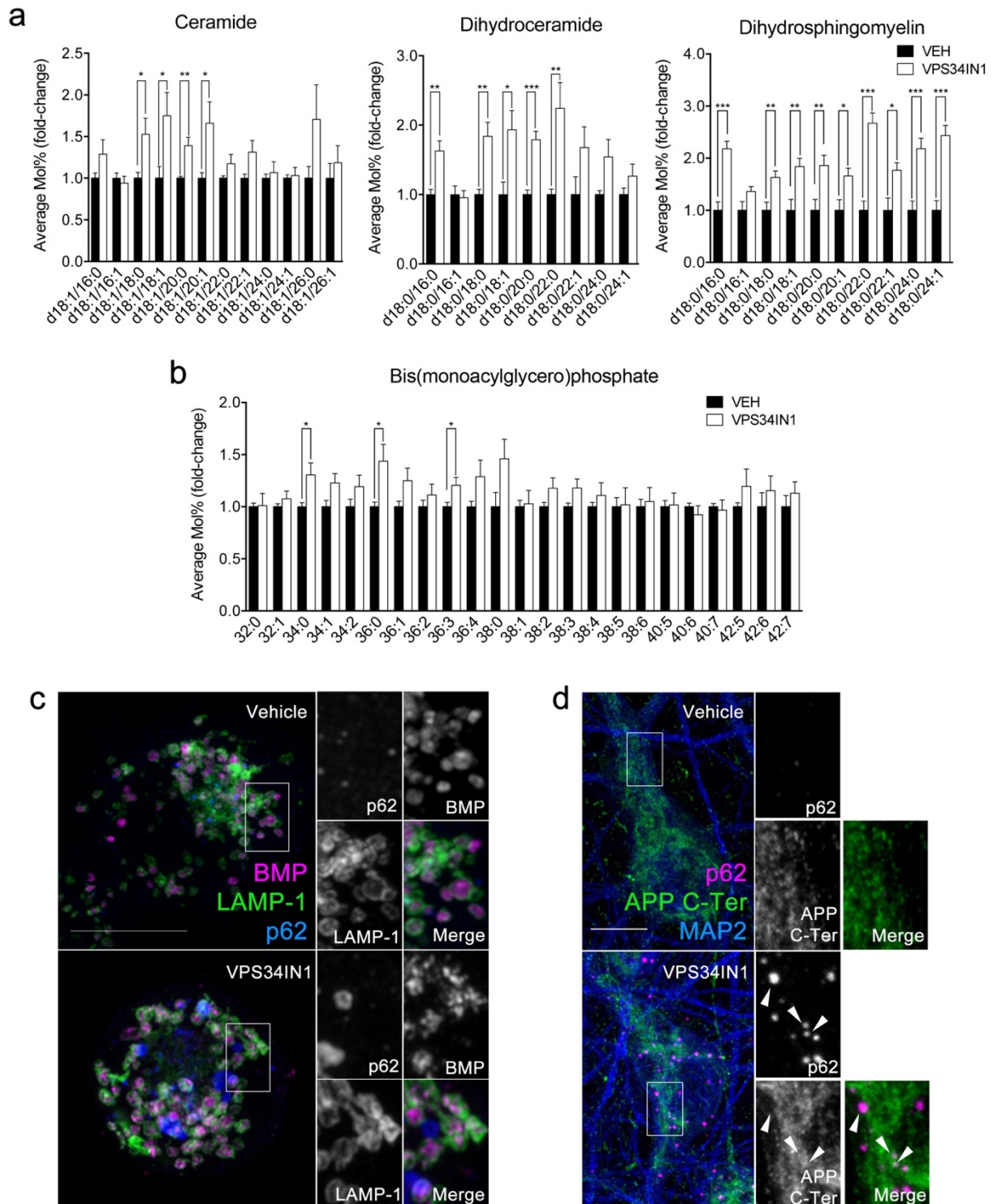
Supplementary Figure 1. VPS34IN1 reduces PI3P production and alters early endosome dynamics. a) Bar diagram showing lipid levels in N2a cells treated with VPS34IN1 at 1μM for 24 hr. Measurements were made by anionic exchange HPLC with suppressed conductivity detection, expressed in Mol% of total anionic phospholipids measured and normalized to vehicle (mean ± SEM, N=8, from two independent experiments). Phosphatidylserine (PS), Phosphatidic Acid (PA), Phosphatidylinositol-4-phosphate (PI4P), Phosphatidylinositol-3-phosphate (PI3P), Phosphatidylinositol-4,5-bisphosphate (PI(4,5)P₂). ***p<0.001 in two-tailed Student's t-test. **b)** Western blot analysis of protein levels of Vps34 interactors in cortical neurons treated with VPS34IN1 at 3μM for 24 hr. Rab7 was used as control. (mean ± SEM, N=4, from two independent experiments). **p<0.01 in two-tailed Student's t-test. **c)** Cortical neuron cell viability measured after treatment with VPS34IN1 at indicated doses for 24 hr (mean ± SEM, N=20, from two independent experiments). **d)** Western blot analysis of endosomal protein levels of N2a cells treated with VPS34IN1 at 3μM for 3 hr. Cell extracts were subjected to lysis and ultracentrifugation for extraction of soluble (S) or particulate (P) fractions. Values were expressed as fraction of total protein levels (sum of S and P fractions). Tubulin was used as loading control (mean ± SEM, N=3). ***p<0.001 in two-tailed Student's t-test. **e)** Size analysis of Rab5 puncta from cortical neurons treated with vehicle or VPS34IN1 at 3μM for 3 hr (Figure 1a). Bar graphs indicate average Rab5 puncta size, per cell. Puncta were categorized in three size classes for analysis of relative frequency (mean ± SEM, N=55 and 49, resp.). ***p<0.001 in two-tailed Student's t-test.



Supplementary Figure 2. VPS34IN1 delays ligand-induced receptor degradation and APP-CTF lysosomal clearance. **a**) Western Blot analysis of EGFR levels in cultured cortical neurons after EGF stimulation at 200ng/ml and vehicle or VPS34IN1 treatment at 3μM for the indicated time periods (mean ± SEM, N=3). ***p<0.001 in two-way ANOVA repeated measures, Holm-Sidak's multiple comparisons test. **b**) Western Blot analysis of EGFR levels in cultured cortical neurons after treatment as in **a**) plus BafA1 at 50nM for 4 hr. (mean ± SEM, N=3). **p<0.01 in two-way ANOVA repeated measures, Holm-Sidak's multiple comparisons test. **c**) Western Blot analysis of FL-APP and APP-CTF levels in N2a cells after pulse treatment with cycloheximide at 50μg/ml plus vehicle or VPS34IN1 at 1μM for the indicated time periods (mean ± SEM, N=4). ***p<0.001 in two-way ANOVA repeated measures, Holm-Sidak's multiple comparisons test. **d**) Western Blot analysis of FL-APP and APP-CTF levels in N2a cells treated as in **c**) plus XXI γ-inhibitor at 2μM for the indicated time periods (mean ± SEM, N=4). **p<0.01 in two-way ANOVA repeated measures, Holm-Sidak's multiple comparisons test.

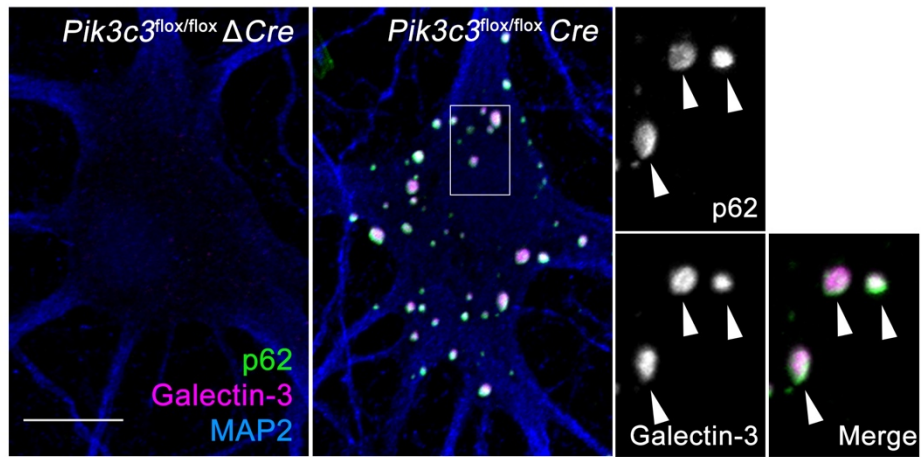


Supplementary Figure 3. VPS34 inhibition blocks autophagosome initiation and causes accumulation of p62 and poly-ubiquitinated proteins. **a**) Western Blot analysis of LC3 lipidation and p62 protein levels in cortical neurons after treatment with vehicle, Bafilomycin A1 (BafA1) at 50nM, VPS34IN1 at 3μM or co-treatment for 3 hr. Bar graphs denote average protein levels normalized to vehicle. (mean ± SEM, N=6 for LC3, N=3 for p62, from two independent experiments). ***p<0.001 in one-way ANOVA, Holm-Sidak's multiple comparisons test. **b**) Ultrastructural electron microscopic analysis of endocytic compartments of primary cortical neurons treated with vehicle or VPS34IN1 for 24 hr. Full arrows, electron-dense vesicles; empty arrows, intraluminal vesicles; e, endosome; m, mitochondrion. Scale bar, 500nm. **c**) Western Blot analysis of ubiquitin and p62 levels in cortical neurons after treatment with VPS34IN1 at 3μM for 24 hr. Bar graph indicates average protein levels normalized to vehicle (mean ± SEM, n=8, from two independent experiments). **p<0.01, ***p<0.001 in two-tailed Student's t-test. **d**) Western blot analysis of Vps34 and p62 levels in *Pik3c3^{fllox/fllox}* cortical neurons virally transduced with inactive (ΔCre) and active *Cre* (*Cre*) recombinase for 7 days. Bar graph indicates average protein levels normalized to ΔCre (mean ± SEM, N=8, from two independent experiments). ***p<0.001 in two-tailed Student's t-test. **e**) Representative confocal images of *Pik3c3^{fllox/fllox}* cortical neurons virally transduced with ΔCre and *Cre* for 7 days. Arrows highlight p62 and ubiquitin colocalization. Scale bar, 10μm.

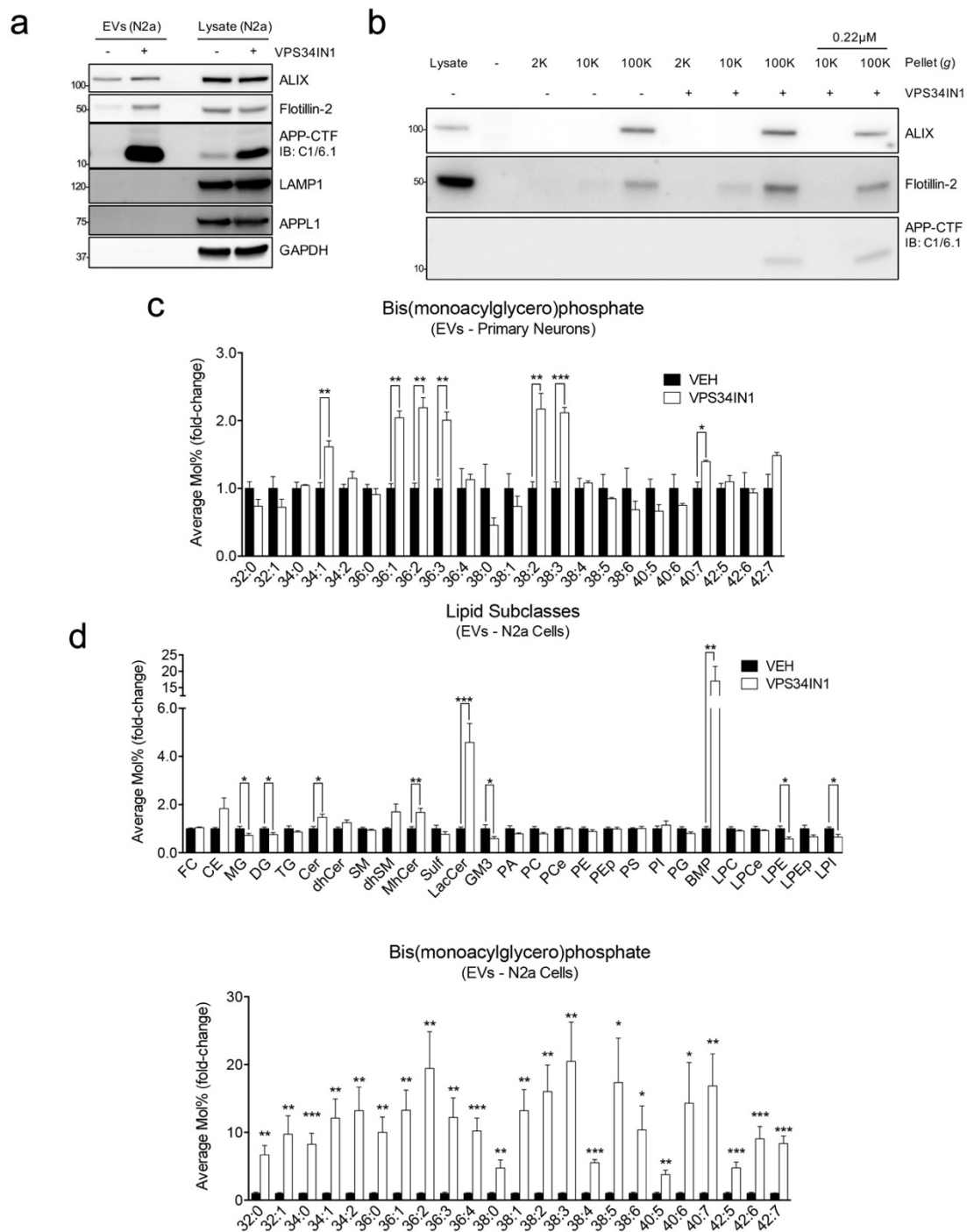


Supplementary Figure 4. Effect of VPS34IN1 treatment on lipid metabolism, BMP and APP localization.

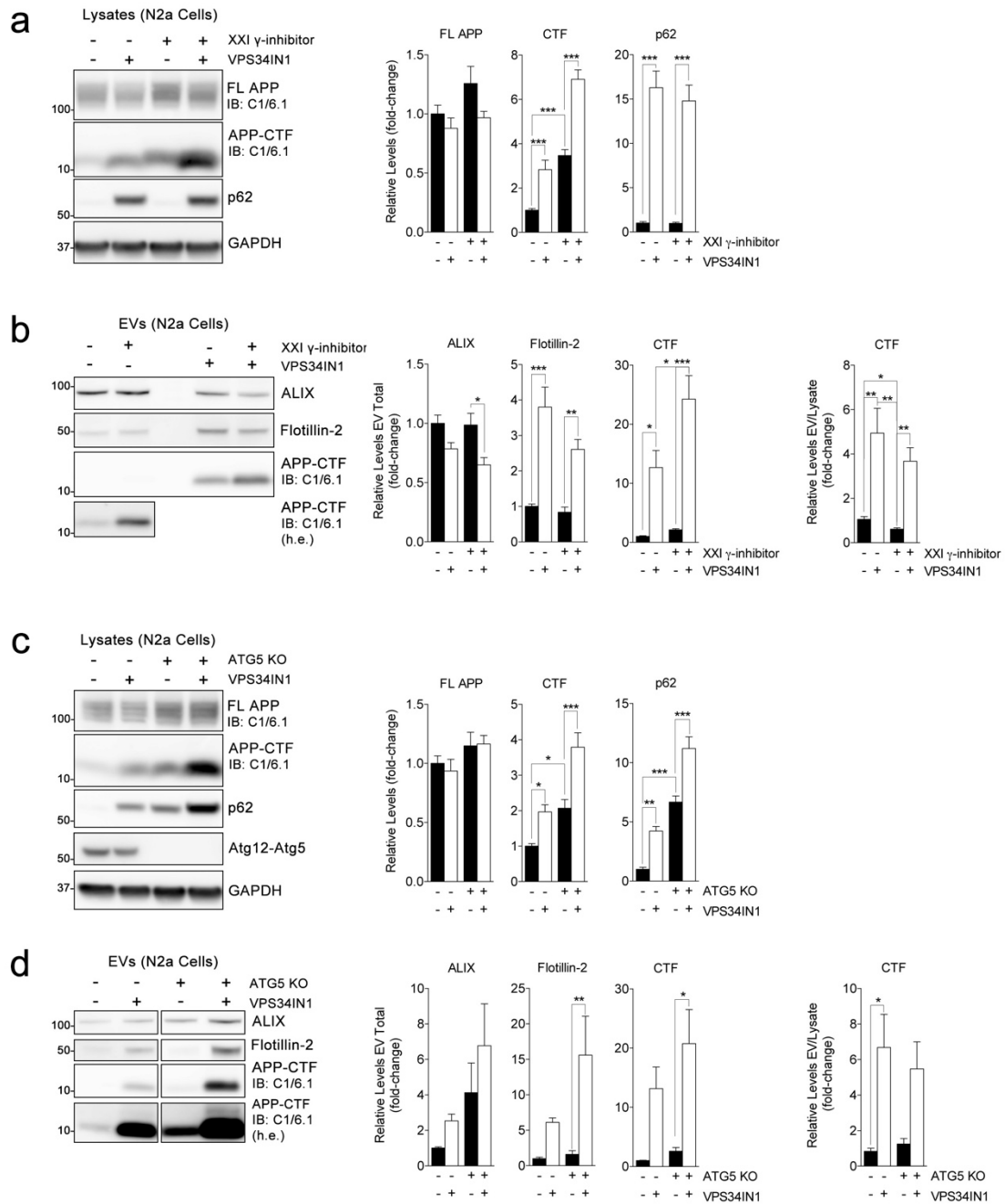
a-b) Molecular species analysis of ceramide (Cer), dihydroceramide (dhCer), dihydrosphingomyelin (dhSM) and Bis(Monoacylglycero)Phosphate (BMP) from primary cortical neurons treated with vehicle or VPS34IN1 at 3 μ M for 24 hr. Values were expressed as average Mol% of total lipid measured, normalized to vehicle. Lipids are annotated per total acyl carbons and degree of unsaturation (mean \pm SEM, N=8, from two independent experiments) * $p < 0.05$, ** $p < 0.01$, *** $p < 0.001$ in two-tailed Student's t-test. **c)** Representative confocal images of N2a cells treated with vehicle or VPS34IN1 at 1 μ M for 24hr and immunostained for LAMP-1, p62 and BMP (see Methods). Airyscan insets highlight luminal enrichment of BMP in LAMP-1-positive compartments in both experimental conditions. Scale bar, 10 μ m. **d)** Representative confocal images of cortical neurons treated with vehicle or VPS34IN1 at 3 μ M for 24 hr and immunostained for MAP2, APP cytodomain (C1/6.1) and p62. APP C1/6.1 antibody cross-reacts with both FL-APP and APP-CTFs. Arrows highlight p62-positive structures in proximity to APP signal. Scale bar, 10 μ m.



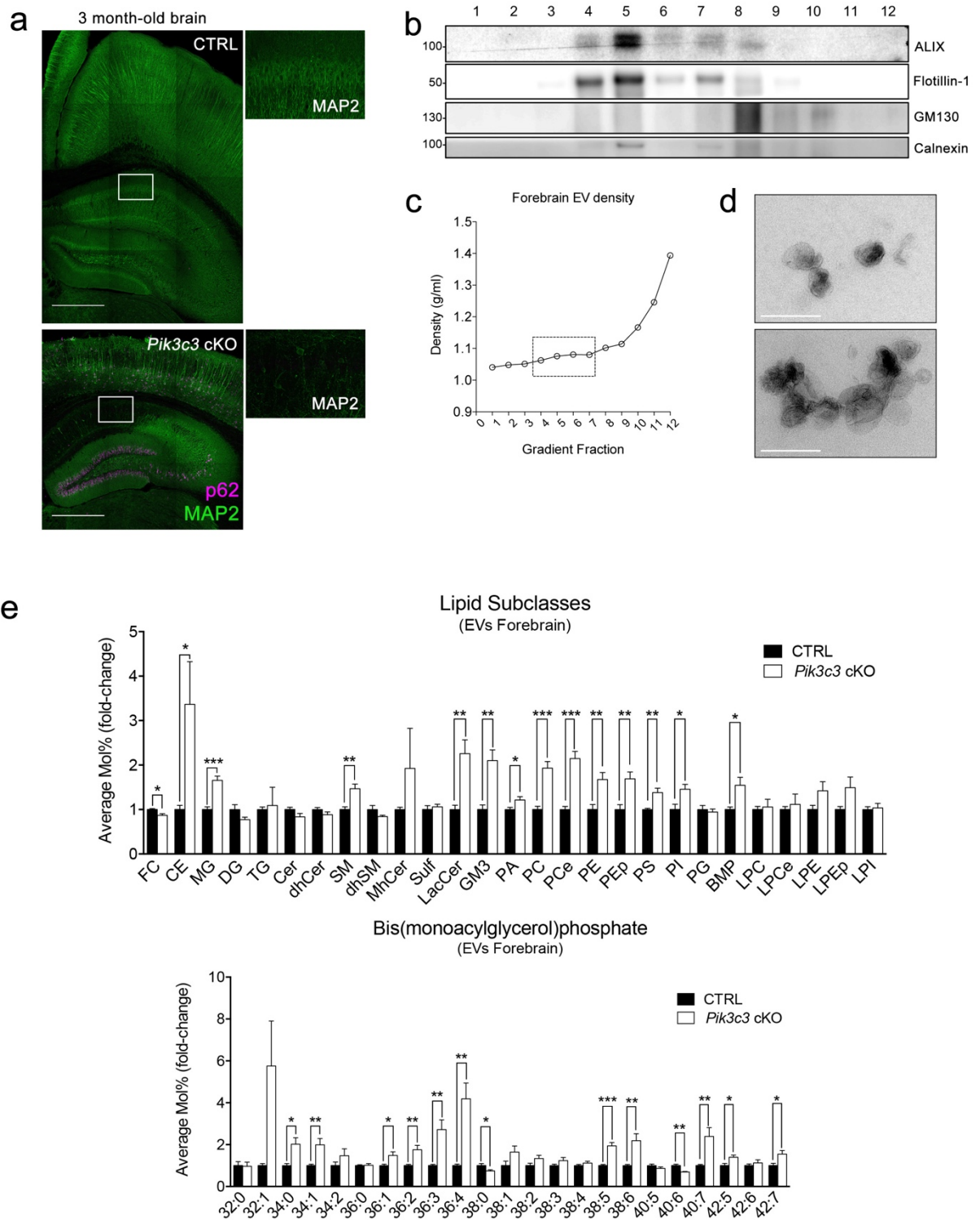
Supplementary Figure 5. Vps34 KO neurons phenocopy endolysosomal membrane damage detected with Vps34 pharmacological inhibition. Representative confocal images of cultured cortical neurons 8 days post lentiviral infection with ΔCre or Cre recombinase. Arrows highlight p62 and galectin-3 colocalization. Scale bar, 10 μ m.



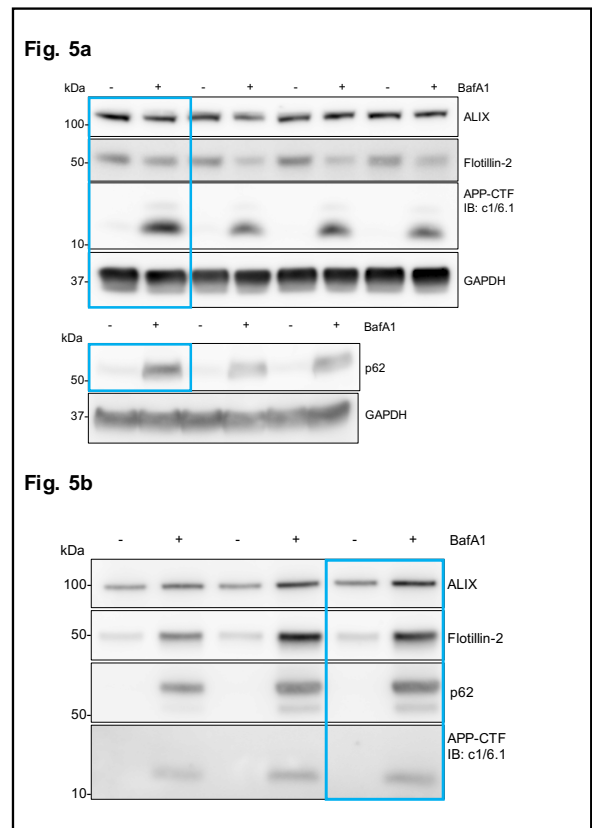
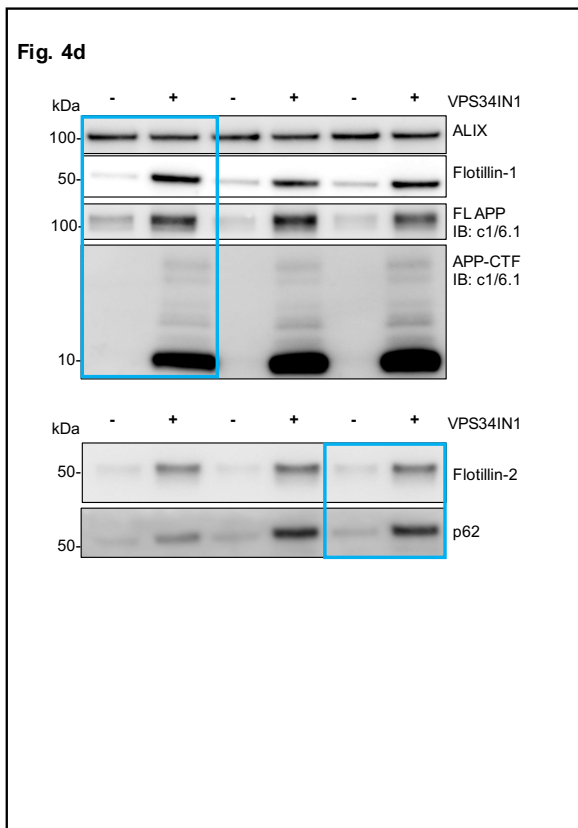
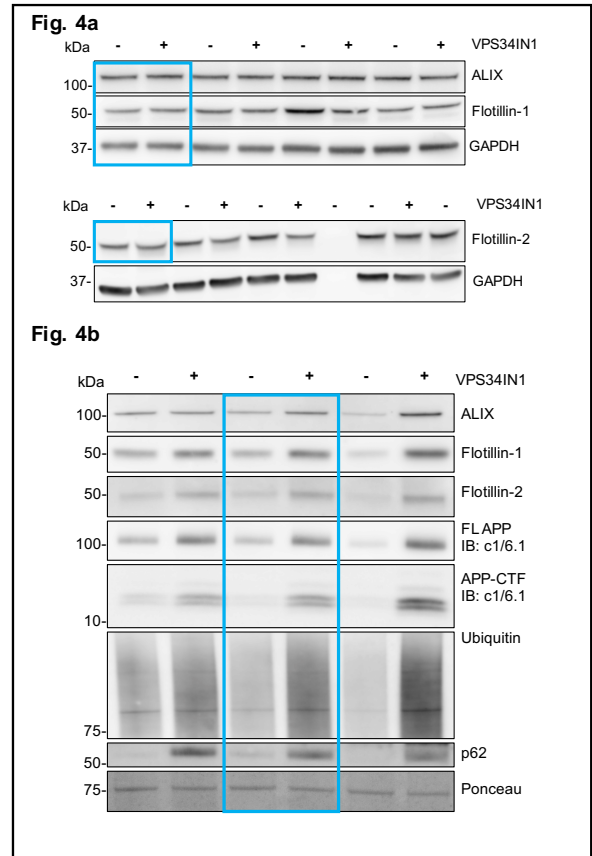
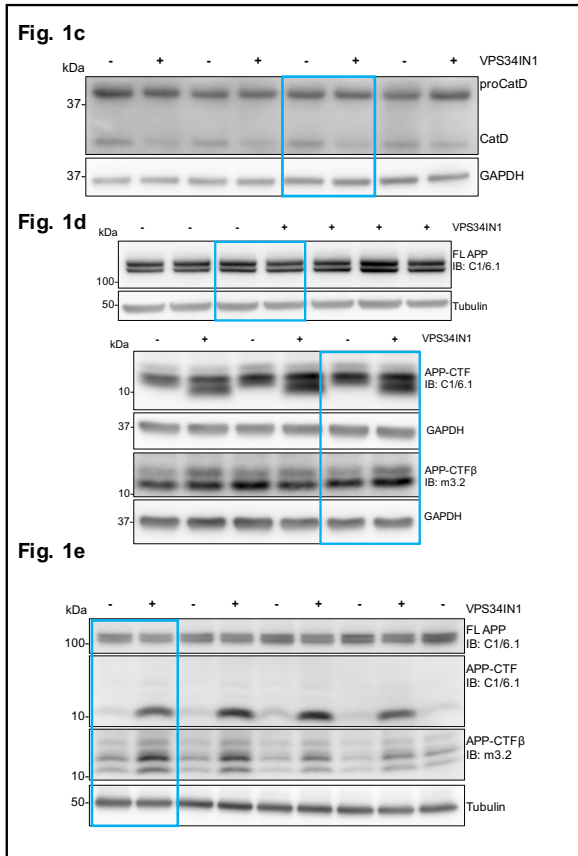
Supplementary Figure 6. EVs secreted upon VPS34IN1 treatment are enriched for multiple BMP species, both in neurons and N2a cells. a-b) Western blot analysis of N2a cell lysates and EV fractions after treatment with vehicle or VPS34IN1 at $1\mu\text{M}$ for 24hr. Note exclusion of late endosome/lysosomal marker LAMP-1, early endosome marker APPL1 and cytosolic protein GAPDH from EV preparations. **b)** Cell media was sequentially ultracentrifuged at indicated g 's or alternatively filtered with a $0.22\mu\text{m}$ filter and ultracentrifuged at $100,000g$. EV markers were enriched and APP-CTFs exclusively present in the $100,000g$ pellet. **c)** Molecular species analysis of BMP extracted from EVs purified from cortical neuron culture media after treatment with vehicle or VPS34IN1 at $3\mu\text{M}$ for 24 hr. Values were expressed as average Mol% of total lipid measured, normalized to vehicle. Lipids are annotated per total acyl carbons and degree of unsaturation (mean \pm SEM, $N=3$ each from a pool of two biological replicates) **d)** Upper panel, LC-MS analysis of lipids extracted from EVs collected from N2a cell culture media after treatment with vehicle or VPS34IN1 at $1\mu\text{M}$ for 24 hr. Lower panel, molecular species analysis of BMP from EVs collected from N2a cell culture media under the same treatment conditions. Values were expressed as average Mol% of total lipids measured, normalized to vehicle (mean \pm SEM $N=7$ each from a pool of two biological replicates) * $p<0.05$, ** $p<0.01$, *** $p<0.001$ in two-tailed Student's t-test.



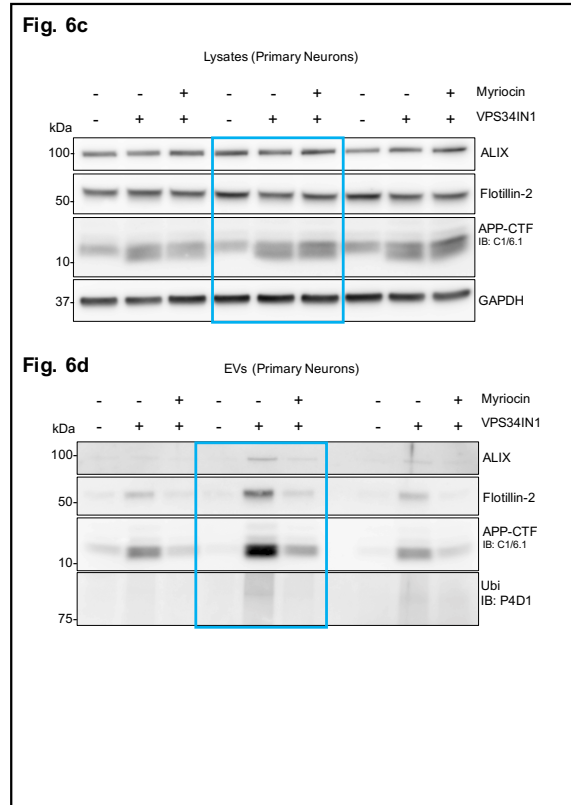
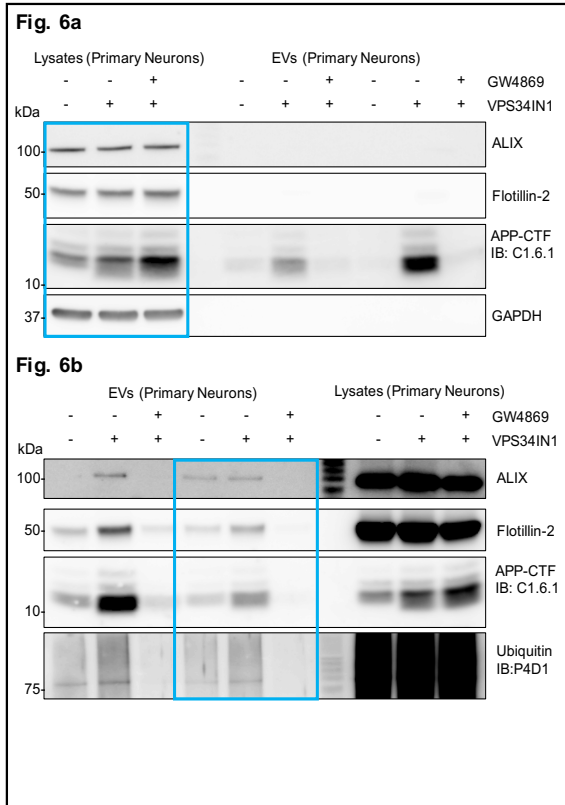
Supplementary Figure 7. Secretion of exosomal APP-CTFs does not simply reflect cellular accumulation of APP-CTFs. a-b) Western blot analysis of cell lysates and EVs from N2a cells treated with vehicle, XXI γ -inhibitor at 2 μ M, VPS34IN1 at 1 μ M or co-treated for 24 hr. EV protein levels were normalized to lysate total protein (EV total) or lysate levels of the corresponding protein (EV/Lysate ratio). Bar graph denotes average protein levels normalized to vehicle (mean \pm SEM, N=5-6, from two independent experiments). * $p < 0.05$, ** $p < 0.01$, *** $p < 0.001$ in one-way ANOVA, Holm-Sidak's multiple comparisons test. **c-d)** Western blot analysis of cell lysates and EVs from ATG5-KO N2a and isogenic control cells treated with vehicle or VPS34IN1 at 1 μ M for 24 hr. EV protein levels were normalized to lysate total protein (EV total) or lysate levels of the corresponding protein (EV/Lysate ratio). Bar graph denotes average protein levels normalized to control cells. (mean \pm SEM, N=5-6, from two independent experiments). * $p < 0.05$, ** $p < 0.01$, *** $p < 0.001$ in one-way ANOVA, Holm-Sidak's multiple comparisons test.



Supplementary Figure 8. *In vivo* Vps34 cKO causes age-dependent neurodegeneration and secretion of EVs with a distinct lipid signature. a) Brain sections from *Pik3c3^{lox/lox}* (CTRL) and *Pik3c3^{lox/lox} Camk11a-Cre* (*Pik3c3* cKO) mice at 3 months immunostained for MAP2 and p62. Scale bar, 500µm. **b-d)** Validation of EVs purified from wild-type C57BL/6 mice and floated on an Optiprep gradient. **b)** Western blot analysis demonstrates the presence of exosomal markers ALIX and flotillin-1 in fractions 4-7. These fractions were pooled for downstream analysis. **c)** Density of recovered fractions, measured by refractometry. **d)** Representative wide-field EM images of EVs purified from wild-type C57BL/6 mice. Scale bar, 200nm. **e)** Upper panel, LC-MS analysis of lipids extracted from EVs collected from CTRL or *Pik3c3* cKO mice at 2 months. Lower panel, molecular species analysis of BMP. Values were expressed as average Mol% of total lipids measured, normalized to vehicle (mean ± SEM N=6, from two independent experiments) * p<0.05, ** p<0.01, *** p<0.01 in two-tailed Student's t-test.



Supplementary Figure 9. Extended data of Western Blot cropped in main and supplementary figures.
Blue rectangles indicate lanes cropped.



Supplementary Figure 9 (continued).

Fig. 7b

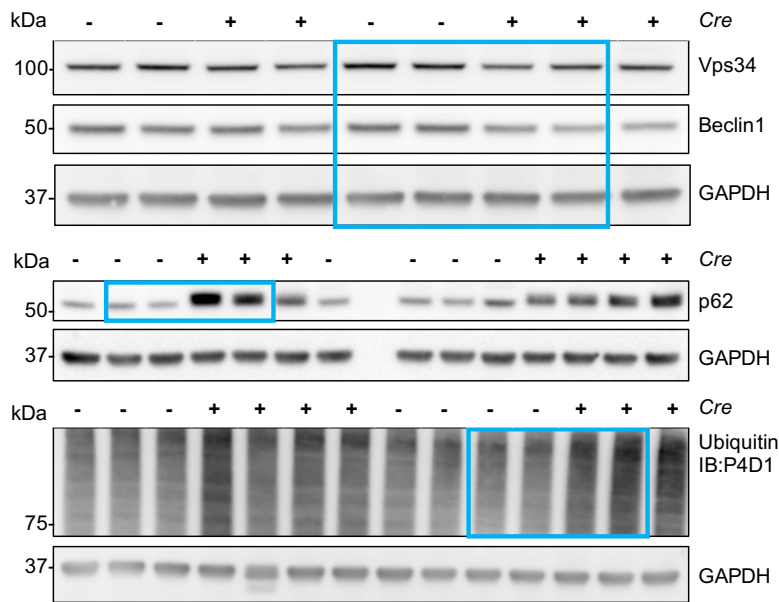


Fig. 7c

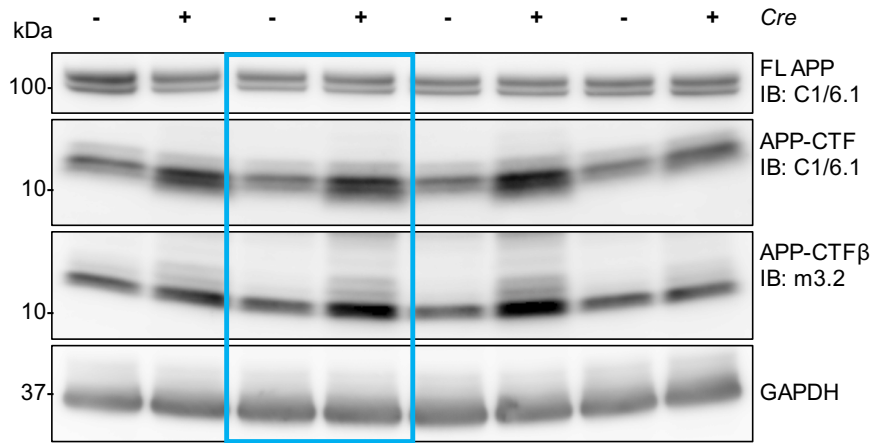
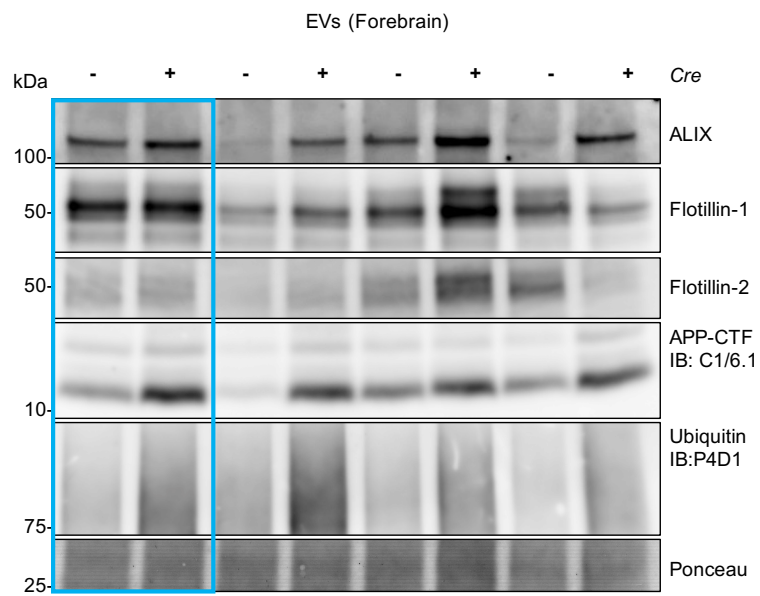
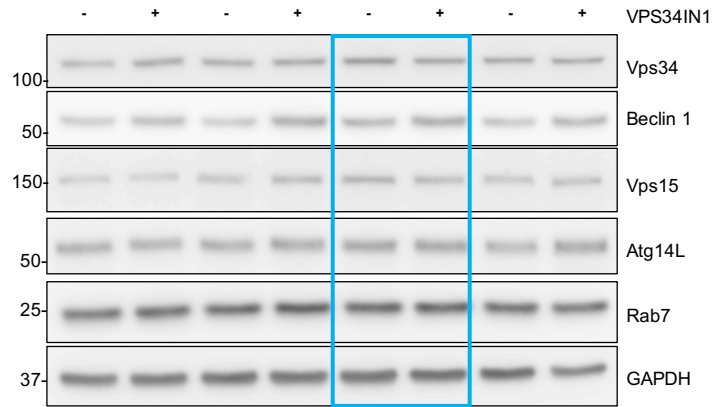


Fig. 7f

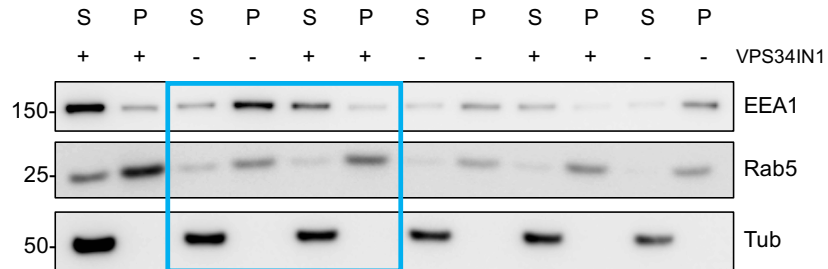


Supplementary Figure 9 (continued).

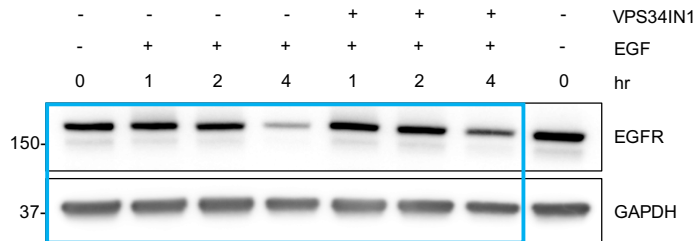
Supplementary Fig. S1b



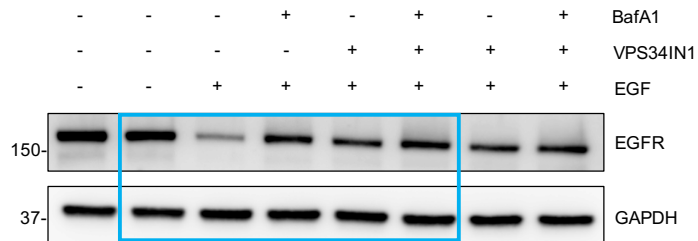
Supplementary Fig. S1d



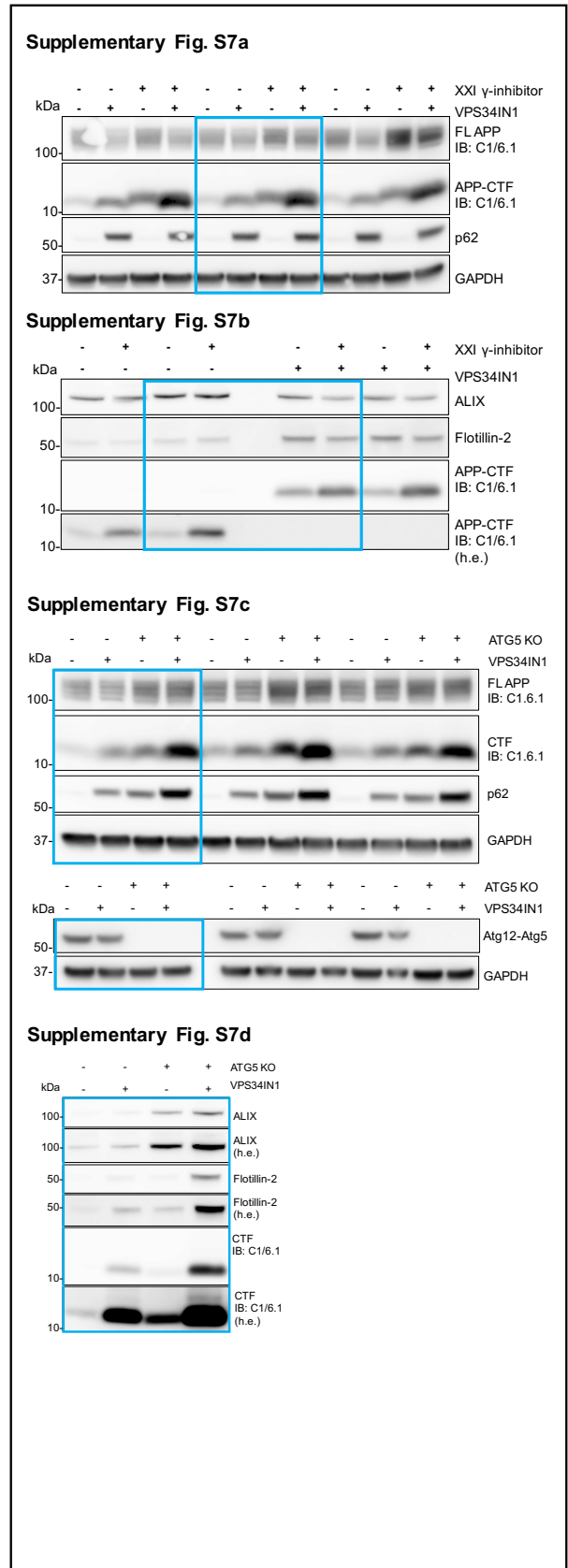
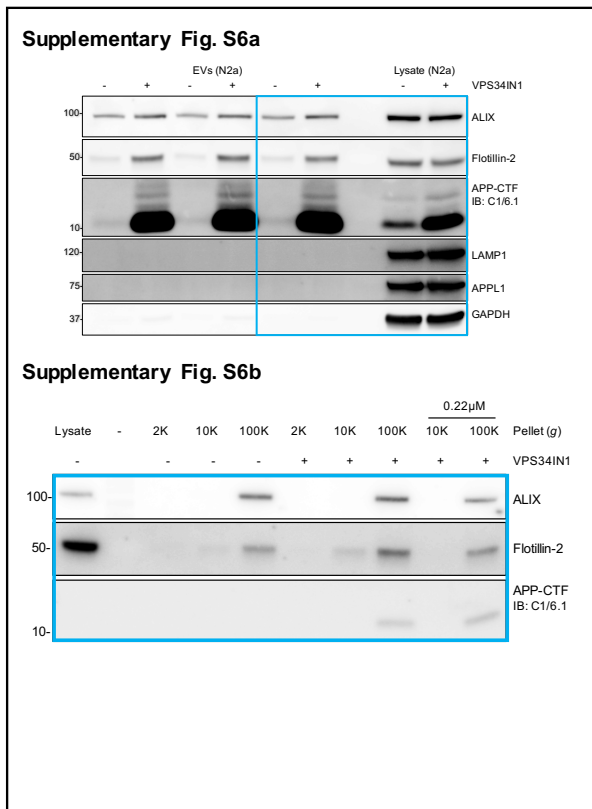
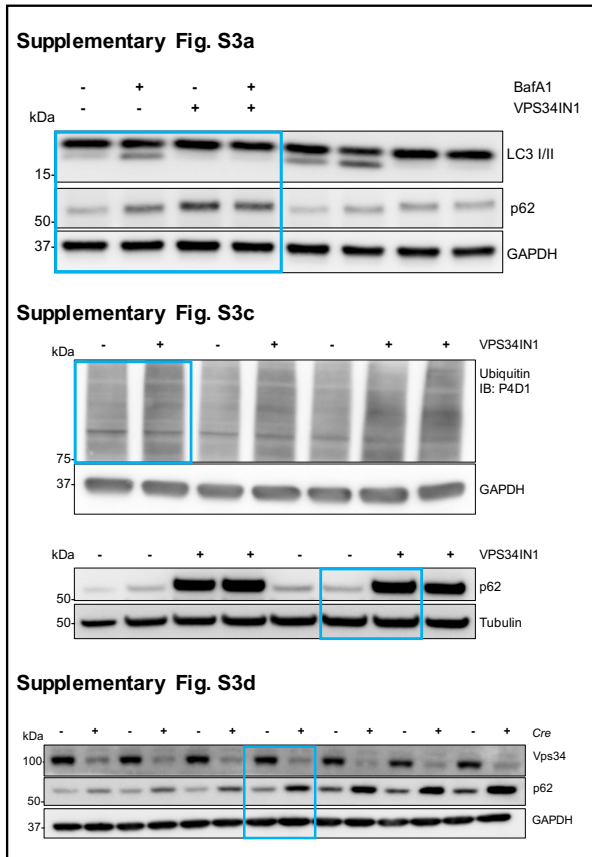
Supplementary Fig. S2a



Supplementary Fig. S2b



Supplementary Figure 9 (continued).



Supplementary Figure 9 (continued).

Figure 1				
Fig.	Test		p value	Sig.
Fig.1A	2t t-test	EEA1 Size	1E-23	***
Fig.1A	2t t-test	EEA1 Intensity	3E-18	***
	2t t-test	Rab5 Intensity	5E-15	***
Fig.1B	2t t-test	APPL1/Rab5 Coloc.	3E-15	***
Fig.1C	2t t-test	Total CatD	0.515	
	2t t-test	CatD/Total CatD	8E-06	***
Fig.1D	2t t-test	APP	0.8791	
	2t t-test	CTF	0.0009	**
	2t t-test	CTFβ	0.0045	**
	2t t-test	Aβ40	0.0037	**
	2t t-test	Aβ42	0.0347	*
Fig.1E	2t t-test	APP	0.3483	
	2t t-test	CTF	0.0005	***
	2t t-test	CTFβ	2E-05	***
	2t t-test	Aβ40	4E-07	***
	2t t-test	Aβ42	2E-07	***

Figure 2				
Fig.	Test		p value	Sig.
Fig.2A	2t t-test	LC3 Intensity	0.0001	***
	2t t-test	P62 Intensity	0.0001	***

Figure 3					
Fig.	Test		p value	Sig.	
Fig.3A	2t t-test	FC	0.8617		
	2t t-test	CE	0.8247		
	2t t-test	MG	0.4392		
	2t t-test	DG	0.2778		
	2t t-test	TG	0.6804		
	2t t-test	Cer	0.026	*	
	2t t-test	dhCer	0.0016	**	
	2t t-test	SM	0.497		
	2t t-test	dhSM	0.0022	**	
	2t t-test	MhCer	0.2317		
	2t t-test	Sulf	0.1093		
	2t t-test	LacCer	0.2228		
	2t t-test	GM3	0.6619		
	2t t-test	PA	0.7622		
	2t t-test	PC	0.3272		
	2t t-test	PCe	0.763		
	2t t-test	PE	0.2654		
	2t t-test	PEp	0.3738		
	2t t-test	PS	0.8714		
	2t t-test	PI	0.6845		
	2t t-test	PG	0.8493		
	2t t-test	BMP	0.2739		
	2t t-test	LPC	0.1501		
	2t t-test	LPCe	0.1249		
	2t t-test	LPE	0.8075		
	2t t-test	LPEp	0.4128		
	2t t-test	LPI	0.2446		
	Fig.3B	2t t-test	Galectin-3 Puncta	1E-09	***
		2t t-test	Gal-3/P62 Coloc	5E-23	***
		2t t-test	Ub/Gal-3 Coloc	1E-08	***

Figure 4					
Fig.	Test		p value	Sig.	
Fig.4A	2t t-test	ALIX	0.3625		
	2t t-test	Flotillin-1	0.5513		
	2t t-test	Flotillin-2	0.6205		
Fig.4B	Total Levels		-		
	2t t-test	ALIX	0.0024	**	
	2t t-test	Flotillin-1	0.0005	***	
	2t t-test	Flotillin-2	0.0005	***	
	2t t-test	APP	3E-06	***	
	2t t-test	CTF	0.0002	***	
		EV/Lysate Ratio		-	
	2t t-test	APP	3E-06	***	
	2t t-test	CTF	0.0004	***	
	Fig.4C	2t t-test	FC	0.0275	*
		2t t-test	CE	0.7373	
		2t t-test	MG	0.254	
		2t t-test	DG	0.0282	*
		2t t-test	TG	0.0071	**
		2t t-test	Cer	0.0355	*
2t t-test		dhCer	0.0022	**	
2t t-test		SM	0.1963		
2t t-test		dhSM	0.0019	**	
2t t-test		MhCer	0.0047	**	
2t t-test		Sulf	0.2482		
2t t-test		LacCer	0.0386	*	
2t t-test		GM3	0.8147		
2t t-test		PA	0.0181	*	
2t t-test		PC	0.0239	*	
2t t-test	PCe	0.1052			
2t t-test	PE	0.0082	**		
2t t-test	PEp	0.0003	***		
2t t-test	PS	0.0613			
2t t-test	PI	0.4017			
2t t-test	PG	0.0298	*		
2t t-test	BMP	0.0001	**		
2t t-test	LPC	0.1833			
2t t-test	LPCe	0.1479			
2t t-test	LPE	0.563			
2t t-test	LPEp	0.3508			
2t t-test	LPI	0.0123	*		
Figure 4D	Total Levels		-		
	2t t-test	ALIX	0.0407	*	
	2t t-test	Flotillin-1	0.003	**	
	2t t-test	Flotillin-2	0.0002	***	
	2t t-test	APP	0.0045	**	
	2t t-test	CTF	1E-05	***	
		EV/Lysate Ratio		-	
	2t t-test	APP	0.0035	**	
	2t t-test	CTF	8E-05	***	
	Figure 4E	2t t-test	Cer	0.0146	*
		2t t-test	dhSM	0.0545	
		2t t-test	MhCer	0.0033	**
		2t t-test	LacCer	0.0007	***
		2t t-test	BMP	0.0035	**

Supplementary Table 1. Statistical analysis information for main and supplementary Figures. *p<0.05, **p<0.01, ***p<0.001, color-coded by light pink, pink and red, respectively. 2t t-test: two-tailed unpaired Student's t-test. TW RM ANOVA: two-way repeated measure ANOVA.

Figure 5				
Fig.	Test		p value	Sig.
Fig.5A	2t t-test	ALIX	0.2607	
	2t t-test	Flotillin-2	0.0048	**
	2t t-test	p62	0.017	*
	2t t-test	CTF	0.001	***
Fig.5B		Total Levels	-	
	2t t-test	ALIX	0.349	
	2t t-test	Flotillin-2	0.0011	**
	2t t-test	p62	0.0001	***
	2t t-test	CTF	7E-05	***
		EV/Lysate	-	
Fig.5C	2t t-test	p62	0.0021	**
	2t t-test	CTF	0.2975	
	2t t-test	FC	0.0064	**
	2t t-test	CE	0.1745	
	2t t-test	MG	1E-05	***
	2t t-test	DG	0.3059	
	2t t-test	TG	4E-05	***
	2t t-test	Cer	6E-05	***
	2t t-test	dhCer	0.0014	**
	2t t-test	SM	1E-05	***
	2t t-test	dhSM	0.0631	
	2t t-test	MhCer	2E-05	***
	2t t-test	Sulf	0.003	**
	2t t-test	LacCer	0.003	**
	2t t-test	GM3	5E-08	***
	2t t-test	PA	0.3485	
	2t t-test	PC	0.0071	**
	2t t-test	PCe	0.0133	*
	2t t-test	PE	0.4178	
	2t t-test	PEp	0.0223	*
	2t t-test	PS	0.0347	*
	2t t-test	PI	0.9844	
	2t t-test	PG	0.6833	
	2t t-test	BMP	0.0004	***
2t t-test	LPC	0.12		
2t t-test	LPCe	0.0168	*	
2t t-test	LPE	0.0426	*	
2t t-test	LPEp	0.0232	*	
2t t-test	LPI	0.0059	**	

Figure 6				
Fig.	Test		p value	Sig.
Fig.6A	ANOVA	ALIX	0.8744	
	ANOVA	Flotillin-2	0.5153	
	ANOVA	CTF	0.0007	***
Fig.6B		Total Levels	-	
	ANOVA	ALIX	0.0047	**
	ANOVA	Flotillin-2	0.003	**
	ANOVA	Ubiquitin	0.0025	**
	ANOVA	CTF	0.0178	*
Fig.6C		EV/Lysate	-	
	ANOVA	CTF	0.0053	**
	ANOVA	ALIX	0.2541	
Fig.6D	ANOVA	Flotillin-2	0.8619	
	ANOVA	CTF	0.0296	*
		Total Levels	-	
Fig.6D	ANOVA	ALIX	0.0188	*
	ANOVA	Flotillin-2	0.0021	**
	ANOVA	Ubiquitin	0.0357	*
	ANOVA	CTF	0.0008	***
	ANOVA	CTF	0.0018	**

Figure 7				
Fig.	Test		p value	Sig.
Fig.7B	2t t-test	Vps34	0.0108	*
	2t t-test	Beclin1	0.0006	***
	2t t-test	Ubiquitin	0.0065	**
	2t t-test	p62	2E-05	***
Fig.7C	2t t-test	APP	0.7117	
	2t t-test	CTF	8E-05	***
	2t t-test	CTFβ	0.0018	**
	2t t-test	Aβ40	0.4371	
Fig.7D	2t t-test	Aβ42	0.1916	
	2t t-test	FC	0.939	
	2t t-test	CE	0.0001	***
	2t t-test	MG	0.0213	*
	2t t-test	DG	0.2751	
	2t t-test	TG	0.2605	
	2t t-test	Cer	0.0004	***
	2t t-test	dhCer	9E-05	***
	2t t-test	SM	0.9547	
	2t t-test	dhSM	0.3687	
	2t t-test	MhCer	0.7653	
	2t t-test	Sulf	0.9122	
	2t t-test	LacCer	0.4254	
	2t t-test	GM3	0.2524	
	2t t-test	PA	0.5384	
	2t t-test	PC	0.746	
	2t t-test	PCe	0.3982	
	2t t-test	PE	0.2223	
	2t t-test	PEp	0.2003	
	2t t-test	PS	0.4086	
	2t t-test	PI	0.7895	
	2t t-test	PG	0.3333	
	2t t-test	BMP	1E-05	***
	2t t-test	LPC	0.3307	
2t t-test	LPCe	0.1355		
2t t-test	LPE	0.4904		
2t t-test	LPEp	0.0145	*	
2t t-test	LPI	0.2606		
Fig.7E	2t t-test	ALIX	0.0367	*
	2t t-test	Flotillin-1	0.7494	
	2t t-test	Flotillin-2	0.6487	
	2t t-test	Ubiquitin	0.0426	*
Fig.7F	2t t-test	CTF	0.0383	*
	2t t-test	SM	0.0031	**
	2t t-test	LacCer	0.0029	**
2t t-test	BMP	0.016	*	

Sup. Fig. 1				
Fig.	Test		p value	Sig.
Sup.Fig.1A	2t t-test	Cardiolipin	0.7509	
	2t t-test	PS	0.5823	
	2t t-test	PA	0.6082	
	2t t-test	PI4P	0.2895	
	2t t-test	PI3P	1E-06	***
	2t t-test	PI(4,5)P ₂	0.0656	
Sup.Fig.1B	2t t-test	Vps34	0.5148	
	2t t-test	Beclin1	0.0061	**
	2t t-test	Vps15	0.6898	
2t t-test	Atg14L	0.4353		
Sup.Fig1C	ANOVA	Viability	0.6848	
Sup.Fig1D	2t t-test	EEA1	4E-05	***
	2t t-test	Rab5	0.7388	
Sup.Fig1E	2t t-test	Rab5 Size	6E-05	***
	2t t-test	<0.19	0.0002	***
	2t t-test	0.20-0.23	0.8745	
	2t t-test	>0.23	0.0004	***

Sup. Fig. 2				
Fig.	Test		p value	Sig.
Sup.Fig2A	TW RM ANOVA	EGF (time)	0.0015	**
	TW RM ANOVA	EGF (treatment)	0.0001	***
Sup.Fig2B	TW RM ANOVA	EGF	0.0001	***
	TW RM ANOVA	EGF (treatment)	0.0001	***
Sup.Fig2C	TW RM ANOVA	APP (time)	0.0001	***
	TW RM ANOVA	APP (treatment)	0.8116	
	TW RM ANOVA	CTF (time)	0.0214	**
Sup.Fig2D	TW RM ANOVA	CTF (treatment)	0.0001	***
	TW RM ANOVA	APP (time)	0.0001	***
	TW RM ANOVA	APP (treatment)	0.9518	
	TW RM ANOVA	CTF (time)	0.0001	***
TW RM ANOVA	CTF (treatment)	0.0106	**	

Sup. Fig. 3				
Fig.	Test		p value	Sig.
Sup.Fig3A	ANOVA	LC3	0.0001	***
	ANOVA	p62	0.0001	***
Sup.Fig3C	2t t-test	Ubiquitin	0.0038	**
	2t t-test	p62	1E-08	***
Sup.Fig3D	2t t-test	Vps34	2E-09	***
	2t t-test	p62	0.0002	***

Sup. Fig. 4				
Fig.	Test		p value	Sig.
Sup.Fig4A	2t t-test	Cer d18:1/16:0	0.1415	
	2t t-test	Cer d18:1/16:1	0.5691	
	2t t-test	Cer d18:1/18:0	0.0217	*
	2t t-test	Cer d18:1/18:1	0.0314	*
	2t t-test	Cer d18:1/20:0	0.0019	**
	2t t-test	Cer d18:1/20:1	0.0254	*
	2t t-test	Cer d18:1/22:0	0.1501	
	2t t-test	Cer d18:1/22:1	0.0558	
	2t t-test	Cer d18:1/24:0	0.639	
	2t t-test	Cer d18:1/24:1	0.7768	
	2t t-test	Cer d18:1/26:0	0.1295	
	2t t-test	Cer d18:1/26:1	0.5	
	2t t-test	dhCer d18:0/16:0	0.002	**
	2t t-test	dhCer d18:0/16:1	0.7802	
	2t t-test	dhCer d18:0/18:0	0.0016	**
	2t t-test	dhCer d18:0/18:1	0.0136	*
	2t t-test	dhCer d18:0/20:0	5E-05	***
	2t t-test	dhCer d18:0/20:1	0.245	
	2t t-test	dhCer d18:0/22:0	0.0054	**
	2t t-test	dhCer d18:0/22:1	0.1026	
	2t t-test	dhCer d18:0/24:0	0.0557	
	2t t-test	dhCer d18:0/24:1	0.201	
	2t t-test	dhSM d18:0/16:0	8E-05	***
	2t t-test	dhSM d18:0/16:1	0.0778	
	2t t-test	dhSM d18:0/18:0	0.0066	**
	2t t-test	dhSM d18:0/18:1	0.0061	**
	2t t-test	dhSM d18:0/20:0	0.0095	**
	2t t-test	dhSM d18:0/20:1	0.0214	*
	2t t-test	dhSM d18:0/22:0	2E-05	***
	2t t-test	dhSM d18:0/22:1	0.0149	*
	2t t-test	dhSM d18:0/24:0	0.0006	***
	2t t-test	dhSM d18:0/24:1	0.0001	***

Sup. Fig. 4 (continued)				
Fig.	Test		p value	Sig.
Sup.Fig4B	2t t-test	BMP 32:0	0.9303	
	2t t-test	BMP 32:1	0.3449	
	2t t-test	BMP 34:0	0.0225	*
	2t t-test	BMP 34:1	0.0547	
	2t t-test	BMP 34:2	0.1636	
	2t t-test	BMP 36:0	0.0199	*
	2t t-test	BMP 36:1	0.076	
	2t t-test	BMP 36:2	0.3763	
	2t t-test	BMP 36:3	0.0337	*
	2t t-test	BMP 36:4	0.1071	
	2t t-test	BMP 38:0	0.0635	
	2t t-test	BMP 38:1	0.8475	
	2t t-test	BMP 38:2	0.119	
	2t t-test	BMP 38:3	0.0735	
	2t t-test	BMP 38:4	0.4153	
	2t t-test	BMP 38:5	0.9221	
	2t t-test	BMP 38:6	0.7454	
	2t t-test	BMP 40:5	0.8991	
	2t t-test	BMP 40:6	0.4208	
	2t t-test	BMP 40:7	0.7563	
	2t t-test	BMP 42:5	0.2667	
2t t-test	BMP 42:6	0.4433		
2t t-test	BMP 42:7	0.4175		

Sup. Fig. 6				
Fig.	Test		p value	
Sup.Fig6C	2t t-test	BMP 32:0	0.1342	
	2t t-test	BMP 32:1	0.2589	
	2t t-test	BMP 34:0	0.6485	
	2t t-test	BMP 34:1	0.007 **	
	2t t-test	BMP 34:2	0.2679	
	2t t-test	BMP 36:0	0.4379	
	2t t-test	BMP 36:1	0.0011 **	
	2t t-test	BMP 36:2	0.0021 **	
	2t t-test	BMP 36:3	0.0053 **	
	2t t-test	BMP 36:4	0.6879	
	2t t-test	BMP 38:0	0.2203	
	2t t-test	BMP 38:1	0.3737	
	2t t-test	BMP 38:2	0.0097 **	
	2t t-test	BMP 38:3	0.0009 ***	
	2t t-test	BMP 38:4	0.6315	
	2t t-test	BMP 38:5	0.5007	
	2t t-test	BMP 38:6	0.3857	
	2t t-test	BMP 40:5	0.1165	
	2t t-test	BMP 40:6	0.2984	
	2t t-test	BMP 40:7	0.0144 *	
	2t t-test	BMP 42:5	0.4465	
	2t t-test	BMP 42:6	0.8001	
	2t t-test	BMP 42:7	0.0851	
	Sup.Fig6D	2t t-test	FC	0.2806
		2t t-test	CE	0.0869
		2t t-test	MG	0.0484 *
		2t t-test	DG	0.0363 *
2t t-test		TG	0.3229	
2t t-test		Cer	0.0146 *	
2t t-test		dhCer	0.0807	
2t t-test		SM	0.396	
2t t-test		dhSM	0.0545	
2t t-test		MhCer	0.0033 **	
2t t-test		Sulf	0.2264	
2t t-test		LacCer	0.0007 ***	
2t t-test		GM3	0.0478 *	
2t t-test		PA	0.1255	
2t t-test		PC	0.0796	
2t t-test		PCe	0.9517	
2t t-test		PE	0.2858	
2t t-test		PEp	0.8876	
2t t-test		PS	0.9538	
2t t-test		PI	0.4861	
2t t-test		PG	0.088	
2t t-test		BMP	0.0035 **	
2t t-test		LPC	0.3595	
2t t-test		LPCe	0.4741	
2t t-test		LPE	0.0119 *	
2t t-test		LPEp	0.0657	
2t t-test		LPI	0.0235 *	

Sup. Fig. 6 (continued)			
Fig.	Test		p value
Sup.Fig6D	2t t-test	BMP 32:0	0.0014 **
	2t t-test	BMP 32:1	0.0075 **
	2t t-test	BMP 34:0	0.0008 ***
	2t t-test	BMP 34:1	0.0018 **
	2t t-test	BMP 34:2	0.0043 **
	2t t-test	BMP 36:0	0.0017 **
	2t t-test	BMP 36:1	0.0014 **
	2t t-test	BMP 36:2	0.0052 **
	2t t-test	BMP 36:3	0.0021 **
	2t t-test	BMP 36:4	0.0004 ***
	2t t-test	BMP 38:0	0.0085 **
	2t t-test	BMP 38:1	0.0019 **
	2t t-test	BMP 38:2	0.0025 **
	2t t-test	BMP 38:3	0.0056 **
	2t t-test	BMP 38:4	4E-07 ***
	2t t-test	BMP 38:5	0.0282 *
	2t t-test	BMP 38:6	0.0211 *
	2t t-test	BMP 40:5	0.001 **
	2t t-test	BMP 40:6	0.0465 *
	2t t-test	BMP 40:7	0.0057 **
	2t t-test	BMP 42:5	0.0009 ***
	2t t-test	BMP 42:6	0.0007 ***
	2t t-test	BMP 42:7	2E-05 ***

Sup. Fig. 7				
Fig.	Test		p value	Sig.
Sup.Fig7A	ANOVA	FL APP	0.0603	
	ANOVA	CTF	0.0001	***
	ANOVA	p62	0.0001	***
Sup.Fig7B	ANOVA	ALIX	0.0093	**
	ANOVA	Flotillin-2	0.0001	***
	ANOVA	CTF	0.0001	***
Sup.Fig7C	ANOVA	CTF Ratio	0.0005	***
	ANOVA	FL APP	0.2306	
	ANOVA	CTF	0.0001	***
Sup.Fig7D	ANOVA	p62	0.001	**
	ANOVA	ALIX	0.063	
	ANOVA	Flotillin-2	0.0048	**
ANOVA	CTF	0.0029	**	
ANOVA	CTF Ratio	0.0046	**	

Sup. Fig. 8			
Fig.	Test	p value	Sig.
Sup.Fig8E	2t t-test	FC	0.0109 *
	2t t-test	CE	0.0344 *
	2t t-test	MG	0.0002 ***
	2t t-test	DG	0.096
	2t t-test	TG	0.8334
	2t t-test	Cer	0.1055
	2t t-test	dhCer	0.1583
	2t t-test	SM	0.0031 **
	2t t-test	dhSM	0.1275
	2t t-test	MhCer	0.3294
	2t t-test	Sulf	0.5763
	2t t-test	LacCer	0.0029 **
	2t t-test	GM3	0.0019 **
	2t t-test	PA	0.0364 *
	2t t-test	PC	0.0002 ***
	2t t-test	PCe	6E-05 ***
	2t t-test	PE	0.0056 **
	2t t-test	PEp	0.0043 **
	2t t-test	PS	0.004 **
	2t t-test	PI	0.0186 *
	2t t-test	PG	0.6317
	2t t-test	BMP	0.016 *
	2t t-test	LPC	0.766
	2t t-test	LPCe	0.6409
	2t t-test	LPE	0.0932
	2t t-test	LPEp	0.0745
	2t t-test	LPI	0.7726
	2t t-test	BMP 32:0	0.8988
	2t t-test	BMP 32:1	0.0514
	2t t-test	BMP 34:0	0.0101 *
	2t t-test	BMP 34:1	0.0094 **
	2t t-test	BMP 34:2	0.2265
	2t t-test	BMP 36:0	0.8914
	2t t-test	BMP 36:1	0.0262 *
	2t t-test	BMP 36:2	0.0062 **
	2t t-test	BMP 36:3	0.0041 **
	2t t-test	BMP 36:4	0.0017 **
	2t t-test	BMP 38:0	0.0401 *
	2t t-test	BMP 38:1	0.1012
	2t t-test	BMP 38:2	0.1181
	2t t-test	BMP 38:3	0.1616
	2t t-test	BMP 38:4	0.2484
	2t t-test	BMP 38:5	0.0002 ***
	2t t-test	BMP 38:6	0.0055 **
	2t t-test	BMP 40:5	0.206
	2t t-test	BMP 40:6	0.001 **
	2t t-test	BMP 40:7	0.0081 **
2t t-test	BMP 42:5	0.0203 *	
2t t-test	BMP 42:6	0.4607	
2t t-test	BMP 42:7	0.0231 *	

Chapter 2.2

André M. Miranda, Francisca Vaz Bravo, Robin B. Chan, Nuno Sousa, Gilbert Di Paolo, Tiago Gil

Oliveira

Differential lipid composition and regulation along the hippocampal longitudinal axis

(Manuscript to be submitted)

(2018)

Differential lipid composition and regulation along the hippocampal longitudinal axis

André Miguel Miranda^{1,2,3,4}, Francisca Vaz Bravo^{1,2}, Robin B. Chan^{3,4}, Nuno Sousa^{1,2}, Gilbert Di Paolo^{3,4},
Tiago Gil Oliveira^{1,2*}

¹ Life and Health Sciences Research Institute (ICVS), School of Medicine, University of Minho, Braga 4710-057, Portugal

² ICVS/3B's, PT Government Associate Laboratory, Braga/Guimarães 4710-057, Portugal

³ Department of Pathology and Cell Biology, Columbia University Medical Center, New York City, NY 10032, USA.

⁴ Taub Institute for Research on Alzheimer's disease and the Aging Brain, Columbia University Medical Center, New York City, NY 10032, USA.

Correspondence should be addressed to T.G.O. (e-mail: tiago@med.uminho.pt)

Abstract

Lipids are major constituents of the brain and growing evidence implicates their role in physiological and pathological processes. The hippocampus is a complex brain structure involved in learning, memory and emotional responses and its functioning is also affected in various brain disorders. Despite conserved intrinsic circuitry, behavioral and anatomical studies suggest the existence of a structural and functional organization along its longitudinal axis, endowed with specific cognitive operations. Here, we used an unbiased mass spectrometry approach to characterize the lipid composition of the dorsal and ventral areas of the rat hippocampus. Additionally, we evaluated the susceptibility of each region to lipid modulation by corticosterone, an important mediator of the neuropathological effects of stress. First, we confirmed a conserved intrinsic composition of the hippocampal subregions relatively to other brain areas. We observed a continuous molecular gradient along the longitudinal axis of the hippocampus, and specifically the dorsal and ventral extremities differed significantly from each other, particularly in the abundance of sphingolipids and phospholipids. Additionally, we found that chronic exposure to corticosterone induced significant remodeling of both regions of the hippocampus. While the majority of the alterations induced by corticosterone were identical and thus preserved the biochemical coherence between dorsal and ventral hippocampus, region-specificity was also noted, suggesting the modulation of specific lipid pathways. Thus, our results confirm a multipartite view of the hippocampus based on its lipid signature and highlight lipid metabolism as an important mediator of glucocorticoid signaling with potential implications for conditions associated with stress, namely mood and neurodegenerative disorders.

Introduction

Lipids are a group of varied molecules that are critical for proper brain function. While recent advances in the areas of genomics and proteomics have extensively broadened our knowledge on the molecular landscape of the distinct brain regions, the study of the lipidome has been lagging behind due to technical limitations and difficulty in translating molecular profiles to cognitive function (Wenk 2010; Miranda and Oliveira 2015; Brügger 2014). The increased accessibility to approaches such as mass spectrometry (MS)-based lipidomics and *in vivo* manipulation of lipid signaling pathways, by means of transgenic mice or viral mediated expression of lipid enzymes, now allows a more comprehensive study of the role of lipids in brain function (Aureli et al. 2015; Cermenati et al. 2015). Indeed, while multiple studies particularly focused on specific lipid signaling pathways, exploratory MS-based approaches have allowed the lipidomic profiling of human and animal brains, including identification of characteristic lipid signatures associated with specific pathological conditions (Bozek et al. 2015; Chan et al. 2012; Mapstone et al. 2014).

The hippocampus is a fundamental brain structure critically involved in learning and memory. These functions are believed to be differentially regulated by subregions along the longitudinal axis of the hippocampus, dorsal and ventral respectively (Strange et al. 2014). A dominant view in the field for a long time implicated the dorsal hippocampus particularly in cognitive function (*e.g.* spatial memory) while the ventral hippocampus mediated emotional responses (Strange et al. 2014; Kheirbek et al. 2013; McHugh et al. 2011; Bannerman et al. 2014). While the basic intrinsic circuitry of the hippocampus is conserved along its longitudinal axis (*e.g.*, CA1–3 and DG), it is also well established that connectivity to cortical and subcortical areas is regionally dependent (Strange et al. 2014). In addition to the extrinsic circuitry, functional differentiation of hippocampal subregions along the axis may also be imposed through distinct autonomous cellular properties. For instance, dorsal and ventral hippocampus differ in intrinsic electrophysiological properties such as paired pulse facilitation and the ability to induce long-term potentiation (Pinto et al. 2014; Maggio and Segal 2007). Moreover, the recent development of new genomic-scale tools has allowed a new mapping of the anatomical boundaries of the hippocampus along its longitudinal axis (Thompson et al. 2008; Shah et al. 2017).

Stress can be perceived as an endogenous or exogenous challenge to an individual's homeostasis. Intense or prolonged exposure to stressors are known to elicit deleterious adaptive mechanisms, with particular functional and structural impact in the hippocampus (McEwen and Gianaros 2011; Lucassen et al. 2014). While stressful events are associated with a variety of mental

disorders, chronic stress in rodents induces responses such as dendritic atrophy and important functional correlates as depressive- and anxious-like behavior and learning and memory deficits (Nuno Sousa and Almeida 2012; Lucassen et al. 2014). A significant portion of the pathological effects of chronic stress are believed to be mediated by prolonged release of glucocorticoids, namely corticosterone (CORT) in rodents. While stress is known to induce remodeling of the hippocampal intrinsic and extrinsic circuitry, it is possible that some of the functional phenotypes may rely on a bi-modal response mediated by the dorsal and ventral hippocampus, respectively. Interestingly, CORT receptors are differentially expressed along the hippocampal axis. High-affinity mineralocorticoid receptors (MR) and low-affinity glucocorticoid receptors (GR) are each more highly expressed in the ventral and dorsal hippocampus, respectively (Segal, Richter-Levin, and Maggio 2010). The distinct affinity of receptors to CORT may thus explain a more homeostatic role for MR in basal settings and an on-demand GR activation in response to increased levels of CORT, which may be instrumental for the deleterious effect of chronic stress (Nuno Sousa, Cerqueira, and Almeida 2008). Thus, dichotomy of regional corticosteroid receptor expression may underlie the distinct responses of dorsal and ventral hippocampus to stress stimuli. Recently, we have found that a chronic unpredictable stress paradigm inversely affected dorsal and ventral hippocampus CA3 arborization (atrophy vs hypertrophy, respectively), while only the ventral hippocampus displayed altered electric properties (Pinto et al. 2014). Together with additional evidence for differential responses to stimuli along the longitudinal hippocampal axis, it is therefore critical to identify the molecular pathways that provide hippocampal subregions their identity and determine region specific adaptive responses, namely to stress and CORT signaling.

To test whether lipid composition can also be used as an anatomical marker of the distinct longitudinal sections of the hippocampus, we performed a broad-scale lipid analysis of dorsal, intermediate and ventral hippocampus and compared it to other brain areas. We found that the hippocampus shows a continuous gradient along its axis, with a greater distinction between the dorsal and ventral subregions. Specifically, we found the dorsal hippocampus to be specifically enriched for phosphatidic acid (PA) and other glycosphingolipids in general. Moreover, while CORT treatment caused an overall similar effect in both regions, suggesting stimulation of similar regulatory mechanisms, we found region-specific modulation of lipid species, suggesting distinct action of lipid enzymes in the dorsal and ventral hippocampus, respectively. Altogether, our findings support a biochemical model in which the hippocampus can be partitioned in subregions based on lipid

composition. This suggests that modulation of the underlying lipid signaling cascades may contribute to regional functional correlates.

Results

Regional lipid heterogeneity in the rodent brain

For a better understanding of the lipid composition of the rodent brain, we performed a comprehensive MS-based lipidomic analysis of distinct brain regions, namely the hippocampus, prefrontal cortex (PFC), amygdala and cerebellum in male Wistar rats injected with vehicle (VEH; see Methods for details). Based on the literature supporting molecular and functional heterogeneity along its longitudinal axis, we subdivided the hippocampus in dorsal, intermediate and ventral portions (Strange et al. 2014).

In order to analyze the compositional similarity and disparity between regions, we plotted a heat-map of standard scores (Z score) of the average mol% of each lipid class per region, taking as reference value the mean of all regions pooled (Fig. 1). First, we observed a high degree of similarity, expressed as lower modular Z scores (lighter blue and red shades), between the three hippocampal regions (dorsal, intermediate and ventral) relatively to the other three brain regions (PFC, amygdala and cerebellum) under study. In these specifically, we found the dorsal hippocampus to show higher similarity with the intermediate than the ventral hippocampus, consistent with the proposed continuous gradient of molecular identity along dorsal-ventral axis, where distinctions are more obvious between the poles (Thompson et al. 2008; Shah et al. 2017). The other three brain regions showed a high degree of differentiation comparatively to the hippocampal sub-regions and between themselves.

Specifically, the dorsal and intermediate hippocampus were the most enriched for glycosphingolipids, monoglycosyl- and lactosylceramides and sulfatides (HexCer, LacCer and Sulf, resp.). The PFC showed the highest abundance of glycerolipids, such as PA, phosphatidylcholine (PC), PC esters (PCe), phosphatidylethanolamine (PE), PE plasmogen (PEp) and lysolipid derivatives lysophosphatidylcholine esters and lysophosphatidylethanolamine plasmogen (LPCe and LPEp, resp.). The amygdala was particularly enriched in cholesterol esters (CE) and lysophosphatidylcholine (LPC) while the cerebellum showed the highest enrichment for free cholesterol (FC), glycosylated sphingolipids and sulfatides. Remarkably, this region also showed an enrichment in the abundance of the atypical glycerophospholipid bis(monoacylglycero)phosphate (BMP) and its precursor phosphatidylglycerol (PG). Our findings were confirmed and validated by performing the same analysis

in a previously published cohort of control adult rats (CTRL; not injected with vehicle) (Supplementary Fig. 1) (T G Oliveira et al. 2015). Altogether, our results highlight the heterogeneity of lipid composition between distinct brain regions and identify a continuous molecular gradient along the longitudinal axis of the hippocampus.

Distinct lipid signature of dorsal and ventral hippocampus

We focused our analysis on directly comparing the composition of the dorsal and ventral hippocampus (Fig. 2a). In VEH animals, the ventral hippocampus showed reduced levels of FC and Chol 27-OH, as well sphingolipids HexCer, LacCer and Sulf and the atypical phospholipids BMP and acylphosphatidylserine (aPS) comparatively to the dorsal hippocampus. On the contrary, the ventral hippocampus was particularly enriched in dihydrosphingomyelin (dhSM). To account for the reduced abundance of sphingolipids, the ventral hippocampus was enriched in most abundant glycerophospholipids, namely PC by near 2-fold and PCe, PE, PS, LPCe and lysophosphatidylethanolamine (LPE) by 1.5-fold. Of note, while PC levels were increased, PA, the product of PC hydrolysis by phospholipase D, was significantly decreased by ~20%. Importantly, overlapping results were observed in CTRL rats, with the exception of lack of significant changes between hippocampal regions in PCe, PE ($p=0.08$ and 0.06 , resp.). Perhaps due to reduced levels of PE in the ventral hippocampus in CTRL rats, higher levels of LPE were not detected and LPEp were significantly reduced by 25% (Supplementary Fig. 2).

While lipid classes are generally defined and classified by their polar head group, the acyl chains linked to their backbone show great variety in length and saturation, with important functional implications (Fahy et al. 2005; Miranda and Oliveira 2015). In general, the degree of length and saturation provides distinct physical properties to membranes, namely thickness, fluidity and microdomain assembly (Holthuis and Menon 2014; Simons and Sampaio 2011). Therefore, we analysed the acyl composition of glycerolipids (glycerophospholipids and DG) and sphingolipids in VEH animals (Fig. 2b). We found that the ventral hippocampus was enriched in glycerolipids containing both shorter 34 carbons (C) and over 40C length acyl-chains, at the significant expense of intermediate 36C and 38C chains. Moreover, glycerolipids from this region also showed higher abundance of poly-unsaturated chains with over 6 double-bonds, at the expense of less saturated lipid species, namely containing 1 to 2 double-bonds. Inversely, sphingolipids from the ventral hippocampus were significantly shorter, with higher abundance of 18C and 20C acyl chains and lower

24C, comparatively to the dorsal portion. Contrarily to glycerolipids, sphingolipids were more saturated in the ventral hippocampus than in dorsal.

Due to the bimodal effect in the metabolically related lipids classes (e.g. PC, PA and DG) in both experimental groups (CTRL and VEH), we directly compared the abundance of all lipid species detected by LC-MS (see Supplementary Fig. 3 for all lipid species detected). In both groups, the ventral hippocampus showed significantly decreased levels for most of PA species, particularly those with decreased unsaturated bonds (0 to 2 double bonds). Inversely, the ventral hippocampus was enriched for PC species, with no predilection for acyl-chain and saturation profile. Therefore, the dorsal and ventral hippocampus differ significantly in their lipid composition, with decreased levels of glycosylated sphingolipids and PA specifically in the ventral area, while acyl chain composition of glycerolipids and sphingolipids also varies, with inversed chain length and saturation profiles between both lipid categories.

Corticosterone treatment affects the dorsal and ventral hippocampus differentially

Chronic stress exposure culminates in the release of glucocorticoids such as CORT in rodents which is believed to mediate a myriad of pathologic effects of prolonged stress. While CORT may bind both MR and GR, the lower affinity for the later limits GR activity under basal conditions except for occurrence of high CORT levels as in chronic stress (Nuno Sousa, Cerqueira, and Almeida 2008). Thus, to test whether high CORT levels modulate the lipid landscape of the hippocampus in a region specific manner, we subjected a group of animals to daily subcutaneous injections of synthetic CORT (N Sousa et al. 2000; Cerqueira et al. 2007).

In the dorsal hippocampus, the most prominent change at the lipid class level was a significant ~2-fold increase in CE (Fig. 3a; Supplementary Fig. 4). Levels of LPC and BMP were decreased by 10-20% and APS increased by 25% (Fig. 3a). Additionally, we found increases in multiple species of other classes of neutral lipids, namely DG and TG, although no significant increase in the total abundance of the class was found, neither any specific acyl chain enrichment pattern (Supplementary Fig. 4). Of note, we also found multiple increases in the relative abundance of HexCer(s) (Supplementary Fig. 4). Curiously, PA species showed a bimodal distribution: shorter species, namely 32:0, 32:1 and 34:2 were found increased, while 38:1 and 38:2 were decreased (Supplementary Fig. 4). Likewise, shorter phosphatidylinositol (PI) species were also found increased (34:0, 34:1, 36:1 and 36:2) (Supplementary Fig. 4).

In the ventral hippocampus, we found overlapping effects, yet of commonly higher magnitude (Fig. 3b). First, CE increases matched the phenotype seen in the dorsal region. As for neutral lipids, we found a significant increase in the abundance of DG, which included higher abundance of an increased number of DG species comparatively to the dorsal pole, as well as an increased number of altered TG species (Supplementary Fig. 4). Contrarily, while HexCer species were unchanged in the ventral hippocampus, increases were found in multiple ceramide (Cer) and dhSM species (Supplementary Fig. 4). Specifically, overlapping acyl-chain profiles were detected in the latter lipid classes, particular Cer and dhSM 22:0, 26:0, 26:1, suggesting a specific subset species from these classes may be under specific regulation of mediators of CORT signaling. However, in contrast to the dorsal region, the ventral hippocampus only revealed increases in PA species, not only 32:1 and 34:2, but also 34:1 and 40:6 (Supplementary Fig. 4). Finally, the same PI species found to be increased in the dorsal hippocampus were also upregulated in the ventral pole after CORT treatment, in addition to multiple unsaturated PS species (32:1, 34:1, 36:2, 38:3, 40:5, 40:6 and 42:5) (Supplementary Fig. 4).

Considering the region-specific impact of CORT treatment in particular lipid species (e.g. DG, TG, HexCer), we calculated the ratio of the abundance of each of the lipid species detected in both hippocampal regions and the degree of *biochemical coherence* between VEH and CORT animals (Fig. 4). We found that a very reduced number of lipids (11 out of ~300) had their *coherence* significantly changed (PEp 36:0, PS 32:0, LPC 16:0, LPCe 20:1, DG30:1/14:0, DG36:0/18:0, Cer 24:1, dhSM 22:1, HexCer 18:1, Lac18:0 and LacCer 20:0). However, in line with the already mentioned region-specific lipid changes, we were able to detect subtle changes in metabolically related lipid classes. A trend for increased ventral/dorsal ratio for PA in CORT animals contrasted with a trend for decreased PC ratios, suggesting a preferred increase in PA species as seen in Supplementary Fig. 4. Also, our results suggest a substitution of PE by PEp and a trend for TG and DG enrichment in the ventral hippocampus upon elevated CORT levels. We further detected a trend from decreased ratios of LacCer and HexCer, as CORT significantly upregulated multiple HexCer species and LacCer 20:0 in the dorsal but not ventral hippocampus. Reflecting the loss of abundance in complex sphingolipids, the ventral hippocampus showed a trend for enrichment of Cer and dhSM. Thus, our results suggest that elevated levels of CORT do not interfere with the global molecular landscape characteristic of the dorsal and ventral poles of the hippocampus, predominantly characterized by the relative abundance of lipid classes, but rather modulate the abundance of a particular subsets of lipid species in a region-specific manner.

Discussion

Here, we present the first detailed analysis of the lipid composition along the hippocampal longitudinal axis. First, we compared the three sub-regions of the hippocampus (dorsal, intermediate and ventral) to other brain regions, namely the PFC, amygdala and cerebellum. Consistent with the preserved intrinsic architecture of the hippocampus along its axis, we found higher similarity (*i.e.* less variance) between the different hippocampal sub-regions than the other brain regions (Strange et al. 2014). Importantly, we found a higher similarity between the dorsal and intermediate hippocampus than ventral, supporting a continuous gradient along the dorsal-ventral axis. In addition to the baseline differences between the hippocampus extremities, we found that CORT, a known mediator of chronic stress exposure, individually impacts the lipid composition of each of the regions.

Our previous study of the impact of a chronic stress paradigm in the brain lipidome highlighted the PFC as the region more susceptible to lipid modulation (T G Oliveira et al. 2015). In fact, we found that PFC is the most abundant in sphingomyelin, which may thus explain the increased predisposition to elevated Cer levels upon stress stimulation (*e.g.*, through SM hydrolysis by sphingomyelinases) comparatively to other areas as the hippocampus. In fact, previous studies have implicated the direct action of antidepressants through modulation of sphingomyelinases, which are likely critical for the homeostatic control of the molecular identity of this brain region (Gulbins et al. 2013). Moreover, we found the cerebellum to be the region mostly enriched for free cholesterol and the atypical phospholipid BMP, predominantly found in the intraluminal vesicles of late endosomes and lysosomes (Bissig and Gruenberg 2013). Interestingly, the cerebellum is characteristically susceptible to neuronal loss in the lysosomal storage disorder Niemann-Pick Type C (Evans and Hendriksz 2017). Loss of function in the late endosome/lysosome proteins NPC1 and NPC2 leads to the accumulation of free cholesterol in these endocytic compartments, which secondarily disrupts trafficking and turnover of sphingolipids and BMP (Neefjes and van der Kant 2014; Kobayashi et al. 1999). This disruption of lipid trafficking results in Alzheimer's disease-like pathology, including neurofibrillary tangles and neuronal loss (Malnar et al. 2014). Thus, the baseline lipid composition of the distinct brain regions may provide important hints about regional susceptibility to impairment of specific lipid pathways in different disease contexts and therefore allow the prioritization of specific therapeutical approaches, such as modulators of sphingolipid metabolism or cholesterol and BMP in depression and Niemann-Pick Type C, respectively.

The comparison of the lipid composition between dorsal and ventral hippocampus in two groups of adult rats (CTRL and VEH) revealed robust and reproducible observations. Specifically, we

found an enrichment for complex glycosphingolipids in the dorsal hippocampus, at the expense of simpler sphingolipids (SM and dhSM) and glycerophospholipids in general. An exception for PA was noted, which was more abundant in the dorsal pole. It will now be crucial to identify the mechanisms underlying the region-specific molecular landscape. The differential expression of lipid metabolizing enzymes and cellular composition are likely the strongest candidates. While the network of lipid metabolites is extremely complex, wide-scale sequencing studies will certainly be fundamental to address this question.

Moreover, we studied the differential effect of elevated CORT levels, an experimental model of glucocorticoid-mediated chronic stress. CORT similarly induced an upregulation of CE and downregulation of BMP in both hippocampal poles. Interestingly, CE accumulation is increasingly seen as a hallmark of neurodegeneration, with reports in both human and mouse models of AD, progranulin-linked frontotemporal dementia and aging (Chan et al. 2012; Evers et al. 2017; Rodriguez-Navarro et al. 2012). The mechanism for CE increase is not yet clear in any of the scenarios, neither whether this is a neuron-specific phenotype. Recently, we have reported that depletion of brain phosphatidylinositol-3-phosphate levels in mice, as seen for AD patients, induces lysosomal defects and leads to an abrupt accumulation of CE prior to extensive neurodegeneration (Miranda et al. 2018). While Merrill *et al* report a partial enrichment of CE in neuron cell bodies relatively to the brain parenchyma, increase in CE in primary neuronal cultures upon phosphatidylinositol-3-phosphate depletion was not detected, thus we do not exclude that elevated CE levels, mediated by CORT, may result from contribution of non-neuronal cells, such as astrocytes and microglia, which are also known to be subject to glucocorticoid signaling (Bridges, Slais, and Syková 2008; Carter, Hamilton, and Thompson 2013).

Despite the common effect of CORT in lipid classes as CE and TG in both hippocampal regions, we also found that CORT treatment preferentially upregulated PA species in the ventral hippocampus than in dorsal. Our analysis revealed a partially overlapping effect of CORT, PA 32:1 and PA 34:2 were equally upregulated in the dorsal and ventral hippocampus, while changes in the ventral hippocampus were of higher magnitude. However, in the dorsal portion, PA 32:0 was also upregulated and PA 38:1 and 38:2 significantly decreased, while in the ventral area no decreases were detected. PA 34:1 and PA 40:6 were also increased in the later. Of note, DG, which may derive from dephosphorylation of PA, was also differently affected, with increases in multiple species, spanning different acyl-chain and saturation profiles. Interestingly, levels of highly abundant PC were not affected. Two possible mechanisms may account for these observations. First, sequential PC

breakdown by phospholipase D, including isoforms 1 and 2, may account for increased levels in PA (Oliveira and Di Paolo 2010). In fact, in a mouse model of familial AD, increased levels of specific PA species (PA 34:2) were normalized by genetic ablation of PLD2 (Oliveira et al. 2010). Thus, these results reflect a putative differential effect of CORT in PA metabolism in both regions by recruitment of species-specific metabolizing enzymes. Moreover, we found the dorsal hippocampus to be enriched for PA of different acyl-chain lengths, namely 32, 34, 36 and 38C. Vermeren et al recently reported that genetic ablation of PLD2 levels reduces the abundance of PA 32 and 34 by ~5% (Vermeren et al. 2016). Thus, the more predominant increase in 32 and 34C found in the ventral hippocampus upon CORT treatment may be mediated by on-demand PLD2 recruitment specifically. Increased PLD2 activity, as seen in AD transgenic model, may mediate some of the effects of stress on ventral hippocampus remodeling. However, increased levels of DG either suggest increased PA dephosphorylation, perhaps as a compensatory buffering mechanisms to normalize PA levels, or *de novo* synthesis (Carrasco and Mérida 2007). Since TG levels are increased upon CORT treatment, particularly in the ventral hippocampus, it is possible that increased lipase function causes increased DG levels which in turn may be phosphorylated by DAG kinases to produce PA. Beyond the important role as a fundamental substrate for phospholipid synthesis, DG and PA are also signaling molecules, acting as second messenger (Oliveira and Di Paolo 2010; Carrasco and Mérida 2007). Importantly, PA is implicated in the regulation of mTOR activity. The mTOR kinase is part of a complex that regulates important aspects of signal transduction and metabolism. In fact, mTOR modulation by on-demand synthesis of PA may not only have repercussions in metabolic effects but also mediate synaptic and dendritic plasticity such as increased dendritic arborization of the ventral hippocampus in response to chronic stress or elevated glucocorticoids (Polman et al. 2012; Pinto et al. 2014; Henry et al. 2018). Indeed, mTOR activation has been implicated in dendrite growth and complexity (Kumar 2005). In addition, metabolism of DG and PA have been intrinsically involved in secretory function, including not only synaptic vesicles and neurotransmitter release but also synaptic vesicle recycling (Goldschmidt et al. 2016; Lee, Kim, and Tanaka-Yamamoto 2016; Almena and Mérida 2011). Thus, future studies on the role of local modulation of lipid metabolizing enzymes should complement lipidomic analysis with functional readouts, namely electrophysiology or other events occurring at the synaptic level.

Importantly, a limitation of our study is that the lipid profiles here described were performed in macrodissected tissue. While still informant about the overall composition of the distinct subregions of the hippocampus, we lack the spatial resolution to characterize the longitudinal lipid variability in

each of the hippocampal subregions (e.g. CA1-3). Therefore, the use of newly developed techniques as matrix-assisted laser desorption/ionization based imaging mass spectrometry (MALDI-IMS) will allow further insights on the lipid profile of brain regions *in situ* (Hanrieder et al. 2013; Nielsen et al. 2016). While initial MALDI studies were limited by biochemical resolution (*i.e.*, classes and species of lipids analyzed) or required multiple specimens for analysis, these have been overcome by bi- and trimodal MALDI (Hanrieder et al. 2013; Thomas et al. 2012). As such, combined protein and lipid MALDI-IMS was recently used to characterize the distinct layers of the cerebellum at a cellular resolution and the association of lipids with amyloid-beta plaques (Kaya et al. 2017). Therefore, this technique may prove as a valuable resource for a detailed characterization of the hippocampal subregions. Moreover, in light of the abovementioned implications of the highlighted lipids, neuronal loss, astroglial recruitment or synaptic and dendritic plasticity may be differentially modulated in the dorsal and ventral hippocampus by regional lipid environments. While our approach does not take into account the differential contribution of the different cell types in the brain parenchyma, future approaches may be complemented by single cell tissue dissociation and purification of different cell populations, as previously performed in the field of transcriptomics (Zhang et al. 2014; Merrill et al. 2017). In addition to the cell diversity, the distinct extrinsic circuit of the hippocampus may also contribute to local lipids profiles. It is believed that neuronal polarity is associated with differential distribution of different lipid classes and species (Yang et al. 2012; Antonny et al. 2015). Therefore, regional lipid profiles should be interpreted in the context of the complex brain cellular composition and circuitry.

In summary, our study reveals a distinct lipid composition in different brain regions that may have an impact in regional susceptibility to specific lipid-related pathologies. Importantly, we outline a new molecular identity of the hippocampus along its longitudinal axis, highlighting the distinct lipid landscape of the dorsal and ventral poles. The implication of common, but also distinct, lipid pathways in the mediation of effects glucocorticoid signalling opens new avenues for the study of the specific role of the dorsal and ventral hippocampus in several-stress related conditions, including mood and neurodegenerative disorders. A thorough knowledge of the boundaries within the hippocampal axis will also provide new tools to understand and manipulate each region's function, both in health and disease.

Methods

Animals and treatments

All animals experiments were conducted in full compliance with European Union Directive 86/609/EEC. Adult 2-month old male Wistar rats (Charles River Laboratories) were housed in groups of 2 under standard laboratory conditions (lights on from 8:00 A.M. to 8:00 P.M.; room temperature 22°C; ad libitum access to food and drink). Animals were assigned to daily handling (CTRL; control group); a 4-week protocol of daily injections with vehicle (VEH; sesame oil) or synthetic corticosterone (CORT; 40 mg/kg) (Sigma-Aldrich) (T G Oliveira et al. 2015).

Lipids analysis

Animals were killed by decapitation, brains immediately macro-dissected, frozen in liquid nitrogen and stored at -80 °C until further processing. Lipids were extracted using a modified Bligh-Dyer procedure as previously described (Chan et al. 2012; Miranda et al. 2018). Briefly, frozen tissue was resuspended and homogenized in a solution of methanol:chloroform (2:1) and lipids extracted using chloroform:KCl (3:2, 1 M). Extracts were spiked with appropriate internal standards and analyzed using a 6490 Triple Quadrupole LC/MS system (Agilent Technologies) (Chan et al. 2012; T G Oliveira et al. 2015). Individual lipid concentration was calculated by referencing to appropriate internal standards (T G Oliveira et al. 2015). Lipid concentration was normalized by molar concentration across all species detected for each sample, and expressed as relative mean mol%. The nomenclature abbreviations are: FC, free cholesterol; 24-OHC, 24(S)-hydroxycholesterol; CE, cholesteryl ester; DG, diacylglycerol; TG, triacylglycerol; Cer, ceramide; SM, sphingomyelin; dhSM, dihydrosphingomyelin; HexCer, hexosylceramide; Sulf, sulfatides; Sulf(2OH), 2-hydroxy N-acyl sulfatide; LacCer, lactosylceramide; PA, phosphatidic acid; PC, phosphatidylcholine; PCe, ether phosphatidylcholine; PE, phosphatidylethanolamine; PEp, plasmalogen phosphatidylethanolamine; PG, phosphatidylglycerol; PI, phosphatidylinositol; PS, phosphatidylserine; LPC, lysophosphatidylcholine; LPCe, ether lysophosphatidylcholine; LPE, lysophosphatidylethanolamine; LPEp, plasmalogen lysophosphatidylethanolamine; LPI, lysophosphatidylinositol; BMP, bis(monoacylglycero)phosphate; APS, acyl-phosphatidylserine.

Statistical Analysis

Statistical analysis was performed using Prism software (Graphpad). All the data are given as mean \pm s.e.m. for a given N of biological replicates (see each figure legend for exact details). For comparison of two experimental conditions, two-tailed Student's t test was performed.

References

- Almena, María, and Isabel Mérida. 2011. "Shaping up the Membrane: Diacylglycerol Coordinates Spatial Orientation of Signaling." *Trends in Biochemical Sciences*. doi:10.1016/j.tibs.2011.06.005.
- Antonny, Bruno, Stefano Vanni, Hideo Shindou, and Thierry Ferreira. 2015. "From Zero to Six Double Bonds: Phospholipid Unsaturation and Organelle Function." *Trends in Cell Biology* 25 (7). Elsevier Ltd: 427–36. doi:10.1016/j.tcb.2015.03.004.
- Aureli, Massimo, Sara Grassi, Simona Prioni, Sandro Sonnino, and Alessandro Prinetti. 2015. "Lipid Membrane Domains in the Brain." *Biochimica et Biophysica Acta (BBA) - Molecular and Cell Biology of Lipids* 1851 (8). Elsevier B.V.: 1006–16. doi:10.1016/j.bbalip.2015.02.001.
- Bannerman, David M., Rolf Sprengel, David J. Sanderson, Stephen B. McHugh, J. Nicholas P. Rawlins, Hannah Monyer, and Peter H. Seeburg. 2014. "Hippocampal Synaptic Plasticity, Spatial Memory and Anxiety." *Nature Reviews Neuroscience* 15 (3). Nature Publishing Group: 181–92. doi:10.1038/nrn3677.
- Bissig, Christin, and Jean Gruenberg. 2013. "Lipid Sorting and Multivesicular Endosome Biogenesis." *Cold Spring Harbor Perspectives in Biology*. Cold Spring Harbor Laboratory Press. doi:10.1101/cshperspect.a016816.
- Bozek, Katarzyna, Yuning Wei, Zheng Yan, Xiling Liu, Jieyi Xiong, Masahiro Sugimoto, Masaru Tomita, et al. 2015. "Organization and Evolution of Brain Lipidome Revealed by Large-Scale Analysis of Human, Chimpanzee, Macaque, and Mouse Tissues." *Neuron*, 695–702. doi:10.1016/j.neuron.2015.01.003.
- Bridges, Nikola, Karel Slais, and Eva Syková. 2008. "The Effects of Chronic Corticosterone on Hippocampal Astrocyte Numbers: A Comparison of Male and Female Wistar Rats." *Acta Neurobiologiae Experimentalis* 68 (2): 131–38. <http://www.ncbi.nlm.nih.gov/pubmed/18511949>.
- Brügger, Britta. 2014. "Lipidomics: Analysis of the Lipid Composition of Cells and Subcellular Organelles by Electrospray Ionization Mass Spectrometry." *Annual Review of Biochemistry* 83: 79–98. doi:10.1146/annurev-biochem-060713-035324.
- Carrasco, Silvia, and Isabel Mérida. 2007. "Diacylglycerol, When Simplicity Becomes Complex." *Trends in Biochemical Sciences*. doi:10.1016/j.tibs.2006.11.004.
- Carter, Bradley S., David E. Hamilton, and Robert C. Thompson. 2013. "Acute and Chronic Glucocorticoid Treatments Regulate Astrocyte-Enriched mRNAs in Multiple Brain Regions in Vivo." *Frontiers in Neuroscience* 7 (August). *Frontiers*: 139. doi:10.3389/fnins.2013.00139.
- Cermenati, Gaia, Nico Mitro, Matteo Audano, Roberto C. Melcangi, Maurizio Crestani, Emma De Fabiani, and Donatella Caruso. 2015. "Lipids in the Nervous System: From Biochemistry and Molecular Biology to Patho-Physiology." *Biochimica et Biophysica Acta (BBA) - Molecular and Cell Biology of Lipids* 1851 (1). Elsevier B.V.: 51–60. doi:10.1016/j.bbalip.2014.08.011.
- Cerqueira, João J, François Mailliet, Osborne F X Almeida, Thérèse M Jay, and Nuno Sousa. 2007. "The Prefrontal Cortex as a Key Target of the Maladaptive Response to Stress." *The Journal of Neuroscience : The Official Journal of the Society for Neuroscience* 27 (11): 2781–87. doi:10.1523/JNEUROSCI.4372-06.2007.
- Chan, Robin B., Tiago G. Oliveira, Ety P. Cortes, Lawrence S. Honig, Karen E. Duff, Scott a. Small, Markus R. Wenk, Guanghou Shui, and Gilbert Di Paolo. 2012. "Comparative Lipidomic Analysis of Mouse and Human Brain with Alzheimer Disease." *Journal of Biological Chemistry* 287: 2678–88. doi:10.1074/jbc.M111.274142.
- Evans, William R H, and Chris J Hendriksz. 2017. "Niemann-Pick Type C Disease - the Tip of the Iceberg? A Review of Neuropsychiatric Presentation, Diagnosis and Treatment." *BJPsych Bulletin* 41 (2). Royal College of Psychiatrists: 109–14. doi:10.1192/pb.bp.116.054072.
- Evers, Bret M, Carlos Rodriguez-Navas, Rachel J Tesla, Gang Yu, Charles L White Iii, Joachim Herz Correspondence, Janine Prange-Kiel, et al. 2017. "Lipidomic and Transcriptomic Basis of Lysosomal Dysfunction in Progranulin Deficiency." *CellReports* 20: 2565–74. doi:10.1016/j.celrep.2017.08.056.
- Fahy, Eoin, Shankar Subramaniam, H Alex Brown, Christopher K Glass, Alfred H Merrill, Robert C Murphy, Christian R H Raetz, et al. 2005. "A Comprehensive Classification System for Lipids." *Journal of Lipid Research* 46 (5): 839–61. doi:10.1194/jlr.E400004-JLR200.
- Goldschmidt, Hana L, Becky Tu-Sekine, Lenora Volk, Victor Anggono, Richard L Haganir, and Daniel M Raben. 2016. "DGK θ Catalytic Activity Is Required for Efficient Recycling of Presynaptic Vesicles at Excitatory Synapses." *Cell Reports* 14 (2). Elsevier: 200–207. doi:10.1016/j.celrep.2015.12.022.
- Gulbins, Erich, Monica Palmada, Martin Reichel, Anja Lüth, Christoph Böhmer, Davide Amato, Christian P Müller, et al. 2013. "Acid Sphingomyelinase-Ceramide System Mediates Effects of Antidepressant Drugs." *Nature Medicine* 19 (7): 934–38. doi:10.1038/nm.3214.
- Hanrieder, Jörg, Nhu T. N. Phan, Michael E. Kurczyk, and Andrew G. Ewing. 2013. "Imaging Mass Spectrometry in Neuroscience." *ACS Chemical Neuroscience* 4 (5). American Chemical Society: 666–79. doi:10.1021/cn400053c.
- Henry, Fredrick E., Xiao Wang, David Serrano, Amanda S. Perez, Cynthia J. L. Carruthers, Edward L. Stuenkel, and Michael

- A. Sutton. 2018. "A Unique Homeostatic Signaling Pathway Links Synaptic Inactivity to Postsynaptic mTORC1." *The Journal of Neuroscience* 38 (9): 2207–25. doi:10.1523/JNEUROSCI.1843-17.2017.
- Holthuis, Joost C M, and Anant K Menon. 2014. "Lipid Landscapes and Pipelines in Membrane Homeostasis." *Nature* 510 (7503): 48–57. doi:10.1038/nature13474.
- Kaya, Ibrahim, Dimitri Brinet, Wojciech Michno, Mehmet Başkurt, Henrik Zetterberg, Kaj Blenow, and Jörg Hanrieder. 2017. "Novel Trimodal MALDI Imaging Mass Spectrometry (IMS3) at 10 μm Reveals Spatial Lipid and Peptide Correlates Implicated in A β Plaque Pathology in Alzheimer's Disease." *ACS Chemical Neuroscience* 8 (12): 2778–90. doi:10.1021/acscchemneuro.7b00314.
- Kheirbek, Mazen A., Liam J. Drew, Nesha S. Burghardt, Daniel O. Costantini, Lindsay Tannenholz, Susanne E. Ahmari, Hongkui Zeng, André A. Fenton, and René Hen. 2013. "Differential Control of Learning and Anxiety along the Dorsoventral Axis of the Dentate Gyrus." *Neuron* 77 (5): 955–68. doi:10.1016/j.neuron.2012.12.038.
- Kobayashi, T, M H Beuchat, M Lindsay, S Frias, R D Palmiter, H Sakuraba, R G Parton, and J Gruenberg. 1999. "Late Endosomal Membranes Rich in Lysobisphosphatidic Acid Regulate Cholesterol Transport." *Nature Cell Biology* 1 (2): 113–18. doi:10.1038/10084.
- Kumar, Vikas. 2005. "Regulation of Dendritic Morphogenesis by Ras-PI3K-Akt-mTOR and Ras-MAPK Signaling Pathways." *Journal of Neuroscience* 25 (49): 11288–99. doi:10.1523/JNEUROSCI.2284-05.2005.
- Lee, Dongwon, Eunjoon Kim, and Keiko Tanaka-Yamamoto. 2016. "Diacylglycerol Kinases in the Coordination of Synaptic Plasticity." *Frontiers in Cell and Developmental Biology* 4 (August). *Frontiers*: 92. doi:10.3389/fcell.2016.00092.
- Lucassen, Paul J., Jens Pruessner, Nuno Sousa, Osborne F X Almeida, Anne Marie Van Dam, Grazyna Rajkowska, Dick F. Swaab, and Boldizsár Czéh. 2014. "Neuropathology of Stress." *Acta Neuropathologica* 127 (1): 109–35. doi:10.1007/s00401-013-1223-5.
- Maggio, Nicola, and Menahem Segal. 2007. "Unique Regulation of Long Term Potentiation in the Rat Ventral Hippocampus." *Hippocampus* 17 (1): 10–25. doi:10.1002/hipo.20237.
- Malnar, Martina, Silva Hecimovic, Niklas Mattsson, and Henrik Zetterberg. 2014. "Bidirectional Links between Alzheimer's Disease and Niemann-Pick Type C Disease." *Neurobiol Dis* 72 Pt A: 37–47. doi:10.1016/j.nbd.2014.05.033.
- Mapstone, Mark, Amrita K Cheema, Massimo S Fiandaca, Xiaogang Zhong, Timothy R Mhyre, Linda H MacArthur, William J Hall, et al. 2014. "Plasma Phospholipids Identify Antecedent Memory Impairment in Older Adults." *Nature Medicine* 20 (4). Nature Publishing Group: 415–18. doi:10.1038/nm.3466.
- McEwen, Bruce S., and Peter J. Gianaros. 2011. "Stress- and Allostasis-Induced Brain Plasticity." *Annual Review of Medicine* 62 (1). *Annual Reviews* : 431–45. doi:10.1146/annurev-med-052209-100430.
- McHugh, Stephen B., Marianne Fillenz, John P. Lowry, J. Nicolas P. Rawlins, and David M. Bannerman. 2011. "Brain Tissue Oxygen Amperometry in Behaving Rats Demonstrates Functional Dissociation of Dorsal and Ventral Hippocampus during Spatial Processing and Anxiety." *European Journal of Neuroscience* 33 (2): 322–37. doi:10.1111/j.1460-9568.2010.07497.x.
- Merrill, Collin B., Abdul Basit, Andrea Armirotti, Yousheng Jia, Christine M. Gall, Gary Lynch, and Daniele Piomelli. 2017. "Patch Clamp-Assisted Single Neuron Lipidomics." *Scientific Reports* 7 (1). Nature Publishing Group: 5318. doi:10.1038/s41598-017-05607-3.
- Miranda, André M., Zofia M. Lasiecka, Yimeng Xu, Jessi Neufeld, Sanjid Shahriar, Sabrina Simoes, Robin B. Chan, Tiago Gil Oliveira, Scott A. Small, and Gilbert Di Paolo. 2018. "Neuronal Lysosomal Dysfunction Releases Exosomes Harboring APP C-Terminal Fragments and Unique Lipid Signatures." *Nature Communications* 9 (1). Nature Publishing Group: 291. doi:10.1038/s41467-017-02533-w.
- Miranda, André Miguel, and Tiago Gil Oliveira. 2015. "Lipids under Stress - a Lipidomic Approach for the Study of Mood Disorders." *BioEssays* 37 (11): 1226–35. doi:10.1002/bies.201500070.
- Neeffjes, Jacques, and Rik van der Kant. 2014. *Stuck in Traffic: An Emerging Theme in Diseases of the Nervous System. Trends in Neurosciences. Vol. 37. Elsevier Current Trends.* doi:10.1016/j.tins.2013.11.006.
- Nielsen, Mette M. B., Kate L. Lambertsen, Bettina H. Clausen, Morten Meyer, Dhaka R. Bhandari, Søren T. Larsen, Steen S. Poulsen, Bernhard Spengler, Christian Janfelt, and Harald S. Hansen. 2016. "Mass Spectrometry Imaging of Biomarker Lipids for Phagocytosis and Signalling during Focal Cerebral Ischaemia." *Scientific Reports* 6 (1). Nature Publishing Group: 39571. doi:10.1038/srep39571.
- Oliveira, T G, R B Chan, F V Bravo, a Miranda, R R Silva, B Zhou, F Marques, et al. 2015. "The Impact of Chronic Stress on the Rat Brain Lipidome." *Molecular Psychiatry*, no. November 2014. Nature Publishing Group: 1–9. doi:10.1038/mp.2015.14.
- Oliveira, Tiago Gil, Robin B Chan, Huasong Tian, Mikael Laredo, Guanghou Shui, Agnieszka Staniszewski, Hong Zhang, et al. 2010. "Phospholipase d2 Ablation Ameliorates Alzheimer's Disease-Linked Synaptic Dysfunction and Cognitive Deficits." *The Journal of Neuroscience : The Official Journal of the Society for Neuroscience* 30 (49): 16419–28. doi:10.1523/JNEUROSCI.3317-10.2010.
- Oliveira, Tiago Gil, and Gilbert Di Paolo. 2010. "Phospholipase D in Brain Function and Alzheimer's Disease." *Biochimica et Biophysica Acta (BBA) - Molecular and Cell Biology of Lipids* 1801 (8). Elsevier B.V.: 799–805.

- doi:10.1016/j.bbalip.2010.04.004.
- Pinto, V., J. C. Costa, P. Morgado, C. Mota, a. Miranda, F. V. Bravo, T. G. Oliveira, J. J. Cerqueira, and N. Sousa. 2014. "Differential Impact of Chronic Stress along the Hippocampal Dorsal-Ventral Axis." *Brain Structure and Function*, 1–8. doi:10.1007/s00429-014-0713-0.
- Polman, J. Annelies E, Richard G Hunter, Niels Speksnijder, Jessica M E Van Den Oever, Oksana B Korobko, Bruce S. McEwen, E. Ronald De Kloet, and Nicole A Datson. 2012. "Glucocorticoids Modulate the Mtor Pathway in the Hippocampus: Differential Effects Depending on Stress History." *Endocrinology* 153 (9): 4317–27. doi:10.1210/en.2012-1255.
- Rodriguez-Navarro, Jose Antonio, Susmita Kaushik, Hiroshi Koga, Claudia Dall'Armi, Guanghou Shui, Markus R. Wenk, Gilbert Di Paolo, and Ana Maria Cuervo. 2012. "Inhibitory Effect of Dietary Lipids on Chaperone-Mediated Autophagy." *Proceedings of the National Academy of Sciences of the United States of America* 109 (12): E705-14. doi:10.1073/pnas.1113036109.
- Segal, Menahem, Gal Richter-Levin, and Nicola Maggio. 2010. "Stress-Induced Dynamic Routing of Hippocampal Connectivity: A Hypothesis." *Hippocampus* 20 (12): 1332–38. doi:10.1002/hipo.20751.
- Shah, Sheel, Eric Lubeck, Wen Zhou, and Long Cai. 2017. "seqFISH Accurately Detects Transcripts in Single Cells and Reveals Robust Spatial Organization in the Hippocampus." *Neuron* 94 (4). Cell Press: 752–758.e1. doi:10.1016/J.NEURON.2017.05.008.
- Simons, Kai, and JI Sampaio. 2011. "Membrane Organization and Lipid Rafts." *Cold Spring Harbor ...*, 1–18. <http://cshperspectives.cshlp.org/content/3/10/a004697.short>.
- Sousa, N, Nv Lukoyanov, Md Madeira, Of Almeida, and Mm Paula-Barbosa. 2000. "Reorganization of the Morphology of Hippocampal Neurites and Synapses after Stress-Induced Damage Correlates with Behavioral Improvement." *Neuroscience* 101 (2): 483. <http://www.ncbi.nlm.nih.gov/pubmed/11074170>.
- Sousa, Nuno, and Osborne F X Almeida. 2012. "Disconnection and Reconnection: The Morphological Basis of (Mal)adaptation to Stress." doi:10.1016/j.tins.2012.08.006.
- Sousa, Nuno, João J. Cerqueira, and Osborne F X Almeida. 2008. "Corticosteroid Receptors and Neuroplasticity." *Brain Research Reviews* 57 (2): 561–70. doi:10.1016/j.brainresrev.2007.06.007.
- Strange, Bryan a, Menno P Witter, Ed S Lein, and Edvard I Moser. 2014. "Functional Organization of the Hippocampal Longitudinal Axis." *Nature Publishing Group* 15 (10). Nature Publishing Group: 655–69. doi:10.1038/nrn3785.
- Thomas, Aurélien, Jade Laveaux Charbonneau, Erik Fournaise, and Pierre Chaurand. 2012. "Sublimation of New Matrix Candidates for High Spatial Resolution Imaging Mass Spectrometry of Lipids: Enhanced Information in Both Positive and Negative Polarities after 1,5-Diaminonaphthalene Deposition." *Analytical Chemistry* 84 (4): 2048–54. doi:10.1021/ac2033547.
- Thompson, Carol L., Sayan D. Pathak, Andreas Jeromin, Lydia L. Ng, Cameron R. MacPherson, Marty T. Mortrud, Allison Cusick, et al. 2008. "Genomic Anatomy of the Hippocampus." *Neuron* 60 (6). Elsevier Ltd: 1010–21. doi:10.1016/j.neuron.2008.12.008.
- Vermeren, Matthieu M., Qifeng Zhang, Elizabeth Smethurst, Anne Segonds-Pichon, Heinrich Schrewe, and Michael J. O. Wakelam. 2016. "The Phospholipase D2 Knock Out Mouse Has Ectopic Purkinje Cells and Suffers from Early Adult-Onset Anosmia." Edited by Sally Martin. *PLOS ONE* 11 (9). Public Library of Science: e0162814. doi:10.1371/journal.pone.0162814.
- Wenk, Markus R. 2010. "Lipidomics: New Tools and Applications." *Cell* 143 (6). Elsevier Inc.: 888–95. doi:10.1016/j.cell.2010.11.033.
- Yang, Hyun-Jeong Jeong, Yuki Sugiura, Koji Ikegami, Yoshiyuki Konishi, and Mitsutoshi Setou. 2012. "Axonal Gradient of Arachidonic Acid-Containing Phosphatidylcholine and Its Dependence on Actin Dynamics." *Journal of Biological Chemistry* 287 (8). American Society for Biochemistry and Molecular Biology: 5290–5300. doi:10.1074/jbc.M111.316877.
- Zhang, Ye, Kenian Chen, Steven A Sloan, Mariko L Bennett, Anja R Scholze, Sean O'Keeffe, Hemali P Phatnani, et al. 2014. "An RNA-Sequencing Transcriptome and Splicing Database of Glia, Neurons, and Vascular Cells of the Cerebral Cortex." *The Journal of Neuroscience : The Official Journal of the Society for Neuroscience* 34 (36). Society for Neuroscience: 11929–47. doi:10.1523/JNEUROSCI.1860-14.2014.

Acknowledgments

We thank Bowen Zhou from Columbia University for the help in performing the lipidomic analysis. This work was supported by grants from the Fundação para a Ciência e Tecnologia (PD/BD/105915/2014 to A.M.M. and PTDC/SAU-NMC/118971/2010 to T.G.O).

Competing Financial Interest

The authors declare no competing financial interests.

Figure Legends

Figure 1. Lipidomic analysis of brain regions from adult rats. Adult rats were subjected to daily injections of vehicle (VEH) and the annotated brain regions were macrodissected prior to analysis of homogenates by LC-MS (see Methods section for details). For lipid nomenclature, see Methods section. Heatmap generated by calculating the standard value of each lipid class (column) using as reference the pooled average relative mol% of all brain regions. Z scores [(mol% of lipid class of each animal – average mol% of lipid class in all brain regions of pool of animals)/standard deviation of average mol% lipid class of all brain regions of pool of animals] represented in gradient color; blue indicates negative Z value; red indicates positive value (lower and higher than reference average, respectively). Each row indicates an individual animal, per brain region (N=9 for dorsal hippocampus, N=10 for all other regions).

Figure 2. Distinct lipid composition of dorsal and ventral hippocampus in adult rats. a)

LC-MS analysis of dorsal and ventral hippocampus macrodissected from adult rats injected with vehicle (VEH). For lipid nomenclature, see Methods section. Bar graphs indicate fold-change of average relative mol% of all lipids measured, normalized to dorsal hippocampus (mean \pm SEM, $N = 9$ for dorsal hippocampus, $N=10$ for ventral hippocampus). Upper panel, heatmap indicates individual fold-change values for average mol% of each lipid class in the ventral hippocampus, normalized to the dorsal hippocampus. Values represented in gradient color. * $p < 0.05$, ** $p < 0.01$ and *** $p < 0.001$ in two-tailed Student's t test. **b)** LC-MS analysis of diacylglycerol/glycerophospholipid and sphingolipid acyl chain. Values expressed as average mol% of total lipid measured, normalized to dorsal hippocampus. Lipids were classified per total acyl carbons and degree of unsaturation (mean \pm SEM, $N=9$ for dorsal hippocampus, $N=10$ for ventral hippocampus) * $p < 0.05$, ** $p < 0.01$ and *** $p < 0.001$ in two-tailed Student's t test.

Figure 3. Similar major effects of corticosterone injections in the lipid composition of dorsal and ventral hippocampus. a-b)

LC-MS analysis of dorsal and ventral hippocampus macrodissected from adult rats submitted to a 4-week protocol of daily injections of corticosterone (CORT) compared to age-matched control injected with vehicle (VEH). For lipid nomenclature, see Methods section. Bar graphs indicate fold-change of average relative mol% of all lipids measured, normalized to VEH (mean \pm SEM, $N = 9$ for dorsal hippocampus of VEH; $N=10$ for remaining groups). Upper panels, heatmap indicates individual fold-change values for average mol% of each lipid

class in CORT, normalized to VEH. Values represented in gradient color. * $p < 0.05$, ** $p < 0.01$ and *** $p < 0.001$ in two-tailed Student's t test.

Figure 4. Specific lipid species are differently regulated in the dorsal and ventral hippocampus by corticosterone. A ventral/dorsal hippocampus ratio for each lipid species detected, for each animal, was calculated in adults rats injected with vehicle (VEH, in grey) or corticosterone (CORT, in red) (mean \pm SEM, $N = 9$ for VEH; $N = 10$ for CORT). * $p < 0.05$, ** $p < 0.01$ and *** $p < 0.001$ in two-tailed Student's t test.

Supplementary Figure 1. Lipidomic analysis of brain regions from control adult rats (not injected; CTRL). Adult rats were handled daily injections and homogenates of the following brain regions were analyzed by LC-MS (see Fig. 1). For lipid nomenclature, see Methods section. Heatmap generated by calculating the standard value of each lipid class (column) using as reference the pooled average relative mol% of all brain regions. Z values [(mol% of lipid class of each animal – average mol% of lipid class in all brain regions of pool of animals)/standard deviation of average mol% lipid class of all brain regions of pool of animals] represented in gradient color; blue indicates negative Z value; red indicates positive value (lower and higher than reference average, respectively). Each row indicates an individual animal, per brain region ($N = 10$ animals).

Supplementary Figure 2. Distinct lipid composition of dorsal and ventral hippocampus in control adult rats (CTRL). a) LC-MS analysis of dorsal and ventral hippocampus macrodissected from adult rats (not injected; CTRL). For lipid nomenclature, see Methods section. Bar graphs indicate fold-change of average relative mol% of all lipids measured, normalized to dorsal hippocampus (mean \pm SEM, $N = 10$ per group). Upper panel, heatmap indicates individual fold-change values for average mol% of each lipid class in the ventral hippocampus, normalized to the dorsal hippocampus. Values represented in gradient color. * $p < 0.05$, ** $p < 0.01$ and *** $p < 0.001$ in two-tailed Student's t test.

Supplementary Figure 3. Comparative lipidome profile of dorsal and ventral hippocampus in adult rats injected with vehicle (VEH) and control adult rats (CTRL). The heatmap represents all lipid species detected by LC-MS in macro-dissected tissue. Lipids were classified per total acyl carbons and degree of unsaturation, respectively. Values represented as

average fold-change of individual species in ventral hippocampus, normalized to dorsal hippocampus (only statistically significant values shown ($p < 0.05$), $N=9$ for dorsal hippocampus in vehicle injected rats; $N=10$ for remaining groups). Results were compared using two-tailed Student's *t*-test.

Supplementary Figure 4. Lipidome profile of dorsal and ventral hippocampus from adult rats submitted to daily injections of corticosterone (CORT) compared to vehicle-treated animals (VEH). The heatmap represents all lipid species detected by LC-MS in macro-dissected tissue. Lipids were classified per total acyl carbons and degree of unsaturation, respectively. Values represented as average fold-change of individual species in dorsal and ventral hippocampus of CORT animals, normalized to vehicle-injected rats (VEH) (only statistically significant values shown ($p < 0.05$), $N=9$ for dorsal hippocampus of VEH; $N=10$ for remaining groups). Results were compared using two-tailed Student's *t*-test.

Figures

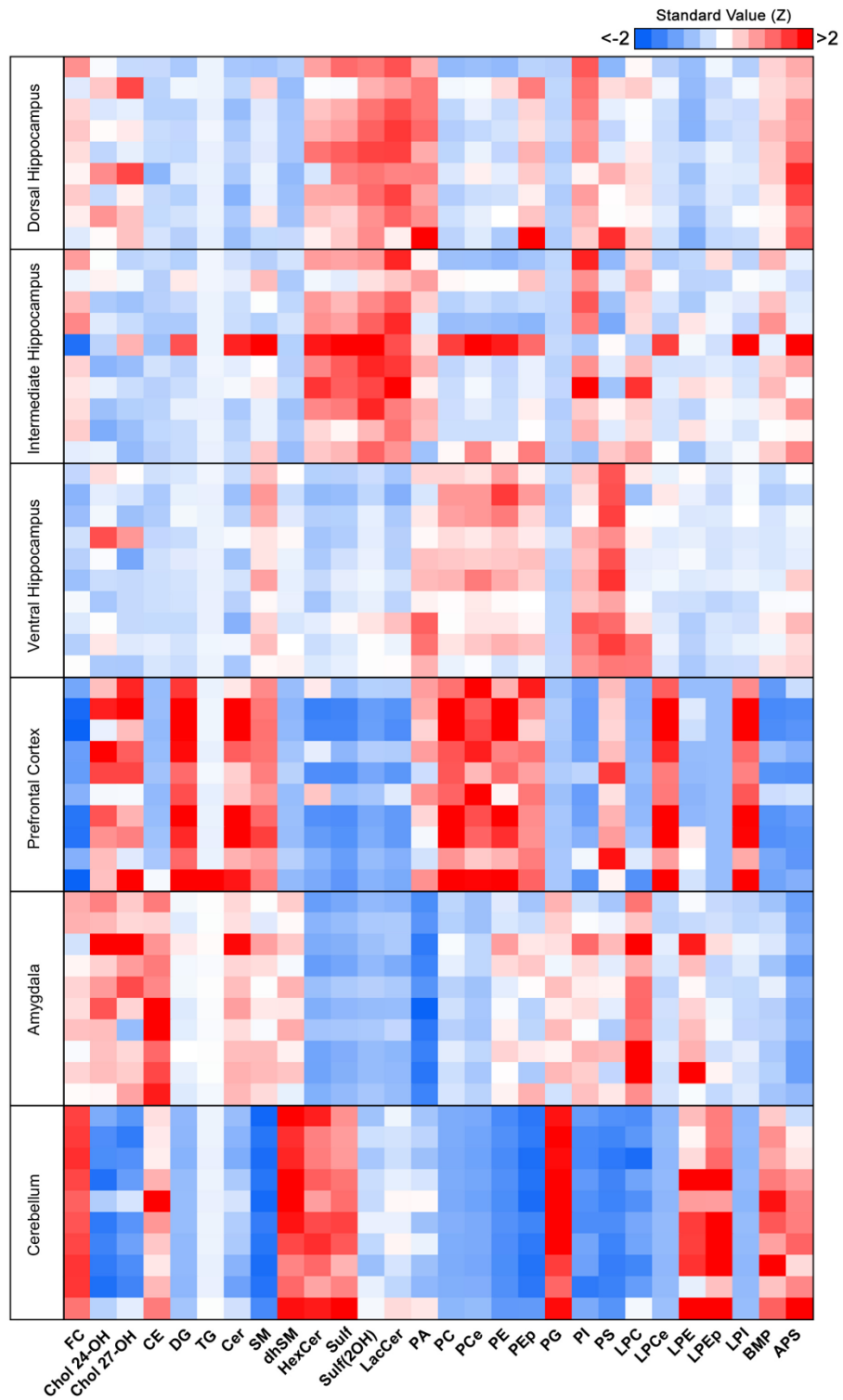


Figure 1 – Miranda *et al.*

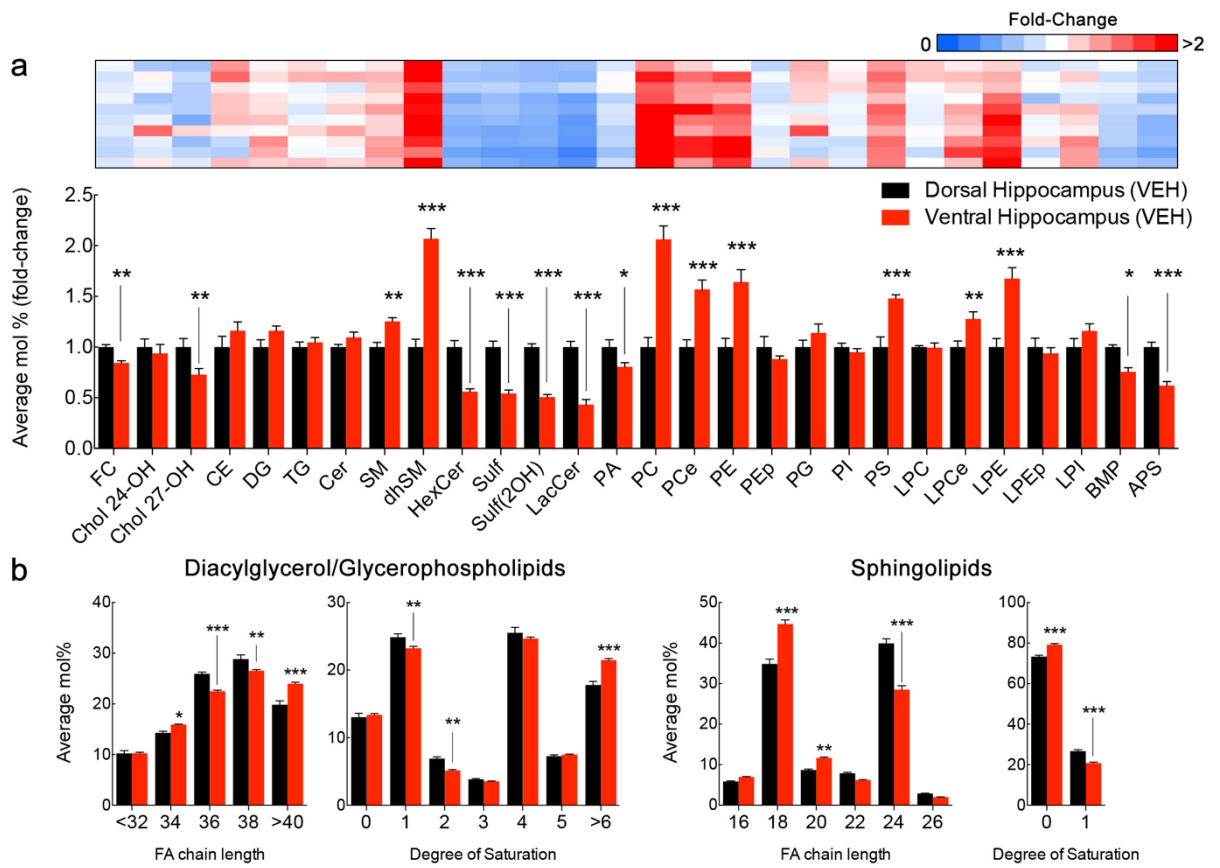


Figure 2 – Miranda *et al.*

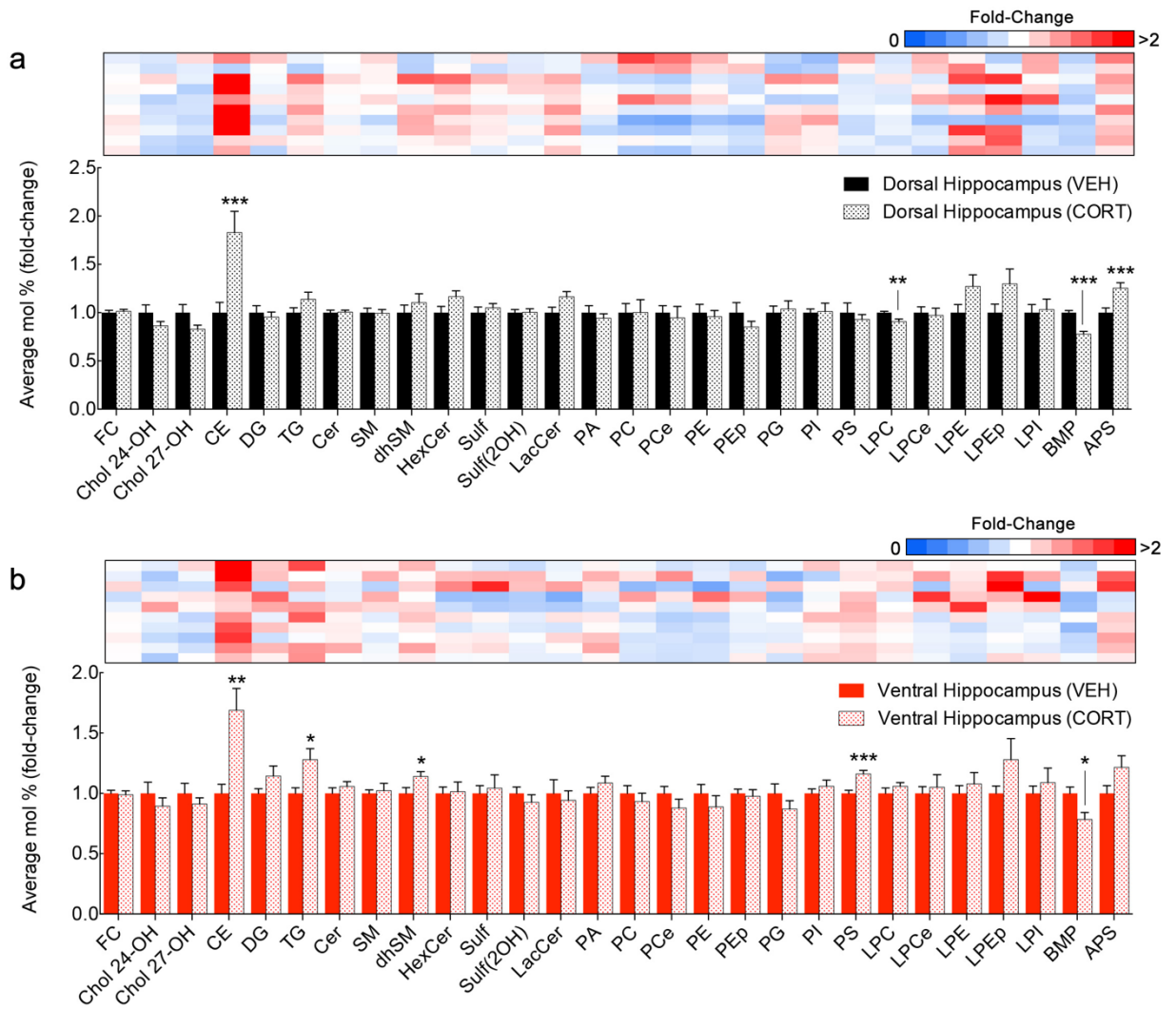


Figure 3 – Miranda *et al.*

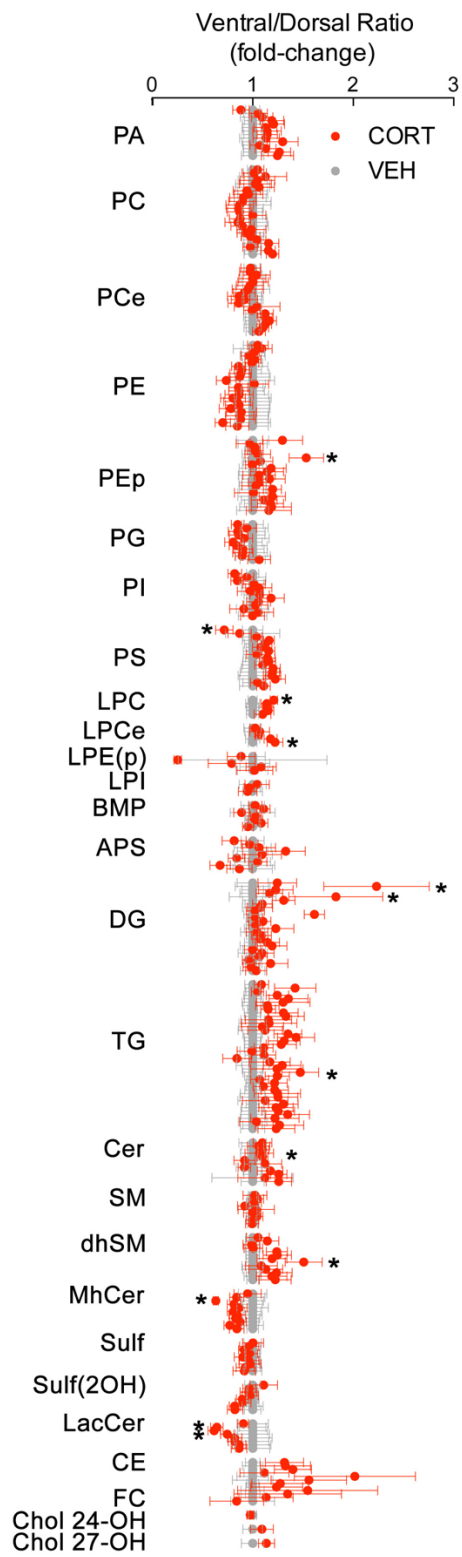
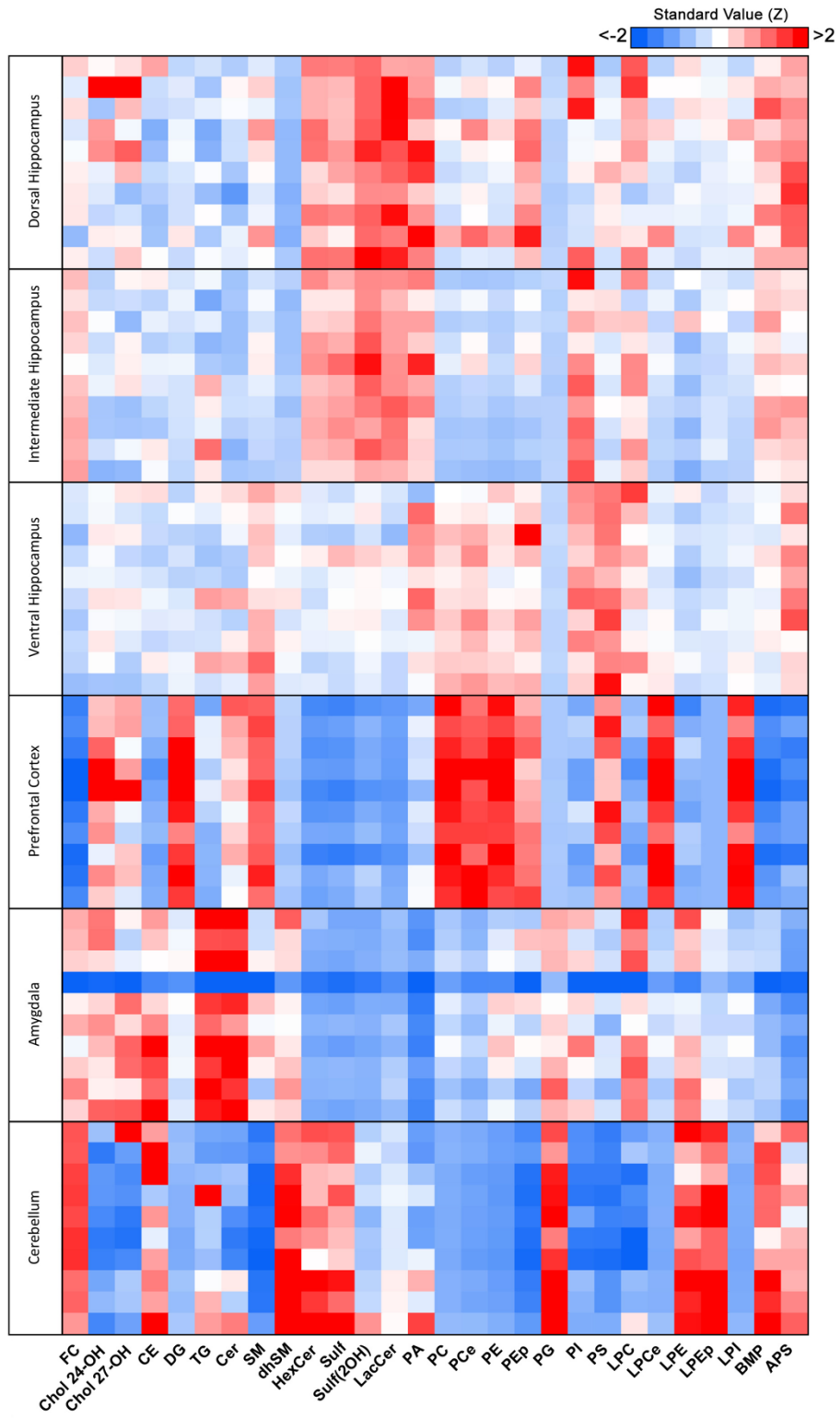
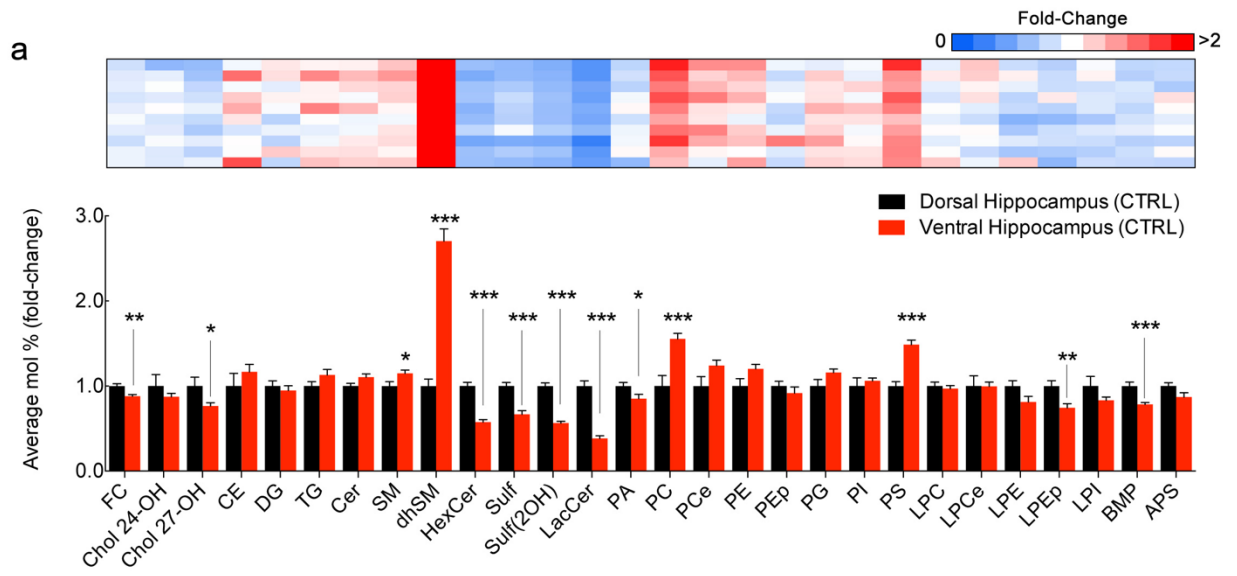


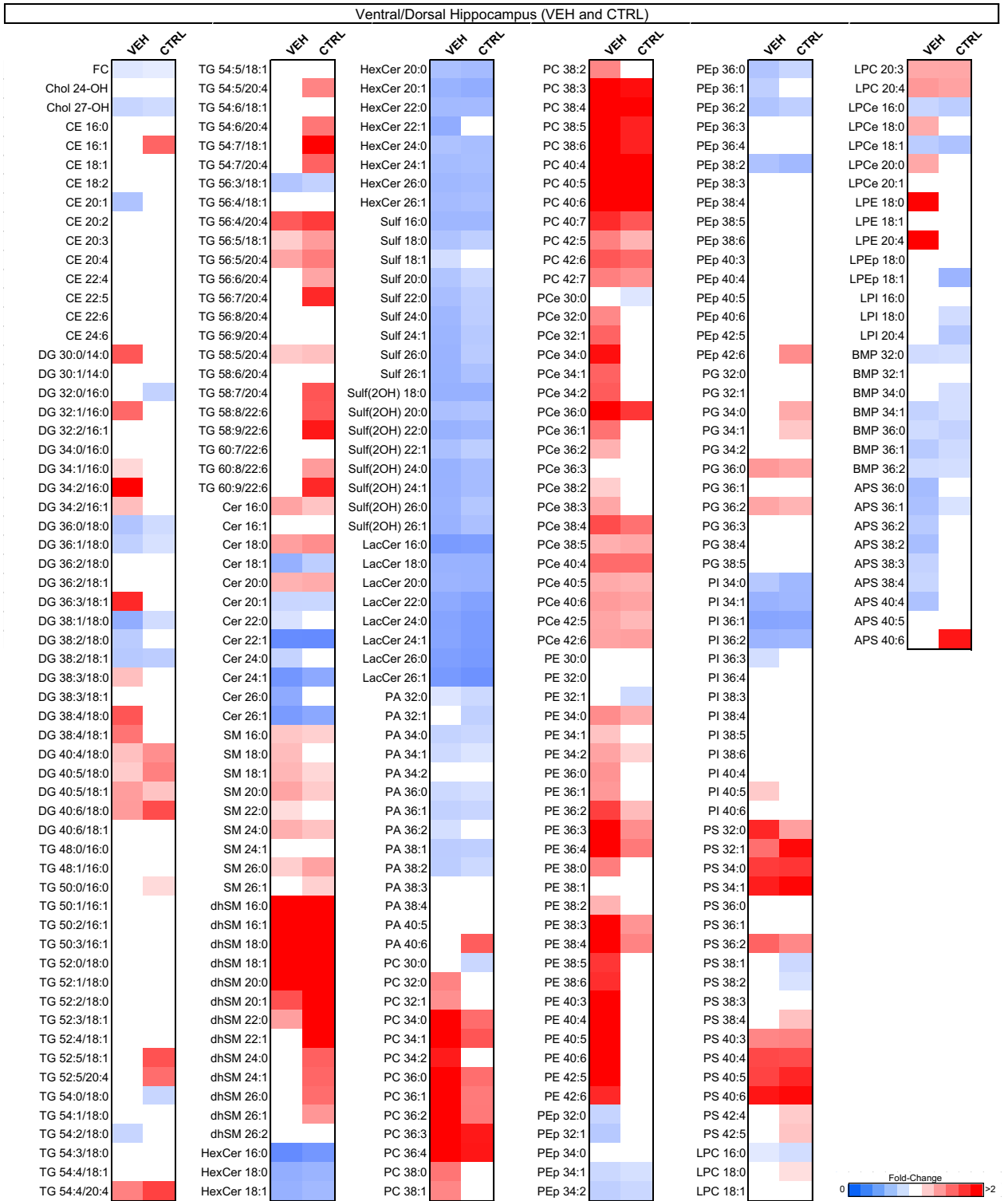
Figure 4 – Miranda *et al.*



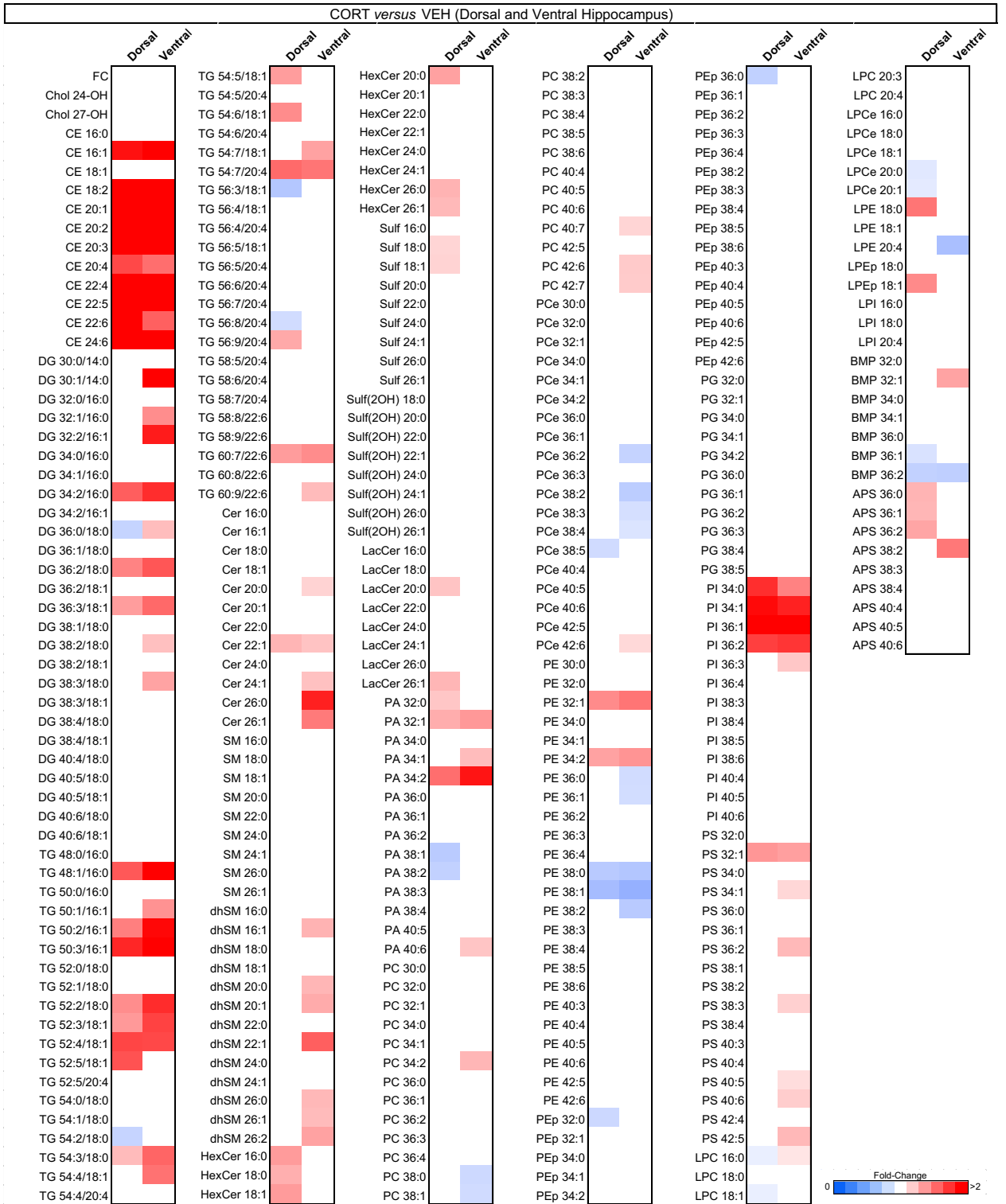
Supplementary Figure 1 – Miranda *et al.*



Supplementary Figure 2 – Miranda *et al.*



Supplementary Figure 3 – Miranda *et al.*



Supplementary Figure 4 – Miranda *et al.*

CHAPTER 3

DISCUSSION, CONCLUSIONS AND FUTURE PERSPECTIVES

DISCUSSION, CONCLUSIONS AND FUTURE PERSPECTIVES

The crucial role of the endolysosomal system for maintenance of neuronal health is supported by evidence that impairment of endosomal traffic or autophagic clearance causes neurodegeneration (Fraldi et al. 2016). Several rare familial, early onset forms of neurodegenerative disorders (e.g., AD, PD and FTD) are associated with gene mutations that facilitate aggregation and reduced clearance of disease-specific proteins (e.g., A β , α -synuclein and tau, respectively). In more common sporadic and late onset forms, genetic polymorphisms conferring slightly elevated risks appear to affect similar pathways (Abeliovich and Gitler 2016; Karch and Goate 2015). Common histological findings implicate morphological and functional deterioration of endosomes, lysosomes and autophagosomes in these disorders, as well as normal aging (Menziés et al. 2017; Kaushik and Cuervo 2015). Altogether, these observations lend support to the growing view that a subset of neurodegenerative disorders may be interpreted as mild, slowly-progressing LSD-like disorders (Nixon, Yang, and Lee 2008; Platt, Boland, and van der Spoel 2012). Hence, it is of the highest priority to identify the culprits for endolysosome destabilization in this context, which will provide not only insights into the mechanisms driving disease onset and progression but also potential diagnostic and prognostic biomarkers and molecular targets of therapeutic value.

Lipids are fundamental molecules for the vesicular organization of intracellular organelles and for cell signaling (Miranda and Oliveira 2015). Notably, dysregulation of lipid metabolism has been implicated in different neurodegenerative disorders (Di Paolo and Kim 2011; Echten-deckert and Walter 2012; Kubo 2016). While the documentation of disease-linked lipid profiles through the use of large-scale mass-spectrometry-based approaches is of critical value for an overview of the metabolic and molecular landscape in each disease, it provides limited insights into whether lipid dysregulation is a cause or consequence of the pathogenic state (Mapstone et al. 2014; Han 2016). Therefore, following the recent report that PI3P is selectively decreased in AD brains and mouse models thereof, and considering the role of this lipid as a master regulator of the endolysosomal and autophagy pathways, we explored the potential of PI3P dysregulation as a factor contributing to AD pathogenesis and neurodegeneration (Morel et al. 2013; Miranda et al. 2018).

Herein, we investigated the impact of neuronal Vps34 inhibition and genetic ablation on endolysosomal function, autophagy and metabolism of APP. We report that blockade of Vps34 function has a profound effect on APP-CTFs and minimally impacts A β . Specifically, APP-CTFs, including the BACE1 product APP-CTF β , accumulate as a result of reduced lysosomal degradation, rather than impaired γ -secretase or autophagy activity. Remarkably, we found that Vps34 inhibition

leads to dysregulation of lipid metabolism, endolysosomal membrane disruption as well as active secretion of a significant amount of APP-CTFs on a subpopulation of exosomes also enriched in ubiquitinated proteins and atypical lipids such as dihydrosphingolipids and BMP. Therefore, our work demonstrates that endolysosomal destabilization may induce the release of potentially toxic cargoes through exosomes, likely as a homeostatic response to counteract inappropriate lysosomal storage, yet possibly facilitating disease propagation.

3.1 PI3P depletion dramatically impairs endolysosomal traffic in neurons

PI3P is primarily synthesized by the lipid kinase Vps34 (Dall'Armi, Devereaux, and Di Paolo 2013). Thus, to address the impact of PI3P depletion in neuronal endolysosomal function, we used a recently developed Vps34 pharmacological inhibitor, VPS34IN1 (Bago et al. 2014). This strategy allowed us to specifically focus on the catalytic activity of Vps34 and by-pass the loss of scaffolding function associated with genetic ablation of Vps34, which destabilizes its interacting partners, namely Beclin 1 and Vps15, and likely interferes with endosomal traffic and cell signaling through protein complex destabilization (Devereaux et al. 2013; Jaeger and Wyss-Coray 2010; Gstrein et al. 2018).

First, we analyzed the morphology of early endocytic compartments upon Vps34 inhibition. We detected an enlargement of EEA1-positive endosomes, similarly to what had been reported with Vps34 silencing (Devereaux et al. 2013; Morel et al. 2013). Since Vps34 negatively regulates Rab5, we hypothesized that Rab5 activation could occur in compensation to decreased PI3P levels (Law et al. 2017). In fact, we also found that Rab5 is likely hyperactive since Rab5-positive endosomes were not only enlarged but also showed higher fluorescence intensity (*i.e.*, membrane recruitment of Rab5). In addition, Rab5 co-localization with APPL1, an endosomal marker known to associate with PI3P-negative endosomes, was increased (Zoncu et al. 2009). Importantly, Rab5 anomalies have been reported in pre-clinical stages of AD, induced pluripotent stem cell-derived neurons generated from familial and late onset AD patients and in Down Syndrome patients, who develop early onset AD neuropathology (Cataldo et al. 2000; Jiang et al. 2010; Israel et al. 2012; Wiseman et al. 2015). While seen as one of the earliest pathological events in AD, even preceding other autophagy- and lysosome-related disturbances also reported in this disease, the mechanisms driving dysregulation of the endocytic pathway are still not known (Peric and Annaert 2015). This question has potentially major implications for the pathogenesis of AD because many of the associated genetic risk factors are involved in early endosome biology (*e.g.*, *BIN1*, *SORL1*, *CD2AP*, *PICALM*), mostly affecting the balance of trafficking in and out of this compartment including membrane recycling, retromer

transport and lysosomal degradation (Small et al. 2017). Dysregulation of this pathway may enhance coincidental localization of APP and BACE-1, which leads to enhanced amyloidogenic cleavage of APP and a secondary perturbation of endosomal trafficking through accumulation of toxic APP metabolites (Jiang et al. 2010; Xu et al. 2016). Notably, APP-CTF β has been recently found to stabilize Rab5 in endosomal membranes through interaction with APPL1 and drive endosomal enlargement (Kim et al. 2016). Here, since we show that depletion of PI3P facilitates Rab5-APPL1 interaction, it could consequently be a primary cause of endosomal enlargement, while secondary accumulation of APP-CTF β exacerbates this phenotype. Alternatively, increased endosomal size may also be due to defects in endosomal maturation (*i.e.*, Rab5 to Rab7 conversion), excessive endosomal homotypic fusion or defective tubulation or retrograde trafficking from endosomes, all of which have been linked to decreased Vps34 function (Schink, Tan, and Stenmark 2016).

Next, we found that Vps34 inhibition more dramatically affects APP-CTF metabolism than A β secretion. Remarkably, APP-CTF accumulation induced by VPS34IN1 was enhanced in the presence of a pharmacological γ -secretase inhibitor, suggesting that APP-CTF accumulation derives from impaired endosomal sorting and lysosomal degradation and not by defects in γ -secretase function. Also, we observed the same phenotype in gene-edited Atg5 KO N2a cells after Vps34 kinase inhibition, suggesting that APP-CTF accumulation originates from other aspects of endolysosomal dysfunction than VPS34IN1-induced autophagy blockade. Interestingly, Beclin 1 silencing also causes accumulation of APP-CTFs but instead increases secretion of A β , as seen with Vps34 silencing (Jaeger et al. 2010; Tian et al. 2011; Morel et al. 2013). While these observations appear to be at odds with our findings, our results are supported by experiments using other pharmacological inhibitors of Vps34, wortmannin and 3-methyladenine, albeit of low specificity, both of which decrease A β secretion (Yu et al. 2005; Petanceska and Gandy 1999). This discrepancy may therefore reflect kinase-dependent *vs.* scaffolding effects of Vps34. Alternatively, increased A β secretion by Vps34 and Beclin 1 silencing may be explained by accumulation of autophagosomes, structures enriched for γ -secretase proteins and A β production, which otherwise are not found in VPS34IN1-treated neurons (Yu et al. 2005). While we were not able to precisely determine intracellular A β levels, we hypothesize that decreased secretion associated with Vps34 inhibition is due increased cellular retention of A β peptides. In fact, inhibition of autophagy through genetic ablation of Atg7 causes intracellular accumulation of A β while secondary induction of autophagy, through inhibition of mTOR or proteasome, increases A β secretion (Nilsson et al. 2013; Agholme et al. 2012). Also, inhibition of ESCRT-mediated sorting of APP and APP-CTFs through silencing of Hrs and Tsg101, which sort

ubiquitinated cargoes into ILVs in a PI3P-dependent fashion, is associated with decreased A β secretion, which is instead retained intracellularly (Edgar et al. 2015). While both of these processes are linked to Vps34 mediated function, consequent accumulation of APP and APP-CTFs in the limiting membrane of MVEs facilitates A β generation by presenilin-2, which is predominantly found in this compartment and promotes cellular retention of A β (Sannerud et al. 2016). Therefore, it will be interesting to test whether presenilin-2 is indeed responsible for impaired secretion of A β upon PI3P depletion. Finally, *in vivo* genetic ablation of *Pik3c3* (the gene encoding Vps34) did not affect total soluble A β levels. Clearly, the relationship between PI3P-mediated cellular events and A β metabolism is not yet fully understood and is worthy of further attention in the future. In fact, understanding the causes of intracellular A β accumulation is of highest priority as this event occurs in early stages of AD onset, preceding build-up of extracellular plaques, and coincides with potentially reversible synaptic and behavioral defects (Billings et al. 2005; Tomiyama et al. 2010; LaFerla, Green, and Oddo 2007). Independently of A β -mediated toxicity, accumulation of APP-CTF β is also of great relevance as a common hallmark of AD-pathology and known to induce age-dependent neurodegeneration and cognitive impairment (Yang et al. 2003; Kim et al. 2016; Oster-Granite et al. 1996; Rockenstein et al. 2005; Tamayev et al. 2012). Interestingly, overexpression of this APP metabolite induces accumulation of electron-dense granular inclusions and lysosome-like structures, similarly to *in vitro* pharmacological inhibition of Vps34 (Oster-Granite et al. 1996; Kaur et al. 2017). Therefore, our findings suggest a primary association of decreased PI3P levels and early cellular events potentially leading to AD pathogenesis.

A key finding reported in this work is that reduction of PI3P severely impairs lysosomal function, causing accumulation of endolysosomal and autophagy cargoes, including both proteins and lipids, which is reminiscent of cellular models of LSDs, particularly Niemann-Pick Type C (Maulik et al. 2015; Boland et al. 2010). We detected a significant impairment of general lipid homeostasis upon deficiency of PI3P *in vivo* and *in vitro*, including accumulation of ceramides, dihydroceramides and BMP. Of note, sphingolipid accumulation induces cytopathological features of AD, including disruption of autophagy/lysosomal clearance and accumulation of APP-CTFs, supporting the idea that PI3P depletion precipitates changes in endolysosomal membrane lipid composition of pathological relevance (Tamboli et al. 2011). Coincidentally, we detected the formation and accumulation of poly-ubiquitinated inclusions that co-localized with the autophagy receptor p62 in neuronal somas. Ultrastructural analysis revealed the presence of small, membrane-bound electron dense lysosome-like structures. These structures resembled electron-dense p62-positive inclusions formed upon

inhibition of autophagy inhibition (Kishi-Itakura et al. 2014). The observation that these structures did not co-localize with the autophagosomal marker LC3 and were not sorted to the lumen of LAMP-1 late endosomes/lysosomes highlights the critical role of PI3P in phagophore formation and lysosomal delivery of autophagy cargo. We also found that ubiquitin/p62-positive structures co-localized with galectin-3, an endogenous cytosolic protein commonly used as a probe for endolysosomal permeabilization (Maejima et al. 2013). We attempted to identify these compartments but found no co-localization of galectin-3/p62 puncta with any canonical endosomal markers [e.g. Rab5, Rab7, EEA1, LAMP-1, LAMP-2, Vps35 (data not shown)] other than flotillin-1 and -2. While flotillins are commonly associated with membrane domains enriched for sphingolipids and cholesterol and thus confirm the membrane-bound nature of galectin-3 inclusions, we are unsure if they correspond to a specific subset of endocytic compartments that are more prone to membrane damage in the context of endolysosomal dysfunction or to the generality of compartments that happen to become permeabilized upon Vps34 inhibition. A possible explanation for the loss of molecular identity is that permeabilization may trigger destabilization of the low-affinity binding of endosomal markers that typically characterize these compartments or luminal diffusion of hydrolytic enzymes that cause their cleavage. Compartmental accumulation of sphingolipids and cholesterol, known to occur in intermediate endosomal structures as a result of lysosomal dysfunction, may also be a primary cause of membrane destabilization (Gabandé-Rodríguez et al. 2014; Cannizzo et al. 2012; Blom et al. 2015; Hernández-Tiedra et al. 2016). The inefficient autophagic clearance of such sphingolipid-enriched compartments could therefore explain the specific intracellular accumulation of ceramides and derivatives in neurons treated with VPS34IN1. Other possible mechanisms, which are not necessarily mutually exclusive, may involve local synthesis of lysolipids which display detergent-like properties; impaired maturation and glycosylation of membrane associated proteins that normally protect membranes from lytic enzymes, and defects in lysosomal acidification or substrate clearance (Gómez-Sintes, Ledesma, and Boya 2016; Li et al. 2016). Interestingly, p62-positive structures adjacent to lysosomes, as seen in Vps34-inhibited neurons, were detected upon lysosome membrane permeabilization mediated by genetic ablation of lysosomal enzyme tripeptidyl peptidase I (TPP1; associated with classic late-infantile neuronal ceroid lipofuscinosis CLN2) and treatment with lysosomotropic agent LeuLeuOMe (Micsenyi et al. 2013). These results thus suggest that lysosomal membrane permeabilization may be a common and important cellular event in LSD-like pathology (Gómez-Sintes, Ledesma, and Boya 2016). Moreover, it may also be of great clinical relevance since unstable lysosomes can potentially be therapeutically targeted with molecular chaperones (Kirkegaard

et al. 2010). Importantly, extracellular aggregates of neurotoxic proteins and peptides as α -synuclein and tau cause endolysosomal membrane rupture, which allows migration to the cytoplasm and aggregation in acceptor cells (Freeman et al. 2013; Calafate et al. 2016; Papadopoulos et al. 2017). Therefore, one of the potential implications of PI3P deficiency in neurodegenerative disorders is increased susceptibility to membrane damage that may facilitate prion-like spreading of aggregate-prone proteins (Walker and Jucker 2015).

Neuronal conditional knock-out of *Pik3c3* causes progressive synaptic loss and extensive gliosis and neurodegeneration (Zhou et al. 2010; L. Wang, Budolfson, and Wang 2011). Interestingly, Vps34 deficiency in sensory neurons did not abolish the ability of forming autophagosomes, suggesting chronic compensatory mechanisms of PI3P synthesis via other PI-3-kinases, although not sufficient to overcome disruption of endosomal compartments (Zhou et al. 2010; Devereaux et al. 2013). In fact, genetic ablation of Vps34 in the forebrain induces a much more dramatic phenotype than deletion of autophagy related genes Atg5 and Atg7, consistent with broader endolysosomal dysfunction than autophagy impairment alone (Komatsu et al. 2006; Hara et al. 2006; L. Wang, Budolfson, and Wang 2011). Importantly, our *in vitro* findings were corroborated by *in vivo* neuronal-specific deletion of Vps34 which phenocopied elevated poly-ubiquitinated proteins and accumulation of sphingolipids and BMP. Remarkably, only APP-CTFs were affected *in vivo*, but not other APP metabolites. Collectively, we note that neuronal conditional knock-out of *Pik3c3* is an excellent model to address endolysosomal defects *in vivo*, particularly since these manifestations precede the onset of neurodegeneration. Moreover, since reactive gliosis and secondary loss of wild-type neurons follow these observations, it will also be an interesting model to study intercellular communication, onset and progression of neuroinflammation, a process in which secretion of lipids and exosomes may play a fundamental role (L. Wang, Budolfson, and Wang 2011; Sundaram et al. 2012)).

3.2 Endolysosomal dysfunction induces secretion of unique exosomes

The endolysosomal pathway is a highly differentiated system that includes multiple control-checkpoints and alternate fates for endosomal cargo (Klumperman and Raposo 2014). Early endosomes are a primary filter for membrane recycling while late endosomes and MVEs mediate retrograde trafficking, lysosomal fusion and secretion of exosomes. The secretion of proteins and lipids that are known to accumulate as a result of disruption of autophagy or lysosome function suggests that exosomes may also contribute to the homeostatic balance of cells and alleviate storage burden (Eitan et al. 2016). While misfolded neurotoxic proteins such as α -synuclein, TDP43, prion-protein,

tau, APP-CTFs and A β have been reported in exosomes, it is still unclear how specific and physiologically relevant exosomal targeting is (Emmanouilidou et al. 2010; Alvarez-Erviti et al. 2011; Iguchi et al. 2016; Y. Wang et al. 2017; Perez-Gonzalez et al. 2012; Sharples et al. 2008; Rajendran et al. 2006).

To address the relationship between endolysosomal dysfunction and exosome secretion, we assessed the release of different exosomal markers upon Vps34 inhibition, in primary cortical neurons and N2a cells. We found that ALIX, flotillin-1 and flotillin-2 were increased in primary neurons following VPS34IN1 treatment whereas only flotillins were increased in N2a cells, but not other markers, including ESCRT-associated ALIX, Hrs, Tsg101 or the tetraspanin CD63. These observations suggest that PI3P depletion upregulates secretion of exosomes in general in neurons while only a specific subpopulation, flotillin-enriched, in N2a cells. We hypothesized that the preferential release of distinct exosome subtypes would translate in a distinct lipid signature of these vesicles, since flotillins are commonly found in lipid rafts, membrane subdomains enriched in cholesterol and sphingolipids. Indeed, we found that, in both neurons and N2a cells, exosomes were enriched in a myriad of sphingolipids, including dhSM, Cer and glycosphingolipids (MhCer and LacCer). In addition, these exosomes were particularly enriched in the atypical phospholipid BMP. Since this lipid is exclusively associated with ILVs, extracellular vesicles enriched in BMP can be defined as *bona fide* exosomes as they are from endosomal origin (Bissig and Gruenberg 2013). Altogether, these observations suggest that depletion of PI3P upregulates exosomal secretion, particularly of exosomes enriched for sphingolipids and BMP. In the future, nanoparticle tracking and gradient fractionation should be performed to unambiguously determine whether PI3P depletion modulates the total number of exosomes secreted or preferential subpopulations of vesicles with characteristic biochemical and morphological traits.

Another outstanding observation was that vesicles secreted upon Vps34 inhibition were enriched for undigested lysosomal cargo, which had been found to accumulate intracellularly, namely APP-CTFs, p62 and poly-ubiquitinated proteins (Figure 1). Interestingly, we show that exosomes predominantly transport mature, glycosylated full-length APP (as noted in the band shift to heavier weight in EV preparations comparatively to lysates) but, notably, are even more enriched in APP-CTFs. In fact, increased APP-CTF/APP ratio suggests that these vesicles are of endosomal origin as the initial α - and β -cleavage occurs predominantly in the endocytic pathway, as observed and suggested by others (Langui et al. 2004; Perez-Gonzalez et al. 2012; Laulagnier et al. 2017; Vingtdoux et al. 2007).

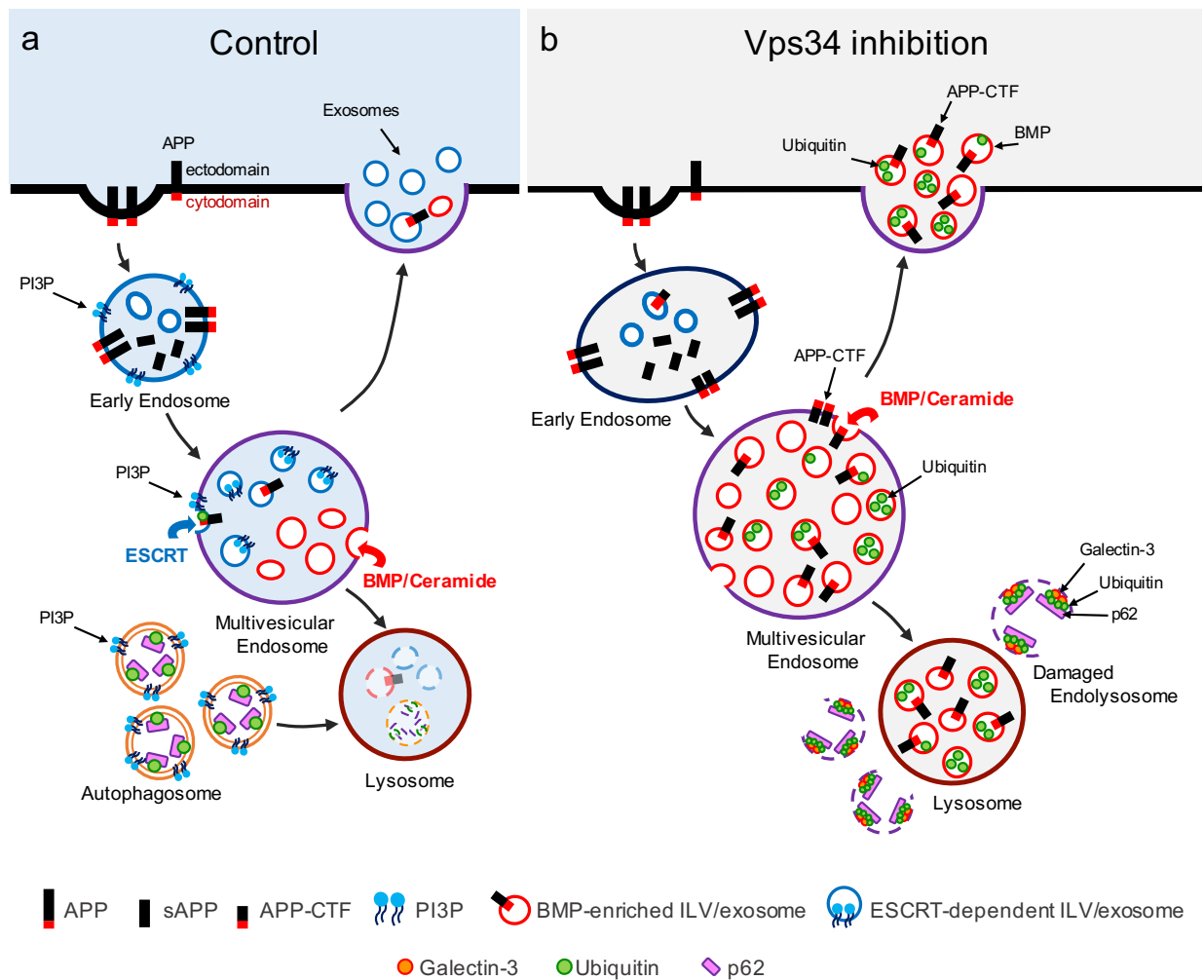


Figure 1. Vps34 inhibition causes endolysosomal dysfunction and enhanced release of atypical exosomes harboring poly-ubiquitinated proteins, APP-CTFs and the atypical phospholipid BMP.

a) In control cells, newly synthesized APP traffics to the plasma membrane (not shown), where it undergoes clathrin-mediated endocytosis and sorting into PI3P-enriched early endosomes. The acidic endosomal lumen is optimal for amyloidogenic processing by BACE1. APP-CTFs and a pool of full length APP are sorted to intraluminal vesicles (ILVs) of multivesicular endosomes (MVEs) via the ESCRT pathway, which requires PI3P and ubiquitination of lysine residues of the APP cytodomain. APP-CTFs are then be processed into A β , degraded in lysosomes or secreted in exosomes upon fusion of MVEs with the plasma membrane. Of note, under control conditions, exosomes are largely devoid of BMP. In a separate pathway, autophagosome formation and maturation also requires PI3P and mediate clearance of cytosolic cargoes and damaged organelles labelled with autophagy receptors (*e.g.*, p62) upon their fusion with the endolysosomal system. b) Vps34 inhibition causes enlargement of Rab5-positive early endosomes which are enriched for endosomal adaptor APPL1 instead of PI3P-binding protein, EEA1 (not shown). Through pleiotropic effects on the endolysosomal system, Vps34 inhibition causes accumulation of proteins and lipids in MVEs and lysosomes, resulting in a fraction of them undergoing physical damage, as denoted by the enrichment of galectin-3 on p62- and ubiquitin-positive structures. While PI3P deficiency reduces ESCRT-dependent sorting of cargoes, including APP, into ILVs, local synthesis of ceramide by nSMase2 facilitates ILV sorting and secretion of poly-ubiquitinated proteins, APP-CTFs and BMP in exosomes, alleviating lysosomal burden (Miranda and Di Paolo, *in press*).

Until recently, only a limited number of studies had described the presence of APP-CTFs in exosomes. In these reports, increased APP-CTF exosomal sorting was associated with increased

cellular levels alone, either by overexpression or pharmacological inhibition of γ -secretase. Here, we show that APP-CTFs are increasingly sorted to exosomes upon endolysosomal dysfunction, to a greater extent than intracellular accumulation. In fact, we directly compared PI3P inhibition (*i.e.*, endolysosomal dysfunction) to inhibition of γ -secretase alone (*i.e.*, APP-CTF accumulation alone), both of which cause an equivalent accumulation of intracellular APP-CTFs, and found a profound difference between both treatment conditions. APP-CTF enrichment in exosomes was significantly higher after VPS34IN1 treatment. As to better understand the sorting mechanisms underlying this phenotype, we found that mutated APP-CTFs lacking ubiquitination sites in the cytodomain, which are not efficiently sorted to the lumen of enlarged endosomes via ESCRT, are still released through exosomes as efficiently as wild-type APP-CTF upon Vps34 inhibition (data not shown) (Williamson et al. 2017). Interestingly, a recent study also reported sorting of APP-CTFs in atypical CD63-negative exosomes, which specifically bind to neurons but not glial cells *in vitro* (Laulagnier et al. 2017). Together with our results, this observation suggests that exosomes containing APP-CTFs, and those secreted upon Vps34 inhibition, are largely independent from ESCRT machinery and tetraspanins. Supporting this view, inhibiting nSMAse2 or *de novo* sphingolipid synthesis dramatically reduced APP-CTF exosomal secretion. While the existence of exosome subtypes is relatively well established, a fundamental question yet to be answered is whether these subpopulations co-reside or derive from distinct endosomal compartments (van Niel, D'Angelo, and Raposo 2018; Kowal et al. 2016). There is a longstanding view that PI3P- and BMP-positive ILVs are segregated from each other within MVEs, similarly to CD63- and ESCRT-dependent ILVs (Gillooly et al. 2000; Stuffers et al. 2009; Edgar, Eden, and Futter 2014). Importantly for neurodegenerative disorders, nSMAse2 has been specifically implicated in exosomal secretion of APP-CTFs, tau, TDP43 and prion-protein and exacerbation of AD-pathology in a transgenic mouse model (Miranda et al. 2018; Asai et al. 2015; Iguchi et al. 2016; Guo, Bellingham, and Hill 2015; Dinkins et al. 2014; Dinkins et al. 2016). This suggests that perhaps not all subpopulations of exosomes are constitutively secreted, but rather under control of specific regulatory pathways. In this line, we confirmed that inhibition of lysosomal V-ATPase using bafilomycin-A1 mimicked the effects of PI3P depletion, including increased exosomal sorting of APP-CTFs, flotillins and lipids as sphingolipids and BMP. Supporting evidence of lysosomal pH-dependent exosome secretion implicates the lysosomal and proteostatic status of the cell as major determinant for the release of at least a subset of exosomes, characterized by undigested lysosomal cargo (Edgar et al. 2016; H. Guo et al. 2017; Eitan et al. 2016). Altogether, we can only assume for now that exosome secretion results from a balance of distinct biogenic processes occurring in different maturation stages

or subpopulations of MVEs that likely depend on the nature of the cargo and regulatory checkpoints mediated by homeostatic state of the cell.

Regarding the downstream impact of exosome secretion, our work suggests that exosome release is a cell autonomous pathway that facilitates elimination of undigested and potentially toxic lysosomal cargoes, which are not efficiently degraded in the context of lysosome destabilization or pH neutralization. Concerning APP-CTF secretion, their exosomal elimination may decrease their inherent cellular toxicity and reduce deleterious A β production. However, Laulagnier and colleagues have reported that APP-CTF β in exosomes can be captured and processed by target neurons' γ -secretase and thus transfer A β production downstream (Laulagnier et al. 2017). Similar mechanisms may also apply to transfer of other aggregate-prone proteins found in exosomes such as aberrant tau, α -synuclein and TDP-43. Therefore, the right balance should be achieved in mitigating intracellular accumulation and toxicity through exosome release but also preventing propagation of pathology. In this context, future studies should address whether neuronal exosomes triggered by lysosomal dysfunction are endowed with any signaling properties and whether they induce a beneficial or deleterious response. The identification of the mediators of cell-type exosome targeting will therefore allow fine tuning of the pathophysiological consequences of this communication.

The observation of unique lipid and proteins signatures of exosomes secreted in the context of endolysosomal dysfunction also has critical implications for biomarker discovery. Indeed, increased levels of BMP are a common feature of several LSDs, including NPC, and have been described in neurodegenerative disorders such as AD and Lewy body disease (Simons et al. 2000; Chan et al. 2012; Clark et al. 2015). Regardless of the physiological functions of BMP, which include biogenesis of ILVs, regulation of lysosomal lipases and storage of endolysosomal cholesterol, our study suggests that levels of BMP in body fluids, such as serum, plasma, cerebrospinal fluid and urine, can be indicative of endolysosomal dysfunction (Bissig and Gruenberg 2013; Chevallier et al. 2008; Kolter and Sandhoff 2005). While BMP is known to be detectable in plasma or urine (typically as a measure of phospholipidosis), more accurate measurements of this lipid may require the purification of exosomes from these body fluids (Meikle et al. 2008; Fuji et al. 2015). A key question not addressed in our study is whether BMP is co-enriched with APP-CTF solely on neuronal or different cell types. Moreover, further effort should be employed to confirm if these two proposed reporters of endolysosomal function co-reside in the same or separate exosomal subpopulations and whether BMP is required for secretion of APP-CTF and other endolysosomal cargo in exosomes, a question that may be addressed by identification and manipulation of BMP-synthesizing enzymes. Interestingly, APP-

CTFs have also been reported in human CSF, suggesting that they can be helpful biomarkers in clinical settings, possibly as diagnostic reporters lysosomal dysfunction or as pharmacodynamic biomarkers informing on therapeutic efficacy (García-Ayllón et al. 2017). Therefore, the use of APP-CTFs and BMP as biomarkers should thus be broadly explored in in the context of LSDs and neurodegeneration.

3.3 Heterogeneous lipid composition and modulation of distinct brain regions

In this study, we also analyzed and compared the lipid composition of the hippocampus, prefrontal cortex, amygdala and cerebellum. Given the body of literature pointing to the anatomical and functional organization of the hippocampus along its longitudinal axis, we subdivided the hippocampus in three equipartitioned dorsal, intermediate and ventral regions (Strange et al. 2014). We observed a high degree of similarity between the three hippocampal sections relatively to the other three brain regions under study, confirming a conserved intrinsic structure within this region. Importantly, continuous gradient of lipid identity along dorsal-ventral axis which suggests that the molecular make-up of the hippocampal poles may underlie its distinct functionality.

Together with the disparity in lipid composition of the distinct brain regions, we detected some regional specificities that, interestingly, correlate with pathological hallmarks. For instance, the prefrontal cortex and the cerebellum were the most enriched in sphingomyelin and BMP, respectively. Our previous work and from others have reported increased ceramide levels in the prefrontal cortex in response to chronic stress. The local enrichment of sphingomyelin in this particular region may thus explain the increased predisposition to increased ceramide signalling upon stress stimulation (*e.g.*, through SM hydrolysis) comparatively to other areas, such as the hippocampus (Gulbins et al. 2013; Oliveira et al. 2015). Likewise, the cerebellum is characteristically susceptible to neuronal loss in Niemann-Pick Type C, which is associated with BMP accumulation (Evans and Hendriksz 2017). Altogether, our integrated lipid profiling of the brain uncovers a new perspective about regional susceptibility to pathological hallmarks of distinct neurodegenerative conditions, which may allow the prioritization of targeted therapeutical approaches.

Furthermore, we directly compared the lipid composition of the dorsal and ventral hippocampus, under control conditions and upon chronic treatment with corticosterone, an important mediator of the neuropathological effects of stress. We found that the dorsal hippocampus is predominantly enriched in sphingolipids and depleted from glycerophospholipids, except phosphatidic acid, comparatively to the ventral hippocampus. Future studies should confirm if differential lipid

enzyme expression is the driving mechanisms for regional lipid landscape. Alternatively, distinct cellular composition (relative abundance of neurons *versus* supporting cells) may also be a contributing factor. In that scenario, complementing single cell dissociation and purification techniques will determine the regional contribution of different cell type populations. Importantly, our results suggest that elevated CORT levels do not interfere with the global lipid assemble characteristic of each of the hippocampal regions, predominantly characterized by the inverse abundance of sphingolipids and glycerophospholipids, but rather modulates specific subsets of lipid species in a region-specific manner. We postulate that these observations stem from differential modulation of lipid enzymes, possibly enzymatic or transcriptional, and the ensuing signaling and metabolic repercussions may be a contributing part to regional synaptic and dendritic plasticity. In light of the common effect of CORT in cholesteryl ester and triglyceride metabolism, it will also be interesting to study the mechanism underlying neutral lipid disturbance and whether disruption of lipid droplets and other aspects of endolysosomal function contributes to the hallmarks of pathological glucocorticoid signaling, including circuitry reorganization and cognitive deficits (Lucassen et al. 2014).

3.4 Conclusion and Future Perspectives

Overall, the main conclusion of this work is the identification of PI3P as a major player in the pathogenesis of neurodegeneration, particularly linked to LSDs and AD. Using a combination of pharmacological and genetic approaches, we show that PI3P deficiency primarily induces severe defects in the endolysosomal pathway, impairing the degradation of APP-CTFs and sphingolipids and causing physical disruption of endolysosomal membranes. We also found that perturbed lysosomal function resulted in the secretion of atypical exosomes, enriched in APP-CTFs, the phospholipid BMP and other undigested lysosomal cargo, revealing a homeostatic response counteracting lysosomal storage. These observations thus highlight the Vps34/PI3P signaling cascade as an appealing therapeutically targetable pathway.

Despite our observations linking endolysosomal and autophagy defects to neurodegeneration, it is still debatable to which extent should autophagy be stimulated or exosome secretion mitigated in this context. While stimulation of autophagy has proven successful in different experimental models of neurodegenerative disorders, commonly over-expressing diseased-linked mutant proteins, this approach may be detrimental in the context of Vps34 dysfunction. Unless endosomal function and lysosomal degradation are efficiently restored, nascent autophagosomes will likely accumulate and aggravate cellular storage burden, including facilitation of A β production or seeding of protein

aggregates (Menzies, Fleming, and Rubinsztein 2015). Alternatively, autophagy induction should be complemented with enhancement of tethering machinery, *via* molecular chaperones promoting endolysosomal fusion, or lysosomal acidification, using acidifying nanoparticles (Lee et al. 2015). Similarly, blockade of exosome secretion may prevent elimination of undigested lysosomal cargo as an alleviating mechanism, namely of APP-CTFs and potentially toxic lipids, thus exacerbating neurotoxicity as a result of their intracellular accumulation. Moreover, upregulation of the coordinated lysosomal expression and regulation (CLEAR) network is an attractive strategy to mitigate LSD-like pathology in neurodegeneration but, in the context of PI3P deficiency, unless the primary event is corrected (*i.e.*, PI3P levels), newly generated lysosomes may also be functionally impaired and instead exacerbate pathology (Martini-Stoica et al. 2016). Thus, given the pleiotropic cascade of LSD-like pathology, effective therapeutic strategies will therefore likely require combined treatments aiming to restore endosomal traffic, lower lipid storage, promote autophagosome formation and finally enhance lysosomal degradation.

Our findings raise several questions of great interest to be addressed in the near future. First, the implications of Vps34 function in APP processing and clearance encourages great interest in studying tau pathology under PI3P depletion. We hypothesize that Vps34 blockade leads to abnormal tau localization and ineffective clearance by autophagy. Remarkably, tau is a proposed substrate of both macroautophagy and chaperone-mediated autophagy (Y. Wang et al. 2009). While inhibition of the first will likely reduce tau clearance, secondary stimulation of chaperone-mediated autophagy in the context of dysfunctional endolysosomes may facilitate oligomeric assembly of tau fragments that act as seeds for further tau aggregation. In addition, disruption of endosomal signaling and kinase-phosphatase activity may also affect tau phosphorylation and downstream pathogenesis. Remarkably, tau has also been identified in exosomes, suggesting that spreading of aggregated tau may occur via exosome transfer (Saman et al. 2012; Y. Wang et al. 2017). Thus, it will be of great importance to determine if endolysosomal dysfunction mediated by deficiency of PI3P also stimulates secretion and propagation of tau. Also, combinatorial genetic, biochemical and imaging experiments may provide clues to the mechanisms required for exosomal sorting of soluble proteins such as tau (*i.e.*, ESCRT-dependent and -independent pathways). *In vivo* ablation of Vps34, particularly using humanized tau models more susceptible to aggregation, will likely prove useful to study tau aggregation and somatodendritic redistribution and complement *in vitro* tau transfer and spreading experiments.

Another important future direction of our studies is the identification of cellular events linking endolysosomal dysfunction to neurodegeneration. Corroborating previous findings from others, we

detected accumulation of poly-ubiquitinated proteins and protein aggregates, as well as potentially toxic lipids at 2 months of age in *Pik3c3*^{+/+} mice (*i.e.*, our new findings), prior to neuronal loss. The later occurrence of neuronal death at 3 months provides us a potentially therapeutic window to mitigate this phenomenon. A combination of transcriptomic and proteomic approaches between these remarkably distinct timepoints may therefore provide us with a solid molecular snapshot linking endolysosomal events and neuronal death, certainly of great utility in the LSD and neurodegeneration field. As for immediate approaches to rescue endolysosomal health, we propose to overexpress members of the Vps34 Complex I/II or upregulate the CLEAR genetic program (*e.g.*, TFEB transduction), both of which have been shown to be beneficial in LSDs (Nemazany et al. 2013; Medina et al. 2011).

Finally, exosomes are a promising theme in the area of biomarker discovery. We propose to analyze APP-CTFs and BMP in purified exosome fractions as biomarkers of neuronal endolysosomal dysfunction. This should initially be tested in the CSF and plasma of preclinical models, ranging from LSD models to transgenic models of neurodegenerative disorders (including AD, PD, ALS, FTD), and ultimately in human subjects.

Altogether, our works emphasizes the importance of studying basic cellular mechanisms such as endosomal traffic and autophagy for a better understanding of the pathogenesis of neurodegeneration and identification of new biomarkers and therapeutic targets in related disorders.

References

- Abeliovich, Asa, and Aaron D Gitler. 2016. "Defects in Trafficking Bridge Parkinson's Disease Pathology and Genetics." *Nature* 539 (7628): 207–16. doi:10.1038/nature20414.
- Agholme, Lotta, Martin Hallbeck, Eirikur Benedikz, Jan Marcusson, and Katarina Kågedal. 2012. "Amyloid- β Secretion, Generation, and Lysosomal Sequestration in Response to Proteasome Inhibition: Involvement of Autophagy." *Journal of Alzheimer's Disease : JAD* 31 (2). IOS Press: 343–58. doi:10.3233/JAD-2012-120001.
- Alvarez-Erviti, Lydia, Yiqi Seow, Anthony H. Schapira, Chris Gardiner, Ian L. Sargent, Matthew J A Wood, and J. Mark Cooper. 2011. "Lysosomal Dysfunction Increases Exosome-Mediated Alpha-Synuclein Release and Transmission." *Neurobiology of Disease* 42 (3). Elsevier Inc.: 360–67. doi:10.1016/j.nbd.2011.01.029.
- Asai, Hirohide, Seiko Ikezu, Satoshi Tsunoda, Maria Medalla, Jennifer Luebke, Tarik Haydar, Benjamin Wolozin, Oleg Butovsky, Sebastian Kügler, and Tsuneya Ikezu. 2015. "Depletion of Microglia and Inhibition of Exosome Synthesis Halt Tau Propagation." *Nature Neuroscience* 18 (11): 1584–93. doi:10.1038/nn.4132.
- Bago, Ruzica, Nazma Malik, Michael J. Munson, Alan R. Prescott, Paul Davies, Eeva Sommer, Natalia Shpiro, et al. 2014. "Characterization of VPS34-IN1, a Selective Inhibitor of Vps34, Reveals That the Phosphatidylinositol 3-Phosphate-Binding SGK3 Protein Kinase Is a Downstream Target of Class III Phosphoinositide 3-Kinase." *Biochemical Journal* 463 (3): 413–27. doi:10.1042/BJ20140889.
- Billings, Lauren M, Salvatore Oddo, Kim N Green, James L McLaugh, and Frank M LaFerla. 2005. "Intraneuronal Abeta Causes the Onset of Early Alzheimer's Disease-Related Cognitive Deficits in Transgenic Mice." *Neuron* 45 (5). Elsevier: 675–88. doi:10.1016/j.neuron.2005.01.040.
- Bissig, Christin, and Jean Gruenberg. 2013. "Lipid Sorting and Multivesicular Endosome Biogenesis." *Cold Spring Harbor Perspectives in Biology*. Cold Spring Harbor Laboratory Press. doi:10.1101/cshperspect.a016816.
- Blom, Tomas, Shiqian Li, Andrea Dichlberger, Nils Bäck, Young Ah Kim, Ursula Loizides-Mangold, Howard Riezman, Robert Bittman, and Elina Ikonen. 2015. "LAPTM4B Facilitates Late Endosomal Ceramide Export to Control Cell Death Pathways." *Nature Chemical Biology* 11 (10): 799–806. doi:10.1038/nchembio.1889.
- Boland, Barry, David A. Smith, Declan Mooney, Sonia S. Jung, Dominic M. Walsh, and Frances M. Platt. 2010. "Macroautophagy Is Not Directly Involved in the Metabolism of Amyloid Precursor Protein." *Journal of Biological Chemistry* 285 (48): 37415–26. doi:10.1074/jbc.M110.186411.
- Calafate, Sara, William Flavin, Patrik Verstreken, and Diederik Moechars. 2016. "Loss of Bin1 Promotes the Propagation of Tau Pathology." *Cell Reports* 17: 931–40. doi:10.1016/j.celrep.2016.09.063.
- Cannizzo, Elvira S., Cristina C. Clement, Kateryna Morozova, Rut Valdor, Susmita Kaushik, Larissa N. Almeida, Carlo Folio, et al. 2012. "Age-Related Oxidative Stress Compromises Endosomal Proteostasis." *Cell Reports* 2 (1). Elsevier: 136–49. doi:10.1016/j.celrep.2012.06.005.
- Cataldo, Anne M, Corrinne M Peterhoff, Juan C Troncoso, Teresa Gomez-Isla, Bradley T Hyman, and Ralph A Nixon. 2000. "Endocytic Pathway Abnormalities Precede Amyloid β Deposition in Sporadic Alzheimer's Disease and Down Syndrome Differential Effects of APOE Genotype and Presenilin." *The American Journal of Pathology* 157 (1). American Society for Investigative Pathology: 277–86. <http://www.ncbi.nlm.nih.gov/pubmed/10880397>.
- Chan, Robin B., Tiago G. Oliveira, Ety P. Cortes, Lawrence S. Honig, Karen E. Duff, Scott a. Small, Markus R. Wenk, Guanghou Shui, and Gilbert Di Paolo. 2012. "Comparative Lipidomic Analysis of Mouse and Human Brain with Alzheimer Disease." *Journal of Biological Chemistry* 287: 2678–88. doi:10.1074/jbc.M111.274142.
- Chevallier, Julien, Zeina Chamoun, Guowei Jiang, Glenn Prestwich, Naomi Sakai, Stefan Matile, Robert G. Parton, and Jean Gruenberg. 2008. "Lysobisphosphatidic Acid Controls Endosomal Cholesterol Levels." *Journal of Biological Chemistry* 283 (41): 27871–80. doi:10.1074/jbc.M801463200.
- Clark, Lorraine N., Robin Chan, Rong Cheng, Xinmin Liu, Naeun Park, Nancy Parmalee, Sergey Kisselev, et al. 2015. "Gene-Wise Association of Variants in Four Lysosomal Storage Disorder Genes in Neuropathologically Confirmed Lewy Body Disease." Edited by Coro Paisan-Ruiz. *PLOS ONE* 10 (5): e0125204. doi:10.1371/journal.pone.0125204.
- Dall'Armi, Claudia, Kelly a Devereaux, and Gilbert Di Paolo. 2013. "The Role of Lipids in the Control of Autophagy." *Current Biology : CB* 23 (1). Elsevier Ltd: R33-45. doi:10.1016/j.cub.2012.10.041.
- Devereaux, Kelly, Claudia Dall'Armi, Abel Alcazar-Roman, Yuta Ogasawara, Xiang Zhou, Fan Wang, Akitsugu Yamamoto, Pietro de Camilli, and Gilbert Di Paolo. 2013. "Regulation of Mammalian Autophagy by Class II and III PI 3-Kinases through PI3P Synthesis." *PLoS ONE* 8 (10): 10–12. doi:10.1371/journal.pone.0076405.
- Di Paolo, Gilbert, and Tae-Wan Kim. 2011. "Linking Lipids to Alzheimer's Disease: Cholesterol and Beyond." *Nature Reviews. Neuroscience* 12 (5). Nature Publishing Group: 284–96. doi:10.1038/nrn3012.
- Dinkins, Michael B., Somsankar Dasgupta, Guanghu Wang, Gu Zhu, and Erhard Bieberich. 2014. "Exosome Reduction in Vivo Is Associated with Lower Amyloid Plaque Load in the 5XFAD Mouse Model of Alzheimer's Disease." *Neurobiology of Aging* 35 (8). Elsevier Ltd: 1792–1800. doi:10.1016/j.neurobiolaging.2014.02.012.
- Dinkins, Michael B, John Enasko, Caterina Hernandez, Guanghu Wang, Jina Kong, Inas Helwa, Yutao Liu, Alvin V. Terry,

- and Erhard Bieberich. 2016. "Neutral Sphingomyelinase-2 Deficiency Ameliorates Alzheimer's Disease Pathology and Improves Cognition in the 5XFAD Mouse." *The Journal of Neuroscience* 36 (33): 8653–67. doi:10.1523/JNEUROSCI.1429-16.2016.
- Echten-deckert, Gerhild Van, and Jochen Walter. 2012. "Progress in Lipid Research Sphingolipids : Critical Players in Alzheimer ' S Disease" 51: 378–93.
- Edgar, James R., Emily R. Eden, and Clare E. Futter. 2014. "Hrs- and CD63-Dependent Competing Mechanisms Make Different Sized Endosomal Intraluminal Vesicles." *Traffic* 15 (2). John Wiley & Sons A/S: 197–211. doi:10.1111/tra.12139.
- Edgar, James R., Katarina Willén, Gunnar K. Gouras, and Clare E. Futter. 2015. "ESCRTs Regulate Amyloid Precursor Protein Sorting in Multivesicular Bodies and Intracellular Amyloid- β Accumulation." *Journal of Cell Science* 128 (14). <http://jcs.biologists.org/content/128/14/2520.long>.
- Edgar, James R, Paul T Manna, Shinichi Nishimura, George Banting, and Margaret S Robinson. 2016. "Tetherin Is an Exosomal Tether." *eLife* 5 (September). eLife Sciences Publications Limited: e17180. doi:10.7554/eLife.17180.
- Eitan, Erez, Caitlin Suire, Shi Zhang, and Mark P. Mattson. 2016. "Impact of Lysosome Status on Extracellular Vesicle Content and Release." *Ageing Research Reviews* 32. Elsevier B.V.: 65–74. <http://dx.doi.org/10.1016/j.arr.2016.05.001>.
- Emmanouilidou, E., K. Melachroinou, T. Roumeliotis, S. D. Garbis, M. Ntzouni, L. H. Margaritis, L. Stefanis, and K. Vekrellis. 2010. "Cell-Produced α -Synuclein Is Secreted in a Calcium-Dependent Manner by Exosomes and Impacts Neuronal Survival." *Journal of Neuroscience* 30 (20): 6838–51. doi:10.1523/JNEUROSCI.5699-09.2010.
- Evans, William R H, and Chris J Hendriksz. 2017. "Niemann-Pick Type C Disease - the Tip of the Iceberg? A Review of Neuropsychiatric Presentation, Diagnosis and Treatment." *BJPsych Bulletin* 41 (2). Royal College of Psychiatrists: 109–14. doi:10.1192/pb.bp.116.054072.
- Fraldi, Alessandro, Andrés D. Klein, Diego L. Medina, and Carmine Settembre. 2016. "Brain Disorders Due to Lysosomal Dysfunction." *Annual Review of Neuroscience* 39 (1): 277–95. doi:10.1146/annurev-neuro-070815-014031.
- Freeman, David, Rudy Cedillos, Samantha Choyke, Zana Lukic, Kathleen McGuire, Shauna Marvin, Andrew M. Burrage, et al. 2013. "Alpha-Synuclein Induces Lysosomal Rupture and Cathepsin Dependent Reactive Oxygen Species Following Endocytosis." Edited by Philipp J. Kahle. *PLoS ONE* 8 (4). Public Library of Science: e62143. doi:10.1371/journal.pone.0062143.
- Fuji, Reina N., Michael Flagella, Miriam Baca, Marco A. S. Baptista, Jens Brodbeck, Bryan K. Chan, Brian K. Fiske, et al. 2015. "Effect of Selective LRRK2 Kinase Inhibition on Nonhuman Primate Lung." *Science Translational Medicine* 7 (273): 273ra15-273ra15. doi:10.1126/scitranslmed.aaa3634.
- Gabandé-Rodríguez, E, P Boya, V Labrador, C G Dotti, and M D Ledesma. 2014. "High Sphingomyelin Levels Induce Lysosomal Damage and Autophagy Dysfunction in Niemann Pick Disease Type A." *Cell Death and Differentiation* 21 (6). Nature Publishing Group: 864–75. doi:10.1038/cdd.2014.4.
- García-Ayllón, María-Salud, Inmaculada Lopez-Font, Claudia P Boix, Juan Fortea, Raquel Sánchez-Valle, Alberto Lleó, José-Luis Molinuevo, Henrik Zetterberg, Kaj Blennow, and Javier Sáez-Valero. 2017. "C-Terminal Fragments of the Amyloid Precursor Protein in Cerebrospinal Fluid as Potential Biomarkers for Alzheimer Disease." *Scientific Reports* 7 (1). Nature Publishing Group: 2477. doi:10.1038/s41598-017-02841-7.
- Gillooly, D. J., I C Morrow, M Lindsay, R Gould, N J Bryant, J M Gaullier, R G Parton, and H Stenmark. 2000. "Localization of Phosphatidylinositol 3-Phosphate in Yeast and Mammalian Cells." *The EMBO Journal* 19 (17): 4577–88. doi:10.1093/emboj/19.17.4577.
- Gómez-Sintes, Raquel, María Dolores Ledesma, and Patricia Boya. 2016. "Lysosomal Cell Death Mechanisms in Aging." *Ageing Research Reviews* 32. Elsevier B.V.: 150–68. doi:10.1016/j.arr.2016.02.009.
- Gstrein, Thomas, Andrew Edwards, Anna Přistoupilová, Ines Leca, Martin Breuss, Sandra Pilat-Carotta, Andi H. Hansen, et al. 2018. "Mutations in Vps15 Perturb Neuronal Migration in Mice and Are Associated with Neurodevelopmental Disease in Humans." *Nature Neuroscience* 21 (February). Springer US. doi:10.1038/s41593-017-0053-5.
- Gulbins, Erich, Monica Palmada, Martin Reichel, Anja Lüth, Christoph Böhmer, Davide Amato, Christian P Müller, et al. 2013. "Acid Sphingomyelinase-Ceramide System Mediates Effects of Antidepressant Drugs." *Nature Medicine* 19 (7): 934–38. doi:10.1038/nm.3214.
- Guo, Belinda B., Shayne A. Bellingham, and Andrew F. Hill. 2015. "The Neutral Sphingomyelinase Pathway Regulates Packaging of the Prion Protein into Exosomes." *Journal of Biological Chemistry* 290 (6): 3455–67. doi:10.1074/jbc.M114.605253.
- Guo, Huishan, Maneka Chitiprolu, Luc Roncevic, Charlotte Javalet, Fiona J. Hemming, My Tran Trung, Lingrui Meng, et al. 2017. "Atg5 Disassociates the V 1 V 0 -ATPase to Promote Exosome Production and Tumor Metastasis Independent of Canonical Macroautophagy." *Developmental Cell* 43 (6): 716–730.e7. doi:10.1016/j.devcel.2017.11.018.
- Han, Xianlin. 2016. "Lipidomics for Studying Metabolism." *Nature Reviews Endocrinology* 12 (11). Nature Publishing Group: 668–79. doi:10.1038/nrendo.2016.98.

- Hara, Taichi, Kenji Nakamura, Makoto Matsui, Akitsugu Yamamoto, Yohko Nakahara, Rika Suzuki-Migishima, Minesuke Yokoyama, et al. 2006. "Suppression of Basal Autophagy in Neural Cells Causes Neurodegenerative Disease in Mice." *Nature* 441 (7095): 885–89. doi:10.1038/nature04724.
- Hernández-Tiedra, Sonia, Gemma Fabriàs, David Dávila, Íñigo J. Salanueva, Josefina Casas, L. Ruth Montes, Zuriñe Antón, et al. 2016. "Dihydroceramide Accumulation Mediates Cytotoxic Autophagy of Cancer Cells via Autolysosome Destabilization." *Autophagy* 12 (11). Taylor & Francis: 2213–29. doi:10.1080/15548627.2016.1213927.
- Iguchi, Yohei, Lara Eid, Martin Parent, Geneviève Soucy, Christine Bareil, Yuichi Riku, Kaori Kawai, et al. 2016. "Exosome Secretion Is a Key Pathway for Clearance of Pathological TDP-43." *Brain* 139 (12): 3187–3201. doi:10.1093/brain/aww237.
- Israel, Mason A., Shauna H. Yuan, Cedric Bardy, Sol M. Reyna, Yangling Mu, Cheryl Herrera, Michael P. Hefferan, et al. 2012. "Probing Sporadic and Familial Alzheimer's Disease Using Induced Pluripotent Stem Cells." *Nature* 482 (7384). Nature Publishing Group: 216–20. doi:10.1038/nature10821.
- Jaeger, Philipp A, Fiona Pickford, Chung-Huan Sun, Kurt M Lucin, Eliezer Masliah, and Tony Wyss-Coray. 2010. "Regulation of Amyloid Precursor Protein Processing by the Beclin 1 Complex." *PLoS ONE* 5 (6): e111102. doi:10.1371/journal.pone.0011102.
- Jaeger, Philipp a, and Tony Wyss-Coray. 2010. "Beclin 1 Complex in Autophagy and Alzheimer Disease." *Archives of Neurology* 67 (10): 1181–84. doi:10.1001/archneurol.2010.258.
- Jiang, Ying, Kerry A Mullaney, Corrinne M Peterhoff, Shaoli Che, Stephen D Schmidt, Anne Boyer-Boiteau, Stephen D Ginsberg, Anne M Cataldo, Paul M Mathews, and Ralph A Nixon. 2010. "Alzheimer's-Related Endosome Dysfunction in Down Syndrome Is A -Independent but Requires APP and Is Reversed by BACE-1 Inhibition." *Proceedings of the National Academy of Sciences* 107 (4). National Academy of Sciences: 1630–35. doi:10.1073/pnas.0908953107.
- Karch, Celeste M., and Alison M. Goate. 2015. "Alzheimer's Disease Risk Genes and Mechanisms of Disease Pathogenesis." *Biological Psychiatry*. doi:10.1016/j.biopsych.2014.05.006.
- Kaur, G, M Pawlik, S E Gandy, M E Ehrlich, J F Smiley, and E Levy. 2017. "Lysosomal Dysfunction in the Brain of a Mouse Model with Intraneuronal Accumulation of Carboxyl Terminal Fragments of the Amyloid Precursor Protein." *Molecular Psychiatry* 22 (7). Nature Publishing Group: 981–89. doi:10.1038/mp.2016.189.
- Kaushik, Susmita, and Ana Maria Cuervo. 2015. "Proteostasis and Aging." *Nature Medicine* 21 (12). Nature Publishing Group: 1406–15. doi:10.1038/nm.4001.
- Kim, S, Y Sato, P S Mohan, C Peterhoff, A Pensalfini, A Rigoglioso, Y Jiang, and R A Nixon. 2016. "Evidence That the rab5 Effector APPL1 Mediates APP-βCTF-Induced Dysfunction of Endosomes in Down Syndrome and Alzheimer's Disease." *Molecular Psychiatry* 21 (5): 707–16. doi:10.1038/mp.2015.97.
- Kirkegaard, Thomas, Anke G Roth, Nikolaj H T Petersen, Ajay K Mahalka, Ole Dines Olsen, Irina Moilanen, Alicja Zyllicz, et al. 2010. "Hsp70 Stabilizes Lysosomes and Reverts Niemann-Pick Disease-Associated Lysosomal Pathology." *Nature* 463 (7280): 549–53. doi:10.1038/nature08710.
- Kishi-Itakura, Chieko, Ikuko Koyama-Honda, Eisuke Itakura, and Noboru Mizushima. 2014. "Ultrastructural Analysis of Autophagosome Organization Using Mammalian Autophagy-Deficient Cells." *Journal of Cell Science* 127 (22): 4984–4984. doi:10.1242/jcs.164293.
- Klumperman, Judith, and Graça Raposo. 2014. "The Complex Ultrastructure of the Endolysosomal System." *Cold Spring Harbor Perspectives in Biology* 6 (10). Cold Spring Harbor Laboratory Press: a016857. doi:10.1101/cshperspect.a016857.
- Kolter, Thomas, and Konrad Sandhoff. 2005. "PRINCIPLES OF LYSOSOMAL MEMBRANE DIGESTION: Stimulation of Sphingolipid Degradation by Sphingolipid Activator Proteins and Anionic Lysosomal Lipids." *Annual Review of Cell and Developmental Biology* 21 (1). Annual Reviews: 81–103. doi:10.1146/annurev.cellbio.21.122303.120013.
- Komatsu, M, S Waguri, T Chiba, S Murata, J Iwata, I Tanida, T Ueno, et al. 2006. "Loss of Autophagy in the Central Nervous System Causes Neurodegeneration in Mice." *Nature* 441 (7095): 880–84. doi:10.1038/nature04723.
- Kowal, Joanna, Guillaume Arras, Marina Colombo, Mabel Jouve, Jakob Paul Morath, Bjarke Prindal-Bengtson, Florent Dingli, Damaris Loew, Mercedes Tkach, and Clotilde Théry. 2016. "Proteomic Comparison Defines Novel Markers to Characterize Heterogeneous Populations of Extracellular Vesicle Subtypes." *Proceedings of the National Academy of Sciences* 113 (8): E968–77. doi:10.1073/pnas.1521230113.
- Kubo, Shin-ichiro. 2016. "Membrane Lipids as Therapeutic Targets for Parkinson's Disease: A Possible Link between Lewy Pathology and Membrane Lipids." *Expert Opinion on Therapeutic Targets* 20 (11): 1301–10. doi:10.1517/14728222.2016.1086340.
- LaFerla, Frank M., Kim N. Green, and Salvatore Oddo. 2007. "Intracellular Amyloid-β in Alzheimer's Disease." *Nature Reviews Neuroscience* 8 (7): 499–509. doi:10.1038/nrn2168.
- Langui, Dominique, Nadège Girardot, Khalid Hamid El Hachimi, Bernadette Allinquant, Véronique Blanchard, Laurent Pradier, and Charles Duyckaerts. 2004. "Subcellular Topography of Neuronal Abeta Peptide in APPxPS1 Transgenic

- Mice." *The American Journal of Pathology* 165 (5): 1465–77. doi:10.1016/S0002-9440(10)63405-0.
- Laulagnier, Karine, Charlotte Javalet, Fiona J. Hemming, Mathilde Chivet, Gaëlle Lachenal, Béatrice Blot, Christine Chatellard, and Rémy Sadoul. 2017. "Amyloid Precursor Protein Products Concentrate in a Subset of Exosomes Specifically Endocytosed by Neurons." *Cellular and Molecular Life Sciences*, February 27. doi:10.1007/s00018-017-2664-0.
- Law, Fiona, Jung Hwa Seo, Ziqing Wang, Jennifer L. DeLeon, Yousstina Bolis, Ashley Brown, Wei-Xing Zong, Guangwei Du, and Christian E. Rocheleau. 2017. "The VPS34 PI3K Negatively Regulates RAB-5 during Endosome Maturation." *Journal of Cell Science* 130 (12): 2007–17. doi:10.1242/jcs.194746.
- Lee, Ju Hyun, Mary Kate McBrayer, Devin M. Wolfe, Luke J. Haslett, Asok Kumar, Yutaka Sato, Pearl P Y Lie, et al. 2015. "Presenilin 1 Maintains Lysosomal Ca²⁺ Homeostasis via TRPML1 by Regulating vATPase-Mediated Lysosome Acidification." *Cell Reports* 12 (9). The Authors: 1430–44. doi:10.1016/j.celrep.2015.07.050.
- Li, Yuan, Baohui Chen, Wei Zou, Xin Wang, Yanwei Wu, Dongfeng Zhao, Yanan Sun, et al. 2016. "The Lysosomal Membrane Protein SCAV-3 Maintains Lysosome Integrity and Adult Longevity." *Journal of Cell Biology* 215 (2): 167–85. doi:10.1083/jcb.201602090.
- Lucassen, Paul J., Jens Pruessner, Nuno Sousa, Osborne F X Almeida, Anne Marie Van Dam, Grazyna Rajkowska, Dick F. Swaab, and Boldizsár Czéh. 2014. "Neuropathology of Stress." *Acta Neuropathologica* 127 (1): 109–35. doi:10.1007/s00401-013-1223-5.
- Maejima, Ikuko, Atsushi Takahashi, Hiroko Omori, Tomonori Kimura, Yoshitsugu Takabatake, Tatsuya Saitoh, Akitsugu Yamamoto, et al. 2013. "Autophagy Sequesters Damaged Lysosomes to Control Lysosomal Biogenesis and Kidney Injury." *The EMBO Journal* 32: 2336–47. doi:10.1038/emboj.2013.171.
- Mapstone, Mark, Amrita K Cheema, Massimo S Fiandaca, Xiaogang Zhong, Timothy R Mhyre, Linda H MacArthur, William J Hall, et al. 2014. "Plasma Phospholipids Identify Antecedent Memory Impairment in Older Adults." *Nature Medicine* 20 (4). Nature Publishing Group: 415–18. doi:10.1038/nm.3466.
- Martini-Stoica, Heidi, Yin Xu, Andrea Ballabio, and Hui Zheng. 2016. "The Autophagy-Lysosomal Pathway in Neurodegeneration: A TFEB Perspective." *Trends in Neurosciences* 39 (4). Elsevier Ltd: 221–34. doi:10.1016/j.tins.2016.02.002.
- Maulik, Mahua, Kyle Peake, Ji Yun Chung, Yanlin Wang, Jean E. Vance, and Satyabrata Kar. 2015. "APP Overexpression in the Absence of NPC1 Exacerbates Metabolism of Amyloidogenic Proteins of Alzheimer's Disease." *Human Molecular Genetics* 24 (24): 7132–50. doi:10.1093/hmg/ddv413.
- Medina, Diego L, Alessandro Fraldi, Valentina Bouche, Fabio Annunziata, Gelsomina Mansueto, Carmine Spampinato, Claudia Puri, et al. 2011. "Transcriptional Activation of Lysosomal Exocytosis Promotes Cellular Clearance." *Developmental Cell* 21 (3): 421–30. doi:10.1016/j.devcel.2011.07.016.
- Meikle, Peter J., Stephen Duplock, David Blacklock, Phillip D. Whitfield, Gemma Macintosh, John J. Hopwood, and Maria Fuller. 2008. "Effect of Lysosomal Storage on Bis(monoacylglycerol)phosphate." *Biochemical Journal* 411 (1). <http://www.biochemj.org/content/411/1/71>.
- Menzies, Fiona M., Angeleen Fleming, Andrea Caricasole, Carla F. Bento, Stephen P. Andrews, Avraham Ashkenazi, Jens Füllgrabe, et al. 2017. "Autophagy and Neurodegeneration: Pathogenic Mechanisms and Therapeutic Opportunities." *Neuron* 93 (5): 1015–34. doi:10.1016/j.neuron.2017.01.022.
- Menzies, Fiona M., Angeleen Fleming, and David C. Rubinsztein. 2015. "Compromised Autophagy and Neurodegenerative Diseases." *Nature Reviews Neuroscience* 16 (6). Nature Publishing Group: 345–57. doi:10.1038/nrn3961.
- Micsenyi, Matthew C, Jakub Sikora, Gloria Stephney, Kostantin Dobrenis, and Steven U Walkley. 2013. "Lysosomal Membrane Permeability Stimulates Protein Aggregate Formation in Neurons of a Lysosomal Disease." *The Journal of Neuroscience: The Official Journal of the Society for Neuroscience* 33 (26): 10815–27. doi:10.1523/JNEUROSCI.0987-13.2013.
- Miranda, André M., Zofia M. Lasiacka, Yimeng Xu, Jessi Neufeld, Sanjid Shahriar, Sabrina Simoes, Robin B. Chan, Tiago Gil Oliveira, Scott A. Small, and Gilbert Di Paolo. 2018. "Neuronal Lysosomal Dysfunction Releases Exosomes Harboring APP C-Terminal Fragments and Unique Lipid Signatures." *Nature Communications* 9 (1). Nature Publishing Group: 291. doi:10.1038/s41467-017-02533-w.
- Miranda, André Miguel, and Tiago Gil Oliveira. 2015. "Lipids under Stress - a Lipidomic Approach for the Study of Mood Disorders." *BioEssays* 37 (11): 1226–35. doi:10.1002/bies.201500070.
- Morel, Etienne, Zeina Chamoun, Zofia M Lasiacka, Robin B Chan, Rebecca L Williamson, Christopher Vetanovetz, Claudia Dall'Armi, et al. 2013. "Phosphatidylinositol-3-Phosphate Regulates Sorting and Processing of Amyloid Precursor Protein through the Endosomal System." *Nature Communications* 4 (January): 2250. doi:10.1038/ncomms3250.
- Nemazanyy, Ivan, Bert Blaauw, Cecilia Paolini, Catherine Caillaud, Feliciano Protasi, Amelie Mueller, Tassula Proikas-Cezanne, et al. 2013. "Defects of Vps15 in Skeletal Muscles Lead to Autophagic Vacuolar Myopathy and Lysosomal Disease." *EMBO Molecular Medicine* 5 (6). EMBO Press: 870–90. doi:10.1002/emmm.201202057.
- Nilsson, Per, Krishnapriya Loganathan, Misaki Sekiguchi, Yukio Matsuba, Kelvin Hui, Satoshi Tsubuki, Motomasa Tanaka, Nobuhisa Iwata, Takashi Saito, and Takaomi C. C. Saido. 2013. "A β Secretion and Plaque Formation Depend on

- Autophagy." *Cell Reports* 5 (1). The Authors: 61–69. doi:10.1016/j.celrep.2013.08.042.
- Nixon, Ralph A., Dun-Sheng Yang, and Ju-Hyun Lee. 2008. "Neurodegenerative Lysosomal Disorders: A Continuum from Development to Late Age." *Autophagy* 4 (5). Taylor & Francis: 590–99. doi:10.4161/auto.6259.
- Oliveira, T G, R B Chan, F V Bravo, a Miranda, R R Silva, B Zhou, F Marques, et al. 2015. "The Impact of Chronic Stress on the Rat Brain Lipidome." *Molecular Psychiatry*, no. November 2014. Nature Publishing Group: 1–9. doi:10.1038/mp.2015.14.
- Oster-Granite, M L, D L McPhie, J Greenan, and R L Neve. 1996. "Age-Dependent Neuronal and Synaptic Degeneration in Mice Transgenic for the C Terminus of the Amyloid Precursor Protein." *The Journal of Neuroscience : The Official Journal of the Society for Neuroscience* 16 (21): 6732–41. <http://www.ncbi.nlm.nih.gov/pubmed/8824314>.
- Papadopoulos, Chrisovalantis, Philipp Kirchner, Monika Bug, Daniel Grum, Lisa Koerver, Nina Schulze, Robert Poehler, et al. 2017. "VCP/p97 Cooperates with YOD1, UBXD1 and PLAA to Drive Clearance of Ruptured Lysosomes by Autophagy." *The EMBO Journal* 36 (2): 135–150. doi:10.15252/embj.
- Perez-Gonzalez, Rocio, Sebastien A. Gauthier, Asok Kumar, and Efrat Levy. 2012. "The Exosome Secretory Pathway Transports Amyloid Precursor Protein Carboxyl-Terminal Fragments from the Cell into the Brain Extracellular Space." *Journal of Biological Chemistry* 287 (51): 43108–15. doi:10.1074/jbc.M112.404467.
- Peric, Aleksandar, and Wim Annaert. 2015. "Early Etiology of Alzheimer's Disease: Tipping the Balance toward Autophagy or Endosomal Dysfunction?" *Acta Neuropathologica* 129 (3): 363–81. doi:10.1007/s00401-014-1379-7.
- Petanceska, Suzana S., and Sam Gandy. 1999. "The Phosphatidylinositol 3-Kinase Inhibitor Wortmannin Alters the Metabolism of the Alzheimer's Amyloid Precursor Protein." *Journal of Neurochemistry* 73 (6). Blackwell Science Ltd.: 2316–20. doi:10.1046/j.1471-4159.1999.0732316.x.
- Platt, Frances M, Barry Boland, and Aarnoud C van der Spoel. 2012. "The Cell Biology of Disease: Lysosomal Storage Disorders: The Cellular Impact of Lysosomal Dysfunction." *The Journal of Cell Biology* 199 (5): 723–34. doi:10.1083/jcb.201208152.
- Rajendran, Lawrence, Masanori Honsho, Tobias R Zahn, Patrick Keller, Kathrin D Geiger, Paul Verkade, and Kai Simons. 2006. "Alzheimer's Disease Beta-Amyloid Peptides Are Released in Association with Exosomes." *Proceedings of the National Academy of Sciences of the United States of America* 103 (30): 11172–77. doi:10.1073/pnas.0603838103.
- Rockenstein, Edward, Michael Mante, Michael Alford, Anthony Adame, Leslie Crews, Makoto Hashimoto, Luke Esposito, Lennart Mucke, and Eliezer Masliah. 2005. "High β Secretase Activity Elicits Neurodegeneration in Transgenic Mice Despite Reductions in Amyloid- β Levels." *Journal of Biological Chemistry* 280 (38): 32957–67. doi:10.1074/jbc.M507016200.
- Saman, Sudad, Won Hee Kim, Mario Raya, Yvonne Visnick, Suhad Miro, Sarmad Saman, Bruce Jackson, et al. 2012. "Exosome-Associated Tau Is Secreted in Tauopathy Models and Is Selectively Phosphorylated in Cerebrospinal Fluid in Early Alzheimer Disease." *Journal of Biological Chemistry* 287 (6): 3842–49. doi:10.1074/jbc.M111.277061.
- Sannerud, Ragna, Cary Esselens, Paulina Ejsmont, Rafael Mattera, Leila Rochin, Arun Kumar Tharkeshwar, Greet De Baets, et al. 2016. "Restricted Location of PSEN2/ γ Secretase Determines Substrate Specificity and Generates an Intracellular A β Pool." *Cell* 166 (1). Elsevier: 193–208. doi:10.1016/j.cell.2016.05.020.
- Schink, Kay O., Kia-Wee Tan, and Harald Stenmark. 2016. "Phosphoinositides in Control of Membrane Dynamics." *Annual Review of Cell and Developmental Biology* 32 (1): 143–71. doi:10.1146/annurev-cellbio-111315-125349.
- Sharples, Robyn A, Laura J Vella, Rebecca M Nisbet, Ryan Naylor, Keyla Perez, Kevin J Barnham, Colin L Masters, and Andrew F Hill. 2008. "Inhibition of Gamma-Secretase Causes Increased Secretion of Amyloid Precursor Protein C-Terminal Fragments in Association with Exosomes." *FASEB Journal : Official Publication of the Federation of American Societies for Experimental Biology* 22 (5). Federation of American Societies for Experimental Biology: 1469–78. doi:10.1096/fj.07-9357com.
- Simons, K., J. Gruenberg, D.A. Brown, E. London, K. Simons, E. Ikonen, A.G. Ostermeyer, et al. 2000. "Jamming the Endosomal System: Lipid Rafts and Lysosomal Storage Diseases." *Trends Cell Biol* 10 (0). Elsevier: 459–62. doi:10.1016/S0962-8924(00)01847-X.
- Small, Scott A., Sabrina Simoes-Spassov, Richard Mayeux, and Gregory A. Petsko. 2017. "Endosomal Traffic Jams Represent a Pathogenic Hub and Therapeutic Target in Alzheimer's Disease." *Trends in Neurosciences* 40 (10): 592–602. doi:10.1016/j.tins.2017.08.003.
- Strange, Bryan a, Menno P Witter, Ed S Lein, and Edvard I Moser. 2014. "Functional Organization of the Hippocampal Longitudinal Axis." *Nature Publishing Group* 15 (10). Nature Publishing Group: 655–69. doi:10.1038/nrn3785.
- Stuffers, Susanne, Catherine Sem Wegner, Harald Stenmark, and Andreas Brech. 2009. "Multivesicular Endosome Biogenesis in the Absence of ESCRTs." *Traffic* 10 (7): 925–37. doi:10.1111/j.1600-0854.2009.00920.x.
- Sundaram, J. R., E. S. Chan, C. P. Poore, T. K. Pareek, W. F. Cheong, G. Shui, N. Tang, C.-M. Low, M. R. Wenk, and S. Kesavapany. 2012. "Cdk5/p25-Induced Cytosolic PLA2-Mediated Lysophosphatidylcholine Production Regulates Neuroinflammation and Triggers Neurodegeneration." *Journal of Neuroscience* 32 (3): 1020–34. doi:10.1523/JNEUROSCI.5177-11.2012.

- Tamayev, Robert, Shuji Matsuda, Ottavio Arancio, and Luciano D'Adamio. 2012. "β but Not γSecretase Proteolysis of APP Causes Synaptic and Memory Deficits in a Mouse Model of Dementia." *EMBO Molecular Medicine* 4 (3): 171–79. doi:10.1002/emmm.201100195.
- Tamboli, Irfan Y, Heike Hampel, Nguyen T Tien, Karen Tolksdorf, Bernadette Breiden, Paul M Mathews, Paul Saftig, Konrad Sandhoff, and Jochen Walter. 2011. "Sphingolipid Storage Affects Autophagic Metabolism of the Amyloid Precursor Protein and Promotes Abeta Generation." *The Journal of Neuroscience : The Official Journal of the Society for Neuroscience* 31 (5): 1837–49. doi:10.1523/JNEUROSCI.2954-10.2011.
- Tian, Yuan, Victor Bustos, Marc Flajolet, and Paul Greengard. 2011. "A Small-Molecule Enhancer of Autophagy Decreases Levels of Abeta and APP-CTF via Atg5-Dependent Autophagy Pathway." *The FASEB Journal : Official Publication of the Federation of American Societies for Experimental Biology* 25 (6): 1934–42. doi:10.1096/fj.10-175158.
- Tomiyama, Takami, Shogo Matsuyama, Hiroyuki Iso, Tomohiro Umeda, Hiroshi Takuma, Kiyuhisa Ohnishi, Kenichi Ishibashi, et al. 2010. "A Mouse Model of Amyloid Beta Oligomers: Their Contribution to Synaptic Alteration, Abnormal Tau Phosphorylation, Glial Activation, and Neuronal Loss in Vivo." *The Journal of Neuroscience : The Official Journal of the Society for Neuroscience* 30 (14). Society for Neuroscience: 4845–56. doi:10.1523/JNEUROSCI.5825-09.2010.
- van Niel, Guillaume, Gisela D'Angelo, and Graça Raposo. 2018. "Shedding Light on the Cell Biology of Extracellular Vesicles." *Nature Reviews Molecular Cell Biology*. Nature Publishing Group. doi:10.1038/nrm.2017.125.
- Vingtdoux, Valérie, Malika Hamdane, Anne Loyens, Patrick Gelé, Hervé Drobeck, Séverine Bégard, Marie Christine Galas, et al. 2007. "Alkalizing Drugs Induce Accumulation of Amyloid Precursor Protein by-Products in Luminal Vesicles of Multivesicular Bodies." *Journal of Biological Chemistry* 282 (25): 18197–205. doi:10.1074/jbc.M609475200.
- Walker, Lary C, and Mathias Jucker. 2015. "Neurodegenerative Diseases: Expanding the Prion Concept." *Annual Review of Neuroscience* 38 (1): 87–103. doi:10.1146/annurev-neuro-071714-033828.
- Wang, L., K. Budolfson, and F. Wang. 2011. "Pik3c3 Deletion in Pyramidal Neurons Results in Loss of Synapses, Extensive Gliosis and Progressive Neurodegeneration." *Neuroscience* 172. Elsevier Inc.: 427–42. doi:10.1016/j.neuroscience.2010.10.035.
- Wang, Yipeng, Varun Balaji, Senthilvelrajan Kaniyappan, Lars Krüger, Stephan Irsen, Katharina Tepper, Ramreddy Chandupatla, et al. 2017. "The Release and Trans-Synaptic Transmission of Tau via Exosomes." *Molecular Neurodegeneration* 12 (1): 5. doi:10.1186/s13024-016-0143-y.
- Wang, Yipeng, Marta Martinez-Vicente, Ulrike Krüger, Susmita Kaushik, Esther Wong, Eva Maria Mandelkow, Ana Maria Cuervo, and Eckhard Mandelkow. 2009. "Tau Fragmentation, Aggregation and Clearance: The Dual Role of Lysosomal Processing." *Human Molecular Genetics* 18 (21): 4153–70. doi:10.1093/hmg/ddp367.
- Williamson, Rebecca L., Karine Laulagnier, André Miguel Miranda, Marty A. Fernandez, Michael S. Wolfe, Rémy Sadoul, and Gilbert Di Paolo. 2017. "Disruption of Amyloid Precursor Protein Ubiquitination Selectively Increases Amyloid Beta (Aβ 40 Levels via Presenilin 2-Mediated Cleavage." *Journal of Biological Chemistry*, October. American Society for Biochemistry and Molecular Biology, jbc.M117.818138. doi:10.1074/jbc.M117.818138.
- Wiseman, Frances K., Tamara Al-Janabi, John Hardy, Annette Karmiloff-Smith, Dean Nizetic, Victor L. J. Tybulewicz, Elizabeth M. C. Fisher, and André Strydom. 2015. "A Genetic Cause of Alzheimer Disease: Mechanistic Insights from Down Syndrome." *Nature Reviews Neuroscience* 16 (9). Nature Publishing Group: 564–74. doi:10.1038/nrn3983.
- Xu, Wei, April M. Weissmiller, Joseph A. White, Fang Fang, Xinyi Wang, Yiwen Wu, Matthew L. Pearn, et al. 2016. "Amyloid Precursor Protein-mediated Endocytic Pathway Disruption Induces Axonal Dysfunction and Neurodegeneration." *The Journal of Clinical Investigation* 126 (5). American Society for Clinical Investigation: 1815–33. doi:10.1172/JCI82409.
- Yang, Li-Bang, Kristina Lindholm, Riqiang Yan, Martin Citron, Weiming Xia, Xiao-Li Yang, Thomas Beach, et al. 2003. "Elevated βSecretase Expression and Enzymatic Activity Detected in Sporadic Alzheimer Disease." *Nature Medicine* 9 (1): 3–4. doi:10.1038/nm0103-3.
- Yu, W. Haung, Ana Maria Cuervo, Asok Kumar, Corrinne M. Peterhoff, Stephen D. Schmidt, Ju-Hyun Lee, Panaiyur S. Mohan, et al. 2005. "Macroautophagy—a Novel βAmyloid Peptide-Generating Pathway Activated in Alzheimer's Disease." *The Journal of Cell Biology* 171 (1): 87–98. doi:10.1083/jcb.200505082.
- Zhou, Xiang, Liangli Wang, Hiroshi Hasegawa, Priyanka Amin, Bao-Xia Han, Shinjiro Kaneko, Youwen He, and Fan Wang. 2010. "Deletion of PIK3C3/Vps34 in Sensory Neurons Causes Rapid Neurodegeneration by Disrupting the Endosomal but Not the Autophagic Pathway." *Proceedings of the National Academy of Sciences of the United States of America* 107: 9424–29. doi:10.1073/pnas.0914725107.
- Zoncu, Roberto, Rushika M Perera, Daniel M Balkin, Michelle Pirruccello, Derek Toomre, and Pietro De Camilli. 2009. "A Phosphoinositide Switch Controls the Maturation and Signaling Properties of APPL Endosomes." *Cell* 136 (6). Elsevier Ltd: 1110–21. doi:10.1016/j.cell.2009.01.032.

CHAPTER 4

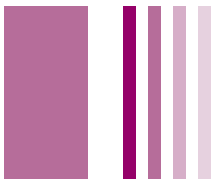
ANNEXES

André Miguel Miranda, Tiago Gil Oliveira

Lipids under stress - a lipidomic approach for the study of mood disorders

BioEssays (2015)

DOI 10.1002/bies.201500070



Lipids under stress – a lipidomic approach for the study of mood disorders

André Miguel Miranda¹⁾²⁾ and Tiago Gil Oliveira^{1)2)*}

The emerging field of lipidomics has identified lipids as key players in disease physiology. Their physicochemical diversity allows precise control of cell structure and signaling events through modulation of membrane properties and trafficking of proteins. As such, lipids are important regulators of brain function and have been implicated in neurodegenerative and mood disorders. Importantly, environmental chronic stress has been associated with anxiety and depression and its exposure in rodents has been extensively used as a model to study these diseases. With the accessibility to modern mass-spectrometry lipidomic platforms, it is now possible to snapshot the extensively interconnected lipid network. Here, we review the fundamentals of lipid biology and outline a framework for the interpretation of lipidomic studies as a new approach to study brain pathophysiology. Thus, lipid profiling provides an exciting avenue for the identification of disease signatures with important implications for diagnosis and treatment of mood disorders.

Keywords:

■ brain; chronic stress; lipid; lipidomics; mass spectrometry; mood disorders

Introduction

Lipids constitute a diverse group of molecules that are fundamental for the structural organization and signaling regulation of cells. Their vast physicochemical diversity reflects their multiple functions at the cellular level, from modulation of the chemical and mechanical properties of membranes to protein trafficking, ion channel functioning and cell-to-cell communication [1]. While the research areas of genomics and proteomics have been extensively explored in the past few years, the study of the lipidome has been lagging behind essentially due to technical limitations. The recent improvement in analytical techniques, such as mass spectrometry (MS)-based lipidomics, currently allows a comprehensive study of the lipid profile of different systems, from cells to tissues or whole organisms, in an attempt to understand the role of lipids in physiology and pathological signaling events [2].

The study of lipids is particularly challenging, for lipid structure is immensely varied and lipid species can be dynamically interchangeable. The classical definition of a lipid is a molecule soluble in organic solvents. However, certain lipids present such a polarity that they are easily diffused in the aqueous phase when performing organic solvent-based lipid extraction [3]. Consequently, a thorough qualitative and quantitative analysis of the lipidome of a

DOI 10.1002/bies.201500070

¹⁾ Life and Health Sciences Research Institute (ICVS), School of Health Sciences, University of Minho, Campus Gualtar, Braga, Portugal

²⁾ ICVS/3B's - PT Government Associate Laboratory, Braga/Guimarães, Portugal

*Corresponding author:

Tiago Gil Oliveira

E-mail: tiago@ecsau.de.uminho.pt

Abbreviations:

AA, arachidonic acid; **ACAT 1**, cholesterol acyltransferase 1; **AD**, Alzheimer's Disease; **Cer**, ceramide; **CORT**, corticosterone; **CUS**, chronic unpredictable stress; **DG**, diacylglycerol; **ER**, endoplasmic reticulum; **GC**, glucocorticoids; **lysoPC**, lysophosphatidylcholine; **MALDI-TOF-MSI**, matrix-assisted laser desorption/ionization-time of flight/mass-spectrometry imaging; **MCI**, mild cognitive impairment; **MS**, mass-spectrometry; **PA**, phosphatidic acid; **PC**, phosphatidylcholine; **PE**, phosphatidylethanolamine; **PFC**, prefrontal cortex; **PI**, phosphatidylinositol; **PIs**, phosphoinositides; **PLA**, phospholipase A; **PLC**, phospholipase C; **PLD**, phospholipase D; **PS**, phosphatidylserine; **SM**, sphingomyelin; **SREBP2**, sterol regulatory element-binding protein 2; **Sulf-(2OH)**, 2-hydroxy N-acyl sulfate; **TMD**, transmembrane domain.

system requires different analytical approaches directed to each subset of lipid classes [4].

Considering the overwhelming structural diversity of lipids and their role as putative modulators of different aspects of cellular functioning, a tight regulation of its metabolic pathways, both in space and time, is fundamental. Since lipids make up to half of the brain's dry weight, it is not surprising that lipid imbalances are involved in the pathophysiology of different neurodegenerative diseases [5–7]. Indeed, the recent use of MS has allowed the characterization of large-scale changes in lipid profiles both in humans and in animal models of disease [8–10]. This approach has been complemented by studies with genetically modified mice to better understand the role of specific lipids in health and disease [11]. Moreover, the identification of lipidomic signatures as biomarkers for diagnosis and therapeutical responses is an emerging field of study [2].

In this review, we discuss new lipid analytical strategies to study brain pathophysiology in the context of chronic stress and of diseases for which stress is a recognized trigger, such as anxiety and depression [12]. These novel experimental approaches will allow a better understanding of pathophysiological processes and the potential identification of surrogate markers of disease. We outline new ways of interpreting lipidomic data in a disease context and discuss new technical and conceptual challenges for the future.

Understanding the complexity of the brain lipidome

Lipids are crucial structural and functional components of the brain, regulating membrane assembly, vesicle synthesis and trafficking, neurotransmitter release, and signaling propagation [13]. Despite the implication of different lipids in various brain pathologies, mostly through studies focusing on their metabolizing enzymes, we still lack a comprehensive characterization of the brain lipidome and how it is affected by disease. Indeed, a recent MS-based lipidomic study analyzed the composition of different brain regions and non-neural tissues of humans and other animal species and concluded that concentration of lipids in the brain evolved faster when compared to non-neural tissues, with particular acceleration in the cortex [14]. This faster divergence privileges a specific lipid organization of the brain and reinforces the role of lipids in cognition and brain physiology.

Given this plethora of functions, one can be challenged by how lipids are structured and how they relate to other molecules. In mammalian cells, the main lipid categories are sterols (such as cholesterol), glycerophospholipids, and sphingolipids (Fig. 1). Lipids are subdivided on the basis of their chemical structure, namely a hydrophobic tail and a polar head group. The hydrocarbon chain moiety can vary in length, saturation, and hydroxylation, while polar head groups can differ in shape and charge [15]. Theoretically, thousands of lipids may co-exist within the same system and allow cells to organize their internal constituents in discrete organelles, with particular identities

and functions. For instance, the assembly of highly organized lipids in the plasma membrane promotes the existence of a rigid and impermeable barrier between the intra- and extracellular interface, in contrast with the flexible nature of the endoplasmic reticulum (ER), required for biogenic functions, such as synthesis and shuttling of lipids as part of secretory vesicles [16]. These features ultimately determine protein localization, conformation, and function. Finally, since lipids are highly interconvertible molecules and act as substrates to different lipid-modifying enzymes, hydrolytic enzymes are able to breakdown structural membrane components into second messengers [1]. While the hydrophobic product (e.g. diacylglycerol (DG)) is typically sequestered in the membrane of the parent molecule and potentially acts as an anchor signal for protein kinases, the polar structure (e.g. inositol 3-phosphate) is released into the cytoplasm and available to bind receptors and propagate intracellular signaling events, such as signal-induced calcium release [17]. The result of such dynamism is a complex crosstalk between structural components and regulators of cell signaling.

Cholesterol is the most abundant lipid in the brain

Cholesterol is mainly present in myelin sheaths and plasma membranes [18]. There, it resides with other lipid categories in constant molar ratios, namely glycerophospholipids and sphingolipids, such that impairment of this lipid balance is associated with disease [11]. Remarkably, delivery of peripheral lipoproteins across the blood-brain barrier is limited, requiring the cholesterol content of the brain to be mostly dependent on *de novo* synthesis and shuttling between glial cells and neurons [19, 20]. Despite its enrichment in membranes, cholesterol also plays a role in signaling, serving as a precursor to active steroids, such as glucocorticoids (GCs) [11]. These active molecules act as hormones, and differ from protein signaling factors in the sense that they do not typically bind to membrane receptors but rather diffuse across membranes and complex with cytoplasmic/nuclear receptors [21].

Cholesterol plays an important role in membranar lipid packing and raft assembly, which has implications in protein trafficking and folding. As a result, sterol levels are tightly regulated. Excess free cholesterol is converted to cholesteryl esters by the enzyme cholesterol acyltransferase 1 (ACAT 1) for storage in lipid droplets or shuttling to the extracellular milieu [22]. Alternatively, cholesterol conversion to 24S-hydroxycholesterol is the most efficient mechanism for efflux from the brain [23]. While the isoform 27S-hydroxycholesterol can be incorporated in the brain from the periphery, its levels are comparatively low and presents a very active metabolism, hence its contribution to cholesterol homeostasis and brain function is not yet very clear [24–26]. Additionally, mammalian cells have a feedback system in which release of the transcript factor SREBP2 from the ER under sterol depletion, followed by cleavage in the Golgi apparatus and migration through nuclear pores, activates sterol synthesis, and uptake machinery [27].

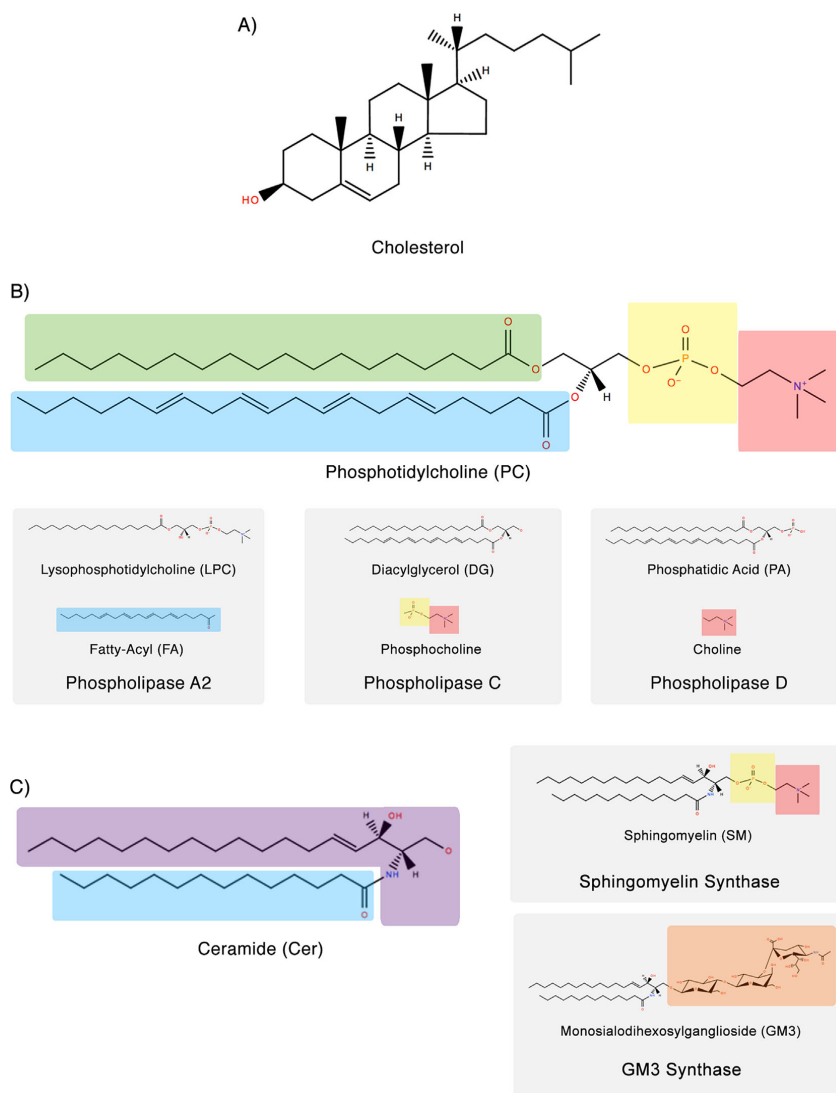


Figure 1. Examples of representative classes of the major lipid categories in mammalian cells. **A:** Cholesterol is the most abundant sterol in mammals. It contains an inflexible four-ring core that confers high hydrophobicity and interferes with acyl packing in membranes, promoting the assembly of lipid microdomains. Cholesterol plays an important role on the physical properties of membranes, namely fluidity, thickness, and permeability. Enzymes, such as ACAT1 and cholesterol 24-hydroxylase, whose activities determine the rate of cholesterol efflux from the brain to periphery, tightly regulate its levels. **B:** Glycerophospholipids are divided in classes according to the nature of the head group linked to the glycerol backbone. These vary in shape and charge, determining their location within membranes in cells. The insight boxes show the site of cleavage by phospholipases A2, C, and D. The respective products contribute to changes in membrane properties, such as induction of curvature (lysoPC and PA), or act as intracellular signaling molecules (fatty acyls and DG). **C:** Sphingolipids contain a sphingoid backbone, which is acylated to form a ceramide. Addition of polar head groups, phosphate or sugars, yields more complex classes, such as phosphosphingolipids and gangliosides. Note the similarity of the building blocks from both categories, suggesting putative steps of crosstalk between lipid metabolizing pathways. Colors: blue and green, fatty-acyl chain; orange, oligosaccharide chain; purple, sphingosine; red, choline; yellow, phosphate group. Lipid structures adapted from LIPID MAPS [114].

Glycerophospholipids are both structural and signaling molecules

Glycerophospholipids rank amongst the most abundant lipids in cells and serve as membrane components and signaling molecules. Their structure is based on a glycerol backbone linked to a polar head group at the position *sn3* and one or two fatty-acyl substituents present at *sn1* and *sn2* positions (Fig. 1B). Examples of different subclasses are phosphatidylcholine (PC), phosphatidylserine (PS), and phosphatidylinositol (PI), which differ among themselves by the addition of a phosphocholine, phosphoserine, or a phosphoinositol ring as head groups, respectively. Further glycerol units – up to two – can be added to synthesize more complex phospholipids, such as bismonoacylglycerophosphate and cardiolipin [15].

The category of glycerophospholipids is a great example of how physicochemically related lipids differ in abundance and localization. For instance, PC is one of the most common glycerophospholipid subclasses in cells and it is a major component of cellular membranes, given its spontaneous propensity to self-assemble in stable bilayer membranes [16]. PS is also abundant in cell membranes and, because of its negatively charged head group, it plays an important role in determining membrane surface charge in the inner leaflet of membranes [28]. In regard to this specific example of non-random distribution of phospholipids, apoptotic pathways can be modulated by the inhibition of translocases and activation of scramblases that induce a randomization of the transbilayer gradient, resulting in external exposure of PS and clearance of apoptotic bodies by phagocytes [29, 30]. Moreover, other less abundant glycerophospholipids, such as phosphoinositides (PIs), have been reported to provide an identity code to membrane compartments with a major impact in protein recruitment and signaling pathways [31]. Similarly to sterols, glycerophospholipids also display feedback control mechanisms that can respond to specific changes in lipid concentration or physicochemical properties of membranes, such as curvature stress [16].

Sphingolipids regulate the assembly of membrane domains

Sphingolipids differ from the previous lipid category in the substitution of the glycerol backbone by sphingosine. They can be subdivided into sphingosine derivatives, ceramides (Cer) (with the addition of a fatty acid), and more complex sphingolipids with phosphate or carbohydrate head groups. Glycosphingolipids are classified based on the charge and number of carbohydrate head groups [15]. The simplest of these have a single moiety linked to Cer (glucosyl- or galactosylceramide), but more complex structures called gangliosides include oligosaccharide chains containing sialic acid groups [32].

Given their long and saturated fatty acid chains, sphingolipids present a tall, straight, and narrow cylindrical shape. This feature allows the assembly of highly ordered solid-gel phase membrane domains, named by some authors as lipid rafts, structures of higher complexity than initially predicted by the fluid-mosaic model [33]. These detergent-

resistant membrane domains are also enriched in cholesterol, which facilitates lateral association and mobility, and modulates membrane thickness, with implications for protein recruitment and sorting [11, 34].

Lipid metabolic networks are intrinsically connected

Understanding the dynamics behind lipid diversity is an essential step to unveil their biological function and relevance. Most de novo lipid synthesis takes place in the ER [35]. Here, phospholipids and sterols are produced and shuttled to the Golgi and plasma membrane through secretory vesicles or pipelines orchestrated by lipid transfer proteins [36, 37]. In the case of sphingolipids, the Cer backbone is synthesized and transported from the ER to the Golgi apparatus where it is then converted to sphingomyelin (SM) by sphingomyelin synthases (SMS). Consistently, sterols preferably accumulate in the Golgi where stabilization with long, saturated acyl chains of SM and derivatives afford protection of the hydrophobic core from the cytosol [38]. The gradient of sterol and sphingolipids along the secretory pathway is conserved by the exclusion of both from coat protein I vesicles that retrogradely transport proteins and lipids back to the ER [39]. Additionally, some lipid metabolizing enzymes show different affinities for fatty acyls and generate distinctive lipid subspecies with a unique fatty acyl length and saturation, e.g. ceramide synthases and phospholipases A. These may present distinct subcellular localizations, and therefore mediate specific functions [40]. Moreover, some lipids present concentrations of different order of magnitude such that minor disturbances in their levels may result in larger impacts in their relative counterparts, within the same lipid category, e.g. relatively small fluctuations in SM and PC breakdown may result in two or more fold-change increases in Cer or PA, respectively [40]. The crosstalk between metabolic pathways of distinct lipid categories, such as the step mediating SM synthesis from the transfer of the polar head group from the glycerophospholipid PC to the sphingolipid Cer, adds another level of complexity to the integrated system of lipid metabolism [40]. These points of connection between multiple-lipid pathways may allow a small disturbance in a specific metabolic branch to propagate to other lipid categories. Such phenomena impair the overall lipid shape equilibrium, in which the interplay between the abundance of each lipid species and acyl chain composition are tightly controlled to ensure the appropriate membrane properties for organelle function. For a more detailed discussion of membrane sensing, cross-talk and compensatory mechanisms between lipid pathways, see [16, 41].

Lipids determine the properties of membranes—from shape to function

Eukaryotic cells have evolved to form a complex membrane system that allows compartmentalization of the cell into

different organelles, where specific cellular functions occur, such as post-translational modification and maturation of proteins, spatial and temporal sorting, degradation, and recycling of long-lived compounds and damaged organelles [31]. Consistent with their functional complexity relatively to prokaryotes is the sophistication of their lipidomes [42]. Although lipid classes are generally defined by their polar head group, the fatty acids linked to their backbone may still vary in length and saturation, increasing the number of possible subspecies of lipids within the same class exponentially.

We have discussed that different lipids present different shapes and biochemical behaviors when assembled together in the same membranes. In general, the length of a phospholipid is proportional to the number of carbon atoms and inversely proportional to the degree of saturation (presence of double bonds). Taking into consideration the geometry of their polar head, lipids can assume different shapes, such as cylindrical or conical forms. These changes in geometry predict the shape of membranes, inducing planar or curved structures, respectively. Interestingly, a cylindrical phospholipid such as PC can be rapidly catabolized into conical lipids, through hydrolysis to diacylglycerol (DG) or phosphatidic acid (PA), by phospholipase C (PLC) and phospholipase D (PLD), respectively, or converted in an inverted-conical lysophosphatidylcholine (lysoPC) through the release of a fatty acyl chain by phospholipase A (PLA). Accordingly, cells defective in PS upregulate the similarly charged and shaped PI as a compensatory mechanism and another example of possible functional redundancy arises from the similarity between conical phosphatidylethanolamine (PE) and PA [16].

It is, therefore, possible for a membrane to assume different physical properties through the modulation of its lipids, namely thickness, fluidity, raft assembly, or surface charge [43]. Experimental evidence suggests that enrichment of sterols in the plasma membrane, in addition to saturated lipids, causes an increase in its thickness comparatively to other compartments, such as the ER. Not only the transmembrane domains (TMD) of plasma membrane proteins are longer than those located in the ER, but also proteins with smaller TMD are more easily segregated from this compartment when cholesterol is added, suggesting a model of hydrophobic matching [44].

Another key feature of membranes is the propensity to form microdomains, such as lipid rafts [6]. These lipid rafts were reported to be particularly enriched in cholesterol and sphingolipids with long and saturated fatty acids, a feature allowing an ordered sorting and interdigitation of their long chains between both leaflets [45]. These specific lipid microdomain structures function as specialized docks for localized cellular processes and have an important impact in disease physiology [5, 46]. Consistently, perturbation of sphingolipid metabolism results in altered protein compartmentalization through loss of assembly of these domains [43]. However, lipid rafts are not exclusively packed with sphingolipids and sterols but also contain glycerophospholipids, such as PC, its degree of recruitment being dependent on its level of saturation [34]. Indeed, sphingolipid depletion is compensated by synthesis of highly ordered and cylindrical saturated phospholipids [41]. Such planar structures allow a

more ordered state and the likelihood to be recruited and included in rafts. Additionally, the extent of phospholipid saturation determines membrane adsorption of cytosolic proteins by allowing packing defects that anchor hydrophobic motifs [47].

Altogether, manipulation of membrane composition regulates protein trafficking and folding and adjust flexibility to ease the mechanical forces exerted by proteins, such as to induce membrane curvature to facilitate vesicle fusion for neurotransmitter release or vesicle budding for synaptic vesicle recycling [48, 49].

Lipid imbalance is a hallmark of the stressed brain

In modern societies, the exposure to environmental stress is an increasing challenge. While physiological mechanisms to respond to acute stress are fundamental for the survival of an organism, the continuous or prolonged exposure to stress stimuli can have a deleterious impact. This maladaptive response includes functional and morphological impairment in various brain regions, such as the hippocampus and the prefrontal cortex (PFC). Consequently, chronic stress affects brain functions, such as learning and memory, decision making, emotional responses, and underlies the pathophysiology of various brain disorders, namely anxiety, depression and Alzheimer's disease (AD) [50–57].

The response to chronic stress involves a fast activation of the sympathetic nervous system, followed by a slower activation of the hypothalamic-pituitary-adrenal axis that culminates in the release of glucocorticoids (GCs), such as cortisol in primates and corticosterone (CORT) in rodents. GCs are believed to mediate a significant part of the pathologic effects of chronic stress and lead to structural and functional hippocampal impairment, with remarkable behavioral perturbations [52, 58–60]. Considering the multifaceted role of lipids in brain function, their implication in stress-related disorders, such as major depression and anxiety, is not surprising [61]. In fact, lipid-modifying enzymes have been reported to act downstream of GC signaling pathways and to be subject of modulation by antidepressant treatment [62, 63]. Dietary intake of lipids, namely poly-unsaturated fatty acids (e.g. docosahexaenoic acid (DHA)) affects the brain lipid composition in a region specific manner and impacts behavior [64–67]. Glycerolipid metabolism has been implicated in the pathology of depression, from increased turnover of phospholipids to single nucleotide polymorphisms in related enzymes that confer higher risk for bipolar disorder [68]. Increased sphingolipid breakdown and Cer production has also been linked to depressive-like behavior and neuro-inflammation, and has been postulated as a pharmacological target of tricyclic antidepressants [61, 62]. Multiple studies suggest a connection between aberrant lipid metabolism and the neurobiology of depression through deregulation of monoaminergic transmission or neurogenesis [68]. In addition, indirect pathways may occur, such as lipid deficiency-induced inflammation and aberrant lipid transport from the periphery to the brain [69, 70].

Taken together, certain specific lipid classes may be directly implicated in brain disorders. Considering the impact of dietary lipid intake and pharmacological intervention in brain lipid metabolism, it was thus timely and informative to conduct a comprehensive lipidomic profile of the brain under conditions of stress.

Lipidomic analysis of the chronic-stressed brain

In order to understand the impact of chronic stress exposure on the rat brain lipidome, we employed a detailed MS-based lipidomic analysis of different brain regions from animals submitted to a 4-week chronic unpredictable stress paradigm (Table 1) [12, 53]. In the next sections, we detail a basic framework to conduct a lipidomic study and dissect the metabolic implications for lipid signaling from this pathological context.

Snapshotting lipid pathways

A possible initial approach to characterize the lipidome of a system is to analyze the abundance of lipid categories referenced to a control group. Given the diverse biochemical properties of the mammalian lipidome, particularly in terms of polarity, different extraction methods need to be employed for a full characterization. The use of a modified Bligh and Dyer method allows an efficient and reproducible lipid extraction of the major lipid classes soluble in organic solvents [71]. After extraction, lipid classes are identified by a combined liquid chromatography-mass spectrometry approach and quantified, in molar values, by spiking with appropriate internal standards. With such a broad analysis, it is possible to integrate multiple lipid metabolic pathways and denote whether changes in a lipid class are in concert with levels of metabolically related products and whether any compensatory mechanisms are activated in a diseased setting.

Table 1. Changes in rat brain lipid composition induced by chronic unpredictable stress exposure [12].

Brain region	Lipid changes
Prefrontal cortex	Decrease in glycerophospholipids (PC, PCe, PE)
	Increase in lysophospholipids (lysoPC ^a , lysoPE)
	Decrease in sphingolipids (SM ^a and dhSM)
	Increase in sphingomyelin derivatives (Cer, LacCer)
Hippocampus	Decrease in PC
	Increase in PI
	Decrease in SM
	Increase in sphingomyelin derivatives (Cer, dhSM)
Amygdala	Increase in sulfatide derivatives (Sulf(2OH))
Cerebellum	No significant changes

^aLipid changes correlated with serum CORT levels ($R^2 > 0.4$)

While the present method is successful for the isolation of most lipid species, accurate measurement of highly polarized lipids (e.g. complex gangliosides) is hampered by their retention in the aqueous phase or need for alternative extraction methods for their purification [72]. Complementing strategies, such as high-performance liquid chromatography or the use of isotope-tagged derivatives, are required for the characterization of low-abundant lipids and isoform specific phospholipids, e.g. PI(3)P and PI(4)P [73–75]. Even though the use of the present tools only allows the identification of high-order relative fold changes, it has proven successful in the collection of a macro-snapshot of the lipid molecular species involved in disease pathology [8, 76].

Despite the common practice of using tissue homogenates in lipidomic approaches to identify lipid alterations in brain disorders, it is important to consider that whole tissue is composed of multiple cell types, such as neuronal and glial cells, each of which harbors its own lipid composition, enhancing the level of complexity of interpreting large-scale data sets [8, 63, 77, 78]. Indeed, we found significant differences between the lipid compositions of the different brain regions assessed [12]. Consequently, regional cellular heterogeneity is a potential major contribute for lipid disparity among different brain regions. Alternative approaches to complement this tissue analysis include the use of micro-dissection techniques or in vitro cell-type specific studies. Ultimately, a complete spatial characterization of the cell lipidome would require the analysis of the composition of particular organelles or more spatially defined structures in the central nervous system, through different biochemical fractionation and purification methods [79, 80]. This would be of particular relevance considering that bulk lipids determine the physical properties of membranes, modulate cellular protein machinery, and influence organelle functionality. The increase in spatial resolution can also be addressed by imaging lipid distribution in frozen brain sections using matrix-assisted laser desorption/ionization – time of flight/mass-spectrometry imaging (MALDI-TOF/MSI) [81, 82]. Nevertheless, the cost for topographical specificity is the reduced number of lipid species able to be identified, comparatively to other more established MS methods. Finally, the set-up of pulse and chase experiments in vitro, combined with the use of fluorescently tagged lipid binding domains, caged lipids, or direct labeling of lipids (e.g. deuterated lipids), can provide unique information about their exact location and how dynamically they change positions [83–86].

Knowing lipids from the inside: Fatty-acyl profile and metabolizing enzymes

The structural diversity of lipid classes impacts membrane function and interaction with the surrounding environment. This is of particular importance in brain functioning and neuronal processes. Neuronal communication relies on complex mechanisms mediating chemical synapses, from neurotransmitter release to sensing and signal initiation and propagation. Lipids are involved not only in synaptic vesicle fusion, and thus neurotransmitter release, but also in the activity of neurotransmitter receptors, ion channel

conductivity, and intracellular signaling cascades [87–89]. Another level of complexity on top of the diversity of lipid heads, that define each lipid class, is the variability of the carbon chain length and degree of saturation of the fatty acyls that ultimately determine the membrane biophysical properties [90]. These include lipid packing, fluidity and propensity to raft assembly. While in MS lipid ions are identified by their mass/charge ratio, such analysis is not directly informative about their fatty-acyl composition other than the total number of carbons and saturated bonds in the molecule. Therefore, to determine the nature of the fatty acids in a specific lipid, it is necessary to fragment lipids and detect the resulting products, yielding a head group and one or two fatty acids, whether it is a lyso- or phospholipid, respectively [43]. We have recently characterized the profile of the fatty-acyl chains of phospholipids, sphingolipids, and other neutral lipids in different brain regions and how these are affected by the exposure to chronic stress. In addition to a generalized increase in glycerophospho- and sphingolipid hydrolysis, we reported a decrease in shorter fatty-acyl phospholipids/DG in the PFC and an increase in 38 carbon and four-double bond phospholipids/DG in the hippocampus [12]. This accumulation of longer, unsaturated species suggests the incorporation of arachidonic acid (AA) – with the following “number of carbons”: “double bonds” composition – 20:4 – as part of the fatty acyl composition. AA is a known mediator of inflammation, is positively correlated with age-induced changes and has also been described to be enriched in a different rat model of depressive-like behavior [91, 92]. In contrast, diets rich in polyunsaturated fatty acids, such as fish oil diet, show an increase in short, unsaturated DHA-containing phospholipids, which are proposed to be neuroprotective and anxiolytic [93, 94]. Of note, patients with depression were found to have an altered ratio of n-6/n-3 polyunsaturated fatty acids in peripheral blood and these changes may reflect an altered brain lipid composition, considering these fatty acids are also used as substrates in brain lipid synthesis [95–98].

Another piece of relevant information obtained from depicting lipid subspecies is the possible modulation of their metabolic enzymes. Some lipid modifying enzymes have been extensively implicated in brain disorders and proposed to be modulated at the level of protein expression as well as phosphorylation status [99–101]. Given the observed increase in glycerophospholipid and sphingolipid breakdown after exposure to chronic stress, we quantified the mRNA levels of the lipid enzymes most likely to underlie the observed findings (Fig. 2). We found no changes in the transcript levels of several PLA2, PLD, and sphingomyelinase isoforms [12]. These results suggest a complex and yet to be identified mechanism of post-transcriptional lipid enzyme regulation, which could involve altered protein synthesis, post-translational modifications, altered trafficking, or enzymatic activity.

Specific lipid imbalances are correlated with biological mediators of chronic stress

Depression and anxiety disorders are examples of the impact of the allostatic load caused by chronic stressors. In a recent study, we showed that the long-term consequences of

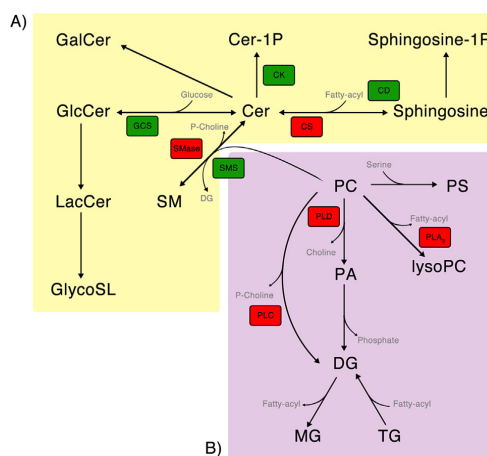


Figure 2. Pathways of sphingolipid and glycerophospholipid metabolism. **A:** Brain Cer levels are increased under conditions of stress [12, 61]. Such flux in sphingolipid metabolism is likely to occur due to increased hydrolysis of SM by sphingomyelinases but can also be related to increased de novo formation (enzymes highlighted in red). To alleviate Cer burden, sphingolipid breakdown may be reduced by pharmacological inhibition of SMases or stimulation of both SM and glycosphingolipid synthesis (highlighted in green). Alternatively, Cer may be hydrolyzed by ceramidases or phosphorylated to ceramide 1-phosphate by ceramide kinases. **B:** Glycerophospholipid metabolism is impaired under chronic stress with concerted PC breakdown and increase in its metabolites LysoPC, PA, and DAG, possibly by increased PLA, PLD, and PLC enzyme activity, respectively (highlighted in red). Decreased PC levels have been reported in animal models of neurodegenerative diseases and genetic ablation of the highlighted enzymes confers protection from synaptic and cognitive impairment. In addition, studies have shown decreased plasma PC levels and increased cerebrospinal fluid PC metabolites in patients with AD [115]. Abbreviations: CD, ceramidase; Cer, ceramide; Cer-1P, ceramide 1-phosphate; CK, ceramide kinase; CS, ceramide synthase; DG, diacylglycerol; GalCer, galactosylceramide; GCS, glucosylceramide synthase; GlcCer, glucosylceramide; GlycoSL, glycosphingolipids; LacCer, lactosylceramide; LysoPC, lysophosphatidylcholine; MG, monoacylglyceride; PA, phosphatidic acid; PC, phosphatidylcholine; PLA2, phospholipase A2; PLC, phospholipase C; PLD, phospholipase D; PS, phosphatidylserine; P-Choline, phospho-choline; SM, sphingomyelin; SMase, sphingomyelinase; SMS, sphingomyelin synthase; Sphingosine-1P, sphingosine-1-phosphate; TG, triacylglyceride.

exposure to stress leads to an imbalance in lipid homeostasis in specific brain areas [12]. However, chronic stress also affects many other physiological parameters. As previously mentioned, the response to chronic stress in the rodent involves an increase in CORT blood levels, which partly modulates its deleterious effects [102]. We reasoned that specific lipid changes could potentially be correlated with CORT blood levels [103, 104]. To further validate our hypothesis, we performed a full-scale unbiased correlation analysis between the abundance of over 300 quantifiable lipid species and the serum levels of CORT, in each brain region. With such an approach, we extended our analysis to the level of the individual within each group. This is particularly important

considering that individual humans and animals present different responses to stress, hence the concept of resilience [105]. These distinct responses to the same stimulus are linked to specific molecular alterations and genetic susceptibility and should be considered in studies addressing depressive-like behaviors [106–108]. Our results reinforced the initial findings: in the PFC, phospholipid, and sphingolipid breakdown correlated with serum CORT. Although correlation does not imply causation, such strong coherence suggests that these metabolic pathways are involved and possibly mediate stress responses. Further agreement with previous studies implicating these metabolizing enzymes in other cognitive disorders increase the relevance of such observations [62, 76, 109]. Other appealing approaches to screen the role of lipid imbalances in brain dyshomeostasis would be to correlate their levels to other known biological parameters, such as behavioral changes, electrophysiological activity, or morphological remodeling, including synaptic plasticity and neurogenesis. These findings should be followed by validation studies using genetic or pharmacological approaches targeting lipid modulating enzymes.

Lipid signatures as biomarkers for neurodegenerative disorders

The prevalence of neurological and psychiatric disorders is on the rise, and brings with it a considerable economic burden [110]. Continuous efforts have been implemented in order to early diagnose, prevent, halt, or reverse these disorders. Presently, it is still a major challenge to diagnose mood disorders and to predict their disease progression and response to therapy. Moreover, some cognitive disorders, such as AD, still rely on *post-mortem* evaluation for its diagnosis [111]. There is thus the need to develop new diagnostic and disease progression biomarkers. Not surprisingly, lipidomic studies are arising as potential means to find lipid signatures that identify specific disease states. Importantly, while it is still unclear the biological implication of these lipid signatures in disease physiology, their clinical relevance arises from the reproducibility amid independent studies and consistency between human and animal models of disease [8, 73, 78]. In the context of AD, a recent study has reported a blood-based lipid profile for successful detection of preclinical AD and prediction of phenocconversion to either mild cognitive impairment (MCI) or AD within 2–3 years [112]. The untargeted metabolomics and lipidomic profiling resulted in the identification of 10 metabolites, namely PC and acylcarnitine species, which could be used as a diagnostic tool. Therefore, it is now essential to extend the approach of lipid profiling to other neurological and psychiatric diseases, such as chronic stress associated disorders. It would be interesting to understand whether human studies present similar pathological signatures to the ones observed in rodent models. For the time being, magnetic resonance imaging spectroscopy methods have enabled non-invasive measurements of choline-containing molecules, further implicating phospholipid membrane metabolism in mood disorders, such as schizophrenia and depression [113]. Additional studies co-analyzing brain data with blood and CSF samples will not

only be useful in setting new diagnostic biomarkers, but also predicting prognosis and therapy response. Given the complexity of the lipidome in terms of lipid categories, classes, and subclasses, only large post-processing and integrative methods of data analysis will allow researchers to uncover the many important roles of these highly modulatable molecules and transform lipidomic profiling in a routine and cost-effective procedure, readily available for patient care.

Conclusions and outlook

Lipidomic MS methods have opened new avenues in the analysis of biological samples. Since lipids are major constituents of the brain, these new analytical techniques provide new insights in the understanding of brain physiology and pathophysiology. Lipidomic studies allow the identification of altered lipid pathways and lipid signatures associated with a disease state. From now on, it will be fundamental to characterize the impact on the lipidome of genetic manipulation, pharmacological modulation, or exposure to different environmental factors, such as diet, exercise, and psychosocial stressors. Since lipids are intrinsically metabolically connected, lipidomic mappings will provide us the framework to correctly apply lipid-modifying therapies and use lipid signatures for diagnosis, prognosis, and therapeutic response in a given disease state.

Acknowledgments

We would like to thank Nuno Sousa for critical reading of the manuscript. André Miranda is funded by Fundação para a Ciência e Tecnologia (PD/BD/105915/2014). Tiago Gil Oliveira is funded by Fundação para a Ciência e Tecnologia (PTDC/SAU-NMC/118971/2010).

The authors have declared no conflicts of interest.

References

1. **Piomelli D, Astarita G, Rapaka R.** 2007. A neuroscientist's guide to lipidomics. *Nat Rev Neurosci* **8**: 743–54.
2. **Wenk MR.** 2010. Lipidomics: new tools and applications. *Cell* **143**: 888–95.
3. **Brügger B.** 2014. Lipidomics: analysis of the lipid composition of cells and subcellular organelles by electrospray ionization mass spectrometry. *Annu Rev Biochem* **83**: 79–98.
4. **Wenk MR.** 2005. The emerging field of lipidomics. *Nat Rev Drug Discov* **4**: 594–610.
5. **Di Paolo G, Kim T-W.** 2011. Linking lipids to Alzheimer's disease: cholesterol and beyond. *Nat Rev Neurosci* **12**: 284–96.
6. **Simons K, Ehehalt R.** 2002. Cholesterol, lipid rafts, and disease. *J Clin Invest* **110**: 597–603.
7. **Wymann MP, Schneider R.** 2008. Lipid signalling in disease. *Nat Rev Mol Cell Biol* **9**: 162–76.
8. **Chan RB, Oliveira TG, Cortes EP, Honig LS, et al.** 2012. Comparative lipidomic analysis of mouse and human brain with Alzheimer disease. *J Biol Chem* **287**: 2678–88.
9. **Prasad MR, Lovell MA, Yatin M, Dhillon H, et al.** 1998. Regional membrane phospholipid alterations in Alzheimer's disease. *Neurochem Res* **23**: 81–8.
10. **Han X.** 2005. Lipid alterations in the earliest clinically recognizable stage of Alzheimer's disease: implication of the role of lipids in the pathogenesis of Alzheimer's disease. *Curr Alzheimer Res* **2**: 65–77.

11. **Cermenati G, Mitro N, Audano M, Melcangi RC**, et al. 2015. Lipids in the nervous system: From biochemistry and molecular biology to pathophysiology. *Biochim Biophys Acta* **1851**: 51–60.
12. **Oliveira TG, Chan RB, Bravo FV, Miranda A**, et al. 2015. The impact of chronic stress on the rat brain lipidome. *Mol Psychiatry*, in press, doi: 10.1038/mp.2015.14.
13. **Delisi LE**. 2009. Handbook of neurochemistry and molecular neurobiology. *Handb Neurochem Mol Neurobiol Schizophr* **27**: 107–241.
14. **Bozek K, Wei Y, Yan Z, Liu X**, et al. 2015. Organization and evolution of brain lipidome revealed by large-scale analysis of human, chimpanzee, macaque, and mouse tissues. *Neuron* **85**: 695–702.
15. **Fahy E, Subramaniam S, Brown HA, Glass CK**, et al. 2005. A comprehensive classification system for lipids. *J Lipid Res* **46**: 839–61.
16. **Holthuis JCM, Menon AK**. 2014. Lipid landscapes and pipelines in membrane homeostasis. *Nature* **510**: 48–57.
17. **Thatcher JD**. 2010. The inositol trisphosphate (IP3) signal transduction pathway. *Sci Signal* **3**: tr.
18. **Hartmann T, Kuchenbecker J, Grimm MOW**. 2007. Alzheimer's disease: the lipid connection. *J Neurochem* **103 Suppl**: 159–70.
19. **Dietschy JM, Turley SD**. 2001. Cholesterol metabolism in the brain. *Curr Opin Lipidol* **12**: 105–12.
20. **Bazinete RP, Layé S**. 2014. Polyunsaturated fatty acids and their metabolites in brain function and disease. *Nat Rev Neurosci* **15**: 771–85.
21. **Arevalo M-A, Azcoitia I, Garcia-Segura LM**. 2014. The neuroprotective actions of oestradiol and oestrogen receptors. *Nat Rev Neurosci* **16**: 17–29.
22. **Chang T-Y, Chang CCY, Ohgami N, Yamauchi Y**. 2006. Cholesterol sensing, trafficking, and esterification. *Annu Rev Cell Dev Biol* **22**: 129–57.
23. **Björkhem I**. 2006. Crossing the barrier: oxysterols as cholesterol transporters and metabolic modulators in the brain. *J Intern Med* **260**: 493–508.
24. **Heverin M, Bogdanovic N, Lütjohann D, Bayer T**, et al. 2004. Changes in the levels of cerebral and extracerebral sterols in the brain of patients with Alzheimer's disease. *J Lipid Res* **45**: 186–93.
25. **Lütjohann D, Breuer O, Ahlborg G, Nennesmo I**, et al. 1996. Cholesterol homeostasis in human brain: evidence for an age-dependent flux of 24S-hydroxycholesterol from the brain into the circulation. *Proc Natl Acad Sci USA* **93**: 9799–804.
26. **Zhang D-D, Yu H-L, Ma W-W, Liu Q-R**, et al. 2015. 27-Hydroxycholesterol contributes to disruptive effects on learning and memory by modulating cholesterol metabolism in the rat brain. *Neuroscience* **300**: 163–73.
27. **Radhakrishnan A, Goldstein JL, McDonald JG, Brown MS**. 2008. Switch-like control of SREBP-2 transport triggered by small changes in ER cholesterol: a delicate balance. *Cell Metab* **8**: 512–21.
28. **Kay JG, Grinstein S**. 2013. Phosphatidyserine-mediated cellular signaling. *Adv Exp Med Biol* **991**: 177–93.
29. **Kodigepalli KM, Bowers K, Sharp A, Nanjundan M**. 2015. Roles and regulation of phospholipid scramblases. *FEBS Lett* **589**: 3–14.
30. **Williamson P, Schlegel RA**. 2002. Transbilayer phospholipid movement and the clearance of apoptotic cells. *Biochim Biophys Acta* **1585**: 53–63.
31. **Di Paolo G, De Camilli P**. 2006. Phosphoinositides in cell regulation and membrane dynamics. *Nature* **443**: 651–7.
32. **Maceyka M, Spiegel S**. 2014. Sphingolipid metabolites in inflammatory disease. *Nature* **510**: 58–67.
33. **Nicolson GL**. 2014. The fluid-mosaic model of membrane structure: still relevant to understanding the structure, function and dynamics of biological membranes after more than 40 years. *Biochim Biophys Acta* **1838**: 1451–66.
34. **Dawson G**. 2015. Measuring brain lipids. *Biochim Biophys Acta* **1851**: 1026–39.
35. **Van Meer G, Voelker DR, Feigenson GW**. 2008. Membrane lipids: where they are and how they behave. *Nat Rev Mol Cell Biol* **9**: 112–24.
36. **Lev S**. 2010. Non-vesicular lipid transport by lipid-transfer proteins and beyond. *Nat Rev Mol Cell Biol* **11**: 739–50.
37. **Schauder CM, Wu X, Saheki Y, Narayanaswamy P**, et al. 2014. Structure of a lipid-bound extended synaptotagmin indicates a role in lipid transfer. *Nature* **510**: 552–5.
38. **Mesmin B, Maxfield FR**. 2009. Intracellular sterol dynamics. *Biochim Biophys Acta* **1791**: 636–45.
39. **Shevchenko A, Simons K**. 2010. Lipidomics: coming to grips with lipid diversity. *Nat Rev Mol Cell Biol* **11**: 593–8.
40. **Hannun Y a, Obeid LM**. 2008. Principles of bioactive lipid signalling: lessons from sphingolipids. *Nat Rev Mol Cell Biol* **9**: 139–50.
41. **De Kroon AIPM, Rijken PJ, De Smet CH**. 2013. Checks and balances in membrane phospholipid class and acyl chain homeostasis, the yeast perspective. *Prog Lipid Res* **52**: 374–94.
42. **Simons K, Sampaio J**. 2011. Membrane organization and lipid rafts. *Cold Spring Harb Perspect Biol* **3**: a004697.
43. **Klose C, Surma MA, Simons K**. 2013. Organellar lipidomics-background and perspectives. *Curr Opin Cell Biol* **25**: 406–13.
44. **Mouritsen OG**. 2011. Model answers to lipid membrane questions. *Cold Spring Harb Perspect Biol* **3**: 1–5.
45. **Holthuis JC, Pomorski T, Riggers RJ, Sprong H**, et al. 2001. The organizing potential of sphingolipids in intracellular membrane transport. *Physiol Rev* **81**: 1689–723.
46. **Vetrivel KS, Thinakaran G**. 2010. Membrane rafts in Alzheimer's disease beta-amyloid production. *Biochim Biophys Acta* **1801**: 860–7.
47. **Antony B, Vanni S, Shindou H, Ferreira T**. 2015. From zero to six double bonds: phospholipid unsaturation and organelle function. *Trends Cell Biol* **25**: 427–36.
48. **McMahon HT, Gallop JL**. 2005. Membrane curvature and mechanisms of dynamic cell membrane remodeling. *Nature* **438**: 590–6.
49. **Oliveira TG, Di Paolo G**. 2010. Phospholipase D in brain function and Alzheimer's disease. *Biochim Biophys Acta* **1801**: 799–805.
50. **Lupien SJ, McEwen BS, Gunnar MR, Heim C**. 2009. Effects of stress throughout the lifespan on the brain, behaviour and cognition. *Nat Rev Neurosci* **10**: 434–45.
51. **Pinto V, Costa JC, Morgado P, Mota C**, et al. 2015. Differential impact of chronic stress along the hippocampal dorsal-ventral axis. *Brain Struct Funct* **220**: 1205–12.
52. **Sousa N, Almeida OFX**. 2012. Disconnection and reconnection: the morphological basis of (mal) adaptation to stress. *Trends Neurosci* **35**: 742–51.
53. **Cerqueira JJ, Mailliet F, Almeida OFX, Jay TM**, et al. 2007. The prefrontal cortex as a key target of the maladaptive response to stress. *J Neurosci* **27**: 2781–7.
54. **Dias-Ferreira E, Sousa JC, Melo I, Morgado P**, et al. 2009. Chronic stress causes frontostriatal reorganization and affects decision-making. *Science* **325**: 621–5.
55. **Roosendaal B, McEwen BS, Chattarji S**. 2009. Stress, memory and the amygdala. *Nat Rev Neurosci* **10**: 423–33.
56. **Catania C, Sotiropoulos I, Silva R, Onofri C**, et al. 2009. The amyloidogenic potential and behavioral correlates of stress. *Mol Psychiatry* **14**: 95–105.
57. **Bessa JM, Ferreira D, Melo I, Marques F**, et al. 2009. The mood-improving actions of antidepressants do not depend on neurogenesis but are associated with neuronal remodeling. *Mol Psychiatry* **14**: 739.
58. **Sousa N, Lukoyanov N, Madeira M, Almeida O**, et al. 2000. Reorganization of the morphology of hippocampal neurites and synapses after stress-induced damage correlates with behavioral improvement. *Neuroscience* **101**: 483.
59. **Sousa N, Cerqueira JJ, Almeida OFX**. 2008. Corticosteroid receptors and neuroplasticity. *Brain Res Rev* **57**: 561–70.
60. **Sousa N, Almeida OFX**. 2002. Corticosteroids: sculptors of the hippocampal formation. *Rev Neurosci* **13**: 59–84.
61. **Kornhuber J, Müller CP, Becker KA, Reichel M**, et al. 2014. The ceramide system as a novel antidepressant target. *Trends Pharmacol Sci* **35**: 293–304.
62. **Gulbins E, Palmada M, Reichel M, Luth A**, et al. 2013. Acid sphingomyelinase-ceramide system mediates effects of antidepressant drugs. *Nat Med* **19**: 934–8.
63. **Lee LH-W, Shui G, Farooqui A a, Wenk MR**, et al. 2009. Lipidomic analyses of the mouse brain after antidepressant treatment: evidence for endogenous release of long-chain fatty acids?. *Int J Neuropsychopharmacol* **12**: 953–64.
64. **Levant B, Ozias MK, Carlson SE**. 2007. Specific brain regions of female rats are differentially depleted of docosahexaenoic acid by reproductive activity and an (n-3) fatty acid-deficient diet. *J Nutr* **137**: 130–4.
65. **Prasad A, Prasad C**. 1996. Short-term consumption of a diet rich in fat decreases anxiety response in adult male rats. *Physiol Behav* **60**: 1039–42.
66. **Ortolani D, Oyama LM, Ferrari EM, Melo LL**, et al. 2011. Effects of comfort food on food intake, anxiety-like behavior and the stress response in rats. *Physiol Behav* **103**: 487–92.
67. **Buchenaer T, Behrendt P, Bode FJ, Horn R**, et al. 2009. Diet-induced obesity alters behavior as well as serum levels of corticosterone in F344 rats. *Physiol Behav* **98**: 563–9.

André M. Miranda, Gilbert Di Paolo

**Endolysosomal dysfunction and exosome secretion: implications for
neurodegenerative disorders**

Microreview - Cell Stress

(accepted April 2018)

Endolysosomal dysfunction and exosome secretion: implications for neurodegenerative disorders

André M. Miranda^{1,2,3,4} and Gilbert Di Paolo^{1,2,5,*}

¹ Department of Pathology and Cell Biology, Columbia University Medical Center, New York City, NY 10032, USA.

² Taub Institute for Research on Alzheimer's disease and the Aging Brain, Columbia University Medical Center, New York City, NY 10032, USA.

³ Life and Health Sciences Research Institute (ICVS), School of Medicine, University of Minho, Braga 4710-057, Portugal

⁴ ICVS/3B's, PT Government Associate Laboratory, Braga/Guimarães 4710-057, Portugal

⁵ Present address: Denali Therapeutics, South San Francisco, CA 94080, USA

*Correspondence should be addressed to G.D.P. (e-mail: dipaolo@dnli.com)

Keywords: extracellular vesicles, endomembrane damage, galectin-3, phosphoinositide, phosphatidylinositol-3-phosphate, lysobisphosphatidic acid, LBPA, sphingolipids, phospholipids.

Growing evidence suggests that endolysosomal and autophagic defects are key pathogenic processes in various neurodegenerative disorders, including Alzheimer's disease (AD), Parkinson's disease (PD), frontotemporal dementia (FTD) and amyotrophic lateral sclerosis (ALS). The causal relationship between these defects and neurodegeneration is supported by human genetic studies identifying disease mutations in genes controlling endolysosomal function and autophagy. The canonical view is that defects in these processes lead to impaired lysosomal clearance of proteins prone to form toxic oligomeric assemblies and/or aggregates, ultimately resulting in cellular pathologies that define these disorders. Because lysosomes mediate the clearance of a large number of lipids, lipid storage is frequently associated with compromised endolysosomal and autophagic function. However, an emerging notion, supported by our recent study on class III phosphatidylinositol 3-kinase (PI3K) Vps34, is that neuronal endolysosomal and autophagic dysfunction can manifest itself with the occurrence of physically damaged endomembranes and with the release of exosomes enriched for Amyloid Precursor Protein COOH-terminal fragments (APP-CTFs) as well as atypical phospholipid bis(monoacylglycero)phosphate (BMP). Here, we summarize our recent findings and their potential implications in the context of lysosomal biology, lipid signaling and neurodegenerative diseases.

A master regulator of both endolysosomal function and autophagy is Vps34 and its lipid product phosphatidylinositol-3-phosphate (PI3P) through which the lipid kinase exerts most of its biological actions in eukaryotic cells. A host of PI3P effectors have been characterized and shown to mediate processes as diverse as endosomal fusion, retrograde transport, sorting of cargoes into intraluminal vesicles (ILVs) of multivesicular endosomes as well as autophagosome biogenesis and maturation. Interfering with the signaling of PI3P and its metabolite PI(3,5)P₂ has been implicated in neurodegeneration, as PI3P deficiency was reported in the brain of AD patients and the pathway was genetically linked to ALS and PD. Accordingly, genetic disruption of the Vps34-encoding gene (*Pik3c3*) in mice leads to major neuronal loss, suggesting that ablation and pharmacological inhibition of Vps34 are appropriate models to study the causal relationship between endolysosomal/autophagic defects and neurodegeneration.

Prompted by our findings showing that PI3P is deficient in the brain of AD patients and mouse models thereof, we investigated the consequences of Vps34 kinase inhibition or genetic ablation on autophagy, endolysosomal function and APP processing. We observed that reducing PI3P levels in

primary cortical neurons or the neuronal cell line N2a blocks autophagy initiation, causes an increase in autophagy receptor/substrate p62 and polyubiquitinated protein levels and slows degradation of APP-CTFs, including APP-CTF β , the BACE1-derived substrate processed by γ -secretase into amyloid- β (A β). As APP-CTFs accumulate following Vps34 inhibition, it is reasonable to assume that γ -secretase-mediated processing of these fragments is not efficient enough to downregulate their levels. In fact, A β levels were found to be decreased upon Vps34 inhibition.

Given the impact of Vps34 inhibition on endolysosomal function, we hypothesized it may also impair the metabolism of lipids and specifically, those degraded in lysosomes. Using lipidomics, we found that Vps34 inhibition increases levels of specific sphingolipids, namely ceramides and dihydrosphingolipids, somewhat reminiscent of some lysosome storage disorders (LSDs). While dysregulated ceramide metabolism can trigger cytotoxic signaling cascades, including apoptosis and necroptosis, missorting and accumulation of these sphingolipids in membrane subdomains may destabilize lipid bilayers and cause their permeabilization. Thus, we examined levels and subcellular localization of galectin-3, which, similar to other galectins, is a cytosolic lectin with high affinity for glycan β -galactosides that are enriched in the luminal leaflet of endocytic organelles. Thus, intracellular galectin-3 accumulation in the form of ubiquitin-positive puncta denotes permeabilization of endolysosomal membranes, as others have reported. We observed that inhibition or genetic ablation of Vps34 in primary cortical neurons causes accumulation of galectin-3/ ubiquitin/ p62-positive structures (Fig. 1). However, those puncta were also positive for cholesterol/sphingolipid-rich membrane marker flotillin, yet, negative for LAMP-1 (although they lied in close proximity to LAMP-1-positive late endosomes/lysosomes), suggesting that they were organelles of endocytic origin lacking standard markers for those compartments. APP did not appear to concentrate on these organelles either. We speculated that their permeabilization causes loss of specific endolysosomal markers through excessive proteolysis. Importantly, accumulation of p62, ubiquitin and galectin-3 on those physically compromised organelles suggested that they are targeted to the autophagy pathway but not properly cleared by lysophagy (*i.e.*, a selective form of autophagy clearing damaged lysosomes), as Vps34 inhibition blocks autophagy initiation. What mechanisms account for endomembrane damage and what endolysosomal compartments are permeabilized in response to Vps34 inhibition? While we have not answered this question, we hypothesized that altered trafficking along the endolysosomal pathway causes secondary accumulation of sphingolipids and possibly sterols, which, in turn, leads to destabilization and permeabilization of endolysosomal membranes. Alternate explanations include increased oxidative stress or loss of glycocalyx coating of their luminal leaflets

through missorting of glycoproteins. It will thus be fundamental to better characterize the identity of these damaged structures, perhaps via immunoisolation combined with proteomic and lipidomic analyses. Future work will address whether endolysosomal membrane permeabilization is a common pathogenic process in neurodegenerative disorders associated with LSDs and whether blocking it confers therapeutic benefits.

Another key finding reported in our study is that Vps34 inhibition causes robust secretion of exosomes enriched for APP-CTFs (Fig. 1). Exosomes are small vesicles secreted upon fusion of multivesicular endolysosomal compartments with the plasma membrane and correspond to the ILVs of those organelles. There is significant heterogeneity in the types of internal vesicles based on their differential protein and lipid composition, and logically, this heterogeneity is carried over in exosomes when internal vesicles are secreted. For instance, it has been reported that internal vesicles can be either PI3P- or BMP-positive, although no studies had reported the presence of either of those lipids in exosomes. Also, whether various subpopulations of exosomes derive from common or distinct endolysosomal compartments remains to be elucidated. We found that by reducing levels of PI3P with the Vps34 inhibitor, the co-secretion of BMP- and APP-CTF-positive exosomes is enhanced, although these molecules may not necessarily reside on the same exosomes (Fig. 1). Pharmacological experiments have begun to delineate the mechanisms responsible for this atypical exosome release. First, it is also triggered by inhibition of the V-type ATPase with Bafilomycin A1 (BafA1), suggesting that elevation of endolysosomal pH may be the underlying mechanism, although neither chloroquine nor NH₄Cl phenocopied these findings, arguing against a simple pH effect (unless BafA1 causes a more sustained increase in endolysosomal pH relative to the other two alkalizers). This may rather reflect an important role of the V-type ATPase in exosome release, as suggested by recent studies. Second, inhibitors of serine palmitoyl transferase and neutral sphingomyelinase 2 both blocked exosomal release of APP-CTFs, suggesting that *de novo* sphingolipid synthesis and ceramide generation are critical. This is consistent with the fact that Vps34 inhibition causes a profound alteration of sphingolipid metabolism, including ceramides. We also note that previous studies from our group have found that the ESCRT pathway, which relies on PI3P primarily due to its ability to recruit ESCRT0/Hrs to endosomal membranes, mediates APP sorting into ILVs and exosome. However, Vps34 inhibition and the ensuing drop in PI3P levels shunt APP/APP-CTFs into an ESCRT-independent pathway, leading to robust exosomal secretion of APP-CTFs. This highlights the plasticity of ILV sorting and exosomal secretion routes for specific cargoes. It remains unclear if BMP is required

for secretion of APP-CTF and other endolysosomal cargo in exosomes, a question that may be addressed by identification of the BMP-synthesizing enzymes and their manipulation.

What could be the purpose of exosome release triggered by endolysosomal dysfunction? Both cell-autonomous and non-autonomous aspects must be considered. Growing evidence indicates that exosomes can serve as vectors for eliminating DNA, proteins or lipids. Our work, along with studies from others, suggests that exosome release is a *bona fide* cell autonomous pathway accounting for the elimination of undesired and/or undigested endolysosomal cargoes, such as toxic proteins or lipids, which cannot be efficiently degraded in lysosomes when the latter are compromised. Concerning APP-CTF β , their exosomal elimination may decrease their inherent cellular toxicity or reduce their processing by γ -secretase into A β , which is also deleterious. Similar mechanisms may apply to aggregate-prone proteins such as tau, α -synuclein (α -syn), and TDP-43, which accumulate primarily in the neurons of patients with AD, PD and ALS/FTD, respectively. In fact, if exosome release is robust enough to eliminate these toxic intracellular proteins, blocking exosomal release may cause their intracellular accumulation and increase their cellular toxicity, perhaps exacerbating intracellular pathologies.

Regarding potential cell non-autonomous functions, growing evidence suggests that exosomes participate in cell-cell communication. In contrast to diffusible, soluble molecules that ensure long-range signaling within a tissue, an organ or an organism, exosomes are more likely to play paracrine roles with limited spreading abilities, unless they reach blood circulation or the cerebrospinal fluid (CSF) or undergo long-range transcytosis along neuronal processes upon internalization. Because exosomes harbor intracellular molecules such as proteins and lipids, the very presence of such molecules on the outer leaflets of their lipid bilayers likely plays a signaling role, driving specificity in cell-cell communication. For instance, the molecules exposed to the surface of exosome could determine what cell types ultimately captures them and transmits their signals, through specific cell surface receptors. In the case of exosomes released upon inducing lysosomal dysfunction in brain tissue, they may carry “eat me signals” destined for immune cells of the brain, such as microglia, which could help eliminating the toxic waste neurons cannot handle. They could also carry danger-associated molecular patterns (DAMPs) stimulating innate immune receptors on astrocytes or microglia, favoring chemotaxis and deleterious gliosis. Future studies will address whether neuronal exosomes triggered by lysosomal dysfunction are endowed with signaling abilities towards glial cells and what the physiological and pathophysiological consequences of this communication are.

In the realm of pathology, exosomes may also contribute to the spreading of neuronal aggregates within the central nervous system, including tau and α -syn pathologies in AD and PD, respectively. While prion-like modalities have been proposed to mediate the spreading of these protein aggregates, the underlying molecular and cellular mechanisms are still unknown. One of the challenges is that tau and α -syn must be unconventionally secreted, re-internalized and crossing the endolysosomal membrane in order to nucleate aggregates in the cytoplasm of “host cells”. While our study has focused primarily on APP-CTFs, other studies have found that lysosomal dysfunction triggers the exosomal secretion of α -syn. Exosomal APP-CTFs themselves have been found by Sadoul and colleagues to be processed by the target neurons' γ -secretase after selective binding of exosomes to, and internalization by, their dendrites. Generally, exosomes represent powerful vectors for cell-cell communication, both in physiology and pathophysiology.

Finally, our work has implications for biomarker discovery. Since lysosomal dysfunction causes robust secretion of APP-CTFs and BMP, measuring those molecules in bodily fluids (*e.g.*, plasma or CSF) of patients and preclinical models for disorders associated with lysosomal dysfunction, including AD, PD, ALS, FTD and obviously LSDs, may be informative, and may also provide novel opportunities in clinical settings for identification of pharmacodynamic biomarkers in relation to treatments that improve or correct lysosomal dysfunction.

Acknowledgements

This work was supported by grants from the Fundação para a Ciência e Tecnologia (PD/BD/105915/2014 to A.M.M.), the National Institute of Health (R01 NS056049 to G.D.P, transferred to Ron K. Liem; and P50 AG008702 to Scott A. Small, Columbia University, New York).

Conflict of Interest

The authors declare no competing financial interests. G.D.P. is a full-time employee of Denali Therapeutics Inc.

Running title

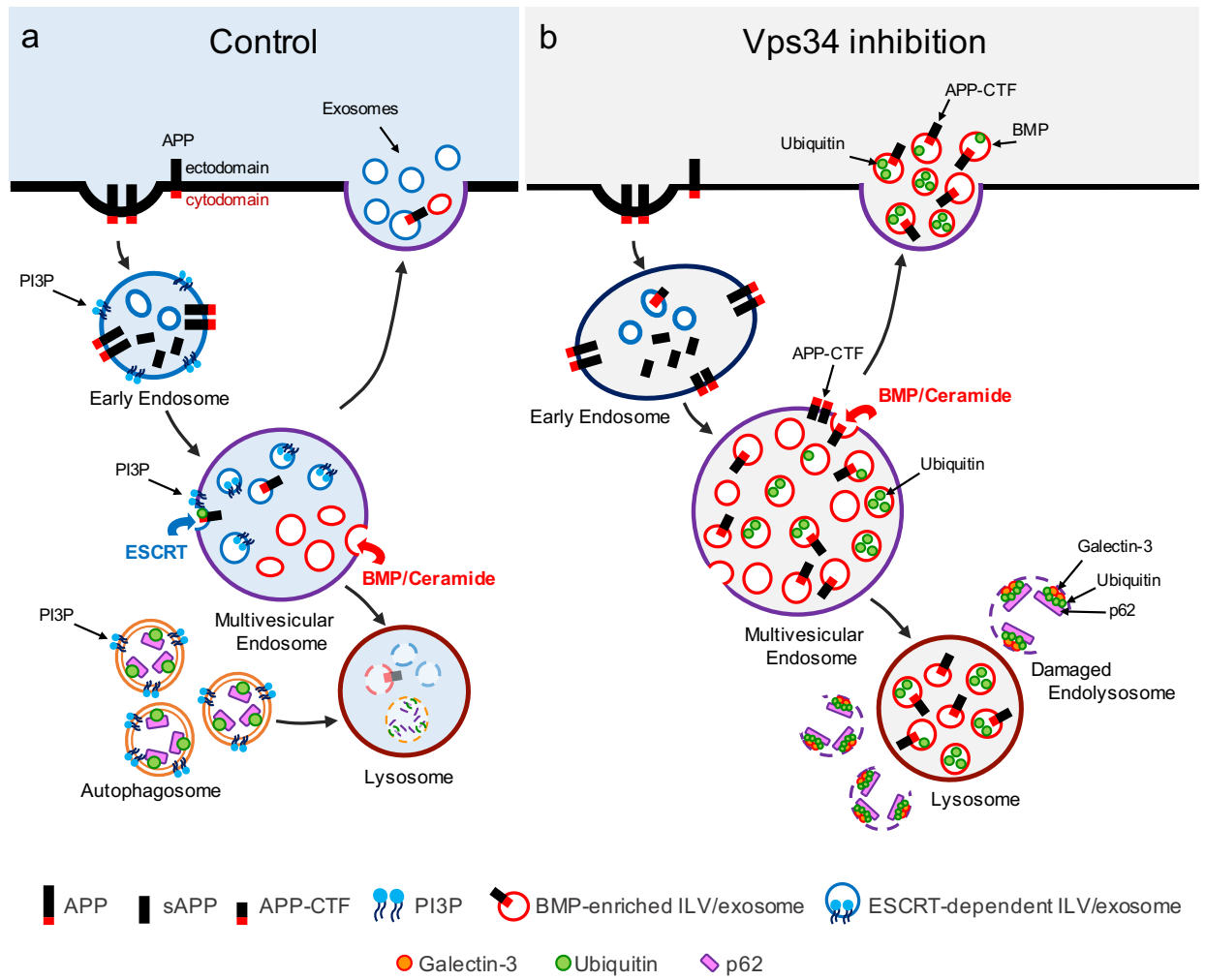
Endolysosomal dysfunction and exosome release

Figure Legend

Figure 1. Vps34 inhibition causes endolysosomal dysfunction and enhanced release of atypical exosomes harboring poly-ubiquitinated proteins, APP-CTFs and the atypical phospholipid BMP.

a) In control cells, newly synthesized APP traffics to the plasma membrane (not shown), where it undergoes clathrin-mediated endocytosis and sorting into PI3P-enriched early endosomes. The acidic endosomal lumen is optimal for amyloidogenic processing by BACE1. APP-CTFs and a pool of full length APP are sorted to intraluminal vesicles (ILVs) of multivesicular endosomes (MVEs) *via* the ESCRT pathway, which requires PI3P and ubiquitination of lysine residues of the APP cytodomain. APP-CTFs can then be processed by γ -secretase into amyloid- β (A β), degraded in lysosomes or secreted in exosomes upon fusion of MVEs with the plasma membrane. Of note, PI3P- and BMP-positive ILVs are segregated from each other within MVEs and, under control conditions, exosomes are largely devoid of BMP. In a separate pathway, autophagosome formation and maturation also requires PI3P and mediate clearance of cytosolic cargoes and damaged organelles labelled with autophagy receptors (*e.g.*, p62) upon their fusion with the endolysosomal system. **b)** Vps34 inhibition causes enlargement of Rab5-positive early endosomes which are enriched for endosomal adaptor APPL1 instead of PI3P-binding protein, EEA1 (not shown). Through pleiotropic effects on the endolysosomal system, Vps34 inhibition causes accumulation of proteins and lipids in MVEs and lysosomes, resulting in a fraction of them undergoing physical damage, as denoted by the enrichment of galectin-3 on p62- and ubiquitin-positive structures. While PI3P deficiency reduces ESCRT-dependent sorting of cargoes, including APP, into ILVs, local synthesis of ceramide by neutral sphingomyelinase 2 facilitates ILV sorting and secretion of poly-ubiquitinated proteins, APP-CTFs and BMP in exosomes, alleviating lysosomal burden. BMP represents a small fraction (< 5%) of phospholipids measured in total exosome derived from N2a cells treated with the Vps34 inhibitor, compared to more abundant phospholipids, such as phosphatidylcholine (PC) (~30%), phosphatidylserine and phosphatidylethanolamine (PE) plasmalogen (~20% each), PE and ether PC (~10% each), although we predict it may be significantly enriched on a subset of exosomes.

Figures



André M. Miranda, Zofia M. Lasiccka, Yimeng Xu, Jessi Neufeld, Sanjid Shahriar, Sabrina Simoes,
Robin B. Chan, Tiago Gil Oliveira, Scott A. Small, Gilbert Di Paolo

**Neuronal lysosomal dysfunction releases exosomes harboring APP C-terminal
fragments and unique lipid signatures**

Peer Review Electronic File

Nature Communications **9**(1):291 (2018)

DOI: 10.1038/s41467-017-02533-w

Editorial Note: Parts of this peer review file have been redacted as indicated to maintain confidentiality.

Reviewers' comments:

Reviewer #1 (Remarks to the Author):

This is an interesting and well done study, investigating the effects of vps34 on endolysosomal function, autophagy and EV release of APP CTFs. The authors find that VPS34 deficiency results in endolysosomal membrane damage, defects in autophagy and increased release of APP CTFs via neutral SMnase dependent EV subtypes which are enriched in BMP.

Also this work is highly relevant and the experiments are technically sound, I have several concerns:

Suppl Fig 1b: The pharmacological inhibition of VPS34 with VPS34iN increases levels of Beclin. Could this explain some of the results? Have the authors recapitulated key in vitro findings with VPS34 knockdown instead? I ask this question also in light of the partially different results obtained in the in vivo situation with cre mediated vps34 knockdown.

Fig 1a: It is difficult to appreciate the enlarged EEA1 endosomes in the VPS34IN1 condition. Would it be possible to find a better image?

Suppl 2b "The remaining degradation was blocked by Baf1" I assume that this conclusion should be based on the comparison of VPS34 inhibition versus VPS34 inhibition +Baf (or have I misunderstood remaining degradation). In that case, I would expect the statistics to compare these two conditions.

Suppl 2d "Gamma secr inhibitor extended APP CTF half-life relative to Cyclohexamide alone, confirming that g secr cleavage is a major pathway for clearance of APP CTFs": Fig 1d compared to 1c seems to show the opposite.

Authors claim that VPS34 inhibition causes decreased lysosomal degradation of APP CTFs. Do APP CTFs accumulate in lysosomes or ILVs during combined g-secretase+Baf treatment?

Fig 3c: could authors also quantify galectin 3/lamp/flot colocalisation or provide better images? they claim that damaged endolysosomes are not efficiently targeted to Lamp1 positive structures upon VPS34. This can not really be judged by the image provided

Fig 4,5, Suppl Fig 6: I think that a quantification of protein release with EVs should be done in all cases by calculating the ratio of protein in EV/lysate and normalize this to control conditions. Otherwise, it is hard to tell, whether an effect is based on differences in protein concentrations in the lysate and a statistical significance cannot be concluded from the histograms if fold changes in EVs are significant and also in lysates but a direct comparison of EV/lysate between 2 conditions could still be not significant. E.g., in Fig. 5 there is a 15 fold enrichment of CTFs in lysates and also in EVs upon Bafilomycin treatment, but there may be no net increase if you quantify EV/lysate.

Fig 6 Here, I am missing the GW4869 condition alone. GW4869 has many additional effects (other than just inhibition of SMnase dep. EV release). Thus, I am wondering, whether it would also inhibit the release of polyubiquitinated proteins if given alone (a finding, which would be contradictory to previous literature)

Fig 7dPurification of brain derived EVs is very controversially discussed. At least the purity of this preparation should be shown by WBs with different markers of potential microsomal contaminations. The same holds true for the cell culture experiments where I have been missing these negative controls (at least it should be shown in one experiment that the quality of the EV preparation is good enough). For the brain derived EVs it would be helpful to provide an EM picture.

Why is there no APP full length present in the brain derived EVs ? It should... also according to the authors own findings from in vitro derived EVs.

Line 438: an "l" is missing in chloroquine

Discussion: Authors should discuss their work in the context of a previous publication by Guix et al., Mol Neurodeg. 2017, which also addresses endolysosomal/autophagy pathways, APP processing, release of APP CTFs by EVs and Abeta generation

Reviewer #2 (Remarks to the Author):

In their paper, Di Paolo and collaborators have analyzed the effects of VPS34 inhibition on endolysosomal and autophagic functions in neuronal cell lines and primary neurons. The rationale evolved from the previous work of the group on the implication of a dysregulated PI3P pathway in AD as well as on the emerging evidence of endolysosomal dysfunctions in early stages of neurodegeneration diseases. VPS34 is a key kinase playing dual roles in endolysosomal trafficking and autophagy through its functional inclusion in distinct regulatory/scaffolding complexes. In the current work they mainly used pharmacological inhibition of VPS34 and report that inactivation of VPS34 strongly affect lipid metabolism resulting in the accumulation of in particular ceramide, sphingomyelin and BMP species accompanied with the promoted secretion of BMP- and ceramide-enriched extracellular vesicles (EVs). In addition, overall these EVs contain as well flotillins and APP (FL and in particular CTFs), while resulting in decreased levels of secreted Abeta. The authors demonstrate elegantly that the APP-CTF accumulation originates from decreased lysosomal degradation and these effects can be countered by inhibitors of sphingomyelinase unequivocally linking the observations to aberrant sphingomyelin metabolism. Finally, they recapitulate part of these findings in vivo using a cKO model for VPS34. Overall the data are of high quality and the strong integration of very good cell biology, with biochemistry and lipidomic profiling makes their story appealing and of potential strong importance. Throughout reading I encountered however some problems with the interpretation of the data which are outlined below is some more detail. Provided that the authors can address

these caveats, a revised manuscript might be considered for publication.

Major compulsory points that require more scrutiny:

There are two major messages in the story, VPS34 deficiency or inactivation triggers a ceramide-driven pathway that shunts APP-CTFs to a subpopulation of EVs and overall this reveals the existence of a homeostatic response that may alleviate the effects of lysosomal dysfunction by secretion of EVs.

My first concern is that while the endolysosomal defects are majorly addressed using a combination of high quality imaging and biochemistry, the story falls short on the fact that all data related to APP and APP-CTFs are only biochemical. Nevertheless, throughout the text strong correlates are made between APP-CTFs accumulation and the observed morphological aberrancies however without actually showing that APP-CTFs indeed accumulate in the same flotilin-/BMP-/ceramide- positive organelles. This part of the story should be significantly improved.

Secondly, I struggle with correlating the imaging data with the interpretations and proposed mechanisms. Upon VPS34 inhibition the authors demonstrate, using high resolution imaging, the appearance of LAMP1-negative, LC3-II negative, but p62-positive organelles that co-stain for ubiquitinated cargo, galectin-3, flotillin-2 (figs 2-3). From this, the authors conclude that VPS34 inhibition blocks initiation of autophagy. However, both p62 and LC3-II are early markers of autophagy initiation and progression: the fact that organelles are positive for p62 might indicate that autophagy is initiated (this would also go in line with the Beclin increase monitored in Suppl Fig1). Moreover, most of the interpretation also clearly points to a defect in lysosomal function (degradation) indicating that autophagosomes might form but cannot fuse with existing lamp1-positive lysosomes. This is in line with their overall conclusion that VPS34 inh and the observed effects on lipid accumulation and APP-CTF build up is strictly related to the role of VPS34 in endolysosomal sorting. In addition, because of the co-localization of Gal3 on the p62-positive organelles, the authors suggest that these are the 'dysfunctional' or damaged (gal3 positive) lysosomes, but strangely they do not contain bona fide lysosomal markers like LAMP proteins. In several images it is also clear that the p62-positive organelles are mostly close to existing LAMP-positive organelles indicating a defect in docking/fusion events. However in the few EM-pictures none such close encounter is seen: instead electron-dense organelles are found close to 'empty' MVBs. If the p62-positive organelles are not related to autophagy, is it possible that they represent the 'empty' MVBs observed by EM (and thus not the electron dense organelles)?

Surprisingly, the authors are not really evaluating the distribution of MVB markers, like some tetraspanins. In addition, they show co-localization of BMP with lysosomes in control cells but not in VPS34 inhibited cells. Maybe visualization of the accumulating lipids (ceramide and LBPA) in control vs VPS34 inh cells, in correlation with an extended set of MVB markers might better elucidate the identity of these organelles. An additional control might be to consider inhibition of the ESCRT pathway in conjunction with VPS34 inhibition as the authors mention that the ceramide-pathway to ILVs is ESCRT independent.

Finally, on page 9 (line 204) the authors hypothesize that the decrease in PI3P, as seen in LSD and following VPS34 inhibition might result in secondary lipid dysregulation. However this is not further discussed. Can the authors speculate how this mechanistically could work? Further, they focus on the most obvious lipids that are accumulating (ceramides, sphingomyelins, BMPs). However, in different cellular models, other lipid species are

significantly downregulated, notably storage lipids and its precursor PA. Others, like lyso-species are higher in EVs of N2A and in hippocampus but lower in EVs of primary neurons. Do the authors have an interpretation for these other changes?

More detailed remarks that should be addressed:

- On few occasions the authors make the strong statement that (early) endosomal enlargement is a 'key endosomal phenotype of AD'. I would be more cautious as these observations are limited to only a few studies. Nevertheless, in neurodegeneration one might indeed focus more on endo-lysosomal transport defects instead of autophagy: this is reviewed recently in Peric et al (*Acta Neuropathologica*, 2015) and might be considered to include as a reference. Related to this, it surprises me that the EE enlargement is so strong, given that the provided confocal images are less convincing. It would be stronger to support this with EM images of EE (given that EM is performed on these cells, this should be feasible to quantify).
- The authors measure in some cases APP-FL but mostly restrict the interpretation to APP-CTF. While for instance in fig 1E, FL is not altered, it increases as well on EVs of primary neurons (4b). Given the variability between observed in effects in different cell lines, it should be more logic to include systematically the CTF/FL ratio. Furthermore, to exclude defects in BACE1 processing, measurements of sAPPbeta should be included.
- Suppl Fig3: panel b and c are inverted in the legends.
- Fig. 4b: Ponceau staining shows equal amount of protein for EVs of control and VPS34 inh neurons. It might suggest that there is not an increase in the number of EVs released, but the released EVs contain more APP/CTF, flotillin etc. Please clarify.
- p12, line 271: the authors refer to fig 4e and suppl fig 5b to show that Cer levels were increased in EVs of N2a but slightly decreased in EVs of primary neurons. The correct figure panel is however fig 4c.
- p15. In their last part the authors recapitulate PI3P-dependent endolysosomal dysfunction in vivo through the analysis of VPS34 cKO mice. It might be informative for the reader to include in suppl data some evidence for a neurodegeneration phenotype in these mice.
- p15, line 362. In EVs isolated from brain not flotillins but Alix is significantly increased: this is a very surprising finding as in cell lines, Alix is mostly not affected but flotillins are increased in EVs following VPS34 inhibition. One could argue a contribution of non-neuronal cells, but this mean that in these cells flotillins are significantly less present to mask their upregulation in neuronal EVs. How to explain this discrepancy?
- p16, line 383: the authors generalize their conclusion ('EVs as part of a homeostatic response counteracting LDSs') too much. They demonstrate that VPS34 inh promotes secretion of a subtype of EVs and that this is related to lysosomal storage defects, not lysosomal storage diseases. The extrapolation to disease models need to be implemented to support this statement.
- p21, line 493-500: please include few references underscoring the link that is made to immune cells, DAMPs etc.

Reviewer #3 (Remarks to the Author):

This manuscript describes the biological effect of inhibition of VPS34, a class III PI 3-kinase regulating endosomal trafficking, on endosomal dysfunction and subsequent accumulation of APP CTF, other endosomal molecules, and their enhanced release in exosomes. The study incorporates comparison of murine neuronal cell line N2a and primary cultured mouse neurons, and detailed characterization of endosomal accumulation of several key markers by high-resolution microscopic imaging techniques. The in vitro findings are partly verified by in vivo study using conditional neuron-specific knockout of VPS34 in forebrain. The study is significant by finding a novel VPS34-dependent pathway of exosome secretion of APP-CTF after endocytic dysfunction, the identification of the new lipid BMP, and the identification of their dependence in sphingomyelin metabolism to ceramide synthesis as determined by GW4869 and myriocin. These findings would have biological implication in generalized exosome secretion mechanism after endocytic dysfunction in many disease conditions, and BMP has a potential for a specific marker for the extracellular vesicles reflecting the intracellular dysfunction of endosome machinery in the affected cells. The study, however, has many data, which are inconsistent among experimental settings and most of them are not well discussed. These have to be clearly addressed.

Major points:

1. There is no introductory description of what p62 expression means in this manuscript. P62 first appears on Fig. 2a (line 185), which is one of key molecules, without description. Please address this in the introduction.
2. Clearly describe and discuss why Beclin1 expression is specifically increased in VPS34IN1-treated group (Fig. S1b) instead of describing that this treatment "did not cause a general downregulation."
3. It is difficult to agree that the diameter of EEA1+ puncta is increased by VPS34IN1 treatment (Fig. 1a), although the reduction of its intensity is agreeable. Immuno-EM of EEA1+ cells will be more conclusive for the morphological analysis.
4. In Fig. 1b, the size of Rab5+ puncta appears to be increased by VPS34IN1 treatment, which is not mentioned in Fig. 1a. Please discuss.
5. The conclusion of the last sentence (line 132-133) is not well supported, since these data are not directly relevant to AD. This has to be rewritten.
6. In Fig. 1d, there is no obvious increase of APP-CTF or APP-CTFbeta fragment in the WB images. This has to be replaced with more representative images. Please also discuss why the effect of VPS34IN1 treatment on APP processing is more significant in N2a cells over primary cultured neurons.
7. The LC3 signal in Fig. 2a-b is almost invisible in all 6 panels. MAP2 signal is also very weak. Ub signal in Fig. 2c is also invisible. Figure 2 images should be replaced with more visually understandable images.
8. In Fig. 3, galectin-3 is a well-accepted marker of phagocytic myeloid cells, and it is rarely detected in neurons. The co-localization of galectin-3 and flotilin-2 in Fig. 3d is also invisible and their quantification is in question. Suggest to delete Fig. 3b-d.
9. In Fig. 4-7, there are WB images of proteins in the purified EV in primary neurons, N2a cells and VPS34 cKO mouse brains. Although the data are of high quality, there are several inconsistent findings, which are not well discussed to understand the differences. For example, Flotilin-1/2 expression is increased by VPS34IN1 treatment in the EV isolated from

primary neurons and N2a cells (Fig. 4b,d) but not in EV isolated from VPS34 cKO mouse brain (Fig. 7d). On the other hand, another EV marker ALIX expression increased by VPS34IN1 treatment in the EV isolated from primary neurons (Fig. 4b) and VPS34 cKO mouse brain (Fig. 7d) but not in EV isolated from N2a cells (Fig. 4d). This indicates that none of the tested EV markers show consistent increase by inhibition or deletion of VPS34, and suggest that the group of EV affected by VPS34 inhibition is highly dependent on the conditions although they are of neuronal origin. This should be clearly discussed.

10. In addition, the expression of full-length APP in the EV is different in these experiments. It is increased by VPS34IN1 treatment in the EV isolated from primary neurons (Fig. 4b) but not in EV isolated from N2a cells (Fig. 4d), and its expression in VPS34 cKO mouse brain is not shown. There is no clear explanation of these inconsistent findings or experimental approach.

11. As for p62 in EV, there are repetitive discussion of the existence of p62 in the EV after VPS34 inhibition in primary cultured neurons and N2a cells (Fig. 4b,d), which suggests the shuttling of dysfunctional endolysosomes to EV as p62-containing complex. However, p62 expression is not shown in the EV fraction isolated from VPS34 cKO mice (Fig. 7d). This is a key conclusive data and should be presented.

12. In Fig. 6b, treatment of cells with nSMase2 inhibitor GW4869 would suppress the total number of EV secreted to the media. Please clarify how much is the input of the EV for each sample.

13. This reviewer disagrees with the conclusion that Atg5 KO has no effect on the secretion of APP-CTF in the EV fraction. Supplementary Fig. 6d shows enhanced accumulation of APP-CTF in ATG5 KO N2a cells, which appears to be more than wildtype N2a cells (lane 1) and is further accumulated by VPS34IN1 treatment (lane 4). This clearly shows that ATG5 deletion inhibit autophagic function and enhances the secretion of APP-CTF in the EV fraction. The authors show the intensity as fold increase of untreated cells, but this is not the correct analysis of band intensity. The band intensity should be quantified on the same SDS-PAGE after loading the same amount of protein from different cell types. The data presentation and interpretation should be thoroughly revised.

14. The Supplementary Fig. 4c does not have the methods to understand how BMP is stained for imaging, and does not appear to be co-localized with LAMP-1. This description (line 213-215) should be revised or replace the data with more representative image.

15. In general, mono-ubiquitination is necessary for the sorting of proteins to ILV via ESCRT machinery, but the protein is deubiquitinated before the insertion into the ILVs. This study repeatedly shows poly-ubiquitinated molecules in the EV fraction (Fig. 4b, 6b, 7d), which is odd but may represent non-ESCRT machinery for the insertion of these molecules to ILVs. Please cite at least one reference reporting the existence of poly-ubiquitinated molecules in the ILVs or exosomes to substantiate the finding.

16. Line 277-278 says "EVs containing BMP can be unambiguously defined as bona fide exosomes". This should be toned down since later in the discussion BMP is described as a unique marker under specific conditions associated with endolysosomal dysfunction (line 471-473).

Minor comments:

1. In Fig. 1c image, please clarify if the CatD refers to only processed CatD or both CatD and proCatD.

Response to reviewers' comments:

Reviewer #1 (Remarks to the Author):

This is an interesting and well done study, investigating the effects of vps34 on endolysosomal function, autophagy and EV release of APP CTFs.

We thank this reviewer for his/her positive comments.

The authors find that VPS34 deficiency results in endolysosomal membrane damage, defects in autophagy and increased release of APP CTFs via neutral SMnase dependent EV subtypes which are enriched in BMP.

Also, this work is highly relevant and the experiments are technically sound, I have several concerns:

1. Suppl Fig 1b: The pharmacological inhibition of VPS34 with VPS34iN increases levels of Beclin. Could this explain some of the results? Have the authors recapitulated key in vitro findings with VPS34 knockdown instead? I ask this question also in light of the partially different results obtained in the in vivo situation with cre mediated vps34 knockdown.

We thank this reviewer for raising this important question. We believe that the 50% increase in Beclin 1 levels observed upon VPS34iN1 treatment *in vitro* is not responsible for the observed phenotypes based on two new lines of evidence: first, conditionally knocking out *Pik3c3/Vps34* in neurons causes a downregulation of Beclin 1 in mouse hippocampi (see revised Figure 7b, with new Beclin 1 immunoblot performed on the same hippocampal extracts/blots) and yet recapitulates the main findings observed *in vitro* using VPS34iN1, including aberrant sphingolipid metabolism and accumulation of p62, poly-ubiquitinated proteins and APP-CTFs. Additionally, brain exosomes from the KO mice also exhibit higher levels of APP-CTFs and the lipid BMP, based on our new lipidomics results (see revised Figure 7g), consistent with the increase we have observed in exosomes produced by VPS34iN1-treated neurons or N2a cells. Second, we have conducted new experiments showing that lentiviral expression of Cre recombinase in *Pik3c3^{fllox/fllox}* primary cortical neurons also recapitulates some of the key phenotypes observed in VPS34iN1-treated neurons, including accumulation of p62, as seen by Western blotting and immunostaining; co-localization of ubiquitin and p62 and, also importantly, recruitment of galectin-3 to p62-positive structures. We have now added these new data in revised Supplementary Figures 3 and 4 and discuss them on page 9 (lines 191-194) and page 10 (line 228-230). Importantly, we show below that Cre-mediated *Vps34* ablation in cultured neurons downregulates Beclin 1 levels (n=2) (Figure 1 for Referees) similarly to what we have previously reported in *Pik3c3* KO MEFs (Devereaux et al. 2013). We now comment on this important point in the discussion from the revised MS, on page 18 (lines 419-422).

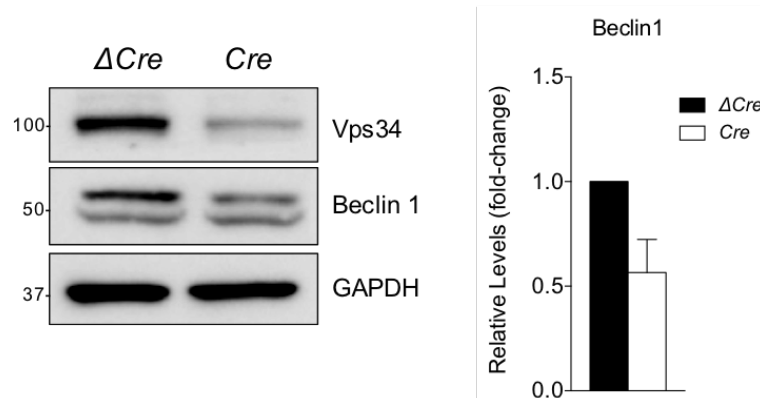


Figure 1. Cre-mediated VPS34 knock-out causes downregulation of Beclin1. Primary neurons derived from *pik3c3^{fllox/fllox}* mice were infected with ΔCre or *Cre* lentivirus at 7 days *in vitro* and processed for western blot analysis 8 days post-infection. Bar graph indicates average protein levels, normalized to ΔCre -infected neurons (mean \pm range, N=2 biological replicates). For quantification of Vps34 knock-out efficiency, please see Supplementary Figure 3d.

2. Fig 1a: It is difficult to appreciate the enlarged EEA1 endosomes in the VPS34IN1 condition. Would it be possible to find a better image?

We have replaced the original pictures with an alternate set of pictures that better show the enlarged EEA1-positive endosomes in revised Figure 1a.

3. Suppl 2b "The remaining degradation was blocked by Baf1" I assume that this conclusion should be based on the comparison of VPS34 inhibition versus VPS34 inhibition +Baf (or have I misunderstood remaining degradation). In that case, I would expect the statistics to compare these two conditions.

We apologize for this omission and thank the reviewer for pointing it out. We have now added the statistical analysis for the direct comparison between Vps34 inhibition and combined treatment with BafA1 at 4 hr post-treatment, with a $p < 0.01$ after a one-way ANOVA using Holm-Sidak's post-test for multiple comparisons. Supplementary Figure 2b has been revised accordingly.

4. Suppl 2d "Gamma secr inhibitor extended APP CTF halflife relative to Cyclohexamide alone, confirming that g secr cleavage is a major pathway for clearance of APP CTFs": Fig 1d compared to 1c seems to show the opposite.

We believe that this reviewer may have been misled by the fact that the treatment duration shown in the x axis for APP-CTF levels is not the same for Supplementary Figure 2c and Figure 2d. Additionally, the y axes are different. With this in mind, we believe that our original interpretation was correct, namely that the γ -inhibitor XXI prolongs the half-life of APP-CTFs in the presence or absence of VPS34IN1. We hope the reviewer now agrees with our interpretation.

5. Authors claim that VPS34 inhibition causes decreased lysosomal degradation of APP CTFs. Do APP CTFs accumulate in lysosomes or ILVs during combined γ -secretase+Baf treatment?

We have previously reported that γ -secretase inhibition causes an increase in APP staining (using anti-cytoplasmic antibodies) throughout the cell, particularly in the endolysosomal system. We invite this reviewer to examine Figure 3 from our previous manuscript (Morel et al. 2013). Given this excess of intracellular APP-CTF observed with γ -secretase inhibition, we do not expect a discernable increase in APP-CTFs with the combined treatments (γ -secretase inhibition + BafA1), in line with the results shown in Supplementary Figure 2 suggesting that γ -secretase inhibition dramatically impairs APP-CTF clearance. However, given our results indicating that BafA1 treatment alone causes efficient sorting of APP-CTFs to exosomes, we hypothesize that APP-CTF accumulation in lysosomes or ILVs might be very transient, prior to release via exocytosis of multivesicular endolysosomal compartments. While it is theoretically an excellent idea to test how much APP-CTFs can accumulate in cells upon combined BafA1 treatment/ γ -secretase inhibition, we feel that it may be a bit tangential to this manuscript, which focuses primarily on Vps34 function. We hope the reviewer agrees with this view.

6. Fig 3c: could authors also quantify galectin 3/lamp/flot colocalisation or provide better images? They claim that damaged endolysosomes are not efficiently targeted to Lamp1 pos structures upon VSP34. This cannot really be judged by the image provided.

Following the reviewer's recommendation, we have replaced the original p62/Galectin-3/LAMP-1 confocal images with better images with slightly enhanced contrast. We have also added a linescan intensity analysis of a p62/galectin-3 structure in the vicinity of LAMP-1-positive membrane where it is obvious that p62/galectin-3 intensity lines peak outside of LAMP-1 intensity profile (see revised Figure 3c). In addition, we have included for the benefit of this reviewer four additional examples from conventional confocal microscopy showing that p62/galectin-3 puncta are largely excluded from the lumen of LAMP-1-positive structures (see Figure 2a for Referees). To support these conclusions, we have also included a distribution/linescan intensity profile from the co-staining of p62/flotillin-2/LAMP-1 after acquiring images with the Airyscan confocal microscope (see Figure 2b for Referees). Please note we also show that p62-positive structures are excluded from the lumen of LAMP-1-positive compartments after VPS34IN1 treatment in revised Figure 2b, even in the presence of BafA1, while these p62-positive structures accumulate luminally in LAMP-1 positive structures after BafA1-alone treatment).

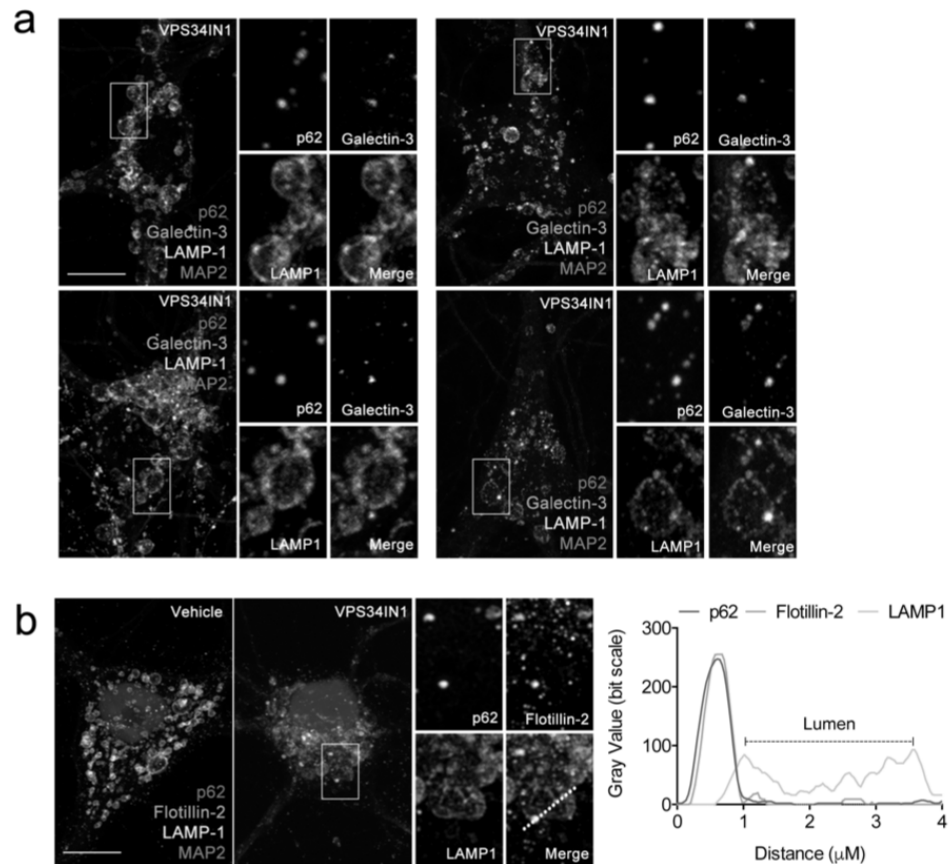


Figure 2. Damaged endolysosomes are not efficiently incorporated in the lumen of LAMP-1-positive compartments. a) Additional representative pictures of cortical neurons treated with VPS34IN1 at 3uM for 24 hr and immunostained for MAP2, p62, galectin-3 and LAMP-1. Regular confocal insets highlight p62/Galectin-3 positive structures repeatedly seen in the periphery, but not lumen, of LAMP-1-positive compartments. **b)** Representative pictures of cortical neurons treated with vehicle or VPS34IN1 at 3uM for 24 hr and immunostained for MAP2, p62, flotillin-2 and LAMP-1. Airyscan insets highlight exclusion of p62/flotillin-2 structures from LAMP-1 lumen. Right panel, line intensity scan of P62/flotillin-2 structure and adjacent LAMP-1 compartment. Scale bar 10 μm .

7. Fig 4,5, Suppl Fig 6: I think that a quantification of protein release with EVs should be done in all cases by calculating the ratio of protein in EV/lysate and normalize this to control conditions. Otherwise, it is hard to tell, whether an effect is based on differences in protein concentrations in the lysate and a statistical significance cannot be concluded from the histograms if fold changes in EVs are significant and also in lysates but a direct comparison of EV/lysate between 2 conditions could still be not significant. E.g., in Fig. 5 there is a 15 fold enrichment of CTFs in lysates and also in EVs upon Bafilomycin treatment, but there may be no net increase if you quantify EV/lysate.

We have followed the reviewer's excellent suggestion. In addition to the previous quantification of protein levels in EVs, we have added bar graphs showing the EV/Lysate ratio for full length APP (FL-APP) and APP-CTFs. Please see updated versions of Figures 4, 5, and 6 as well as Supplementary Figure 7.

8. *Fig 6 Here, I am missing the GW4869 condition alone. GW4869 has many additional effects (other than just inhibition of SMnase dep. EV release). Thus, I am wondering, whether it would also inhibit the release of polyubiquitinated proteins if given alone (a finding, which would be contradictory to previous literature)*

This reviewer is raising a very good point. Given that in our cell types analyzed, GW4869 dramatically decreases exosome release based on the loss of Alix in the EV preparation, we can safely state that the drug causes a decrease in polyubiquitinated proteins associated with EVs. However, we cannot conclude that the ubiquitin signals (which stems from a range of mono-, multi- and polyubiquitinated proteins with different types of K links) serve as sorting signals for delivery into ILVs/exosomes via the canonical ESCRT pathway initiated by ESCRT0/Hrs. In fact, VPS34 inhibition has been shown by our lab (Morel et al. 2013) and many others before us to block the ESCRT pathway, which relies on Vps34's product phosphatidylinositol-3-phosphate (Schink et al. 2013). Therefore, while we do not believe our results contradict the literature, they certainly suggest that many ubiquitinated proteins (some of which could be cytosolic proteins) are sorted into ILVs/exosomes in a PI3P- and ESCRT-independent fashion. This is also consistent with other reports in the literature showing that ubiquitinated proteins can be sorted into ILVs and exosomes (Pisitkun et al. 2004; Huebner et al. 2016).

9. *Fig 7d Purification of brain derived EVs is very controversially discussed. At least the purity of this preparation should be shown by WBs with different markers of potential microsomal contaminations. The same holds true for the cell culture experiments where I have been missing these negative controls (at least it should be shown in one experiment that the quality of the EV preparation is good enough). For the brain derived EVs it would be helpful to provide an EM picture.*

This is a valid concern and we thank this reviewer for raising it. The protocols used for EV purification both *in vivo* and *in vitro* have been extensively validated (Perez-Gonzalez et al. 2012; Kowal et al. 2016; Sharples et al. 2008; Théry et al. 2006), although the consensus is that exosomes obtained from cultured cells are typically purer than those obtained from tissue, for obvious reasons. To address this reviewer's concern, we confirmed the quality of the EV preparation by showing absence of late endosome/lysosomal marker LAMP1, early endosome marker APPL1 and cytosolic protein GAPDH in EVs relatively to cell lysates (Supplementary Figure 5a). In addition, the proteins quantified in EVs (ALIX, flotillin-2 and APP-CTF) were found to be only enriched on the 100,000g pellet (100K) pellet and not the 2K or 10K pellets, which is diagnostic of small EVs (Kowal et al. 2016). Of note, we detected residual signal for flotillin-2 in 10K pellet but the presence of such vesicles is eliminated through filtration using 0.22µm syringe filters as performed for all experiments shown in the manuscript (see Methods). This finding further suggests that the size of the EVs collected is that of typical exosomes (<200 nm). We also note that BMP is enriched on exosomes obtained both *in vitro* and *in vivo* after Vps34 inhibition/ablation (see new data in revised Figure 7g and Supplementary Figure 8d). As explained in our manuscript, the enrichment of BMP, an ILV lipid, on EVs, lends support to the notion that the vesicles we have purified are largely exosomes.

Regarding EV purification from mice, we now include two EM pictures of EVs in revised Supplementary Figure 8 as well as the biochemical characterization of various protein markers from fractions collected after ultracentrifugation of EVs on an Optiprep (iodixanol) gradient. We found that ALIX and flotillin-1 were enriched in fractions 4-7, namely in the range of 1.074-

1.108 g/mL, as previously described in (Greening et al. 2015; Klingeborn et al. 2017). Moreover, Golgi and ER markers GM130 and Calnexin, resp., were enriched in fraction 8-10 and were thus not used for further applications (see revised Supplementary Figure 8b,c,d). We have now updated the Methods section on page 28 (lines 661-693) to summarize our additional efforts to vet the exosome purification protocol.

10. Why is there no APP full length present in the brain derived EVs ? It should... also according to the authors own findings from in vitro derived EVs.

We [redacted] have not been able to detect significant amounts of FL-APP in 15-20ug preparations of brain derived EVs, not only in the mice tested for the purpose of this manuscript but also other animal lines only expressing endogenous wild-type APP. Please note that the APP-CTF/FL-APP ratio is reportedly increased in EVs (Perez-Gonzalez et al. 2012). For the purpose of this revision, we show that EV-associated APP-CTF/FL-APP ratio is increased comparatively to cellular lysates using N2a cells transiently transfected with APP-GFP (see Figure 3a for Referees). Moreover, we show that EVs are enriched for mature, glycosylated FL-APP as noted in the band shift to heavier weight in EV preparation in comparison to lysates, both in primary neurons and in N2a cells (see Figure 3b for Referees). Not only this suggests a de-enrichment of FL-APP in EV preparations, but it also suggests that the APP species detected are of endosomal origin, requiring FL-APP maturation in the Golgi, transport to the plasma membrane via secretory pathway and internalization and sorting into ILVs before release on EVs (Haass et al. 2012).

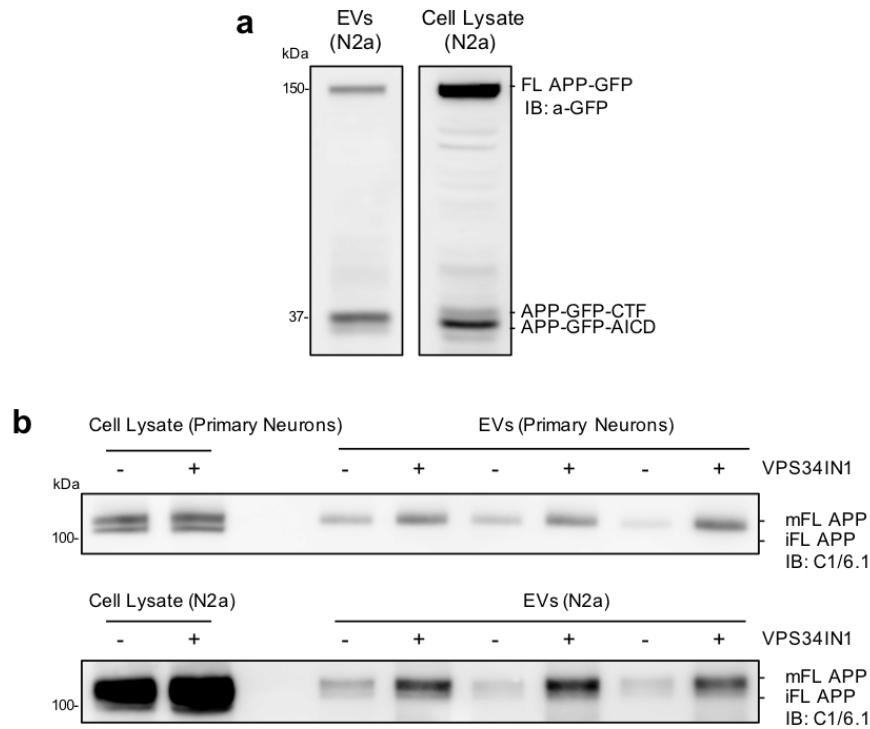


Figure 3. Enrichment of APP-CTF/FL APP ratio in EVs. **a)** N2a cells were transiently transfected with APP-GFP for 24 hours and cell culture media was processed for purification of EVs. APP-GFP-AICD: APP-GFP APP Intracellular Domain (Morel et al. 2013). **b)** Comparison of FL APP migration pattern in SDS-Page between cell lysates and EVs purified from primary cortical neurons or N2a cells treated with VPS34IN1 at 3uM and 1uM for 24hr, respectively.

11. Line 438: an "l" is missing in chloroquine

We thank the reviewer for noting this typo, which has now been corrected.

12. Discussion: Authors should discuss their work in the context of a previous publication by Guix et al., Mol Neurodegen. 2017, which also addresses endolysosomal/autophagy pathways, APP processing, release of APP CTFs by EVs and Abeta generation.

We thank the reviewer for suggesting the inclusion of this paper, which is now cited and discussed on page 20 (lines 476-482).

Reviewer #2 (Remarks to the Author):

In their paper, Di Paolo and collaborators have analyzed the effects of VPS34 inhibition on endolysosomal and autophagic functions in neuronal cell lines and primary neurons. The rationale evolved from the previous work of the group on the implication of a dysregulated PI3P pathway in AD as well as on the emerging evidence of endolysosomal dysfunctions in early stages of neurodegeneration diseases. VPS34 is a key kinase playing dual roles in endolysosomal trafficking and autophagy through its functional inclusion in distinct regulatory/scaffolding complexes. In the current work they mainly used pharmacological inhibition of VPS34 and report that inactivation of VPS34 strongly affect lipid metabolism resulting in the accumulation of in particular ceramide, sphingomyelin and BMP species accompanied with the promoted secretion of BMP- and ceramide-enriched extracellular vesicles (EVs). In addition, overall these EVs contain as well flotillins and APP (FL and in particular CTFs), while resulting in decreased levels of secreted Abeta. The authors demonstrate elegantly that the APP-CTF accumulation originates from decreased lysosomal degradation and these effects can be countered by inhibitors of sphingomyelinase unequivocally linking the observations to aberrant sphingomyelin metabolism. Finally, they recapitulate part of these findings in vivo using a cKO model for VPS34. Overall the data are of high quality and the strong integration of very good cell biology, with biochemistry and lipidomic profiling makes their story appealing and of potential strong importance. Throughout reading I encountered however some problems with the interpretation of the data which are outlined below in some more detail. Provided that the authors can address these caveats, a revised manuscript might be considered for publication.

Major compulsory points that require more scrutiny:

1. There are two major messages in the story, VPS34 deficiency or inactivation triggers a ceramide-driven pathway that shunts APP-CTFs to a subpopulation of EVs and overall this reveals the existence of a homeostatic response that may alleviate the effects of lysosomal dysfunction by secretion of EVs. My first concern is that while the endolysosomal defects are majorly addressed using a combination of high quality imaging and biochemistry, the story falls short on the fact that all data related to APP and APP-CTFs are only biochemical. Nevertheless, throughout the text strong correlates are made between APP-CTFs accumulation and the observed morphological aberrancies however without actually showing that APP-CTFs indeed accumulate in the same flotillin/BMP-/ceramide- positive organelles. This part of the story should be significantly improved.

We are very thankful of the overall positive comments regarding our work. We believe in the correlation of the APP-CTF biochemical data and lipid analysis as samples for protein quantification and lipid quantification have been processed in parallel in order for us to be able to analyze the same exosomal vesicle population.

In an attempt to address this concern, we have immunostained cortical neurons treated with vehicle or VPS34IN1 with antibodies to APP C-terminus (C1/6.1) and p62 (see revised Supplementary Figure 4d). We have focused on p62 because it shows the most robust staining pattern upon Vps34 inhibition and the antibody is of distinct origin (Guinea pig vs mouse, while anti-BMP and anti-flotillin-2 antibodies used in this manuscript are both of mouse origin). In line with our previous manuscript (Morel et al. 2013), few APP/APP-CTF are seen as distinct puncta in the somatodendritic compartment of cortical neurons. Importantly, we found little to no co-localization between APP/APP-CTFs and p62, although some proximity was seen between these two proteins after Vps34 inhibition. We speculate that the increased secretion of APP-CTFs in the form of exosomes is precisely what prevents their dramatic accumulation intracellularly.

2. Secondly, I struggle with correlating the imaging data with the interpretations and proposed mechanisms. Upon VPS34 inhibition the authors demonstrate, using high resolution imaging, the appearance of LAMP1-negative, LC3-II negative, but p62-positive organelles that co-stain for

ubiquitinated cargo, galectin-3, flotillin-2 (figs 2-3). From this, the authors conclude that VPS34 inhibition blocks initiation of autophagy. However, both p62 and LC3-II are early markers of autophagy initiation and progression: the fact that organelles are positive for p62 might indicate that autophagy is initiated (this would also go in line with the Beclin increase monitored in Suppl Fig1). Moreover, most of the interpretation also clearly points to a defect in lysosomal function (degradation) indicating that autophagosomes might form but cannot fuse with existing lamp1-positive lysosomes. This is in line with their overall conclusion that VPS34 inh and the observed effects on lipid accumulation and APP-CTF build up is strictly related to the role of VPS34 in endolysosomal sorting.

There is a large body of evidence indicating that phosphatidylinositol-3-phosphate (PI3P), the product of Vps34, is critical for autophagy initiation (Dall'Armi et al. 2013). p62 serves as an autophagy adaptor binding ubiquitinated cargoes during functional autophagy and it is known to both accumulate and aggregate when autophagy initiation (*i.e.*, autophagosome formation) is blocked (e.g., after silencing ATG9 and FIP200 (Kishi-Itakura et al. 2014)). Given that our results from Figure 2 and Supplementary Figure 3b suggest that Vps34 inhibition prevents formation of LC3-positive puncta (by immunofluorescence) and LC3 lipidation (by Western blot analysis), we have updated the manuscript to clarify that Vps34 impairment specifically blocks autophagy through inhibition of autophagosome formation (page 8, line 172-173). Moreover, we believe this phenotype is independent of Beclin 1 increase because our new data show that p62 accumulation and co-localization with ubiquitin or galectin-3 is recapitulated in Vps34 KO primary cortical cultures, where Beclin 1 protein levels are decreased (please see updated Supplementary Figure 3d,e, Supplementary Figure 5 and our response to reviewer 1's point #1).

3. In addition, because of the co-localization of Gal3 on the p62-positive organelles, the authors suggest that these are the 'dysfunctional' or damaged (gal3 positive) lysosomes, but strangely they do not contain bona fide lysosomal markers like LAMP proteins. In several images, it is also clear that the p62-positive organelles are mostly close to existing LAMP-positive organelles indicating a defect in docking/fusion events. However, in the few EM-pictures none such close encounter is seen: instead electron-dense organelles are found close to 'empty' MVBs. If the p62-positive organelles are not related to autophagy, is it possible that they represent the 'empty' MVBs observed by EM (and thus not the electron dense organelles)?

We thank the reviewer for highlighting this critical point and suggesting an alternate interpretation for our data. In general, we fully agree that the low colocalization between galectin-3 and LAMPs in VPS34IN1-treated neurons is inconsistent with lysosomal damage *per se*. In fact, proximity of galectin-3 to LAMPs rather than luminal staining of galectin-3 suggests that other compartments, likely early-to-late endosomes, may be the damaged entities. For that reason, the term lysophagy (*i.e.*, the autophagy of lysosomes) we have used in the text may therefore be inappropriate, although we note that Maejima *et al.* also show proximity to but not luminal sorting of galectin-3 into LAMP-1 compartments upon lysosome rupture in their seminal lysophagy paper (Maejima et al. 2013). It is also possible that upon rupture, these lysosomal structures may lose common membrane organelle markers, like LAMPs, perhaps via degradation by cytosolic proteases. In our experimental setting, however, we believe that the damaged organelles are of endosomal origin, as these are also flotillin-2 positive. As a result of this helpful and fair criticism, we have now rephrased the text and specifically refer to endolysosomal membrane damage, which is more accurate than "lysosomal damage".

Regarding the second part of the comment, we speculate that the p62-positive structures are the electron-dense membrane enclosed vesicles because of their appearance only after VPS34IN1 treatment and much smaller size than the 'empty' MVBs. We also suggest the empty MVBs to be LAMP1-positive given these are also enlarged upon VPS34IN1 treatment in confocal images (Figure 3c).

4. Surprisingly, the authors are not really evaluating the distribution of MVB markers, like some tetraspanins.

To address this concern, we have transiently transfected N2a cells with CD63-GFP and collected EVs after treatment with VPS34IN1 (see Figure 4 for Referees). We also took this opportunity to analyze the abundance of ESCRT0 and ESCRT1 proteins Hrs and Tsg101, resp. We did not observe any significant increase in any of the markers tested, while the experiment was internally controlled with the enrichment of APP-CTFs after Vps34 inhibition. We believe that secreted tetraspanin levels may reflect the total number of EVs and therefore does not exclude the enrichment of other EV-associated proteins per vesicle, such as flotillins and APP-CTFs. We now briefly mention these results on page 12 (Line 265-268).

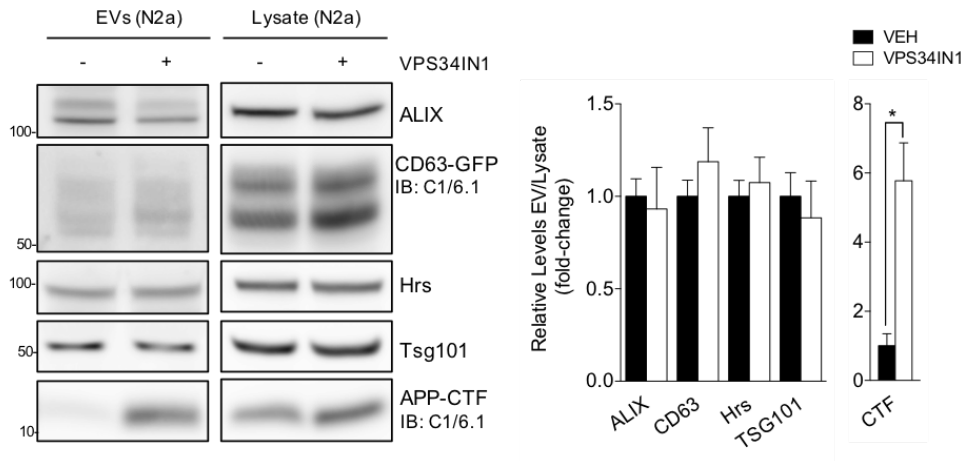


Figure 4. EV secretion of multivesicular body (MVB)-associated markers. a) Western blot analysis of EVs collected from N2a cells transiently transfected with CD63-GFP, treated with vehicle or VPS34IN1 at 1uM for 24hr. EV protein levels were normalized to cell lysate protein concentration and cellular levels of each protein. Bar graph indicates relative protein levels normalized to vehicle (mean \pm SEM, N=3 biological replicates).

5. In addition, they show co-localization of BMP with lysosomes in control cells but not in VPS34 inhibited cells. Maybe visualization of the accumulating lipids (ceramide and LBPA) in control vs VPS34 inh cells, in correlation with an extended set of MVB markers might better elucidate the identity of these organelles.

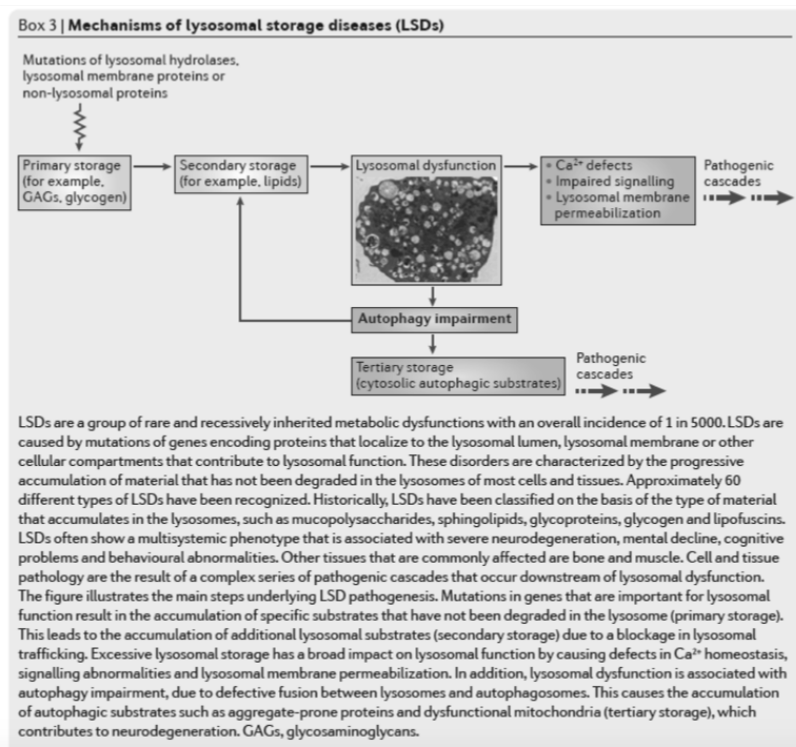
This is a great point and we have now addressed this by conducting immunofluorescence experiments in N2a cells treated with VPS34IN1. We did not observe major differences in anti-BMP stainings between VPS34IN1- and vehicle-treated cells, consistent with the lack of major alterations of BMP levels in cells (as opposed to the dramatic changes observed in exosomes). As a positive control, we found that p62 puncta accumulate in the proximity of LAMP-1 positive compartments in VPS34IN1-treated N2a cells, similar to what we have observed in primary cortical neurons. We show the data in revised Supplementary Figure 4c and modified the text accordingly on page 10 (lines 208-210). Of note, we have not been able to successfully stain ceramide with an antibody, despite multiple attempts in the laboratory.

6. *An additional control might be to consider inhibition of the ESCRT pathway in conjunction with VPS34 inhibition as the authors mention that the ceramide-pathway to ILVs is ESCRT independent.*

This is an interesting suggestion from the reviewer. However, we and others have shown conclusively that Vps34-derived PI3P is critical to initiate the ESCRT pathway, simply because the early component of the ESCRT pathway, ESCRT0/Hrs, is recruited to endosomes precisely via interaction of its FYVE domain with PI3P. While we invite this reviewer to see the supporting evidence in our previous manuscript Morel *et al.* (e.g., Suppl. Figures S5, S6 and S7), there is also seminal work from Stenmark, Emr *et al.* that have shown this in multiple studies (Raiborg *et al.* 2013; Schink *et al.* 2013). Additionally, we have included in the text (page 20, lines 472-475) new data showing that a mutant of APP-GFP lacking all 5 ubiquitination sites in its C-terminus (via lysines-to-arginine mutations) (see (Williamson *et al.* 2017) for characterization of this mutant) is sorted into exosomes as efficiently as APP WT when N2a cells are treated with VPS34IN1, further indicating that Vps34 inhibition triggers an exosome release pathway that is independent of ESCRT.

7. *Finally, on page 9 (line 204) the authors hypothesize that the decrease in PI3P, as seen in LSD and following VPS34 inhibition might result in secondary lipid dysregulation. However, this is not further discussed. Can the authors speculate how this mechanistically could work?*

This is a fantastic question and we could have done a better job explaining our thoughts in the manuscript. To answer it, we invite this reviewer to check Box 3 from a beautifully-written review by Settembre, Ballabio and colleagues (Settembre *et al.* 2013). In essence, it is well established that mutations in lysosomal enzymes, including lipases like glucocerebrosidase, cause enzyme substrate accumulation, which, in turn, perturb the homeostasis of lysosomes through various mechanisms (ion dyshomeostasis, changes in lysosomal membrane composition, alteration of trafficking pathways and delivery of hydrolases to lysosomes, etc...). In the case of Vps34 inhibition, we are probably dealing with pleiotropic effects, ranging from retromer mistrafficking and alteration of mannose-6-phosphate receptor transport to aberrant hydrolase maturation (see for instance Figure 1c for Cathepsin D). In light of this comment, we elaborate on this point on page 18 (line 416-431) of the revised manuscript.



8. Further, they focus on the most obvious lipids that are accumulating (ceramides, sphingomyelins, BMPs). However, in different cellular models, other lipid species are significantly downregulated, notably storage lipids and its precursor PA. Others, like lyso-species are higher in EVs of N2A and in hippocampus but lower in EVs of primary neurons. Do the authors have an interpretation for these other changes?

This is a great question from the reviewer and the short answer is "no", unfortunately. We have set up our lipidomics core several years ago and acquired a wealth of data in various settings, publishing many research papers. When analyzing about 30 lipid subclasses and hundreds of lipid species by LCMS, we typically find many that change. Complicating the interpretation of the data, each lipid is often regulated by multiple enzymes. Our strategy to gain more insights into the physiological and pathophysiological significance of lipid changes is to focus on pathways that can be easily manipulated by pharmacological or molecular genetic tools (although this step requires prioritization of lipid hits to pursue) and determine whether those manipulations alter functional outcomes. We also increasingly combine lipidomics with transcriptomic analyses, in the hope that mRNA changes may inform us on specific enzymes or pathways to further test or characterize.

9. More detailed remarks that should be addressed:

On few occasions the authors make the strong statement that (early) endosomal enlargement is a 'key endosomal phenotype of AD'. I would be more cautious as these observations are limited to only a few studies. Nevertheless, in neurodegeneration one might indeed focus more on endo-lysosomal

transport defects instead of autophagy: this is reviewed recently in Peric et al (Acta Neuropathologica, 2015) and might be considered to include as a reference.

We agree with the reviewer and thank him/her for this suggestion. We have revised our conclusion from Result section number 1 on page 6 (line 125-126). We have also added and discussed the Peric reference in the text on page 17 (line 400).

10. Related to this, it surprises me that the EE enlargement is so strong, given that the provided confocal images are less convincing. It would be stronger to support this with EM images of EE (given that EM is performed on these cells, this should be feasible to quantify).

In response to this comment and reviewer 1's point #2, we have included better pictures of the EEA1 staining in revised Fig. 1a. We hope that the reviewer can better appreciate the enlargement of the endosomal structures. Given that the EEA1-positive endosomal enlargement has been reported in several cell types both at the light and electron microscopic level (Morel et al. 2013; Devereaux et al. 2013; Futter et al. 2001; Jiang et al. 2010; Cossec et al. 2012), we felt that it was unnecessary to perform a time consuming morphometric analysis of ultrastructural analysis, and rather focus on strengthening the most novel aspects of our paper. We hope this reviewer will be clement enough to accept our explanation.

11. The authors measure in some cases APP-FL but mostly restrict the interpretation to APP-CTF. While for instance in fig 1E, FL is not altered, it increases as well on EVs of primary neurons (4b). Given the variability between observed in effects in different cell lines, it should be more logic to include systematically the CTF/FL ratio. Furthermore, to exclude defects in BACE1 processing, measurements of sAPPbeta should be included.

This is an excellent suggestion, partially brought up by reviewer 1 in point #7. We now provide the EV/Lysate ratios for FL-APP and APP-CTFs in Figures 4, 5, 6 and Supplementary Figure 6. Regarding the APP/APP-CTF ratio, we have shown in response to reviewer 1's point #10 that APP-CTFs/FL-APP is increased in EVs.

Regarding the contribution of BACE1 processing to altered APP metabolism caused by Vps34 inhibition, we were not able to detect sAPP β levels in the media of primary neurons. As a reminder, we performed all of our experiments studying endogenous, wild-type murine APP for which sAPP β levels are particularly challenging to detect, comparatively to studies overexpressing human WT or mutated APP. Nevertheless, we believe that an increase in BACE1-mediated processing of APP is unlikely to account for the APP-CTF increase observed upon Vps34 inhibition, given that levels of A β 40 and A β 42 are both decreased. Additionally, both APP-CTF α and APP-CTF β are similarly increased upon Vps34 inhibition, suggesting impaired clearance/processing downstream of α/β -secretase cleavage instead.

12. Suppl Fig3: panel b and c are inverted in the legends.

We thank the reviewer for noting this mistake, which has now been corrected.

13. Fig. 4b: Ponceau staining shows equal amount of protein for EVs of control and VPS34 inh neurons. It might suggest that there is not an increase in the number of EVs released, but the released EVs contain more APP/CTF, flotillin etc. Please clarify.

This is an excellent point raised by the reviewer. To precisely determine the number and amount of exosomes released, we would have to resort to the use of a nanotracker instrument as in (Guix et al. 2017) which unfortunately is not available to us at Columbia University. To the best of our knowledge, we believe that the EV number is not significantly affected after Vps34 inhibition, particularly in N2a cells given the similar levels of EV-associated ALIX, Tsg101, Hrs and CD63-GFP. As mentioned in response to reviewer 2's point #4, we still believe this does not exclude the enrichment of proteins such as flotillins and APP-CTFs in EVs, likely as a subpopulation of these secreted vesicles. We have clarified this ambiguity in the revised manuscript on page 12 (Line 265-268).

14. - p12, line 271: the authors refer to fig 4e and suppl fig 5b to show that Cer levels were increased in EVs of N2a but slightly decreased in EVs of primary neurons. The correct figure panel is however fig 4c.

We thank again the reviewer for noting this mistake, which has now been corrected.

15. - p15. In their last part the authors recapitulate PI3P-dependent endolysosomal dysfunction *in vivo* through the analysis of VPS34 cKO mice. It might be informative for the reader to include in suppl data some evidence for a neurodegeneration phenotype in these mice.

This is a great suggestion. We have collected data on this topic, which we had originally intended for another manuscript. However, we agree it is important to document the extent of neurodegeneration in the mouse model we have used in this manuscript. We have now added new data in revised Figure 7a and Supplementary Figure 8a showing that there is no significant neuronal death at 2 months of age based on MAP2 staining of areas where *CAMKIIa-Cre* expression occurs (e.g. CA1 in the hippocampus) (Wang et al. 2011). Instead, massive loss of neurons is obvious at 3 months of age in the *Vps34* cKO mouse where a dramatic loss of MAP2 immunoreactivity is detected in both hippocampus and cortex, as well as thinning of cortical layers (Supplementary Figure 8a), as also reported by others characterizing the same mice (Wang et al. 2011). We discuss the data on page 15 (line 350-354) in the revised manuscript.

16. - p15, line 362. In EVs isolated from brain not flotillins but Alix is significantly increased: this is a very surprising finding as in cell lines, Alix is mostly not affected but flotillins are increased in EVs following VPS34 inhibition. One could argue a contribution of non-neuronal cells, but this mean that in these cells flotillins are significantly less present to mask their upregulation in neuronal EVs. How to explain this discrepancy?

This is a sharp observation from the reviewer and we have no clear explanation for it, although we can speculate. As pointed out by the reviewer, the EVs purified from the brain reflect the contribution of many cell types, including neurons, astrocytes, microglia and potentially also oligodendrocytes. While we selectively ablate *Vps34* from pyramidal neurons with *CamkIIa-Cre* and can safely conclude that changes in brain EVs by definition originate from those neurons, EV composition changes can also reflect contributions from these other cell types. Additionally, while EVs produced *in vitro* are typically accumulating in the media, there is a lot of evidence that EVs produced *in vivo* are also taken up by cells as part of cell-cell communication. This significantly complicates the interpretation of the results. However, the finding that are most relevant to this paper is that APP-CTFs and BMP levels (as shown in our new results in revised Figure 7g) are increased on purified EVs upon *Vps34* inhibition, both *in vitro* and *in vivo*. We have updated the text in page 21 (line 503-508) as to clarify this discrepancy.

17.- p16, line 383: the authors generalize their conclusion ('EVs as part of a homeostatic response counteracting LDSs') too much. They demonstrate that VPS34 inh promotes secretion of a subtype of EVs and that this is related to lysosomal storage defects, not lysosomal storage diseases. The extrapolation to disease models need to be implemented to support this statement.

We agree with this reviewer and have now toned down this statement, having no evidence that our findings are directly related to a *bona fide* LSD. However, we note that *Vps34* overexpression in myoblasts from patients with Danon disease was shown to alleviate the lysosomal/autophagy defects in this LSD primarily affecting the skeletal muscle (Nemazanyy et al. 2013), which certainly goes in this direction. Please find the revised text on page 17 (line 395-396).

18,- p21, line 493-500: please include few references underscoring the link that is made to immune cells, DAMPs etc.

We have now added the excellent review from Heneka et al. to support these potential implications (Heneka et al. 2014).

Reviewer #3 (Remarks to the Author):

This manuscript describes the biological effect of inhibition of VPS34, a class III PI 3-kinase regulating endosomal trafficking, on endosomal dysfunction and subsequent accumulation of APP CTF, other endosomal molecules, and their enhanced release in exosomes. The study incorporates comparison of murine neuronal cell line N2a and primary cultured mouse neurons, and detailed characterization of endosomal accumulation of several key markers by high-resolution microscopic imaging techniques. The in vitro findings are partly verified by in vivo study using conditional neuron-specific knockout of VPS34 in forebrain. The study is significant by finding a novel VPS34-dependent pathway of exosome secretion of APP-CTF after endocytic dysfunction, the identification of the new lipid BMP, and the identification of their dependence in sphingomyelin metabolism to ceramide synthesis as determined by GW4869 and myriocin. These findings would have biological implication in generalized exosome secretion mechanism after endocytic dysfunction in many disease conditions, and BMP has a potential for a specific marker for the extracellular vesicles reflecting the intracellular dysfunction of endosome machinery in the affected cells. The study, however, has many data, which are inconsistent among experimental settings and most of them are not well discussed. These have to be clearly addressed.

Major points:

1. *There is no introductory description of what p62 expression means in this manuscript. P62 first appears on Fig. 2a (line 185), which is one of key molecules, without description. Please address this in the introduction.*

We apologize for not making this clearer in the original manuscript. We have now provided some background to allow the reader to interpret better our experiments on page 8 (line 173-176) of the revised manuscript.

2. *Clearly describe and discuss why Beclin1 expression is specifically increased in VPS34IN1-treated group (Fig. S1b) instead of describing that this treatment "did not cause a general downregulation."*

We thank the reviewer for pointing out that we have not described these data in the most accurate fashion. We have now corrected the statement by mentioning this increase and its unlikely role in the phenotypes we describe (see also our response to reviewer 1's point #1). Unfortunately, we have no clear explanation for why reducing the kinase activity of Vps34 may increase Beclin 1 levels. Because we do not believe it contributes to the phenotypes we describe, we have decided not to characterize it further.

3. *It is difficult to agree that the diameter of EEA1+ puncta is increased by VPS34IN1 treatment (Fig. 1a), although the reduction of its intensity is agreeable. Immuno-EM of EEA1+ cells will be more conclusive for the morphological analysis.*

Since this point as also raised by reviewers 1 and 2 (points #2 and #10, resp.), we invite this reviewer to read our responses. In essence, we have found better images that reflect our quantifications. Since we have already reported EEA1-positive endosomal enlargement upon Vps34 silencing in neurons and genetic ablation in MEFs (Morel et al. 2013; Devereaux et al. 2013), we have opted to focus on strengthening more novel aspects of our manuscript, rather than investing in a time-consuming immuno-EM analysis of the EEA1 compartment. We hope that this reviewer agrees with this justification.

4. In Fig. 1b, the size of Rab5+ puncta appears to be increased by VPS34IN1 treatment, which is not mentioned in Fig. 1a. Please discuss.

We apologize for omitting this information. We invite the reviewer to examine revised Supplementary Figure 1e which shows the average size of Rab5-positive puncta per cell. Given the marginal increase (4%) in puncta size after Vps34 inhibition, we decided to further characterize Rab5-puncta size distribution. Indeed, Vps34 inhibition caused an increase in the relative frequency of a larger subset of Rab5-positive endosomes (>0.23 μ m, 0.181 \pm 0.010 relative freq. for vehicle and 0.243 \pm 0.014 for VPS34IN1) at the cost of a reduction in smaller endosomes (<0.19 μ m, 0.524 \pm 0.010 relative freq. for vehicle and 0.462 \pm 0.012 for VPS34IN1). However, given the lower frequency of larger endosomes (~20-25%) comparatively to the other two groups of endosomes, these have a minor impact in the total sum of Rab5 size distribution. We have updated the manuscript accordingly on page 6 (lines 122-123).

5. The conclusion of the last sentence (line 132-133) is not well supported, since these data are not directly relevant to AD. This has to be rewritten.

We have rephrased the conclusion as suggested. Please find the revised version on page 6 (lines 125-126).

6. In Fig. 1d, there is no obvious increase of APP-CTF or APP-CTFbeta fragment in the WB images. This has to be replaced with more representative images. Please also discuss why the effect of VPS34IN1 treatment on APP processing is more significant in N2a cells over primary cultured neurons.

We thank this reviewer for pointing this out. We have addressed this point by replacing the original Western blot images with an alternate set in revised Figure 1d. We have also noticed and reported that the phenotype is more dramatic in N2a cells (page 7, line 151-153, and have no other explanation than the fact N2a cells are a cell line with fibroblast features that proliferate, unlike primary neurons. Overall, we feel confident that this finding occurs physiologically because it is observed in primary neurons as well as in mouse brain.

7. The LC3 signal in Fig. 2a-b is almost invisible in all 6 panels. MAP2 signal is also very weak. Ub signal in Fig. 2c is also invisible. Figure 2 images should be replaced with more visually understandable images.

We have replaced the original pictures with an alternate version with higher contrast evidencing all markers.

8. In Fig. 3, galectin-3 is a well-accepted marker of phagocytic myeloid cells, and it is rarely detected in neurons. The co-localization of galectin-3 and flotillin-2 in Fig. 3d is also invisible and their quantification is in question. Suggest to delete Fig. 3b-d.

We thank the reviewer for this fair criticism. We agree that galectin-3 is enriched in phagocytic myeloid cells comparatively with neurons (in fact, the gene encoding galectin-3, *Igals3*, has an 8-fold increase in transcript levels in microglia vs. neurons according to Brain RNA-Seq database developed by Ben Barres *et al.* (Zhang *et al.* 2014)). Despite the low expression levels, we were able to detect galectin-3 in primary neurons using a commercially available antibody for immunocytochemistry. While we use galectin-3 merely as a tool for the detection of endolysosomal membrane damage, which has been previously validated (Maejima *et al.* 2013; Aits *et al.* 2015; Paz *et al.* 2010; Bischoff *et al.* 2012; Papadopoulos *et al.* 2017), we do not exclude expression of other galectin isoforms or their accumulation in p62-positive structures in neuronal cells. As mentioned in response to reviewer 1's point #6, we have updated Figure 3b-d with optimized contrast and added linescan intensity plots (i) confirming luminal exclusion of p62/galectin-3 positive structures from LAMP-1 compartments and (ii) highlighting co-localization of p62/galectin-3/flotillin-2. Accordingly, we have updated the text in page 10 (line

219-222). We would like to keep these figures as we believe that endomembrane damage is a key phenotype of endolysosomal dysfunction induced by Vps34 inhibition.

9. In Fig. 4-7, there are WB images of proteins in the purified EV in primary neurons, N2a cells and VPS34 cKO mouse brains. Although the data are of high quality, there are several inconsistent findings, which are not well discussed to understand the differences. For example, Flotilin-1/2 expression is increased by VPS34IN1 treatment in the EV isolated from primary neurons and N2a cells (Fig. 4b,d) but not in EV isolated from VPS34 cKO mouse brain (Fig. 7d). On the other hand, another EV marker ALIX expression increased by VPS34IN1 treatment in the EV isolated from primary neurons (Fig. 4b) and VPS34 cKO mouse brain (Fig. 7d) but not in EV isolated from N2a cells (Fig. 4d). This indicates that none of the tested EV markers show consistent increase by inhibition or deletion of VPS34, and suggest that the group of EV affected by VPS34 inhibition is highly dependent on the conditions although they are of neuronal origin. This should be clearly discussed.

We hope we have addressed this concern in response to reviewer 2's point #16. We believe that the most relevant finding to this paper is that APP-CTFs and BMP are increasingly sorted to EVs as a result of endolysosomal dysfunction, particularly after Vps34 inhibition. We note, however, that the composition of EVs vary significantly between cell types (Kowal et al. 2016) and may account for the disparities in markers such as ALIX and flotillins across our study models. Accordingly, we have updated the text in page 21 (line 503-508) as to clarify this point.

10. In addition, the expression of full-length APP in the EV is different in these experiments. It is increased by VPS34IN1 treatment in the EV isolated from primary neurons (Fig. 4b) but not in EV isolated from N2a cells (Fig. 4d) and its expression in VPS34 cKO mouse brain is not shown. There is no clear explanation of these inconsistent findings or experimental approach.

We invite the reviewer to examine revised Figure 4d, which confirms that FL-APP is also significantly increased in EVs derived from VPS34IN1-treated N2a cells in comparison to controls. Concerning FL-APP levels in mouse brain EVs, we refer the reviewer to our response to reviewer 1's point #10. Briefly, we and our collaborators have not been able to detect significant amounts of endogenous FL-APP in exosomes derived from the brain of wild-type mice. In addition, we provide data in Figure 3 for Referees showing that EVs have an increased ratio of APP-CTFs/FL-APP relative to lysates and that EVs are enriched for mature, glycosylated FL-APP in our cell culture experiments.

11. As for p62 in EV, there are repetitive discussion of the existence of p62 in the EV after VPS34 inhibition in primary cultured neurons and N2a cells (Fig. 4b,d), which suggests the shuttling of dysfunctional endolysosomes to EV as p62-containing complex. However, p62 expression is not shown in the EV fraction isolated from VPS34 cKO mice (Fig. 7d). This is a key conclusive data and should be presented.

We had previously attempted without success to detect p62 in our original two independent EV purification experiments, although we were able to show p62 immunoreactivity in hippocampal lysates, with an increase in the cKO. During the revision, we conducted an additional third experiment (see Figure 5 for Referees). While we were still not able to detect p62, we confirmed for a third time that EVs derived from cKO mice are enriched for APP-CTFs. We conclude that p62 is therefore not enriched on brain exosomes derived from Vps34 cKO mice, contrary to exosomes derived from neurons/N2a cells treated with VPS34IN1. We mention this point in the revised manuscript on page 16 (lines 374-376).

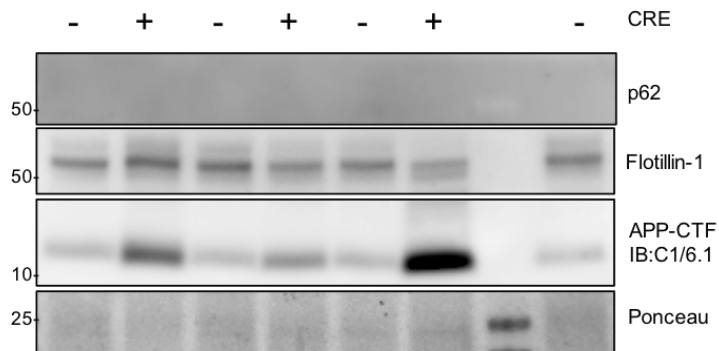


Figure 5. Lack of detection of p62 in EVs derived from mouse brain. EVs were purified from CTRL and cKO mice as described in Method sections and processed for Western Blot analysis.

12. In Fig. 6b, treatment of cells with nSMase2 inhibitor GW4869 would suppress the total number of EV secreted to the media. Please clarify how much is the input of the EV for each sample.

We thank the reviewer for raising this important point. As mentioned in the Methods sections, cells were treated and the same volume of media from each sample was processed for purification of exosomes. In the particular case of GW4869 and myriocin treatment, 1×10^6 neurons were seeded in 6-wells, matured for 15-18 days and incubated in 1.5mL of media during drug treatment. The 100K pellets were resuspended in equal volumes of RIPA buffer and the volume corresponding to approx. 75% of all pelleted material was loaded on SDS-PAGE. Considering we were loading an equivalent volume per sample/cell mass, we normalized the levels of all proteins to the protein concentration of the cell lysate. We clarified this point in the revised Methods section on page 28 (lines 667-669).

13. This reviewer disagrees with the conclusion that Atg5 KO has no effect on the secretion of APP-CTF in the EV fraction. Supplementary Fig. 6d shows enhanced accumulation of APP-CTF in ATG5 KO N2a cells, which appears to be more than wildtype N2a cells (lane 1) and is further accumulated by VPS34IN1 treatment (lane 4). This clearly shows that ATG5 deletion inhibit autophagic function and enhances the secretion of APP-CTF in the EV fraction. The authors show the intensity as fold increase of untreated cells, but this is not the correct analysis of band intensity. The band intensity should be quantified on the same SDS-PAGE after loading the same amount of protein from different cell types. The data presentation and interpretation should be thoroughly revised.

We thank the reviewer for raising this important point and agree in part with his/her assessment. However, while we have updated Supplementary Figure 6 according to the reviewer's recommendation and state that Atg5 KO increases the secretion of APP-CTFs in exosomes, we are still confident regarding our original interpretation, namely that APP-CTF sorting to EVs upon VPS34 inhibition is independent of its role in autophagy impairment. We have updated the text accordingly as to clarify this particular concern on page 13 (line 301-315) of the revised manuscript.

14. The Supplementary Fig. 4c does not have the methods to understand how BMP is stained for imaging, and does not appear to be co-localized with LAMP-1. This description (line 213-215) should be revised or replace the data with more representative image.

We apologize for this omission and for not being clearer in regards to the colocalization between LAMP-1 and BMP. First, we did not mention a specific protocol for BMP staining

because it was performed similarly to the other stainings, as described in the original Methods section. In response to this concern, we now refer the reader to the Methods section in the legend of Supplementary Figure 4c. Secondly, we have rephrased the text on page 10 (line 208-212) to indicate that the BMP immunoreactivity is almost exclusively found in the lumen of LAMP-1-positive compartments rather than co-localizing with LAMP-1, consistent with the notion that it is enriched on intraluminal vesicles (as shown by several other labs (Chevallier et al. 2008; Bissig & Gruenberg 2013; Bache et al. 2003)).

15. *In general, mono-ubiquitination is necessary for the sorting of proteins to ILV via ESCRT machinery, but the protein is deubiquitinated before the insertion into the ILVs. This study repeatedly shows poly-ubiquitinated molecules in the EV fraction (Fig. 4b, 6b, 7d), which is odd but may represent non-ESCRT machinery for the insertion of these molecules to ILVs. Please cite at least one reference reporting the existence of poly-ubiquitinated molecules in the ILVs or exosomes to substantiate the finding.*

We would like to refer the reviewer to two publications reporting and characterizing poly-ubiquitinated proteins in EV fractions (Pisitkun et al. 2004; Huebner et al. 2016). In the first study ubiquitin was detected by LC-MS and immunoblot, spanning a wide molecular mass range from 10kDa to 400kDa, indicating that EVs contained poly-ubiquitinated proteins. The later study reported immunogold labelling of ubiquitin in ILVs and exosomes from human epithelial cells. In addition, they performed LC-MS analysis of poly-ubiquitinated proteins present in exosomes and identified ubiquitin chain in proteins enriched in EVs such as ALIX and TSG101, among others. We are now citing these studies in the revised manuscript in page 11 (line 252-253).

16. *Line 277-278 says" EVs containing BMP can be unambiguously defined as bona fide exosomes". This should be toned down since later in the discussion BMP is described as a unique marker under specific conditions associated with endolysosomal dysfunction (line 471-473).*

We thank the reviewer for pointing out this overstatement, which we have now toned down in the revised manuscript.

Minor comments:

1. *In Fig. 1c image, please clarify if the CatD refers to only processed CatD or both CatD and proCatD.*

We apologize for omitting this information. We have updated Figure 1c mentioning proCatD/CatD.

References

- Aits, S. et al., 2015. Sensitive detection of lysosomal membrane permeabilization by lysosomal galectin puncta assay. *Autophagy*, (August), pp.00–00.
- Bache, K.G. et al., 2003. Hrs regulates multivesicular body formation via ESCRT recruitment to endosomes. *Journal of Cell Biology*, 162(3), pp.435–442.
- Bischoff, V. et al., 2012. Seizure-Induced Neuronal Death Is Suppressed in the Absence of the Endogenous Lectin Galectin-1. *Journal of Neuroscience*, 32(44), pp.15590–15600.
- Bissig, C. & Gruenberg, J., 2013. Lipid sorting and multivesicular endosome biogenesis. *Cold Spring Harbor Perspectives in Biology*, 5(10), p.a016816.
- Chevallier, J. et al., 2008. Lysobisphosphatidic Acid Controls Endosomal Cholesterol Levels. *Journal of Biological Chemistry*, 283(41), pp.27871–27880.
- Cossec, J.-C. et al., 2012. Trisomy for synaptojanin1 in Down syndrome is functionally linked to the enlargement of early endosomes. *Human molecular genetics*, 21(14), pp.3156–72.
- Dall'Armi, C., Devereaux, K. a & Di Paolo, G., 2013. The role of lipids in the control of autophagy. *Current biology : CB*, 23(1), pp.R33-45.

- Devereaux, K. et al., 2013. Regulation of Mammalian Autophagy by Class II and III PI 3-Kinases through PI3P Synthesis. *PLoS ONE*, 8(10), pp.10–12.
- Futter, C.E. et al., 2001. Human VPS34 is required for internal vesicle formation within multivesicular endosomes. *Journal of Cell Biology*, 155(7), pp.1251–1263.
- Greening, D.W. et al., 2015. A Protocol for Exosome Isolation and Characterization: Evaluation of Ultracentrifugation, Density-Gradient Separation, and Immunoaffinity Capture Methods. In *Methods in molecular biology (Clifton, N.J.)*. pp. 179–209.
- Guix, F.X. et al., 2017. Tetraspanin 6: a pivotal protein of the multiple vesicular body determining exosome release and lysosomal degradation of amyloid precursor protein fragments. *Molecular Neurodegeneration*, 12(1), p.25.
- Haass, C. et al., 2012. Trafficking and proteolytic processing of APP. *Cold Spring Harbor perspectives in medicine*, 2(5), p.a006270.
- Heneka, M.T., Kummer, M.P. & Latz, E., 2014. Innate immune activation in neurodegenerative disease. *Nature reviews. Immunology*, 14(7), pp.463–77.
- Huebner, A.R. et al., 2016. Deubiquitylation of Protein Cargo Is Not an Essential Step in Exosome Formation. *Molecular & cellular proteomics : MCP*, 15(5), pp.1556–71.
- Jiang, Y. et al., 2010. Alzheimer's-related endosome dysfunction in Down syndrome is A-independent but requires APP and is reversed by BACE-1 inhibition. *Proceedings of the National Academy of Sciences*, 107(4), pp.1630–1635.
- Kishi-Itakura, C. et al., 2014. Ultrastructural analysis of autophagosome organization using mammalian autophagy-deficient cells. *Journal of Cell Science*, 127(22), pp.4984–4984.
- Klingeborn, M. et al., 2017. Directional Exosome Proteomes Reflect Polarity-Specific Functions in Retinal Pigmented Epithelium Monolayers. *Scientific Reports*, 7(1), p.4901.
- Kowal, J. et al., 2016. Proteomic comparison defines novel markers to characterize heterogeneous populations of extracellular vesicle subtypes. *Proceedings of the National Academy of Sciences*, 113(8), pp.E968–E977.
- Maejima, I. et al., 2013. Autophagy sequesters damaged lysosomes to control lysosomal biogenesis and kidney injury. *The EMBO Journal*, 32, pp.2336–2347.
- Morel, E. et al., 2013. Phosphatidylinositol-3-phosphate regulates sorting and processing of amyloid precursor protein through the endosomal system. *Nature communications*, 4, p.2250.
- Nemazanyy, I. et al., 2013. Defects of Vps15 in skeletal muscles lead to autophagic vacuolar myopathy and lysosomal disease. *EMBO molecular medicine*, 5(6), pp.870–90.
- Papadopoulos, C. et al., 2017. VCP/p97 cooperates with YOD1, UBXD1 and PLAA to drive clearance of ruptured lysosomes by autophagy. *The EMBO Journal*, 36(2), pp.135–150.
- Paz, I. et al., 2010. Galectin-3, a marker for vacuole lysis by invasive pathogens. *Cellular Microbiology*, 12(February), pp.530–544.
- Perez-Gonzalez, R. et al., 2012. The exosome secretory pathway transports amyloid precursor protein carboxyl-terminal fragments from the cell into the brain extracellular space. *Journal of Biological Chemistry*, 287(51), pp.43108–43115.
- Pisitkun, T., Shen, R.-F. & Knepper, M.A., 2004. Identification and proteomic profiling of exosomes in human urine. *Proc. Natl. Acad. Sci. USA*, 101(36), pp.13368–13373.
- Raiborg, C., Schink, K.O. & Stenmark, H., 2013. Class III phosphatidylinositol 3-kinase and its catalytic product PtdIns3P in regulation of endocytic membrane traffic. *The FEBS journal*, 280(12), pp.2730–42.
- Schink, K.O., Raiborg, C. & Stenmark, H., 2013. Phosphatidylinositol 3-phosphate, a lipid that regulates membrane dynamics, protein sorting and cell signalling. *BioEssays*, 35(10), pp.900–912.
- Settembre, C. et al., 2013. Signals from the lysosome: a control centre for cellular clearance and energy metabolism. *Nature reviews. Molecular cell biology*, 14(5), pp.283–296.
- Sharples, R.A. et al., 2008. Inhibition of gamma-secretase causes increased secretion of amyloid precursor protein C-terminal fragments in association with exosomes. *FASEB journal : official*

- publication of the *Federation of American Societies for Experimental Biology*, 22(5), pp.1469–78.
- Théry, C. et al., 2006. Isolation and Characterization of Exosomes from Cell Culture Supernatants. *Current protocols in cell biology / editorial board, Juan S. Bonifacino ... [et al.]*, Chapter 3, pp.1–29.
- Wang, L., Budolfson, K. & Wang, F., 2011. Pik3c3 deletion in pyramidal neurons results in loss of synapses, extensive gliosis and progressive neurodegeneration. *Neuroscience*, 172, pp.427–442.
- Williamson, R.L. et al., 2017. Disruption of amyloid precursor protein ubiquitination selectively increases amyloid beta (A β) 40 levels via presenilin 2-mediated cleavage. *Journal of Biological Chemistry*, p.jbc.M117.818138.
- Zhang, Y. et al., 2014. An RNA-sequencing transcriptome and splicing database of glia, neurons, and vascular cells of the cerebral cortex. *The Journal of neuroscience : the official journal of the Society for Neuroscience*, 34(36), pp.11929–47.

REVIEWERS' COMMENTS:

Reviewer #1 (Remarks to the Author):

I am satisfied with the answers to the concerns raised in my initial review

Reviewer #2 (Remarks to the Author):

The authors have submitted a revised version of their manuscript demonstrating that APP CTF fragments are shunted to a population of EVs upon vps34 inhibition-induced lysosomal dysfunction. After reading their full rebuttal and revised data, I have to conclude that, overall, the authors have significantly improved the manuscript and have addressed my major concerns. The manuscript is now more clearly written out so that the main message is better advocated. In principle I can agree with publication, but have still a few outstanding issues that the authors should consider.

I'm still struggling with the interpretation and identity of the p62-/flotillin-positive organelles. I can agree that the enlarged endosomal structures might be the lamp1-positive organelles, and maybe this should be as such also mentioned in the text (line 184-188). If the dark organelles are suggested to be the p62-organelles, then they are clearly separate organelles. However, the way the authors describe their linescans of the superresolved images remains ambiguous by stating that '... were generally distributed to the periphery of lamp1-positive organelles': it is not clear whether they mean on the periphery of lamp1-positive organelles or clearly a separate organelle closely apposed to endolysosomes. They now more clearly state that the p62-positive organelles are most likely earlier stages of endosomes on which I can agree: having said that, and given the fact that these organelles colocalize with gal3 (and are thus damaged), wouldn't that more agree with the definition of amphisomes or the direct recruitment of the autophagy-machinery to damaged endosomes (as seen in other specific cases of organelle damage like mitophagy, ER-phagy)? To my opinion that would explain the ambiguity on whether autophagy is included or not as this is a specific case of targeting damaged endosomes. I would suggest that the authors should consider incorporating this alternative explanation of their observations and on this population.

Small remark:

- A better contrasted picture for the Lamp1 staining in suppl fig 4C, vps34inh should be provided. It is not so clear (compared to WT) that BMP is in all these lamp1 positive organelles because of the weak signal.
- In the attempt to improve contrast of the Rab5 immunostaining (figure 1a), the increased intensity of rab5 positive structures in VPS34IN1 is completely gone, not only in intensity in individual spots but also in the number of spots (control is far higher compared to the VPS34IN1). Authors should look back at this and find kind of a representative image.
- With respect to the ATG5KO data, the authors now state more explicitly that 'secretion of EVs induced by Vps34 inhibition occurs independently of any autophagic defects and originates from other aspects of endosomal dysfunction' (page 13, l 306-307). Although I agree that the observed effects are majorly coming from endolysosomal regulation, they cannot exclude that there is some component of autophagy involved. Sentence should be

changed to '...occurs independently from major autophagic defects....'.

Reviewer #3 (Remarks to the Author):

The major concerns are all addressed in the revised manuscript and it was really improved in terms of data presentation, description and discussion with adequate citations.

RESPONSE TO REVIEWERS' COMMENTS:

Reviewer #2 (Remarks to the Author):

The authors have submitted a revised version of their manuscript demonstrating that APP CTF fragments are shunted to a population of EVs upon vps34 inhibition-induced lysosomal dysfunction. After reading their full rebuttal and revised data, I have to conclude that, overall, the authors have significantly improved the manuscript and have addressed my major concerns. The manuscript is now more clearly written out so that the main message is better advocated. In principle I can agree with publication, but have still a few outstanding issues that the authors should consider.

I'm still struggling with the interpretation and identity of the p62/flotillin-positive organelles. I can agree that the enlarged endosomal structures might be the lamp1-positive organelles, and maybe this should be as such also mentioned in the text (line 184-188). If the dark organelles are suggested to be the p62-organelles, then they are clearly separate organelles. However, the way the authors describe their linescans of the superresolved images remains ambiguous by stating that '... were generally distributed to the periphery of lamp1-positive organelles': it is not clear whether they mean on the periphery of lamp1-positive organelles or clearly a separate organelle closely apposed to endolysosomes.

We thank the reviewer for requesting a better clarification of this important point. We believe that p62/flotillin-2 positive structures are distinct organelles apposed to LAMP-1 compartments based on the distinct punctate morphology in confocal images and presence of separate electron-dense organelles in electron microscopy. Following the reviewer's request, we have updated the text to clarify this ambiguity (page 9, line 223-227 and page 10, line 266-270).

They now more clearly state that the p62-positive organelles are most likely earlier stages of endosomes on which I can agree: having said that, and given the fact that these organelles colocalize with gal3 (and are thus damaged), wouldn't that more agree with the definition of amphisomes or the direct recruitment of the autophagy-machinery to damaged endosomes (as seen in other specific cases of organelle damage like mitophagy, ER-phagy)? To my opinion that would explain the ambiguity on whether autophagy is included or not as this is a specific case of targeting damaged endosomes. I would suggest that the authors should consider incorporating this alternative explanation of their observations and on this population.

We have updated our manuscript (page 10, line 279) to mention that these damaged organelles are marked for degradation via recruitment of autophagy adapter p62, however lack of PI3P-dependent LC3 lipidation and autophagosome elongation likely prevent their efficient clearance. We have also mentioned another scenario, whereby those damaged structures could be late endosomes or lysosomes that have lost their membrane markers through proteolytic degradation occurring upon loss of membrane integrity (page 11, line 335-337).

Small remark:

- A better contrasted picture for the Lamp1 staining in suppl fig 4C, vps34inh should be provided. It is not so clear (compared to WT) that BMP is in all these lamp1 positive organelles because of the weak signal.

We have updated Supplementary Figure 4C accordingly.

- In the attempt to improve contrast of the Rab5 immunostaining (figure 1a), the increased intensity of rab5 positive structures in VPS34IN1 is completely gone, not only in intensity in individual spots but also in the number of spots (control is far higher compared to the VPS34IN1). Authors should look back at this and find kind of a representative image.

We have updated Figure 1A accordingly with the inclusion of a new set of figures, including super-resolution Airy Scan insets where endosomal enlargement and intensity difference is

now more clear. We also took the opportunity to select a better inset in Fig. 1c that better reflects the luminal localization of CatD after VPS34IN1 treatment.

- With respect to the ATG5KO data, the authors now state more explicitly that 'secretion of EVs induced by Vps34 inhibition occurs independently of any autophagic defects and originates from other aspects of endosomal dysfunction' (page 13, l 306-307). Although I agree that the observe effects are majorly coming from endolysosomal regulation, they cannot exclude that there is some component of autophagy involved. Sentence should be changed to '...occurs independently from major autophagic defects....'.

We agree with the reviewer and have now toned down our original statement as suggested (page 14, line 445).